Role of BK channels in macrophage activation

A thesis submitted by Minae Yoshida to University College London for the Degree of Doctor of Philosophy

March 2017

Department of Neuroscience, Physiology and Pharmacology

University College London, Gower Street, London WC1E 6BT

Declaration

I, Minae Yoshida, confirm that the work presented in this thesis is my own. Where information has been derived from other sources, I confirm that this has been indicated in the thesis.

Abstract

The cells of the immune system expresses an array of different ion channels, yet their roles in these cells are not fully understood. The large-conductance voltage and calcium-activated potassium channel (BK channel) is a potassium ion channel, which is found in a wide variety of cells and tissues. Their biophysical properties and expression in excitable cells are extensively studied. However, their role in immune cells is unclear. In this thesis I have investigated the role of BK channels in macrophages.

The expression of BK channels in the RAW264.7 mouse macrophages cell line was characterised by Western blot, immunofluorescence imaging and electrophysiological recordings. BK channels were predominantly associated with intracellular compartments in resting macrophages. Activation of RAW264.7 with ultrapure lipopolysaccharide (LPS) resulted in the upregulation of BK channel protein on the plasma membrane and the channel activity.

To investigate the function of BK channels in these cells, both genetic and pharmacological approaches were used. These studies suggested that the role of the BK channel in macrophages is dependent on the sub-cellular location of the channel. Importantly this thesis suggests that plasma membrane located BK channels regulate the release of tumour necrosis factor-α (TNF-α) and interleukin-6 receptor α (IL-6Rα) from activated macrophages. IL-6 release was not affected. These results together suggested that a disintegrin and metalloprotease domain 17 (ADAM17) enzyme is negatively regulated by the plasma membrane BK channel.

This thesis proposes a novel interaction between ion channels and the activity of a membrane metalloprotease. This project also identified the dynamic movement of BK channels during activation of macrophages.

ADAM17 regulates the release of a diverse range of proteins including cytokines, growth factors, receptors and adhesion molecules, which are implicated in many fields including immunology, tissue regeneration, neurology and tumour growth. It is anticipated that this finding could stimulate further research.

Acknowledgement

Contents

List of figures

List of tables

List of equation

List of abbreviations

A disintegrin and metalloprotease (ADAM)

A disintegrin and metalloprotease domain 17 (ADAM17)

Activated protein-1 (AP-1)

Ammonium persulfate (APS)

AU rich element (ARE)

AU-rich element RNA-binding protein (AUF1)

Bovine serum albumin (BSA)

Calcium release activated calcium (CRAC)

Calcium release activated channel (CRAC)

Carbon monoxide (CO)

Colony stimulated factor-1 receptor (CSF-1R)

Colony stimulating factor (CSF)

Cyclooxygenase-2 (COX-2)

Damage associated molecular patterns (DAMPs)

Death domain (DD)

Dimethyl sulfoxide (DMSO)

Distilled water (diH$_2$O)

Dithiothreitol (DTT)

Dulbecco's modified eagle medium (DMEM)

ELAV-like protein 4 (HUD)

Enzyme-linked immunosorbent assay (ELISA)

Epidermal growth factor receptor (EGFR)

Eukaryotic translation initiation factor 2 (eIF2)

Eukaryotic translation initiation factor 2B (eIF2B)

Fetal bovine serum (FBS)

Final protein concentration (FPC)

Granulocyte-macrophage colony stimulating factor (GM-CSF)

Heparin-binding epidermal growth factor -like growth factor (HB-EGF)

Horse radish peroxidase (HRP)

Hosphate buffered saline with tween-20 (PBS-T)

Hu-antigen receptor (HUR)

Ibriotoxin (IbTX)

Interleukin (IL)

Interleukin-1 receptor associated kinase-1 (IRAK-1)

Interleukin-1 receptor associated kinase-4 (IRAK-4)

Interleukin-6 receptor α (IL-6Rα)

I kappa B kinase (IKK)

Interferon (IFN)

Interleukin regulatory factor (IRF)

Intracellular adhesion molecule-1 (ICAM-1)

Large conductance voltage- and calcium-activated potassium channel (BK channel)

Leucine-rich repeat (LRR)

Lipopolysaccharide (LPS)

LPS binding protein (LBP)

Methyl-thiazolyl-tetrazolium (MTT)

MicroRNA (miRNA)

Mitogen-activated protein kinase (MAPK)

Mononuclear cells (MNs)

MyD88 adaptor like protein (Mal)

Myloid differentiation factor 2 (MD2)

Myloid differentiation factor 88 (MyD88)

Nitric oxide (NO)

Nonsense mediated decay (NMD)

Nuclear factor-kappa B (NF-κB)

Nuclear factor-kappa B essential modifier (NEMO)

Nuclear localisation signals (NLS)

Open probability (Po)

Pathogen associated molecular patterns (PAMPs)

Pattern recognition receptors (PRRs)

Phorbol 12-myristate 13-acetate (PMA)

Phosphate buffered saline (PBS)

Phosphatidyllinositol-4,5-biphosphate (PtdLns(4,5)P2)

Polymorphonuclear cells (PMNs)

Polyunsaturated fatty acid (PUFA)

Reactive oxygen species (ROS)

Receptor interacting protein (RIP)

Receptor interacting protein homotypic interaction motif (RHIM)

Regulator of nonsense transcripts (UPF)

Regulator of potassium conductance (RCK)

Rel homology domain (RHD)

Ribosomal RNA (rRNA)

RNA induced silencing complex (RISC)

Sodium dodecyl sulfate (SDS)

Sodium dodecyl sulfate polyacrylamide gel electrophoresis (SDS-PAGE)

Sterile alpha and armadillo-motif containing protein (SRAM)

Synaptotagmin XI (SytXI)

Tetraethylammonium chloride (TEA)

Tetramethylethylenediamine (TEMED)

Tissue inhibitor of metalloproteinases-3 (TIMP-3)

Toll-interleukin-1 receptor (TIR)

Toll-interleukin-1 receptor related adaptor molecule (TRAM)

Toll-interleukin-1 receptor-domain containing adaptor inducing interferon-β (TRIF)

Toll-interleukin-1 receptor-domain containing adaptor inducing interferon-β elated adaptor molecule (TRAM)

Toll-like receptor (TLR)

Transcription activation domain (TAD)

Transforming growth factor (TGF)

Transforming growth factor-β activated kinase 1 binding protein 2 (TAB2)

Transforming growth factor-β activated kinase 1 (TAK1)

Transforming growth factor-β activated kinase 1 binding kinase 1 (TBK-1)

Transient receptor potential cation (TRPC)

Transient receptor potential melastatin 2 (TRPM2)

Transient receptor potential vaniloid 2 (TRPV2)

Transmembrane form TNF-α (mTNF-α)

Tris-buffered saline with tween-20 (TBS-T)

Tristetraprolin (TTP)

Tumour necrosis factor receptor (TNFR)

Tumour necrosis factor receptor associated factor (TRAF)

Tumour necrosis factor receptor associated factor 6 regulated I κB activator (TRIKA)

Tumour necrosis factor-α converting enzyme (TACE)

Tumour necrosis factor-α (TNF)

Untranslated terminal region (UTR)

Vascular cell adhesion molecule-1 (VCAM-1)

Chapter 1 Introduction

1.1 Inflammation

1.1.1 General concepts of inflammation

Inflammation is a protective process, which is initiated by a disturbance to cellular or tissue homeostasis. Ultimately the aim of this process is to eliminate the initial or continuing insult, initiate healing and eventually restore normal tissue homeostasis. Although inflammation was first recognised by the Egyptians, *circa* 300 B.C., the visible changes associated with inflammation were first defined by Celsus (approximately 30 B.C.- 38 A.D.) and described as cardinal signs of inflammation. These signs were termed 'redness', 'heat' and 'swelling'. To these was added 'pain' by Virchow and 'loss of function' later by John Hunter (1728-1793 A.D.). Although exact people responsible for the last two signs is still debated. These 'cardinal signs' are caused by the physiological changes in surrounding tissue and the microcirculation, which result in the exudation of plasma and emigration of leukocytes from blood vessels to the area of injury.

The beneficial nature of inflammation was first recognised by Galen (approximately 129-216 A.D.) in the 3rd century A.D. Galen interpreted the inflammation associated with infection has to be beneficial for host wound repair. However the concept that the inflammation was a cause of the disease dominated over ensuing centuries. It was John Hunter in 18th century in his thesis on 'Gun Shot Wounds' who explicitly referred to Inflammation as a physiological or 'salutary', process. He described inflammation response as a salutary process to remove insults and to restore the normal state of the tissue. He expressed his views in following words;

"But if inflammation develops, regardless of the cause, still it is an effort whose purpose is to restore the parts to their natural functions."

In the late 19th to early 20th century, the cellular aspects of inflammatory responses began to be elucidated. Rudolf Virchow (1821-1902 A.D.) began to investigate the cellular components of inflammation, which was followed by the discovery of phagocyte by Eile Metchnikoff (1845-1916 A.D.). This described an important role of phagocytosis in protection against pathogen invasion (Lord Florey, 1970).

It is now established that the inflammatory response is essential in host defence, and an inability to produce a sufficient inflammatory response results in immune deficiency diseases causing life threating infections. Immunodeficiency can occur in both the innate and adaptive immune response. Innate immune deficiencies include chronic granulomatosis diseases, which is caused by genetic defect in the reactive oxygen species producing enzyme, NADPH oxidase (Roos *et al.*, 1996). In severe combined immune deficiency, a deficiency of the adaptive immune system, patients have impairment of T-cell development causes. In both cases patients suffer from opportunistic, severe infections by bacterial, viral and fungal infections (Aloj *et al.*, 2012).

However, beside this 'physiological inflammation', which is essential for continued wellbeing, it is also recognised that the inflammation can cause tissue damage and pathology. Classically, 'pathological inflammation' is associated with excessive and/or an inappropriate inflammatory responses. For example, septic shock and anaphylaxis are associated with excessive inflammatory reactions, which, in severe cases, could lead to the multiple organ failure and death (Boghner and Lichtenstein, 1991; Angus and van der Poll, 2013). Moreover, the general concept of what inflammation is in differing situations is still developing. In past the 15 years, an intermediate tissue condition between normal and inflamed tissue conditions have been introduced and termed 'para-inflammation'. While the exact definition of para-inflammation is still to be determined, this condition refers to prolonged and low grade inflammatory reactions which causes gradual tissue damage and alter responsiveness to endogenous signalling molecules including hormones and neurotransmitters (Medzhitov, 2008). This may contribute to the development of many chronic diseases such as diabetes, arthrosclerosis and neurodegenerative diseases (Nathan, 2002). Inflammation plays an important role in tissue protection and in homeostasis but alternatively, contributes to disease, it is important to investigate the mechanisms and mediators which are responsible for controlling and eliciting this fundamental process.

Central to inflammatory response is the immune system, which has evolved a diverse range of immune cell populations with specialised functions, molecular

signalling pathways and various chemical mediators to bring about the protective effects of inflammation (Medzhitov, 2008). The immune system can be divided into two parts, the innate and adaptive systems. The innate responses provide the first line of defence against many common pathogens. The adaptive immune system evolved later than innate system and importantly, provides the immune systems with a memory and greater response against previously encountered pathogens. The components of innate immune system are important in the initiation of the inflammatory response and provide a bridge to the adaptive system, for example, antigen is presented by macrophages to T cells. (Janeway *et al.*, 2001). The central questions in inflammation research are how do these cells recognise the presence of noxious inflammatory stimuli? And how do they regulate the appropriate responses to these stimuli?

1.1.2 Pattern recognition receptors

Inflammation can be induced by a variety of stimuli including, microbial infections, molecules associated with tissue injury and cell death, tissue neoplasm, and the conditions associated with abnormal tissue conditions/environment, such as obesity, hypoxia and neoplasms (Hotamisligil *et al.*, 1993; Jiang *et al.*, 2005; Akira *et al.*, 2006). The nature of the initial inflammatory insult is important in determining the property and magnitude of subsequent inflammatory response. An efficient inflammatory response results in the most appropriate responses to the stimuli. However, this needs the ability of the immune cells to recognise a broad range of noxious stimuli quickly and to respond rapidly toward the insult. Therefore the principles of "broad", "quick" and "appropriate" are central to inflammation. To accommodate the first two principles, the innate immune system has evolved a series of receptors which recognise differing chemical entities, which are not usually found under normal tissue conditions. These are termed pattern recognition receptors (PRRs). PRRs express the conserved recognition sites, which bind to variable chemical epitopes on invading microorganisms termed pathogen associated molecular patterns (PAMPs), or endogenous chemical moieties associated with cellular stress, damage associated molecular patterns (DAMPs). Some members of PPRs are endocytic, soluble proteins- they sense, are activated and elicit their repose in the extracellular fluid. These endocytic PRRs include Pentaxin, C-type leucine like receptors and the plasma components of complement cascade. Alternatively cell associated PRRs are found on/in host cells and activate the cells inflammatory response. Examples of cell-associated PRRs are toll-like

receptors (TLRs), nucleotide-binding oligomerization domain (NOD)-like receptors, DNA sensors, such as absent in melanoma 2, RNA sensors such as retinoic acid inducible gene-1 and melanoma differentiation-associated protein-5. These cell-associated PRRs are expressed at various cellular locations which include cell/plasma membrane, the cytoplasm and various intracellular compartments. Recently it has been demonstrated that some cell associated PRRs can be found in multiple cellular compartments (Akira *et al.*, 2006). This variation in locations enables the host to respond to different levels of microbial invasions (Takeuchi and Akira, 2010). For example, lipopolysaccharide (LPS), a component of gram-negative bacterial cell wall, is detected by TLR2 heterodimers and/or TLR4 homodimers on the plasma membrane and causes the release of inflammatory cytokines and phagocytosis. Whereas LPS in the cytosol is associated with higher bacterial load and causes the activation of caspase-11 and subsequent cell death (Hagar *et al.*, 2013).

1.2 Toll-like receptor pathways

1.2.1 TLR structure

One of the best characterised families of PRRs is the TLR superfamily. Initially toll receptors, the homology of the TLRs, were discovered in Drosophila. At present, 10 types of TLRs have been identified in human and 13 in mice, Table 1-1. These receptors can be expressed on the plasma or intracellular membranes. The differing subcellular localisation of the receptor is thought to enable effective detection of extracellular or intracellular pathogen as well as allowing the selective recruitment of signalling proteins.

All TLRs contain a ligand binding domain and a toll/interleukin-1 receptor (TIR) homology domain, which are separated by a transmembrane region. The ligand binding site of TLRs consists of a leucine-rich repeat (LRR) of 20-30 amino acids, forming a conserved horseshoe-like tertiary protein structure. The LRRs have a signature consensus sequence motif, L(XX) LXL (XX) NXL (XX) L (XXXXXXX) L (XXX) with N=asparagine, L=leucine and X=any amino acid (Kang and Lee, 2011). These LRR conserved sequences compose the hydrophobic core of the receptor, with variations the X amino acids, influencing its selectivity to particular ligands. LRRs are generally considered as protein binding domains which facilitate protein-protein interactions (Kobe and Deisenhofer, 1995). However due to the slight

variations in its amino acid sequence in TLRs, LRRs in TLRs bind to a chemically more diverse set of ligands (Song and Lee, 2012). These ligands include peptides, lipids and nucleic acids, and possibly oxidised forms of lipoproteins. For example, the absence of asparagine in TLR1, 2, 4 and 6 leads to the formation of a hydrophobic pocket in its LRR region allowing the receptors to bind lipid based ligands. It is therefore not surprising that certain lipids found in bacterial, fungal and viral pathogens or released during tissue stress can act as ligands for TLRs (Song & Lee, 2012). Table 1-1 lists TLRs, their ligands and cellular locations. The molecular mechanisms of ligand binding differ between TLRs, however, they all form dimers when binding to their ligands. These dimers can be homo- or hetero-dimer in nature and once formed, the dimers fold their ligand in the regions between the two LRRs. The dimerization of the receptors is facilitated by the TIR-domains. The TIR-domain is important in the formation of the dimers and the recruitment of the adaptor molecules which also contain TIR-domains.

Five TIR-domain containing adaptor proteins have identified in human. These are myeloid differentiation factor 88 (MyD88), TIR-domain containing adaptor protein inducing IFN-β (TRIF), MyD88 adaptor like protein (Mal), TRIF related adaptor molecule (TRAM) and sterile alpha and armadillo-motif containing proteins (SRAM). Each member of TLR dimers recruits a specific combination of these five adaptor proteins that initiates different but overlapping inflammatory signalling cascades. It was suggested that this specificity, together with the TLRs ligand selectivity, enables the activation of most appropriate immune response directed towards the initiation stimuli (O'Neill and Bowie, 2007). Therefore the combination of receptor locations, ligand binding specificity and selective adaptor protein recruitment allows a quick and appropriate response to a broad class of exogenous and endogenous molecules. It also can be suggested that these combinatory interactions allow a diverse range of signalling cascades to be established. To date TLR4 mediated pathway represents the most well characterised signalling pathway among the TLRs family.

TLR	Species	Localisation	Microbial ligands	Endogenous ligands	Synthetic ligands
TLR1	Human and mouse	Plasma membrane	Triacyl lipoproteins	Unknown	Pam3CSK4
TLR2	Human and mouse	Plasma membrane	Lipoproteins, zymosan, mannan, peptidoglycan, lipoteichoic acid,	Versican	Pam2CSK4, Pam3CSK4
TLR3	Human and mouse	Endolysosomal membrane	Viral dsRNA	mRNA	PolyI:C, polyA:U
TLR4	Human and mouse	Plasma and endolysosomal membrane	LPS	Oxidised low-density lipoprotein, Amyloid-beta	Lipid A derivatives
TLR5	Human and mouse	Plasma membrane	Flagellin	Unknown	Recombinant flagellin
TLR6	Human and mouse	Plasma membrane	Diacyl lipoproteins, lipotechoic acid, zymosan	Oxidised low-density lipoprotein, Amyloid-beta, versican	Macrophage-activating lipopeptide 2, synthetic diacylated lipoproteins, Pam2CSK4
TLR7	Human and mouse	Endolysosomal membrane	Viral and bacterial ssRNA	Immune complexes, self RNA	Thiazoquinoline and imidazoquinoline compounds (e.g. R848, imiquimod)
TLR8	Human and mouse	Endolysosomal membrane	Viral and bacterial ssRNA	Immune complexes, self RNA	Thiazoquinoline and imidazoquinoline compounds (e.g. R848, imiquimod)
TLR9	Human and mouse	Endolysosomal membrane	Viral and bacterial CpG DNA, DNA:RNA hybrids	Chromatin IgG immune complexes, self DNA	Class A, B and C CpG oligodeoxynucleotides
TLR10	Human	Plasma membrane	Unknown	Unknown	Unknown
TLR11	Mouse	Endolysosomal membrane	Profilin and flagellin	Unknown	Unknown
TLR12	Mouse	Endolysosomal membrane	Profilin	Unknown	Unknown
TLR13	Mouse	Endolysosomal membrane	Bacterial 23S ribosomal RNA (rRNA)	Unknown	23S rRNA derived oligoribonucleotide

Table 1-1 TLR superfamily

Table shows the identified members of TLR superfamily in mouse and human. Each member of receptors is activated by specific set of ligand, which can be classified as microbial, endogenous or synthetic in nature.

1.2.2   TLR4

TLR4 has a hydrophobic ligand binding region and as a result as high affinity for lipid based ligands. For example, lipid A epitopes found in LPS is considered to be a most potent activator of this receptor (Raetz and Whitfield, 2002; Kang and Lee, 2011; Song and Lee, 2012). As such LPS are a strong activators of the TLR4 and is strongly implicated in septic shock (Poltorak *et al.*, 1998). Binding of LPS to TLR4 is facilitated by extracellular adaptor proteins, LPS binding protein (LBP) and myeloid differentiation factor 2 (MD2) (Miyake, 2006).LPS binding leads to the formation of TLR4 homodimers and the recruitment of either activated MyD88 and/or TRIF adaptor proteins. Depending on the adaptor protein recruited, MyD88 or TRIF, distinct pathways are activated (Kawai and Akira, 2006).

MyD88 dependent pathway

MyD88 is composed of 296 amino acids with a C-terminus TIR domain and N-terminus death domain. In addition to TLR4 pathway, the protein is recruited by TLR2, TLR5, TLR7 and TLR9. The activation of MyD88 dependent pathway is thought to contribute to strong and rapid inflammatory responses. MyD88 knockout mice have been shown to be highly susceptible to *S. aureus* infections indicating the importance of this pathway in the host's defence against bacterial infections (Takeuchi *et al.*, 2000). In comparison, the activation of MyD88 dependent pathway by LPS injection causes an excessive and destructive inflammation. MyD88 deficiency protects animals from lethal endotoxin shock by decreasing pro-inflammatory cytokine production, including, TNF-α and IL-6 (Kawai *et al.*, 1999). These studies have demonstrate the importance of MyD88 dependent pathway mediated inflammation and a role of this pathway in protection against bacterial infections.

The binding of MyD88 to the activated TLR4 homo-dimer requires another TIR-containing adaptor Mal. Mal functions as a bridge between the TLR4 dimers and MyD88 (Fitzgerald *et al.*, 2001; Horng *et al.*, 2002; Yamamoto *et al.*, 2002). Mal is composed of 235 amino acids with phosphatidyllinositol-4,5-biphosphate (PtdLns(4,5)P_2) binding domains near the N-terminus and a TIR-domain proximal to the C-terminus. The PtdLns(4,5)P_2 binding domain of Mal has been shown to define

its expression on the plasma membrane (Jenkins and Mansell, 2010). The plasma membrane localisation of this adaptor protein serves to set the starting point of MyD88 dependent signalling to the cell surface and enables the death domain (DD) of MyD88 to interact with IL-1R associated kinase-4 (IRAK-4). The IRAK-4 subsequently recruits IL-1R associated kinase-1 (IRAK-1), forming the IRAK-1-IRAK-4 complex. The IRAK-1-IRAK4 complex dissociates from the receptors and interacts with TNF-receptor associated factor 6 (TRAF6), which exists in cytoplasm (Kawai and Akira, 2006). TRAF6 is a RING-finger domain containing protein and functions as an ubiquitin ligase. Together with ubiquitin-conjugating enzyme E2 and ubiquitin-conjugating enzyme 13, TRAF6 mediates the polyubiquitination of substrate proteins at Lys-63. The substrates for this Lys-63 polyubiqutination include the NF-kB essential modifier (NEMO, also IKKγ), and TRAF6 itself (Walsh *et al.*, 2015). Polyubiquitination enables NEMO and TRAF6 to associate with transforming-growth–factor-β-activated kinase 1 (TAK1) and TAK1-binding protein 2 (TAB2). TAK1 is subsequently polyubiquitinated at Lys-63 and this activates the kinase function of the TAK1, initiating two distinct signalling pathways (Wang *et al.*, 2001). In the first pathway, TAK1 phosphorylates IκB kinase β (IKKβ) of IKK complex and increases its enzymatic activity. The IKKβ then phosphorylates a natural inhibitor for NF-κB, IκB. The phosphorylation of IκB acts as a signal for its polyubiqutination and subsequent degradation by the proteasome (Deng *et al.*, 2000; Chen, 2005). The dissociation of IκB from NF-κB leads to NF-κB's translocation to the nucleus and binding to DNA binding sites for NF-κB. NF-κB activation results in the increased expression of pro-inflammatory molecules, including tumour necrosis factor-α (TNF-α), interleukin-6 (IL-6), tumour necrosis factor receptor 1 (TNFR1) and TNFR 2, and adhesion molecules.

The second pathway is mediated by TAK1. TAK1 phosphorylates mitogen-activated protein kinases (MAPKs), including JNK and p38. This phosphorylation ultimately leads to the activation of transcription factor, activated protein-1 (AP-1). This pathway can contributes to both pre- and post-transcriptional regulation of pro-inflammatory mediator release (Kawai and Akira, 2006).

Finally TRAF6 has also been shown to directly activate interleukin regulatory factor 5 (IRF5) and IRF7 by polyuibiutination. This results in the late phase production of TNF-α and production of interferon-α (IFN-α) respectively (Walsh *et al.*, 2015).

TRIF dependent pathway

The second branch of the TLR4 inflammatory signalling occurs via TRIF. This pathway is known to facilitate the later phase activation of NF-κB and has been recognised to contribute to the production of type 1 IFNs. Mice deficient in TRIF have been shown to have a normal early phase activation of NF-κB via the MyD88 dependent pathway, whereas they have an impaired activation of IRF3 and IFN production (Yamamoto *et al.*, 2003a). TRIF is a 712 amino acid protein containing a TIR domain in the central region and recruits receptor interacting protein (RIP) homotypic interaction motif (RHIM) in the C-terminus (Jenkins and Mansell, 2010). TRIF dependent pathways can be initiated from the endosomal membrane and/or the plasma membrane. The TIR-containing adaptor protein, TIR related adaptor molecule (TRAM), has an analogous role to Mal in the TRIF dependent pathway acting as a bridge between TLR4 and TRIF (Yamamoto *et al.*, 2003b). The chemical modification of TRAM is speculated to be crucial in regulating TRIF pathway from differing cellular localisations. In contrast to Mal, TRAM does not contain a PtdLns(4,5)P$_2$ binding domain and therefore does not contribute to its association with the plasma membrane. Mytristoylation of TRAM does enable the TRAM to localise to the plasma membrane and interact with the TLR4 homodimer (Rowe *et al.*, 2006). The second study has also demonstrated that the phosphorylation of TRAM is required for its adaptor function (McGettrick *et al.*, 2006). Once recruited, TRAM mediates trafficking of TLR4 into endosome. Once at the endosomal membrane, TLR4 recruits TRIF (Kagan *et al.*, 2008). Activated TRIF then interacts with TRAF3 and other adaptor molecules. This molecular association leads to auto-ubiquitination of TRAF3 and activation of TANK-1 binding kinase 1 (TBK-1). Finally TBK-1, in conjunction with IKKε, leads to the phosphorylation of IRF3 to induce the type 1 IFNs (Häcker *et al.*, 2011). However TRIF may also contributed to the NF-κB activation and has also been suggested to directly activate TRAF6, leading to the ubiquitination of NF-κB, IRF5 and IRF7 (Sato *et al.*, 2003). Furthermore TRIF is also been shown to activate RIP1 via its C-terminus RHIM domain with the subsequent recruitment of NEMO, resulting in the activation NF-κB (Jenkins and Mansell, 2010).

The TLR4 signalling culminates in the activation of at least 5 transcription factors. These factors upregulate the transcription of genes encoding inflammatory mediators, receptors and cell adhesion molecules. Among these factors, NF-κB is considered to be the most important in inflammation.
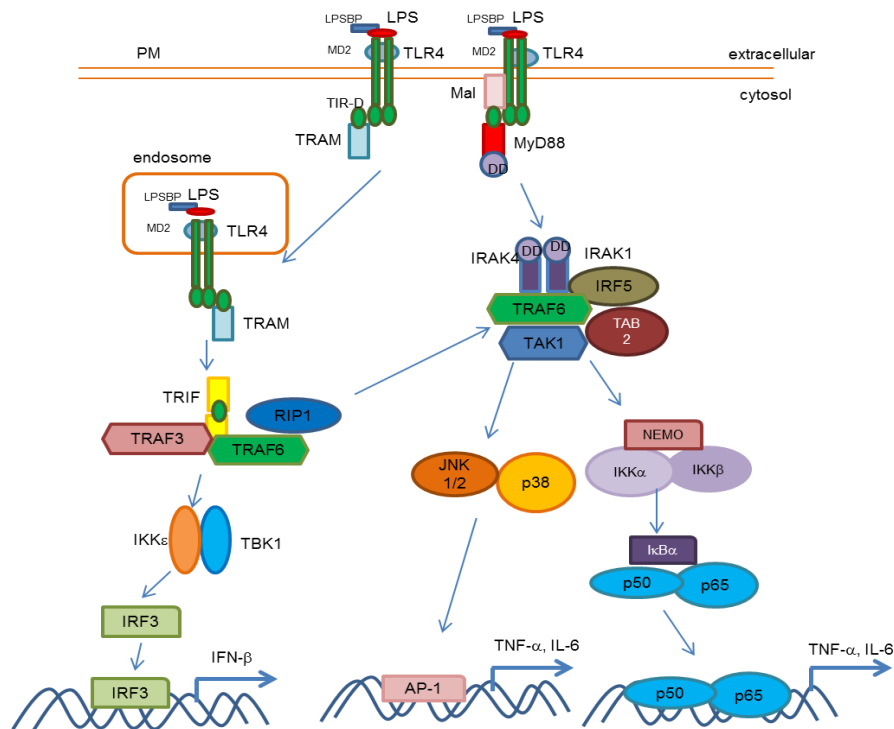
Figure 1-1 TLR4 signalling pathways

LPS binds to TLR4 in conjunction with LPS binding protein (LBP) and myeloid differentiation factor (MD2) and results in the homodimer formation. Activated TLR4 homodimers recruit toll/interleuckin-1 receptor homology domain (TIR) containing adaptor proteins resulting in MyD88 or TRIF dependent signalling pathways. In MyD88 dependent pathway, MyD88 binds to TLR4 homodimers via Mal. Subsequently MyD88 interacts with IL-R associated kinase-4 (IRAK-4) and IRAK-1 via death domain (DD). IRAK-1 and IRAK-4 complex activates TNF-receptor associated factor 6 (TRAF6) and TRAF activates transforming growth factor β activated kinase 1 (TAK1) and TAB2 resulting in activation of NF-κB dimers, p50 and p60 and/or activation of AP-1 via JNK1/2 and p38 MAP kinases. TRIF dependent pathway: LPS bound TLR4 homodimers binds to TIR related adaptor molecule (TRAM) and TRAM facilitate endocytosis of TLR4 complex where the receptor complex activate TRIF. TRIF causes to the activation of TRAF3 and TRAF6 and subsequently TAK-1 binding kinase 1 (TBK-1), which activates IKKε leading to activation of IRF3. TRIF also activate AP-1 and NF-κB via RIP1, which activates TRAK-TAK1 complex. Adapted from O'Neil, L. and Browie, A. (2007) Nature Reviews Immunology, 7 (5) 353-364.

1.2.3   NF-κB

The NF-κB family of transcription factors consist of five members, p65 also called RelA, c-Rel, RelB, p50 (p100 full length precursor) and p52 (p105 full length precursor). These members can form hetero- and homo-dimers resulting in at least 12 different combinations of transcription factors. All five members of NF-κB possess a rel homology domain (RHD) at their N-terminus which facilitates protein dimerization and sequence specific DNA binding (Vallabhapurapu and Karin, 2009). The structure of the RHD has been revealed by X-ray crystallization studies and is composed of two immunoglobulin-like folds, one which facilitates dimerization and the other which mediates DNA recognition. p65, c-Rel and RelB have a transcription activation domain (TAD), which is essential in initiating NF-κB target gene expression, while p50 and p52 lack the TAD domain and require dimerization with other members of the family to initiate protein transcriptions. Alternatively the dimerization of these members can results in blocking of NF-κB transcription sites (Napetschnig and Wu, 2013). The combinations of transcriptionally active NF-κB dimers are suggested to be specific to tissue types and lead to differing upstream signalling pathway and cellular responses. In general, the NF-κB heterodimer composed of p65/p50 is most frequently activated via TLR4 signalling. This p65/p50 dimer is often referred as 'classical NF-κB' and results in the production of pro-inflammatory cytokines.

Under normal conditions, NF-κB dimers are sequestered in the cytoplasm by a family of IκB proteins containing multiple ankyrin repeats which bind to partially mask the nuclear localisation signals (NLS) present in NF-κB dimers. The classical examples are IκBα, IκBβ, and IκBε. Recently it has been shown that some NF-κB proteins, p100 and p105 have ankyrin repeats in C-terminal, which also have IκB like activity. Each IκB member selectively binds to particular sets of NF-κB dimers which have different kinetics for the activation of NF-κB. As described in 1.2.2, TLR4 signalling causes phosphorylation and ubiquitination on IκB resulting in its proteasomal degradation. IκB dissociation from the dimer unmasks the NLS of p65 and causes the nuclear translocation of the NF-κB dimer.

Both MyD88 and TRIF dependent pathway activates NF-κB, however, it was suggested that these pathways regulates different temporal phases of NF-κB

activation (Kawai and Akira, 2006). MyD88 deficient cells have been reported to have impaired NF-κB activation at early time points (2-3 hours) but show a normal peak of the NF-κB transcriptional activation at later time point. However the deletion of MyD88 and TRIF resulted in the essential loss of NF-κB activity. Together these results suggest that while MyD88 pathway is required for an efficient NF-κB activation, TRIF dependent pathway can contribute to the NF-κB when MyD88 is not activated (Yamamoto *et al.*, 2003a). Finally NF-κB leads to the expression of IκB subunit, thus the activation negative regulatory thus establishing a negative feedback loop.

At the cellular level, the activation of the classical NF-κB dimer increases the transcription of genes encoding numerous pro-inflammatory molecules and results in strong inflammatory responses. The expression of proteins induced by NF-κB include cytokines TNF-α, IL-6, IL-1β; growth factors, granulocyte-macrophage colony stimulating factor (GM-CSF); chemokines, IL-8, RANTES, macrophage inflammatory protein-1α; monocyte chemotactic protein-1; and enzymes inducible nitric oxide synthase, phospholipase 2 and cyclooxygenase-2 (COX-2) and adhesion molecules, vascular cell adhesion molecule-1 (VCAM-1), intracellular adhesion molecule-1 (ICAM-1) and E-selectin (Bonizzi and Karin, 2004).

Taken together, we can see the activation of PPRs leads to robust proinflammatory responses via NF-κB activation. While this response has now been characterised in many different cell types, the leukocytes represent the cells most identified with these receptors and pathways in acute inflammation.

1.3   Cells in innate immune system

Leukocytes represent the most important cells in the innate immune system. These cells can be divided into two types, polymorphonuclear cells (PMNs) or mononuclear cells (MNs). These cells can be further subdivided and have clear roles in the development, maintenance and resolution of inflammation. In general, inflammatory response is initiated by tissue resident macrophages or mast cells. This activation results in the migration of PMNs into the site of inflammation, usually neutrophils, followed by the migration of the monocytes/macrophages to the site of inflammation.

It is the macrophage (along the dendritic cells) which represents the conduit between the innate and adaptive immunity, and/or the inflammatory lesion resolution or progression. Due to this, the macrophage has both a large array of PPRs and the ability to produce a diverse range of biological mediators, the production of which is dependent on the extracellular environment the macrophage encounters.

1.4   Macrophages

A wide range of PRRs, including TLR4, and their associated signalling components are found in macrophages (Mukhopadhyay *et al.*, 2009). They are involved in almost all steps of acute inflammatory responses and considered as a major component of innate immune system. In general, macrophages are divided into tissue resident macrophages and inflammatory/migratory macrophages (although in inflammation, the majority of macrophages at sites of inflammation are derive from migratory monocytes). However, macrophages are highly heterogenetic in nature and shows distinct anatomical and biological features depending on the tissue they are located in. For instance, alveolar macrophages (lung), Kupffer cells (liver), Langham cells (skin), peritoneal macrophages (gut) and osteoclast (bones), all have distinct biology and functions. As well as functional and morphological heterogeneity at the tissue level, macrophages from the same tissue also show heterogeneity. For instance, microglia shows diverse morphology depending on the location in the brain and distinct macrophages populations are found within the spleen (Perdiguero and Geissmann, 2016).

Attempts have been made to discover the origin of macrophage, and to classify its diverse populations. The precursor of tissue macrophage populations originates from bone marrow, postnatal spleen, embryonic yok sac (initial source of microglia in mice during development) or foetal liver in the embryo (Davies *et al.*, 2013). During the inflammatory response, bone-marrow derived monocytes in the circulation migrate into the site of inflammation and differentiate into the macrophages. Differentiation of monocytes into macrophages provides important control points of macrophage physiology and differing colony stimulating factors (CSFs) regulate this process depending on the macrophage population. For example, the presence of colony stimulated factor-1 (CSF-1), a ligand for colony stimulated factor-1 receptor (CSF-1R), IL-34, GM-CSF and the expression of CSF-1R are required for the maintenance of tissue resident macrophage populations

(Gordon *et al.*, 2014). CSF-1 is considered to regulate peritoneal macrophages and Kupffer cells differentiation, IL-34 is thought to be required for microglia and Langerhans cells differentiation and GM-CSF for alveolar macrophages differentiation. The differentiation of circulating blood monocytes to macrophages involves the GM-CSF and CSF-1 (Mosser and Edwards, 2008). The identification of the origin of macrophages may provide a clue to inhibit the pathogenic functions of macrophages and CSFs currently represent important targets for controlling macrophage actions in diseases (Lenzo *et al.*, 2012).

During acute inflammatory responses tissue resident macrophages along with mast cells are thought to be the first cells to recognise the inflammatory stimuli via PRRs and as a result the activated macrophages secret a wide range of inflammatory mediators, such as cytokines, chemokines, amines, fatty acid metabolites and complement components. These molecules act on the vascular endothelial cells and increasing its permeability and thus leading to formation of inflammatory oedema. Neutrophils are usually the first cell to migrate to the site of inflammation and there they secret toxic granules containing proteases and release reactive oxygen species (ROS), which attempt to destroy the invading pathogens. Subsequently macrophages are recruited which can phagocytose pathogens, dead cells and/or tissue debris. Due to the different mechanisms of macrophage activation, researchers have attempted to classify macrophages by their activation states. For example a early simple form of classification considered macrophages to be either classically activated (M1) and considered to be proinflammatory macrophages, while alternatively activate macrophages (M2) are associated with the hormonal immunity and wound healing(Mills *et al.*, 2000; Tzachanis *et al.*, 2002; Gordon and Martinez, 2010). These early classification criteria have been developed over past 15 years. While this classification may be useful to obtain detailed information on their response and cell surface molecule expression patterns under extreme conditions *in vitro* and *in vivo*, any group classification criteria may lead to simplistic explanations for macrophages function in the complex tissue environments encountered in pathology (Gordon *et al.*, 2014). Indeed, even within macrophage cell lines, a significant degree of heterogeneity is observed, which is not due to the genetic instability found in some cell lines (Ravasi *et al.*, 2002). Indeed the contribution of macrophage heterogeneity to normal physiological and pathological responses is relatively under-researched area.

In addition to macrophage heterogeneity, another hallmark of macrophage biology is cell plasticity. This is the ability of macrophages to change their array of mediators released in response to extracellular ques. An example of this is the effect of phagocytosis on macrophage function. Originally macrophages were distinguished for their remarkable ability to phagocytose material (Metschnikoff, 1884; Flannagan *et al.*, 2012). Phagocytosis is important during the pro-inflammatory phase of the inflammation, as well as during inflammation resolution, however the molecules release in each of these cases is reported to be pro- or anti-inflammatory in nature respectively. Phagocytosis of invading pathogen or necrotic materials could lead to the release of proinflammatory mediators. In contrast, phagocytosis of apoptotic materials could cause the release of anti-inflammatory materials (Flannagan *et al.*, 2012). However it is important to note that most of these studies are conducted with the purified stimuli, and may not represent the complex tissue environment found in inflammatory lesions. An important question to address is how do macrophages continually regulate the release inflammatory mediators to finesse the body's response to particular noxious stimuli? In macrophages, this exquisite control of mediator release is mediated by the diversity of the PRR expression and intracellular mechanism to finely regulate cytokine release from activated macrophages.

Besides the macrophages role in inflammation the macrophage also play a part in numerous physiological processes. Research has demonstrated their involvement in the development, maintenance of tissue homeostasis, tissue repair and metabolism of nutrients. The role of the macrophage development is seen by the lethal phenotype observed when macrophages population is inhibited in mice (Wynn *et al.*, 2013).

1.4.1   Macrophages production of cytokines

Of central importance to the role of macrophages in inflammation is the production of cytokines. Depending on the definition, to date approximately 130 cytokines have been descried. These cytokines include ILs, CSFs, IFNs, TNF superfamily, chemokines, CCL1-28, CXCL1-17 and CX_3CL-1 and growth factors. These proteins are released from macrophages in response to a diverse range of inflammatory stimuli, which are recognised by various receptors on macrophages, such as PRRs. Along with IL-1β the most important cytokines described are TNF-α and IL-6. These

inflammatory mediators play vital roles in control of innate immune responses and inhibition of these mediators leads to the increased susceptibility to tuberculosis and opportunistic infections. At the same time, these mediators are found upregulated in many inflammatory pathologies including arthritis, atherosclerosis, asthma, neurodegenerative diseases, diabetes, fibrosis and cancer. These mediators represent important therapeutic targets and the understanding of mechanisms by which these mediators are released from macrophages is important (Murray and Wynn, 2011; Arango Duque and Descoteaux, 2014). The classical stimulator for TNF-α and IL-6 production is LPS stimulation via TLR4. As discussed, LPS signalling result in the activation of NF-κB.

IL-6 is known as a pleiotropic cytokine with proinflammatory, anti-inflammatory and regenerative actions (Hunter and Jones, 2015). The cytokine induces the acute-phase inflammatory responses as well as the promotion of T cells subtypes and differentiation of B-cells (Klimpel, 1980; Yoshizaki *et al.*, 1984; Woloski and Fuller, 1985; Yasukawa *et al.*, 1987; Kopf *et al.*, 1994). IL-6 elicits its biological responses from the cell mainly via two different signalling pathways. Firstly, signalling through membrane bound IL-6 receptor α (IL-6Rα) and gp130 which is termed classical signalling, and signalling through the soluble form of receptor, IL-6Rα, in combination with membrane bound gp130 is termed trans-signalling, Figure 1-2. IL-6Rα is secreted from leukocytes and the elevated level of IL-6Rα is associated with chronic inflammatory conditions (Jones *et al.*, 2001). Secondly, signalling via IL-6Rα trans-signalling is known to exert proinflammatory action of IL-6 and associated with the pathologies of chronic inflammations including colitis, tissue fibrosis, inflammatory arthritis, allergy, neuroinflammation, cardiovascular diseases and cancers (Campbell *et al.*, 2014; Tanaka *et al.*, 2014). Trans-signalling has also been shown to be important in the recruitment and activation of leukocytes, the development and maintenance of T cell populations and their effector functions (Rose-John and Heinrich, 1994; Jones *et al.*, 2001). IL-6 signalling via membrane bound IL-6Rα is termed classical signalling, which controls an acute inflammatory reaction, apoptosis of immune cells and haematopoiesis (Kopf *et al.*, 1994; Hunter and Jones, 2015). Particularly in brain, the classical signalling is thought to mediate homeostatic processes including energy metabolisms, control of fever, fatigue and loss of appetite (Schöbitz *et al.*, 1995).
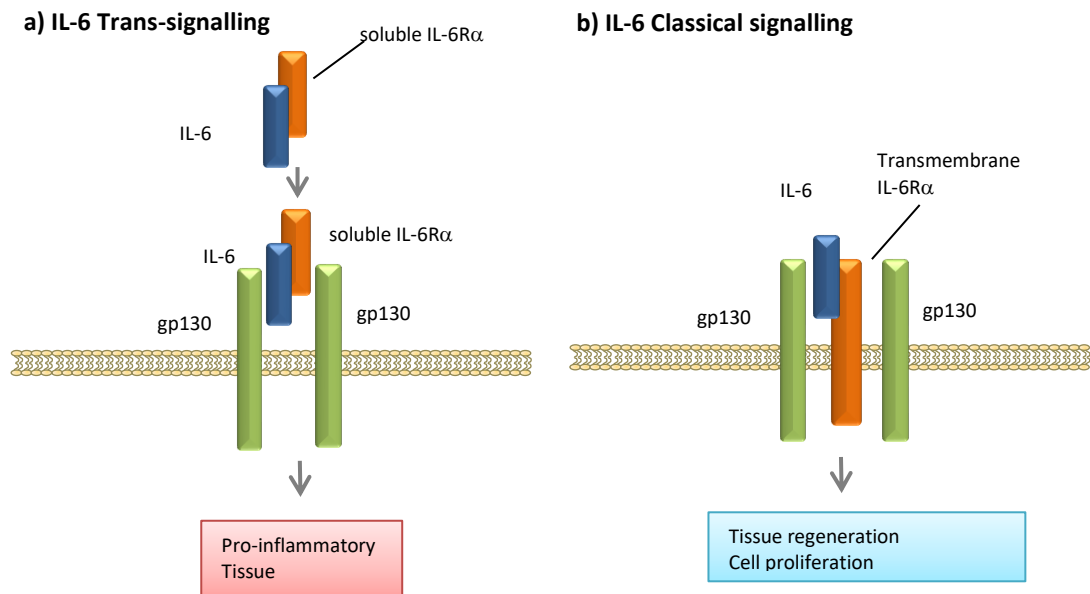
Figure 1-2 Classical and Trans-signalling of IL-6

Two mechanisms of IL-6 signalling. a) Trans-signalling; IL-6 binds to soluble IL-6Rα and the IL-6 and soluble IL-6Rα complex bind to transmembrane protein gp130 on the plasma membrane of cells leading to proinflammatory response. B) Classical signalling: IL-6 bind to plasma membrane bound IL-6Rα and gp130 leading to tissue regeneration/cell proliferation. Adapted from Wolf,J. *et al* (2014) Cytokine, 70:11-20.

TNF-α is a potent inflammatory mediator and considered to be the central to inflammatory responses. The cytokine is not only important in inflammation but also in many fields of biology including neurology, developmental biology and cancer (Aggarwal *et al.*, 2012). Production of this cytokine is regulated at multiple levels- including the transcription of the gene, mRNA stability, message translation, protein transport to the plasma membrane and the final release.

1.4.2   Control of TNF-α mRNA

Activation of TLR4 initiates the rapid transcription of TNF-α in macrophages. The mRNAs of many inflammatory proteins including TNF-α are unstable and represent a control mechanism. In these cases, it is suggested that the mRNA stability is as an important parameter in determining the total amount of cytokine expressed (Rabani *et al.*, 2011). It has been shown that the initial robust production of TNF-α from macrophages is due to the stabilisation of TNF-α mRNA with several mechanisms

being suggested to stabilize the TNF-α mRNA. TNF-α mRNA is also the subject of various post-transcriptional modifications, which include alternative splicing of mRNA, mRNA polyadenylation, and the regulation of initiation and termination of protein translation (Carpenter *et al.*, 2014).

The transcription of TNF-α mRNA during LPS stimulation is rapid and transient, with the transcript also being subject of degradation (Clark *et al.*, 2003). The rate of mRNA decay is very important in determining the extent of translation of TNF-α. The mRNA for TNF-α, is known to express conserved AU rich sequences in the 3' untranslated terminal region (UTR) of the gene and this region is termed AU rich element (ARE). ARE is found in mRNAs of many inflammatory proteins and has been demonstrate to have a key role in destabilizing mRNAs (Shaw and Kamen, 1986; Xu *et al.*, 1997). TNF-α is known to be highly sensitive to degradation and contains the shortest version of ARE, with a 34 nucleotide 6 times AUUUA motifs in the 3'UTRs. However the relation between the length of ARE regions and the cytokine's mRNA stability has yet to be fully characterised. Currently there are 20 ARE-binding proteins described and once bound to the AREs, these proteins stimulate the decay of mRNAs. Among these ARE-binding proteins, tristetraprolin (TTP) and AU-rich element RNA-binding protein (AUF1) have key roles in facilitating the degradation of TNF-α mRNA. Mice lacking TTP or AUF1 have been shown to have excessive inflammatory responses. In comparison, other ARE binding proteins act to stabilise mRNA by competing for binding regions with the "destablizing" ARE binding proteins without destabilizing effect. This in turn limits the effect of these destabilizing ARE-binding proteins. Examples of these "inhibitory" ARE binding proteins include, Y-box binding protein 1, embryonic lethal, abnormal vision (ELAV), Hu-antigen R (HUR) and ELAV-like protein 4 (HUD). The overall relationship between different ARE binding proteins regulates TNF-α mRNA stability. The activation of p38 MAPK downstream of TLR4 activation has been shown to stabilise the ARE containing mRNAs by altering the affinity of ARE binding proteins for the mRNA. For example the phosphorylation of TTP by p38 decreases its affinity to ARE and sequesters the TTP for the degradation (Stoecklin *et al.*, 2004). This favours the binding of HUR to ARE thus stabilising TNF-α mRNA and in turn upregulate its translation (Tiedje *et al.*, 2012). Proteins whose mRNAs are stabilised by p38 include TNF-α, IL-8, IL-1β, COX-2 and GM-CSF (Clark *et al.*, 2003). However it must be noted that HURs are also involved in stabilization of mRNAs of

anti-inflammatory proteins. Therefore the role for HUR in inflammatory conditions is yet to be fully elucidated.

Another element, constitutive decay element, expressed in TNF-α 3'UTR causes the decay of TNF-α mRNA independently of AREs (Stoecklin *et al.*, 2003). Additionally it has emerged that microRNAs (miRNAs) modulate mRNA decay in macrophages. miRNAs are non-coding RNAs which pair to complementary 3'UTR sequences of target mRNAs. This essentially forms a miRNA and mRNA complex causing the inhibition of the target mRNA via RNA induced silencing complex (RISC). The RISC inhibits mRNA translation and/or initiates the decay of target transcript. It has become evident that the miRNAs are important in the control of inflammatory responses in macrophages.

mRNAs which have an extended 3'UTR downstream of a stop codon are down-regulated by the regulator of nonsense transcripts (UPF) proteins, UPF1-3, in the process called nonsense mediated decay (NMD). In this process, phosphorylation of the UPF1 causes the endonucleotic cleavage of the transcript. In macrophages, inhibition of NMD by the deletion of UPF2 upregulates 186 different gene transcripts, suggesting a significant contribution of NMD in the control of mRNA stability (Weischenfeldt *et al.*, 2008).

1.4.3 Translational control of TNF-α

The translation initiation of existing mRNAs allows the rapid production of inflammatory mediators. This is particularly relevant to innate immune responses which involve fast onset responses. Eukaryotic translation initiation factor 2 (eIF2) is considered to be an important regulator in innate immunity. Eukaryotic translation initiation factor 2B (eIF2B) works via recycling between a GTP active complex and GDP in inactive complex of translation complex. Phosphorylation of eIF2 is known to inhibit its recycling and supresses the translation initiation of cellular mRNAs (Donnelly *et al.*, 2013). In addition, TLR4 or TLR3 activation causes the dephosphorylation of eIF2B via TRIF activation, resulting in frequent activation and translation of protein in comparison cell stressors such as ER stress which inhibits protein translation.

Another structural element which regulates translation is poly (A) tail in 3' end of mRNA. This provides a binding site for a poly (A) binding protein which interacts with various translation initiation factors and is required in translation. TNF-α mRNA is constitutively expressed in resting macrophages. However this constitutively expressed TNF-α mRNA lacks poly (A) tail and therefore cannot produce TNF-α. LPS activation causes the appearance of mRNA TNF-α with poly (A) tail which could enhance the production of TNF-α (Crawford *et al.*, 1997).

1.4.4 Regulation of TNF-α release and actions

Once translated, TNF-α protein starts to accumulate in Golgi complex as early as 20 minutes after cell activation (Shurety *et al.*, 2000) and is directed to the plasma membrane via trans-Golgi network (TGN)-derived vesicle. Once the vesicle is fused with the plasma membrane, TNF-α is expressed as a transmembrane protein trimer consisting of three 26 kDa (mTNF-α) monomers. The final control mechanism for the cytokine is the release from the plasma membrane via ecoto-domain shedding by metalloproteinases (Stow *et al.*, 2009). A disintegrin and metalloproteases protein 17 (ADAM17) or Tumour necrosis factor-α converting enzyme (TACE) is considered to be the main sheddase for TNF-α (Black *et al.*, 1997; Moss *et al.*, 1997). The actions of TNF-α a due to its binding to its receptors, TNFR1, (CD120a, p55) and TNFR2 (CD120b, p75), where it initiates a variety of intracellular cell signalling pathways and leads to the cellular responses (Sedger and McDermott, 2014). Figure 1-3 summarises these TNF-α signalling pathways.

Macrophages are a major source of TNF-α along with other cytokines and control mechanisms for the production and release of these cytokines release are significant in regulating inflammation. It is therefore not surprising that cell signalling mechanisms, which lead to this cytokine release, including TLR4 signalling and secretory pathways are extensively studied in macrophages (Stow *et al.*, 2009; Rutledge *et al.*, 2012). As discussed above, macrophages have a great capacity to sense their surrounding environment via PPRs, initiate cell signalling mechanisms and produce the relevant inflammatory mediators via precise regulation of transcription and post-transcriptional mechanisms. As both sensing its environment and regulation of protein release are regulated at the plasma membrane, it is

surprising that the class of protein intimately involved in membrane biology, namely ion channels, has only received limited attention in the study of macrophage biology. The aim of this thesis is to investigate ion channels in macrophages.
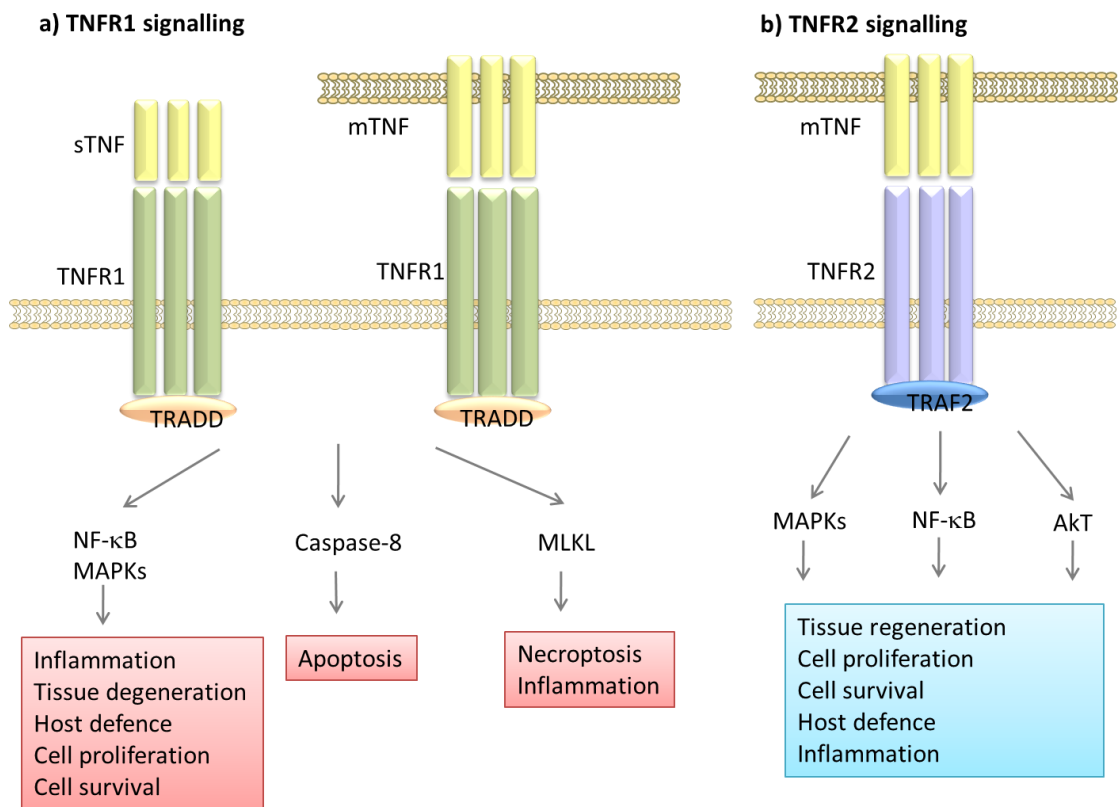
Figure 1-3 TNF-α signalling via TNFR1 or TNFR2

a) Soluble TNF-α (sTNF) and membrane bound TNF-α (mTNF) signal via TNF-α receptor 1 (TNFR1), which contains tumour necrosis factor receptor 1 associated death domain (TRADD) in cytoplasmic region. The ligation of sTNF/mTNF and initiates the activation of transcription of NF-κB, mitogen activated protein kinases (MAPKs), caspase-8 or mixed lineage kinase like protein (MLKL) leading to inflammation, tissue degeneration, apoptosis and/or necrosis. b) mTNF binds to TNFR2 with a higher affinity and via TNF-receptor associated factor 2 (TRAF2), this initiates the activation of MAPKs, NF-κB and protein kinase B (AkT) leading to tissue regeneration, cell survival/proliferation and/or inflammation. Adapted from Kalliolias,G. and Iashkiv, L., (2016) Nature Reviews Rheumatology, 12:4-62.

1.5   Ion channels in immune systems

1.5.1   Evolution of ion channels and function in immune cells

From evolutionary point of view, once the building blocks of life had occurred DNA, RNA and simple proteins, the next important step for life to occur was to bring these molecules close and keep them together, i.e. the packaging of the life chemicals. The answer to this was the evolution of lipid membranes. However the use of membranes to package the chemicals brought a new problem. This was essentially osmotic problems. Again the evolutionary answer to this osmotic problem was the arrival of the channels, which conduct ion species across the membranes. The use of "ion channels" by ancient cells together with protein pumps also allowed the generation of ion gradient, which contributed to the evolution of energy producing pathways such as proton gradient pathways. It is from these beginnings, the ion channel evolved and now play fundamental role in every cell of the body and virtually all physiological responses. Indeed, ion channels are still important in osmotic regulation, for example, the regulation of cell volume as well as in multicellular processes, such as cell signalling and nerve transmission. The activation of these ion channels allows passive movement of sets of ion species across the membranes and this selective movement of ions is essential in regulating cell volume, setting membrane potentials and facilitating cellular signalling processes.

In the cells of immune system, ion channels have also been shown to have important functions. These are not only on general cellular processes, e.g. regulation of cellular volume, but also on specific immune responses. For instance transient receptor potential melastin 2 (TRPM2) or transient receptor potential vaniloid 2 (TRPV2) knock-out mice showed susceptibility to infection with *L.mocytogenes* indicating the importance of these channels in anti-microbial responses. It has also been suggested that there is a link between a mutation in a gene encoding ORAI1, part of the calcium release activated channel (CRAC) and immunodeficiency and autoimmunity, therefore indicating the essential role for these channels in defence mechanisms (Feske, 2009). The role of these ion channels are also studied at the individual cell population level and with T-lymphocyte populations probably the most well studied example. A variety of ion channels are found in T-lymphocytes; CRACs; members of transient receptor potential cation channel subfamily, TRPM2, TRPM4 and TRPM7; voltage gated calcium channels; non-selective cation channel; P_2PX_7; Zinc channels, ZIP3, ZIP6 and ZIP8; potassium

channels, $K_{V1.3}$, $K_{Ca3.1}$, $K_{2P3.1}$; sodium channels; Chloride channels; $GABA_A$ and cystric fibrosis transmembrane conductance regulator. These channels have been reported to be involved in cell proliferation, cell survival and chemotaxis (Launay *et al.*, 2004; Srivastava *et al.*, 2008; Cahalan and Chandy, 2009).

1.5.2 Macrophages and ion channels

Macrophages have been found to express a wide array of ion channels. These include $K_{V1.3}$, $K_{V1.5}$, BK; inward rectifier potassium channels ($K_{ir2.1}$); CRAC channels; voltage-gated proton (H_V) channels; P_2X_7; and TRP channels, TRPC1, TRPC3, TRPC6, TPRM2 and TRPV2 (Gallin, 1984, 1991; Gallin and Sheehy, 1985; DeCoursey and Cherny, 1996; DeCoursey *et al.*, 1996; Berthier *et al.*, 2004; Liu *et al.*, 2007; Nagasawa *et al.*, 2007; Yamamoto *et al.*, 2008; Schilling and Eder, 2009; Finney-Hayward *et al.*, 2010; Gao *et al.*, 2010; Di *et al.*, 2011; Santoni *et al.*, 2013; Stebbing *et al.*, 2015). The role of these ion channels in macrophages is not completely understood and in many instances only investigated in resting macrophages. Several studies have indicated the involvement of proton channels in the NADPH oxidase activity and TRPV2 channels in the macrophage migration. However in comparison to that of the T-lymphocytes or to excitable cells, relatively little research has focused on the role of these ion channels in activated macrophages, Table 1-2.

Ion channels	Macrophage cell type	Reference
$K_{V1.3}$	Human alveolar macrophages	Mackenzie *et al.*, 2003
$K_{Ca1.1}$	PMA differentiated THP-1, Microglia	DeCoursey *et al.*, 1996
$K_{ir2.1}$	PMA differentiated THP-1, J774.1	Gallin., 1985 DeCoursey *et al.*, 1996,
$K_{Ca3.1}$	Microglia, Human PBMCs	DeCoursey and Cherny, 1996 Stebbing *et al.*, 2015
CRAC	Human PBMCs	Gao.*et.al,* 2010
H_V	THP-1,Microglia	Eder and DeCoursey. 2011 Stebbing *et al.*, 2015
P_2X_7	Mouse BMDMs, Microglia	Guerra *et al.*,2003 Cavaliere *et al.*, 2005
TRPC1	7-ketocholesterol stimulated THP-1	Berthier *et al.*, 2004
TRPC3	Rat monocytes	Liu *et al.*, 2007
TRPC6	Human alveolar macrophages	Finney-Hayward *et al.*, 2010
TPRM2	Mouse PBMCs	Di et al., 2011 Yamamoto *et al.*, 2008
TRPV2	Human PBMCs	Santoni *et al.*, 2013

Table 1-2 Ion channel expression in monocytes and macrophages

Reported expression of ion channels in monocytes and macrophages. BMDM: bone marrow derived macrophages, CRAC: Ca^{2+} release-activated channels, $K_{Ca1.1}$: large conductance voltage-and calcium- activated potassium channel (BK channel), K_V: voltage gated potassium channels, $K_{Ca3.1}$: small conductance Ca^{2+}/calmodulin-activated K^+ channel, H_V: voltage-gated proton channel, PBMC: Peripheral blood mononuclear cells, PMA: Phorbol 12-myristate 13-acetate, TRPC: transient receptor potential canonical, TRPM: transient receptor potential melastatin, TRPV: transient receptor potential vanilloid.

1.6   BK channels

As stated above, macrophages express a diverse array of ion channels. One of these channels is the BK channel. The BK channel are characterised by its large conductance and also noted for the diverse range of endogenous modulators which can regulate its opening. These two characteristics suggest that the channel may be involved in multiple cellular functions which allow the integration of extracellular signals into intracellular cell signalling pathways. As macrophages are known to respond to numerous extracellular stimuli, it was speculated that the BK channel could be involved in regulating macrophage functions.

1.6.1   Physiological roles for BK channels

The BK channel, also known as large conductance calcium- and voltage-potassium channel, Maxi-K, Slo-1 or $KCa_{1.1}$, is highly selective to K^+ ions. The channel is characterised by high K^+ selectivity, large conductance (250 pS in symmetrical K^+ concentrations) and its allosteric opening mechanisms by a rise in intercellular Ca^{2+} concentration and membrane depolarization (Cui et al., 2009). The large conductance for K^+ and the unique allosteric opening mechanisms enable BK channel to integrate changes in Ca^{2+} with differing membrane potentials (Hoshi *et al.*, 2013). The opening and closing of the BK channels contribute to fast after-hyperpolarization, regulation of action potential frequency, neurotransmitter release in some neurons (Contreras et al., 2013).

BK channels are ubiquitously expressed. In particular, the function of BK channels in excitable tissues, such as in neurons and smooth muscle cells have been well characterised. For example, BK channels in smooth muscle cells contribute to muscle relaxation and are thought to provide protection from vascular hypertension. It has also been proposed that BK channels have roles in the regulation of circadian rhythm, inducing ethanol tolerance and the generations of nociception, although these channel functions may be location dependant (Contreras *et al.*, 2013; Whitt *et al.*, 2016).   In humans, the dysfunction of BK channels is linked to a number of pathologies including epilepsy, dyskinesia, seizure, incontinence, asthma, hypertension, alcoholism and cancer. Therefore pharmacological modulation of this channel is of clinical interest (Ghatta *et al.*, 2006; Bentzen *et al.*, 2014)

1.6.2   Channel structure and gating mechanisms of BK channels

1.6.2.1   Crystal structure and function

The structure of BK channels has been determined by studies using x-ray crystallography (Wu *et al.*, 2010; Yuan *et al.*, 2010). These studies have revealed the 3D structure of the core part of the human BK channel at a resolution below 10 Å. This core part of the protein contains the gating ring and cytoplasmic Ca^{2+} binding sites. The crystallography was made in absence of Ca^{2+} binding to the channel protein. Thus it is assumed that the described structure represents the closed channel (Yuan *et al.*, 2010).

The core forming part of the channel is composed of four identical α subunits (BKα, Slo-1). The BKα subunit contains approximately 1100 amino acids and is encoded by one gene, *KCNMA1* or alternatively named *SLO-1*. The BKα tetramer can form the functional part of a BK channel but native channels are likely to be associated with auxiliary β and/or γ subunits. The crystal structure defined on the plasma membrane each BKα is formed by seven, S0-S6, transmembrane helices with the extracellular N-terminus, intercellular C-terminus domain with the S5-S6 region forming the selectivity filter of the pore (Wu *et al.*, 2010). Positively charged S2, S3 and S4 together with S1 and S0 serving as the voltage sensor domain. S0 segment has also been shown to contribute to the stabilization of auxiliary subunits expressions, β1-4- and γ1-4-subunits with the BKα protein. The transmembrane region and N-terminus accounts for one third of the amino acid residues of the BKα protein with the remaining part consisting of the cytoplasmic domains. This relatively large cytoplasmic domain contains binding regions for Ca^{2+}, Mg^{2+} and various endogenous signalling molecules (Cui *et al.*, 2009; Contreras *et al.*, 2013; Hoshi *et al.*, 2013).

The crystallography studies showed that four BKα subunits assemble as a gating ring of total eight regulator of conductance of potassium 1 (RCK1) and RCK2 domains (Yuan *et al.*, 2010a). The gating ring of the BK channel has been shown to have a relatively large central hole around 20 Å, which permit ions to move between pore regions into intracellular parts. These RCK1 and 2 have hydrophobic interactions involving residues on α-helices and this hydrophobic interactions

appeared to be conserved among RCK domains. Near to the end of RCK2 domain, there is a high affinity Ca^{2+} binding site. This structure is known as Ca^{2+} bowl, connected by short α helix. The study also showed that the gating ring of the channel is linked to the S5-S6 linker pore-forming region by a strand-like structure which appeared to be free from any non-covalent interaction from other protein residues. This may allow the effective coupling of pore region to gating ring (Yuan *et al.*, 2010).

1.6.2.2   The gating mechanism of BK channels

The precise mechanism by which the voltage sensor and the Ca^{2+} region integrate to cause the opening of the BK channel is still to be elucidated. However, studies suggest that membrane depolarization pushes the positively charged S4 segment toward the extracellular side and this movement rearranges other segments in the voltage sensor region of BKα (S0-S3), which leading to opening of the pore via S6-regulator of potassium conductance (RCK) linker region. For the Ca^{2+} mediated opening, Ca^{2+} binding to the channel causes the release of free energy. It is proposed that this energy is transduced into mechanical force and opens the channel pore. Both the binding of Ca^{2+} and voltage sensor activation increase the probability of the channel opening and these two factors can have synergistic influences on each other's activity. At molecular level, the activation of the voltage sensor domain has been shown to increase the affinity of the channel to Ca^{2+} and the binding of Ca^{2+} enhances the voltage sensor activation. Therefore the activation of both factors is normally required to achieve the maximum probability that the ion conduction gate is open (Open probability: Po) (Cui *et al.*, 2009). This mechanism is in contrast to other K^+ channels including voltage gated K^+ channels and other calcium-activated K^+ channels. In K_v, the activation always causes the opening of the channel due to 4-8 times bigger electric charge on the voltage sensor region than that of BK channels which couples the voltage sensing and pore region tightly. In small and/or intermediate conductance calcium activated K^+ channels, the binding of Ca^{2+} activates the channels. However under certain conditions, the requirement for BK channels to open in the presence of high Ca^{2+} and increased voltage may become redundant. It has been reported that BK channels can open at high membrane voltage without a rise in Ca^{2+}. In addition high intracellular Ca^{2+} has been shown to open the channels at negative voltage (Hoshi *et al.,* 2013). The BKα tetramer can be co-assembled with various combinations of auxiliary subunits, β1-4

and/or γ1-4 in a tissue specific manner, and the assembly with these subunits has an impact on the gating properties of the channel (Kyle and Braun, 2014). The sensitivity of BK channels to the membrane voltage and Ca^{2+} is subject to the expression of these auxiliary subunits. While another divalent ion, Mg^{2+}, is not an activator of the BK channel but has also been reported to enhance the coupling strength between the ion conduction gate and voltage sensor domain at mM concentrations (Cui *et al.*, 2009).

Another mechanism by which BK channel open probability can be changed is via alternative splicing of the BKα gene. As previously stated BKα is encoded by one gene*, KCNMA1*. In the case of BKα it is theoretically possible that the alternative splicing can give rise to variety of polypeptides and some of these variants have been reported to show altered Ca^{2+} sensitivity, channel kinetics, localization and sensitivity to endogenous molecules. However, only several variants are fully characterised to date. Finally post-translational modifications, such as phosphorylation and palmitoylation of BKα proteins can also lead to alterations in BK channel activity and localizations depending on which amino acid residue is modified (Srivastava *et al.*, 2008, Jeffries *et al.*, 2010).
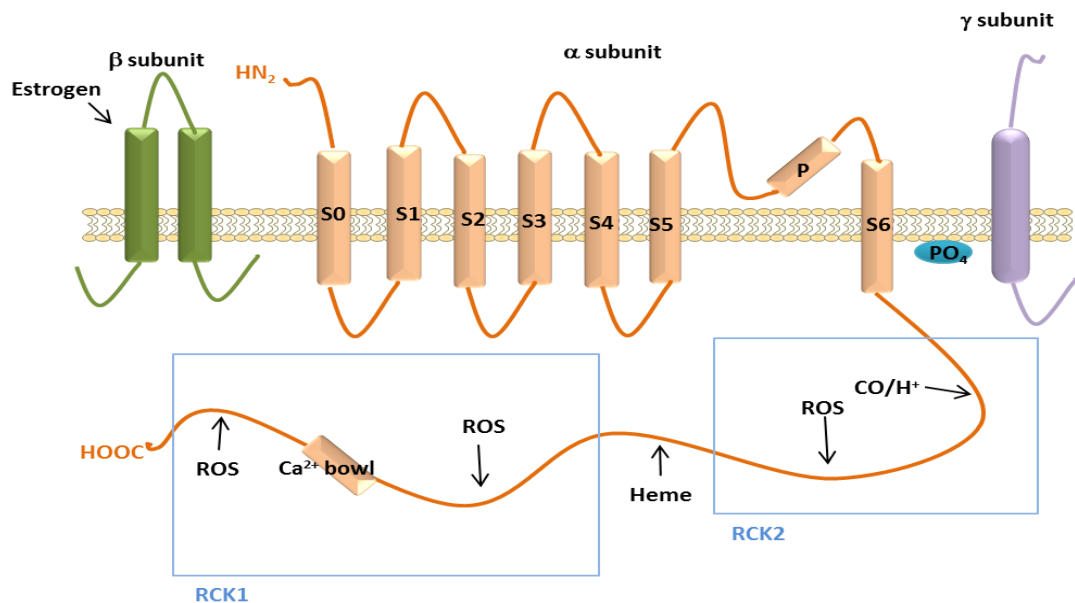
Figure 1-4 BK channel structure and binding sites for endogenous signalling molecules.

BK channel core α subunit is composed of 7 transmembrane (TM) segments, S0-S6, connected through intra- and extracellular loops with the N-terminus facing the extracellular side and C-terminus facing the intracellular side. S1-S4 confers voltage sensing and the C-terminus contains binding sites for Ca^{2+}, Mg^{2+} and the other endogenous molecules, and K^+ ion conducting ring, regulator for conductance of K^+ (RCK) regions. ROS: reactive oxygen species. Adapted from Hou,S. *et al* (2009) Physiology 24(1) :26-35.

1.6.3   BK channel auxiliary subunits

BKα tetramer can form a functional BK channel; however whether the expression of BK channels formed of only a BKα tetramer is present under physiological condition or not is not known. It has been known that BKα tetramer can interact with several auxiliary subunits, β1-4 and/or γ1-3 (Contreras *et al.*, 2012; Zhang and Yan, 2014). It is believed that each BKα monomer can bind one β subunit, therefore the relationship 4 x (1 α subunit to 1 auxiliary β subunit). As previously mentioned the presence of different auxiliary subunits changes the properties of BK channels (Hoshi *et al.*, 2013). It is therefore not surprising that different subunits are found in differing tissues and results in wide range of the biophysical and pharmacological properties of channels. This may equip the channel to facilitate more diverse physiological processes (Orio *et al.*, 2002).

To date the majority of research has focused on the expression and function of the β subunits. The expression of β subunit is known to be tissue specific and was first observed in bovine tracheal smooth muscles. This was later categorized as the $\beta1$ subunit (Knaus *et al.,* 1994a; Orio *et al.,* 2002). To date, four variations of β subunits, $\beta1$, $\beta2$, $\beta3$ and $\beta4$, have been cloned from mammalian tissues (Wallner *et al.*, 1999; Behrens *et al.*, 2000; Brenner *et al.*, 2000). Each β subunit is composed of 2 transmembrane domains, connected by a loop on the extracellular side of the membrane. The expression of these subunit changes the gating properties of the channel. $\beta1$ and $\beta2$ have been shown to increase the sensitivity of the BK channel to Ca^{2+} and voltage, and slows the opening and closing kinetics of the channel. $\beta3$ subunit is known to speed up the deactivation of the channel. The $\beta4$ expression has only been found in the brain tissue (Orio *et al.*, 2002; Contreras *et al.*, 2012, 2013). The BK channels with $\beta4$ subunits has been reported to shows the slower opening and closing kinetics to a greater degree than $\beta1$ and $\beta2$ subunits. In addition the presence of $\beta4$ confers the resistance to the channel blocking peptides, charybdotoxin and iberiotoxin (IbTX) (Meera *et al.*, 2000).

Recently, a second class of BK channels auxiliary subunits have been discovered, which are designated as γ subunits. Four γ subunits have been identified and each subunit has approximate molecular weight of 35 kDa and are single transmembrane proteins. Intriguingly the γ subunits also contain LRRs, which has previously described as the hallmark of PRRs, at their N-terminus (Yan and Aldrich, 2012). The first characterised γ subunit was $\gamma1$, LRRC26. This subunit was discovered in a prostate cancer cell line, LNCaP to shift the half maximal activation voltage of BK channel by approximately -140 mV, allowing channel in absence of intracellular Ca^{2+} (Yan and Aldrich, 2010). It has been suggested that this change in gating properties could allow channels to operate in non-excitable tissues. The other three γ subunits, $\gamma2$ (LRRC52), $\gamma3$ (LRRC55) and $\gamma4$ (LRRC38) respectively, are also known to shift the channel activation voltage toward negative, although to less extent than the $\gamma1$ subunit.

1.6.4 BK channel pharmacology

A wide range of endogenous, natural or synthetic compounds have been identified and/or developed to modulate the activity of BK channels. These compounds interact with BK channels and alter the activation state of the channel in various ways. The inhibitors for the channel have provided useful tools to investigate the functional roles, structure and electrophysiological properties of the channel (Yu *et al.*, 2016). Also much attention has been focused to study the therapeutic potential of the BK modulators (Bentzen *et al.*, 2014). Importantly the BK channel can be regulated by a number of endogenous signalling molecules (Hou *et al.*, 2009). These molecules can be produced by immune cell, which may suggest a link between the inflammatory response and the BK channels.

1.6.4.1 BK channel blockers

BK channels are highly selective for K^+ ions and the application of several cations have been shown to block K^+ conductance by interacting with the conduction gate of BK channels (Carvacho *et al.*, 2008). These cations are H^+, Na^+, Cs^+ and Ba^{2+}, and bind to the gates internally or externally with distinct affinity for each site. The blockade by these cations tends to be affected by membrane voltage, which affects the movement of K^+ ions via the channel. These studies have been used to investigate the nature of pore region and selectivity filter of the channel. For instance, Cs^+ entres the conduction gate regions to cause blockade of BK channels. This blockade has been suggested to be relieved by the large influx of K^+ ions probably due to the higher affinity of the K^+ ion for Cs^+ to the conduction gate (Cecchi *et al.*, 1987). Ba^{2+} blocks BK channels from both external and internal sides but exhibits 1000 fold difference in affinity between the two sides (Vergara *et al.*, 1999).

Tetraethylammonium chloride (TEA) is a non-selective potassium channel blockers but also known to effectively block the BK channel. TEA inhibits BK channels from both side but shows distant affinity with the dissociation constant 0.2 mM when applied internally and 30 mM for the external application (Kaczorowski and Garcia, 1999). Including TEA, quaternary ammonium ions have been characterised to block K_v channels and also shown to block the BK channel with different kinetics. It was suggested that the results possibly reflected the structural similarlities as well as differences between these channels (Villarroel *et al.*, 1988). BK channels are also blocked by Shaker ball peptide, which has been known for its blockade of Shaker K^+ channels.

In addition to these non-selective BK channel blocking compounds, several scorpion toxins have been identified to block BK channels and a few of these toxins are highly selective to BK channels among other ion channels. These peptide toxins include charibdotoxin, slototoxin, martentoxin and iberiotoxin (IbTX). These polypeptide toxins inhibit BK channels by covering the pore region composed by the α subunit tetramer. These peptides are identified to have interaction sites with the β subunits and the affinity and effectiveness are shown to be sensitive to the expression pattern of β subunits (Kaczorowski and Garcia, 1999). Most importantly, IbTX is highly selective to BK channel with the dissociation constant of 1.2 nM and used as the gold standard to inhibit the BK channel (Candia *et al.*, 1992).

A fungal indole alkaloid, paxilline is another selective BK channel inhibitor and alongside IbTX, it is widely used to study the property of the channel. The reagent is a small lipophilic molecule and considered to inhibit the channel at more than one site with distinct affinities (Knaus *et al.*, 1994b; Li and Cheung, 1999; Zhou and Lingle, 2014).

1.6.4.2   BK channel openers

BK channels have been reported to open by several unsaturated cis fatty acid produced in cells. These fatty acids are arachidonic, palmitoleic, eicosapenanoic and eicosatetraynoic acids (Hercule *et al.*, 2007). Also BK channels have been reported to increase opening in response to 17β-estradiol depending on its coexpression with β1 subunit (Valverde *et al.*, 1999). An anti-microbial peptide, β-defensin 2, produced by innate immune cells has also been reported to open the BK channel when the channel is coexpressed with the β1 subunit (Liu *et al.*, 2013). A protecting effect of vasculature has been reported on the application of these BK channel activating molecules (Bentzen *et al.*, 2014).

There found several synthetic compounds to open the BK channel. An anti-estrogen agent, Tamoxifen has been reported to open BK channels which are coexpressed with the β1 subunit (Coiret *et al.*, 2007). Various BK channel activators have been developed by drug companies. Benzimidaolone derivatives NS004 and NS1619 have been used to study the physiological functions of BK channels and therapeutic effect (Olesen *et al.*, 1994). Cym04 is another reported activator of the channel (G *et al.*, 2012). However it also has been noticed that these drugs exhibit mitochondrial

toxicity and low specificity (Bentzen *et al.*, 2014). A newer benximidaxolone derivative, NS11021, is considered to have improved selectivity and effect on BK channel opening (Bentzen *et al.*, 2007). Another activator, the GoSlo-SR family of activators are found to shift the voltage dependence of the BK channels (Roy *et al.*, 2012).It has been reported that compounds naturally found in plants and fungi activate BK channels. Examples of these are dihdrosoyasaponin and DHS-I. These materials have been used in medicines to treat asthma and smooth muscle disorders (Nardi *et al.*, 2003).

These openers for BK channels have been great interest of drug discovery to treat hypotension, vascular hyperactivity, erectile dysfunction, bladder instability, and inflammatory pain, and have studied in clinical trials (Bentzen *et al.*, 2014).

1.6.4.3   BK channel modulation by endogenous signalling molecule

It has become apparent that various endogenous signalling molecules also regulate the opening of BK channels. Importantly in the context of this research, some of these molecules are produced by macrophages during the innate immune responses (Hou *et al.*, 2009). The endogenous molecules which have been speculated to increase the opening of BK channels include protons, carbon monoxide (CO), arachidonic acid metabolites, such as hydroxyeicosatetranoic acids, epoxyeicosatrienoic acids and dihydroxyeicosatrienoic acids; the metabolites of cytochrome P540, epoxygenases, lipoxygenases; the human-β-defensin 2; 17-β-estradiol and unsaturated free fatty acids such as omega-3 docosahexaenoic acids (Baron *et al.*, 1997; Bringmann *et al.*, 1998; Hou *et al.*, 2009; Bentzen *et al.*, 2014). Indeed it has been suggested that the ability of these molecules to modulate BK channels may underlie their physiological and pathophysiological effects (Hercule et al., 2007). For instance, omega-3 docosahexaenoic acid has been demonstrated to lower the blood pressure in wild-type mice, while this was ineffective in BKα knock out mice. 17, 18-epoxyeicosatetraenoic acid has been shown to achieve its vasodilator effect by acting on BK channels (Hercule *et al.*, 2007). Heme has been reported to modulate the activity of the channels, however its effect is more complex. Heme binds to the cytoplasmic region of BKα and increases the Po at negative voltage, however at positive voltages heme decreases Po (Horrigan *et al.*, 2005). Finally ROS, such as hydrogen peroxide (H_2O_2), nitric oxide (NO), peroxynitrite ($ONOO^-$) and super oxide (O^{2-}) have been suggested to inhibit the channel activity via oxidation of Cys911 in the cytoplasmic region (Tang *et al.*, 2004).

Interestingly many of these endogenous BK channel modulators have a role in inflammatory responses. For instance ROS, BK channel inhibitors, are released from macrophages during the early phase of inflammation and may contribute to pro-inflammatory signalling cascades (Tang *et al.*, 2004). In contrast, CO, BK channel opener, has been shown to have anti-inflammatory effects in inflammation. In terms of cell signalling, CO is probably a more likely candidate as a modulator of the channel activity, as CO release is regulated by the enzyme heme oxygenase and the heme oxygenase 1 and 2 are involved in inflammation (Wallace *et al.*, 2015).

A second class of molecules, which have anti-inflammatory effects and also BK channel modulatory effects include arachidonic acid metabolites, including hydroxyeicosatetranoic acids, epoxyeicosatrienoic acid and dihydroxyeicosatrienoic acids. These molecules are associated with the later phase of inflammatory response and the resolution of inflammation (Perretti *et al.*, 2015).

1.6.5   BK channel expression in different cellular locations

As stated above the BK channel can be found in many tissues and exist in many forms. Furthermore the BK channels are expressed in multiple subcellular locations and appear to have tissue and location specific properties/functions. The cellular location in which the BK are found include the plasma membrane, mitochondrial membrane and nuclear envelops (Xu *et al.*, 2002; Douglas *et al.*, 2006; Cui *et al.*, 2009; Li *et al.*, 2014). However the roles for these intracellular BK channels are not completely understood. This may be related to the lack of specific reagents which are required to investigate their activity.

BK channels have many important roles in cell biology, however its function in inflammation is not fully characterised. Interestingly several mediators of inflammation modulate the activity of the channels. The aim of this PhD is to investigate the role of the BK channels in cytokine production during the classical activation of macrophages via TLR4.

1.7 Aims

The overall aim of this thesis is to investigate a role for BK channels in macrophage activation via TLR4. To date, relatively few studies have been carried out on ion channels in macrophages. References to suggest properties related to ion channel ,especially electrophysiology of these cells, are relatively sparse. Therefore this project was also aimed to structure the framework of ion channel research in macrophages. This included the development of methods to research ion channels such as patch clamp technique on macrophages.

A mouse macrophage cell line, RAW264.7, was used throughout the thesis. This is because the cell line is often used in the studies of TLR4 signalling and cytokine production (Rutledge *et al.*, 2012). Macrophages are known to be heterogenetic and plastic in nature. The cell line generally has more stable phenotype and is thought to be suitable for the method development, which aimed on this thesis.

Previous research in the lab had established a role for heme oxygenases and CO in the regulator of inflammatory responses. One of proteins, which has been shown to be regulated by CO are BK channels. In addition, the activation of BK channels is the subject of many factors and importantly this include endogenous molecules which are produced during inflammatory responses. Especially the channels are regulated by CO, whose anti-inflammatory actions have been interest of the laboratory. It is hypothesised the channel may have involvement in inflammatory response.

However the role of BK channel in macrophages had been under-researched. This thesis attempted to establish protocols by which the BK channel expression and activity could be measured in macrophages and carry out initial investigations into the role of the BK channel in macrophages. It was hoped that this research would elucidate the role of BK channel in macrophage activation and possibly indicate a mechanism by which CO regulates macrophage activation.

The release of inflammatory mediators is an important aspect of macrophage activation and has an impact on forming overall inflammatory responses (Medzhitov, 2008; Stow *et al.*, 2009; Arango Duque and Descoteaux, 2014). Therefore this project used the release of cytokines and a cytokine receptor as a measure of macrophage activation.

The research questions to be addressed are following.

1 Establish a model of macrophage activation by TLR4 activation in vitro

To use cytokine release as a measure of inflammatory response, it was necessary to characterise the pattern of protein release during TLR4 activation in RAW264.7 macrophages. These macrophages were stimulated with TLR4 ligand, LPS, and the released levels of cytokines were measured using enzyme-linked immunosorbent assay (ELISA). TNF-α, IL-6 and IL-6Rα are considered to be important in inflammatory pathology and were analysed in this thesis.

2 Do macrophages express BK channels?

Little data is available on the ion channel expression in RAW264.7 macrophages. Especially the expression of BK channels in these cells had not been known. Therefore it was necessary to characterise their expression in RAW264.7 macrophages. The channel expression was studied using 3 different method analysis, Western blot was carried out to assess the expression of the channel, immunofluorescence to visualise the channel location and electrophysiological recordings to determine the activity of the channel. Western blot analysis were carried out at whole cell level and other cellular fractions. As it has been reported that the activation of immune cells alter the expression of K$^+$ channels (Feske *et al.*, 2015), this study was carried out in both resting LPS stimulated macrophages.

3 Are BK channels expressed in macrophages involved in inflammatory response during TLR4 activation?

To study the involvement of BK channels in macrophage activation, the effect of BK channel block by IbTX on cytokine and cytokine receptor release was studied. First whether IbTX has direct effect on cytokine and cytokine receptor release by

macrophages was tested to assess the suitability of this drug to use on macrophages. Once the effect was found, it was aimed to address the mechanism by which the channel inhibition altered the release of TNF-α. This was investigated by different techniques; TNF-α mRNA levels by real time quantitative PCR (RT-qPCR), cellular retention of TNF-α by Western blot.

4 How ADAM17 important in release of cytokine and is BK channel involved in regulating it activity?

The results led the hypothesis that BK channels regulated the main membrane sheddase for TNF-α, ADAM17 (Rose-John, 2013). To assess the effect of IbTX on ADAM17 activity, enzyme activity assay was carried out.

5 Does the genetic inhibition of BK channel have the same effect as pharmacological inhibition?

The results from this pharmacological modulation of channel were further elucidated by genetic inhibition of BK channels by BKα silencing siRNA.It has been reported that macrophages are difficult to transfect siRNA (Forsbach *et al.*, 2012). Therefore, the first experiment aimed to establish a protocol for effective BKα silencing in RAW264.7 macrophages using several transfection reagents and siRNA sequences. The effect was assessed by measuring protein level by Western blot. The effect on the release of cytokines and a cytokine receptor by genetic inhibition of BKα were analysed by ELISA, Western blot and ADAM17 enzyme activity assay.

Chapter 2 Material and method

2.1 Materials

2.1.1 Drugs

Sterile cell culture grade distilled water (diH$_2$O: Thermo Fisher Scientific, U.S.) was used to reconstitute drugs. Sterile filtered cell culture grade dimethyl sulfoxide (DMSO: Sigma Aldrich, UK) was used to reconstitute drugs. Ultrapure LPS from E.coli 0111:B4 strain (Invivogen, U.S.) was reconstituted in diH$_2$O and the stocks were made at the concentration of 5 mg/ml and aliquots were kept in -70°C freezer until required. A BK channel inhibitor, IbTX (Alomone Labs, Israel), was reconstituted in diH$_2$O to the concentration of 10 μM and aliquots were stored in -20°C freezer. Another BK channel inhibitor, Paxilline (R & D Systems, U.S.), was prepared in DMSO at the concentrations of 100 mM and aliquots were stored in -20°C freezer. A general inhibitor for membrane metalloproteases, GM6001 (Enzo Life Sciences, UK) was reconstituted in DMSO at the concentration of 6.75 mM, immediately diluted to 1 in 10 in diH$_2$O to minimize DMSO concentrations and aliquots were stored in -20°C freezer. A selective inhibitor for ADAM17, TAPI-0 (Enzo Life Sciences, UK), was prepared in DMSO at the concentration of 6.75 mM and aliquots were stored in -20°C freezer. NS11021 (Sigma Aldrich, UK) was dissolved in DMSO at the concentration of 100 mM and aliquots were stored in -20°C freezer. Protease inhibitor cocktail (Sigma Aldrich, UK) was prepared in diH$_2$O to 20 times concentrated than working concentrations and aliquots were stored in -20°C freezer. The components of protease inhibitor cocktail and working concentrations are as following; 1 mM AEBSF, 0.8 μM Aprotinin, 50 μM Bestatin, 15 μM E-64, 5 mM EDTA, 20 μM Leupeptin and 10 μM Pepstatin A. TACE substrate II (fluorogenic) (BML-228; Enzo Life Science, UK) were reconstituted in DMSO at the concentration of 6.7 mM and was used in ADAM17 activity assay immediately after reconstitution. When DMSO was used for the reconstitution, the concentration of DMSO in the culture well never exceeded 0.015% in cytokine assays and 0.1% in the ADAM17 activity assays. Table 2-1 shows the summery of drug preparation used in the methods used in the thesis.

Compound	Supplier	Stock conc.	Stock solvent	Final conc. Range	Methods
IbTX	Alomones labs, Israel	10 mM	diH$_2$0	3-1000 nM	ADAM, CA, E, IF, PCR & WB
TEA	Sigma, UK	0.5 M	diH$_2$0	0.6-3 mM	CA & E
LPS	Invivogen, U.S.	5 mg/ml	diH$_2$0	3-1000 ng/ml	ADAM, CA, E, IF, PCR & WB
GM6001	Enzo Life Science, UK	6.75 mM	DMSO	150 nM-15 μM	ADAM, CA & IF
TAPI-0	Enzo Life Science, UK	6.8 mM	DMSO	100 nM-600 nM	ADAM, CA & IF
TACE substrate	Enzo Life Science, UK	6.7 mM	DMSO	5 μM	ADAM
Paxilline	R & D Systems, U.S.	25 mM		25 mM	CA
NS11021	Sigma, UK	100 mM	DMSO	100 nM	ADAM & CA
Protease inhibitor cocktail	Thermo Fisher Scientic U.S.	X 20	diH$_2$O	1 mM AEBSF, 0.8 μM Aprotinin, 50 μM Bestatin, 15 μM E-64, 5 mM EDTA, 20 μM Leupeptin, 10 μM Pepstatin A	WB

Table 2-1 Drugs

Summary of drug preparation, names, sources, stock preparation, final concentration range and methods. IbTX: Iberiotoxin, TEA: Tetradoethyl ammonium, LPS: UltraPure LPS, diH$_2$O: Distilled water, DMSO: Dimethyl sulfoxide. conc.: concentration. ADAM: ADAM17 activity assay, CA: cytokine assay, E: electropysiological recordings, IF: immunofluorescence imaging, PCR: real-time quantitative polymerase chain reaction, WB: Western blot.

2.1.2　Chemicals and reagents

Dulbecco's Modified Eagle Medium (DMEM) (Thermo Fisher Scientific, U.S.) and penicillin/streptomycin concentrate consisted of penicillin 10000 unit/ml and 10 mg/ml streptomycin (Thermo Fisher Scientific, U.S.) were used for cell culture and DMEM was stored at $4^{o}C$ and penicillin/streptomycin was at $-20^{o}C$ respectively. Molecular biology grade, bovine serum albumin (BSA; Sigma UK) was stored at $4^{o}C$. Sterile, cell cluture grade fetal bovine serum (FBS; Thermo Fisher Scientific, U.S.) and goat serum (Thermo Fisher Scientific, U.S.) was stored in $-20^{o}C$. 30% acrylamide/Bis-acrylamide (Sigma, UK), sodium dodecyl sulfate (SDS; Pomega, UK), tetramethylethylenediamine (TEMED; Thermo Fisher Scientific, U.S.), and ammonium persulfate (APS; Sigma, UK) were used to make sodium dodecyl sulfate polyacrylamide gel electrophoresis (SDS-PAGE) gels. Pre-stained protein standards (New England Biolabs, UK) were used as a protein size indicator in Western blot. Other chemicals were purchased from Sigma, UK unless otherwise stated.

2.1.3　Bioassay kits

Mycoprobe (R&D Systems, U.S.) was used to monitor mycoplasma contaminations. Pierce Cell Surface Protein Isolation Kit (Thermo Fisher Scientific, U.S.) was used to isolate the plasma membrane from cells. Enzyme-linked immunosorbent assay (ELISA) kits for mouse TNF-α, IL-6Rα and IL-6 (R & D Systems, U.S.) were used to quantify released cytokines from the cells. RNAsay mini-kit (Qiagen, UK) was used to isolate mRNA from cells. Superscript III Reverse transcriptase kit (Thermo Fisher Scientific, U.S.) was used to construct cDNA from mRNA. Taqman custom gene expression assay kit (Thermo Fisher Scientific, U.S.) for mouse TNF-α and β-actin were used for RT-QPCR.

2.1.4　Buffers and solutions

The formulations for the buffers and solutions used in experiments are summarized in Table 2-2. Chemicals were dissolved in diH$_2$O unless specified. pH of the solution was normally adjusted with 12 N HCl solution and/or 1-3 N NaOH solution. For phosphate buffer used in Rat brain preparation, 1N H$_2$PO$_4$ was used to adjust pH in place of HCl. For electrophysiology solutions free Ca^{2+} concentration in the pipette

solution was estimated from a software, MAXCHELATOR (Stanford University, U.S.) and the osmolality of buffers was measured using an Osmometer (Loser Messetechnik, Germany) where required.

Name	Composition	pH	application
Electrode buffer	192 mM Glycine, 25 mM Tris-Base, 0.1% (v/v) SDS		WB
Phosphate buffered saline (PBS)	137 mM NaCl, 2.7mM KCl, 10 mM Na_2HPO_4, 1.8 mM KH_2PO_4	7.2	ADAM, CA,CI, E, IF, PCR & WB
Phosphate buffered saline with Tween (PBS-T)	137 mM NaCl, 2.7 mM KCl, 10 mM Na_2HPO_4, 1.8 mM KH_2PO_4, 0.1% (v/v) Tween-20	7.2	CA
SDS-PAGE sample buffer 4 times concentrate	62.5 mM Tris-HCl, 20% (v/v) Glycerol, 2% (w/v) SDS, 5% (v/v) β-mercaptoethanol		WB
Tris-buffered saline (TBS)	10 mM Tris (8.4 mM Tris-HCl, 1.6 mM Tris-Base), 100 mM NaCl	7.4	CI &WB
Tris-buffered saline with Tween (TBS-T)	10 mM Tris, 100 mM NaCl, 0.1% (v/v) Tween-20	7.4	CI &WB
Transfer buffer	190 mM Glycine, 25 mM Tris-Base, 20% (v/v) Methanol		WB
Citrate buffer (pH=5.0)	5 mM Citric Acid, 5 mM Tri-sodium citrate	5.0	CA
Mild stripping buffer (pH=2.2)	200 mM Glycine, 1% (w/v) SDS, 1% (v/v) Tween-20, pH set to 2.2 with HCl	2.2	WB
Lysis buffer for nuclei isolation	8 mM Tris-HCl, 2 mM Tris-Base, 10 mM NaCl, 3 mM $MgCl_2$, 0.8% NP-40, Protease inhibitor cocktail	7.5	CI
Quenching solution for cell surface protein isolation	PBS with 100 mM Glycine		CI
Lysis buffer for cell surface protein isolation	PBS with 1% IGEPAL-CA63, Protease inhibitor cocktail		CI
Cell culture freezing solution	10% (v/v) Glycerol, 90% FBS		CC

Wash buffer for cell surface isolation	PBS with 0.1% IGEPAL-CA630, Protease inhibitor cocktail		CI
Kreb's	125 mM NaCl, 26 mM NaHCO$_3$, 2.5 mM KCl, NaH$_2$PO$_4$, 2 5mM D-glucose, 1 mM CaCl$_2$	7.4	E
Phosphate buffer for rat brain preparation	153 μM NaH$_2$PO$_4$,1.46 mM Na$_2$HPO$_4$, 320 mM Sucrose, Adjust pH with H$_2$PO$_4$	7.4	WB
Pipette solution free Ca^{2+} high(1.6 μM)	5 mM EGTA, 20 mM HEPES, 10 mM KCl, 100 mM K-acetate, 1 mM MgCl$_2$, 4 mM CaCl$_2$	7.4	E
Pipette solution free Ca^{2+} low (10 nM)	5 mM EGTA, 20 mM HEPES, 10 mM KCl, 100 mM K-acetate, 1 mM MgCl$_2$, 50 nM CaCl$_2$	7.4	E

Table 2-2 Buffers

Formulations, names, abbreviation, pH of the buffers and solutions and applied techniques. ADAM: ADAM17 activity assay, CA: cytokine assay, E: electrophysiological recordings, IF: immunofluorescence imaging, PCR: real-time quantitative polymerase chain reaction, SDS-PAGE: sodium dodecyl sulphate polyacrylamide gels, WB: Western blot, CI: isolation of cellular fractions. CC: cell culture.

2.1.5   Antibodies

A mouse monoclonal anti-mouse BKα mouse antibody (L6/60; Millipore, UK) and a rabbit polyclonal anti-mouse BKα (APC-107; Almone labs, Israel) were used for BKα identification in Western blot analysis. Both antibodies are designed to bind the intracellular, C-terminal, region of the BKα protein. Antibodies which are directed to the extracellular region of the subunit were avoided due to possible interference with the biotinylation procedure, 2.2.7. This is because the method for the plasma membrane isolation involves covalent modification of the cell surface protein, which could limit the binding of antibody to the extracellular region. L6/60 was used to visualise BKα in immunofluorescence imaging. A rabbit polyclonal anti-ADAM17 antibody (ab2051; abcam, U.S.) was used to assess ADAM17 expression in Western blot.   This antibody is designed to bind to the intracellular, C-terminal, region of ADAM17. For the validation of plasma membrane isolation technique, anti-Akt rabbit polyclonal antibody was used. A rabbit monoclonal anti-mouse TNF-α antibody (D2D4; Cell Signaling Technology, U.S.) was used to detect cellular TNF-α in Western blot. A rabbit polyclonal anti-β-actin antibody (D6A8; Cell Signaling Technology, U.S.) was used as a loading control in Western blot. Goat anti-rabbit IgG horse radish peroxidase (HRP)-linked secondary antibody and horse anti-mouse IgG HRP-linked secondary (Cell Signaling Technology, U.S.) were used to conjugate HRP to primary antibodies in Western blot. Non-specific binding of the secondary antibodies was tested by incubating the samples with the secondary antibodies alone, see 2.2.10.

A mouse monoclonal anti-mouse BKα antibody (L6/60; Millipore, UK) was used to visualize BKα protein in immunofluorescence imaging. Before incubating with L6/60, F(ab)' fragment-affinity purified unconjugated goat anti-mouse IgG (Thermo Fisher Scientific, U.S.) was applied at 1.25 μg/ml to block the binding of the anti-mouse IgG secondary antibody to endogenous mouse Ig. Goat anti-mouse IgG (H&L) secondary antibody Alex Fluor$^®$ 488 conjugate (Thermo Fisher Scientific, U.S.) was used to conjugate fluorescence to primary antibody for immunofluorescence imaging. In order to achieve good signals, experimental conditions, such as antibody concentrations and incubation times were optimised. The optimised experimental conditions are summarised in Table 2-5.

2.2 Methods

2.2.1 Cell culture

RAW264.7 murine macrophage cell line and J774.1 murine macrophage cell line were obtained from the European Collection of Cell Culture. RAW264.7 and J774.1 macrophages were cultured in DMEM containing 10% FBS, 100 unit/ml penicillin and 100 μg/ml streptomycin, referred as culture media in text, in a humidified incubator at 37°C, 5% CO_2. Cells were kept frozen in freezing media consisting of 90% FBS (v/v) and 10% (v/v) glycerol, sterile filtered. The stocks of cells were kept in cryotubes. Each tube contained approximately $5x10^6$ cells in liquid nitrogen. The cells were thawed in water bath at 37°C and immediately transferred to conical bottom tubes supplied with flesh media. To remove any freezing media, tubes were centrifuged at 210 x g, re-suspended in fresh culture media, transferred to the cell culture flasks and cultured in a incubator. The culture media was replaced at 4 hours and 24 hours after thawing to remove dead cells, released molecules and debris. When flasks reached approximately 80% confluency, the cells were passaged using a rubber scraper and a portion of cells were continuously cultured. The passage number did not exceed 16 times. Mycoplasma contamination was routinely tested as described in 2.2.2. Upon thawing and periodically, Nitrite assay, see 2.2.3, was carried out to assess the responsiveness to LPS.

2.2.2 Mycoplasma detection

The presence of mycoplasma contamination was tested using a mycoplasma detection kit, Mycoprobe (R&D Systems, U.S.) following the manufacturer's instruction. To allow the detection of low level of contamination, cell culture media was sampled on day 1 and 3 to determine any increases in signal. The samples were mixed with supplied lysis buffer and hybridized to probes (biotin-labelled capture oligonucleotide probes and digoxigenin-labelled detection probes). Those probes are targeted to the 16S ribosomal RNA (rRNA) of common mycoplasmas. The hybridization solution is transferred to a streptavidin-coated microplate to capture the rRNA/probe hybrid. Following removal of unbound material by wash, an anti-digoxigenin alkaline phosphatase was added. An amplified solution was added and colour develops in proportion to the amount of mycoplasma rRNA. Colour development is stopped and the intensity of the colour is measured using a plate

reader at wavelength 490 nm with correction at 650 nm. An optical density greater than 0.1 indicated the presence of mycoplasma infection and density less than 0.05 indicated the absence of mycoplasma contamination. Signals from day 0 sample and day 3 samples were compared to check change in mycoplasma level.

	Mean O.D.
positive ctrl	1.8163
negative ctrl	0
Day 1	0.0063
Day 3	0.0038

Table 2-3 Mycoplasma test on RAW264.7 cells.

A typical result from mycoplasma test using culture media from RAW264.7 macrophages. Ctrl: control supplied with the kit. O.D.: Optical density. O.D.>0.1: presence mycoplasma infection, O.D. <0.05: absence of mycoplasma infection. Ctrl: control.

2.2.3   Nitrite assay

Macrophages are known to exhibit heterogeneity depending on the environmental cues and origin (Mosser and Edwards, 2008). Pervious work in the lab had found that sub-clones of macrophage cell lines can occur if high passage numbers, 25 times or more, are used, or cells are not continually cultured under optimal conditions. These cells were usually associated with a decrease in their ability to be activated (lack of macrophage response to LPS can also be due to contamination). To use relatively consistent macrophage populations throughout the thesis, the nitrite assay was routinely carried out when each vial was thawed and to monitor the LPS responsiveness of the cells. Macrophages which showed a significant difference to a standard response was discarded and new culture was started.

Activation of macrophages with LPS and IFNγ leads to the generation of nitric oxide (NO) from L-arginine. Nitric oxide synthase 2 inducible derived NO is known to have an antimicrobial activity and possible participates in signal transduction pathways during the inflammatory response. Nitrite assay measures the amount of nitrite in cell culture media and is used to estimate the nitric oxide production. Typical data from experiments were displayed in Figure 2-1. The amount of nitrite in media were measured based on Greiss reaction. The Greiss reaction is a colorimetric assay,

resulting from the formation of pink coloured diazonium salt by addition of sulphate acid on the nitrite. The cells were plated at 1×10^5 per well on 96 well tissue culture plate and incubated overnight. Macrophages were stimulated with 10 or 1000 ng/ml LPS in presence or absence of 100 unit/ml IFNγ. After 24 hours, the media was collected. 50μl of sample was transferred into 96 well plates in duplicate and 100μl of Greiss solution, consisting of equal parts of 0.2% naphthylethylenediamine dihydrochloride, and 2% sulphanilamide in 5% phosphoric acid, added. The optical density was measured in microcell plate with a single wave length at 540 nm. Duplicates were averaged and the nitrite concentration in the samples was calculated against standard (0-100 μM) composed of NaNO$_3$ in diH$_2$O.
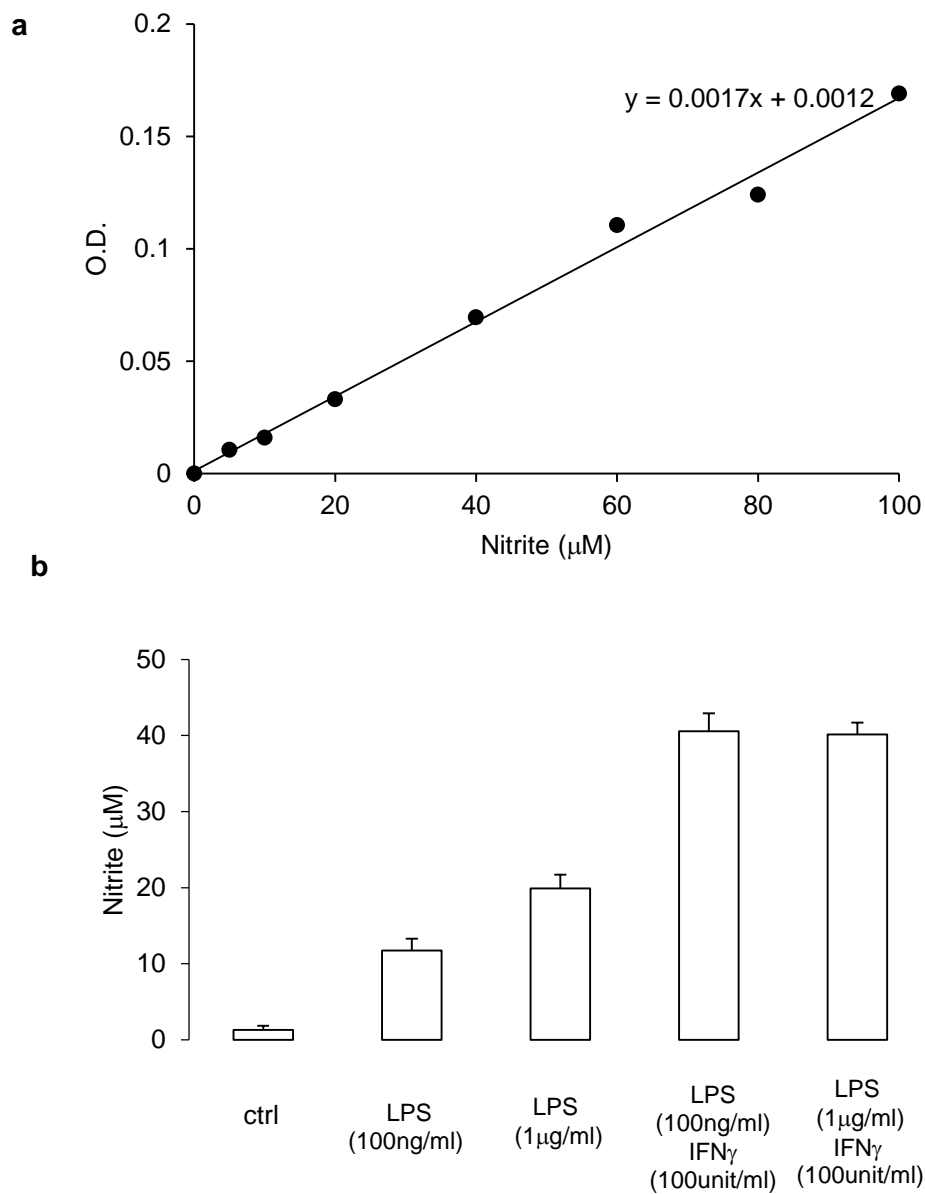
Figure 2-1 Nitrite production from LPS and/or IFNγ activated macrophages

a) A typical nitrate standard plot and b) nitrate production from activated RAW264.7 cells using the Greiss assay. The cells were activated with various combinations of LPS and IFNγ for 24 hours. At 24 hours the conditioned culture media was collected and the nitrite contents were analysed by Greiss reaction. Experiments were routinely carried out and data shown is one example.

2.2.4   MTT assay

Methyl-thiazolyl-tetrazolium (MTT) assay was performed to estimate the effect of drug treatments on the cell viability. NAD(P)H-dependent cellular oxidoreductase enzymes present in mitochondria are capable of reducing yellow coloured tetrazolium salt and this results in the formation of purple coloured precipitated product, formazan. The change in colour is measured by optical density and used to estimate the activity of these enzymes. At the end of experiments, supernatant was removed and thiazolyl salt solution, 0.33 mg/ml Thiazolyl Blue Terazolium Bromide (Alfa Asar, U.S.) in PBS at 37°C was added to each wells. Plates were incubated on a shaker at room temperature until a purple precipitate was visible, typically for 10 minutes. Once the purple precipitate formed the MTT solution was removed, plates dried and the product dissolved in DMSO (Sigma, UK). The sample was pipetted into 96 well-plate wells in duplicate. Optical density of the samples was measured in a microplate reader, Spectra MAXPlus (Molecular Devices, U.S.) at single wave length 545 nm. The values averaged and were compared to non-treated controls.

.

2.2.5   Bradford assay

Protein concentrations in samples were measured by Bradford assay. Bradford assay is a colormetric assay using the dye Comassie Brilliant Blue G-250. When binding to protein, the product was read at 595 nm. The change in optical density was used to calculate the protein contents in the samples. Samples were diluted in PBS so as to fit the range of standard. Protein standard (0-2 mg/ml) was made with BSA in phosphate buffered saline (PBS). 2-5 μl diluted sample and standard was pipetted in duplicates into a 96 well plate. Bradford reagent (Sigma, UK) was diluted 1 in 2 in PBS and added to each well to give sample to reagent ratio of 1 to 50. Optical density was measured in a microplate reader, Spectra MAXPlus (Molecular Devices, U.S.) at single wave length 595 nm. The duplicates were averaged and background signal subtracted. Protein contents in the samples were calculated from the standard.

2.2.6   Whole cell protein preparation for Western blot analysis

After treatment procedures cell were prepared for Western blot analysis as follows. Cells were collected in conical bottom cryotubes with PBS supplied with protease

inhibitor cocktail at 4°C. The tubes were centrifuged at 10000 x g for 7 minutes and supernatant was discarded. Cell pellets were snap frozen in liquid nitrogen and stored in -70 °C freezer until use. The cell pellet was lysed by sonication at 4°C in PBS containing protease inhibitor cocktail. The protein concentration in each sample was measured by Bradford assay, see 2.2.5. Four times concentrate SDS-PAGE sample buffer, 62.5 mM Tris-HCL, 20% (v/v) Glycerol, 2% (w/v) SDS, 5% (v/v) β-mercaptoethanol with trace amount of bromophenol blue was added 3 parts cell sample in PBS. The final protein concentration of the loading sample was 1 mg/ml protein. The following equation 2-1 was used to calculate the proportion of loading buffer, sample and PBS used, with FV being the final volume of sample prepared and FPC being the final protein concentration. The loading sample mixture was boiled in hot water bath for 2-3 minutes. Samples were used immediately or were stored at -20°C until loading.

$$FV = Final\ volume\ (ml)$$

$$SPC = Sample\ protein\ concentration\ \left(\frac{mg}{ml}\right); where\ SPC \geq \frac{1.333mg}{ml}$$

$$FPC = Final\ protein\ concentration = \frac{1mg}{ml}$$

$$\frac{FV}{4} = \boldsymbol{SDSPAGE\ sample\ Loading\ buffer\ (ml)}$$

$$FV * \frac{FPC}{SPC} = \boldsymbol{sample\ (ml)}$$

$$FV - loading\ buffer\ volume - sample\ volume = \boldsymbol{PBS\ (ml)}$$

Equation 2-1 Calculation of Western blot sample volume

This formulation is used to calculate the volume of SDS-PAGE (sodium dodecyl sulfate polyacrylamide gel electrophoresis) sample loading buffer, sample and PBS to prepare samples for Western blot.

2.2.7   Plasma membrane protein isolation

Plasma membrane proteins were isolated using a protein biotinylation and capture method. Pierce Cell Surface Protein Isolation Kit (Thermo Fisher Scientific, U.S.) was used according to manufacturer's guidelines. Isolation of the plasma membrane protein was carried out using 3×10^7 cells per sample. After cell surface proteins were labelled with 1 mg/ml sulfo-NHS-SS-Biotin (Thermo Fisher Scientific, U.S.), the cells were lysed in PBS containing protease inhibitor cocktail and 1% IGAL-CA60 by sonication at 4^oC. The labelled proteins in post nuclear supernatants, separated by centrifugation, were captured with neutroavidn agarose. The captured protein was eluted with SDS-PAGE sample buffer, containing 50 mM 1,4-Dithiothreitol (DTT). The protein contents in elute were measured by Bradford assay. Samples were prepared for Western blot analysis as outlined in 2.2.6. As the total amount of plasma protein obtained is lower than total whole cell protein, the FPC of the loaded sample was 0.2 mg/ml. During the Western blot analysis the absence of the cytosolic protein, Akt, was used to validate plasma membrane isolation process Figure 2-2.
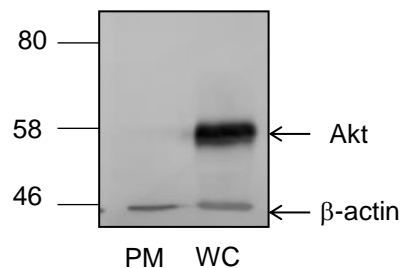
Figure 2-2 Validation of the plasma membrane isolation

Absence of the cytosolic protein Akt in the plasma membrane isolate (PM) and its presence in whole cell lysate (WC) from resting RAW264.7 macrophages. 7 μg protein loaded per lane. Left indicates molecular weight in kDa. β-action was used as a loading control.

2.2.8   Nuclei isolation

Nuclei from RAW264.7 macrophages were isolated using a detergent, NP-40, and low speed centrifugation as previously described (Antalis and Godbolt, 1991). 1×10^7 cells were re-suspended at $4°$C in lysis buffer composed of 8 mM Tris-HCl and 2 mM Tris-Base, 10 mM NaCl, 3 mM $MgCl_2$ and 0.8% NP-40 pH=7.5, Table 2-2, with protease inhibitor cocktail in small tubes with conical bottom. The tubes were

centrifuged twice at 180 x g for 15 minutes. To prevent further lysis of nuclear membranes, NP-40 was washed from the cells by re-suspension with buffer 8 mM Tris-HCl and 2 mM Tris-Base, 10 mM NaCl, 3 mM $MgCl_2$ pH=7.5, Table 2-2, and centrifugation at 180 x g for 10 minutes at 4°C. The obtained nuclei pellets were resuspended in buffer without NP-40. The nuclei integrity was checked using a confocal microscopy by visualizing DNA with DAPI staining. The isolated nuclei was lysed in PBS containing protease inhibitor cocktail by sonication at 4 °C and protein concentrations in the lysate was measured by Bradford assay. Samples were prepared for Western blot analysis as outlined in 2.2.6.

2.2.9   Rat brain homogenise preparation

Rat brain was used as a positive control for BKα detection in Western blot. Rat brain tissue was kindly given by Professor Dickenson's group at the department of Neuroscience, Physiology and Pharmacology in UCL. In his laboratory, all procedures associated with animals were approved by the UK Home Office. The rat brain was homogenised in 5 mM phosphate buffer supplemented with 320 mM sucrose and protease inhibitor cocktail using a glass squeezer. The homogenate was transferred to 1.5 ml conical bottom tubes and span at 800 x g for 5 minutes. The obtained pellet was suspended in the phosphate buffer and lysed in PBS containing protease inhibitor cocktail by sonication at 4°C and protein concentrations in the lysate were measured by Bradford assay. Samples were prepared for Western blot analysis as outlined in 2.2.6.
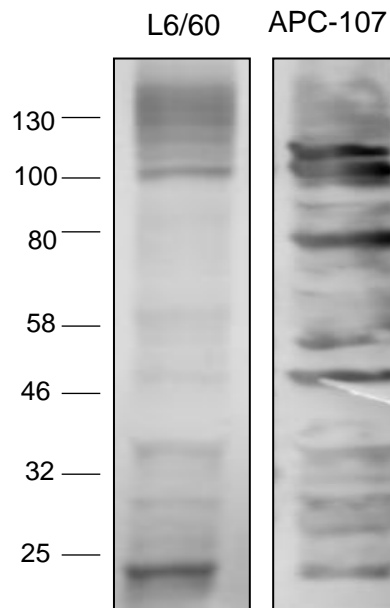
Figure 2-3 BKα expression in rat brain lysate

BKα expression in rat brain lysates was analysed by Western blot using anti-mouse BKα antibodies, L6/60 and APC-107. 10 μg protein was loaded each lane. Left indicates the molecular weight marker in kDa. Experiment was repeated for 5 times with L6/60 and twice with APC-107.

2.2.10 Western blot analysis

Gel casting, sample loading and transfer were performed using Mini-PROTEAN® Tetra Handcast Systems (Bio-rad, UK). SDS-PAGE gels were constructed by free radical polymerization of acrylamide and a monomer cross-linker bis-acrylamide. Pores between the polymers permit the movement of denatured protein in samples. SDS-PAGE gels were hand casted using the casting set in the Mini-PROTEAN® system. First Tris-HCl buffers, diH$_2$O, acrylamide and bis-acrylamide solution were mixed and solution was degassed. Polymerization is initiated by adding APS with TEMED acting as a catalyst. Once the first layer of running gel has set, the second layer was poured. Pore sizes in polyacrylamide gels were determined by the percentage of acrylamide, APS and TEMED. To yield the best separation of the protein samples for the analysis, the composition of the running gel was changed depending on the molecular size of the target protein. For proteins, between 15 kDa and 60 kDa, 12.5% gels were used and for proteins larger than 60 kDa 7.5% gels were used. Stacking gel was made at 4.5%. Table 2-4 summarizes the formulation of the gels, which are total of 50 ml running gel solutions and 20 ml stacking gel

solution, typically used to make 4 gels. Gels were used immediately after pouring or stored in a fridge with hydration for up to one week before use.

Gels are assembled in an electrophoresis chamber. 7 μl pre-stained protein standard was load first lane of gel. Equal amount of sample protein, as prepared in 2.2.6, was loaded on to gels. The amount of protein loaded per lane was typically between 1 to 10 μg. Proteins were separated in the chamber filled with electrode buffer, Table 2-2. A constant voltage of 180 V applied until the protein sample reached the bottom of the gel and this was typically for 1 hour. The gel was assembled in transfer cassette and protein in the gels were transferred to nitrocellulose membranes (Thermo Fisher Scientific, U.S.) in transfer buffer by application of a constant voltage at 100 V for 1 hour.

The membranes were blocked with 5% non-fat milk, 0.01% BSA and 0.1% Tween-20 in tris-buffered saline (TBS) for 2 hours at room temperature with gentle shaking. Subsequently membranes were stained with primary antibodies overnight at 4°C with gentle shaking. The dilution factors and conditions for each primary antibody are summarized in Table 2-5. The membranes were washed with tris-buffered saline with tween-20 (TBS-T) for 10 minutes for 3 times on a shaker. The relevant secondary HRP-linked anti-mouse IgG or anti-rabbit IgG antibodies were applied to the nitrocellulose membranes. Non-specific binding of the secondary antibodies was tested by incubating the samples without primary antibody. Protein bands were visualized by chemiluminescence using Pierce ECL2 Western Blot Substrate (Thermo Fisher Scientific, U.S.) and scanned by a phosphor imager (Typhoon 9410 variable made imager, GE Healthcare UK).

Reagent	Stacking gel (20 ml total)	7.5% running gel (50 ml total)	12% running gel (50 ml total)
30% Acrylamide/bis-acrylamide	2.6 ml	12.5 ml	20 ml
0.5 M Tris-HCl pH 6.8	5 ml	-	-
1.5 M Tris-HCl pH 8.6	-	12.5 ml	12.5 ml
10% SDS	0.2 ml	0.5 ml	0.5 ml
diH$_2$O	12 ml	24.3 ml	16.8 ml
TEMED	20 μl	25 μl	25 μl
10% (w/v) APS	0.1 ml	0.25 ml	0.25 ml
Total volume	20 ml	50 ml	50 ml

Table 2-4 Formulations for SDS-PAGE gel

Formulation of sodium dodecyl sulfate polyacrylamide gel electrophoresis (SDS-PAGE) gels 20 ml of stacking gel solution and 50 ml of running gels. This volume can make up 4 mini-gels (8.6 cm x 6.7 cm). Ammonium persulfate (APS), prepared as 10% (W/W) solution in distilled water (diH$_2$O). TEMED: tetramethylethylenediamin.

2.2.10.1 Calibration of the molecular weight

The molecular weight of protein bands was estimated using a pre-stained colour protein standard. This also confirms the samples on the gels were separated and transferred correctly. The marker is a visible colour (wavelength: 390 -700 nm) when transferred to the nitrocellulose but the colour does not appear when imaged with blue lazer (wavelength : 450 nm).

To calibrate molecular weight, initially the left side of the membrane was cut at each colour indicator so that the marker is visible even under the phosphor-imager. However this process caused damage on the membrane and affected the quality of the image. Thus this calibration was done by matching the final image taken in the phosphor-imager and the photo taken in the same size prior to the application of chemiluminescence reagents as the colour marker fades immediately after the phosphoimage, Figure 2-4a. This analysis was followed in the Western blot and the calibrated molecular weight was indicated as bars, Figure 2-4a and b. These results were recorded in the form presented in Figure 2-4b not in the colour photo shown in Figure 2-4a. Molecular weights are marked as bars shown in Figure 2-4b when the antibody was first used and following blot, the bands at corresponding molecular weights were presented as in Figure 2-4c.

a

The top of membrane

175
130
90
65

58

46

35

25

17

The end of membrane

← 120 kDa

b

175
130
90
65

58

46

35

25

17

← 120 kDa

c

120 kDa →
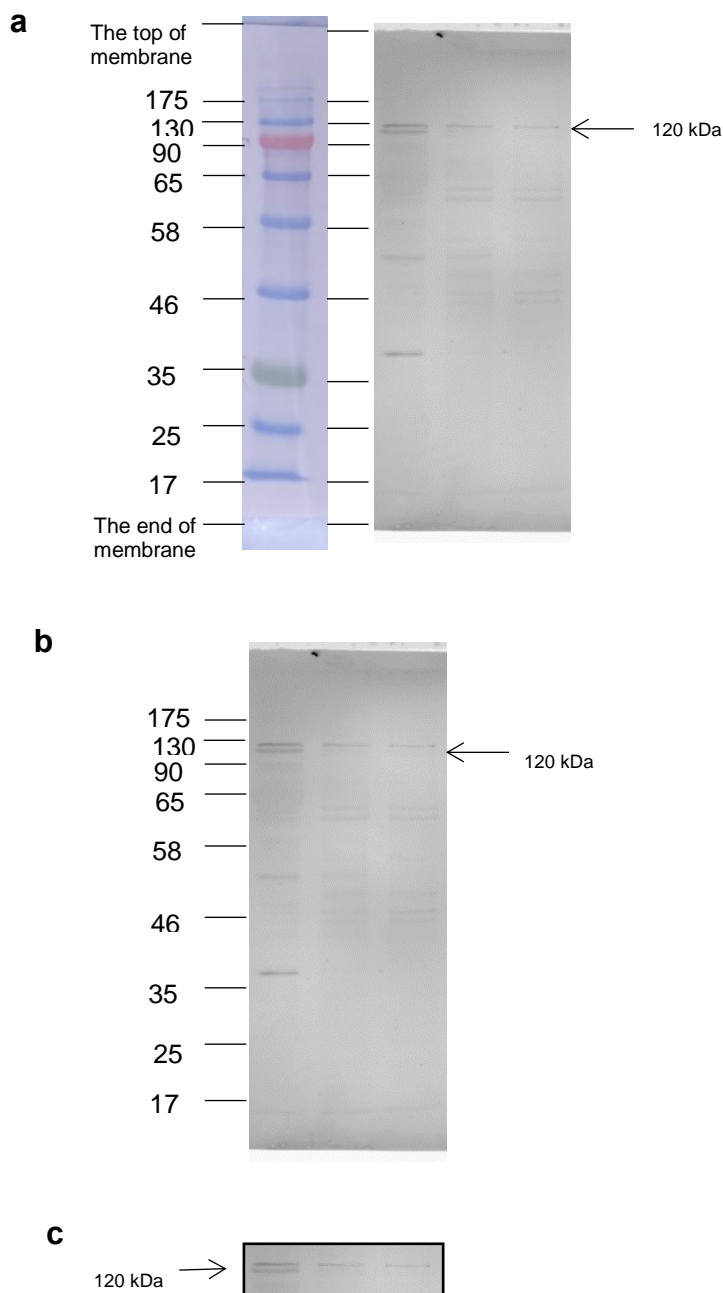
Figure 2-4 Calibration method for molecular weight in Western Blot analysis

a) After sample transfer to nitrocellulose membrane a photograph was taken. After protein bands were developed in a phosphor imager, a) the two images were compared and the molecular weight were annotated on the image as bars. b) Western blot results were recorded with the annotations determined by process. These annotated images b) were used when an antibody was first applied. Subsequent experiments presented c) the bands at relevant molecular weight.

2.2.10.2 Densitometry analysis

Densitometry analysis was carried out to semi-quantify the expression level of the protein bands of interest. The results are presented in order to show the relative expression in the treatment groups compared to control groups. Image Quant 5.2 (Molecular Dynamics, USA) was used for these analyses. Boxes of equal size were drawn around each band. The local median background signals were excluded and band intensity normalized to β-actin in samples prepared from whole cell lysates. Relative band intensities, mean+SEM (n=number of blots used for analysis) of treatment groups were expressed as a ratio of the mean intensity of control bands. The relative expression in treatment groups was presented as ratio to the relevant control group. Therefore statistical analysis has not been made in the densitometry analysis as no bench marking standards was available and only comparison within the same gel can be made.

Primary antibody						Secondary antibody					
Antibody name (Target protein)	Manufacturer	Host species	Dilution	Diluent	Incubation	Antibody name	Manufacturer	Host species	Dilution	Diluent	Incubation
L6/60 (Mouse BKα)	Milipore, UK	Mouse monoclonal	1 in 1000	TBS	Overnight 4 °C	Anti-mouse IgG HRP-linked Antibody	Abcam, U.S.	Horse	1 in 4000	TBS	50 min RT
ab2051(Mouse ADAM17)	Abcam, U.S.	Rabbit polyclonal	1 in 750	TBS	Overnight 4 °C	Anti-rabbit IgG HRP-linked Antibody	Cell Signaling Technology, U.S.	Goat	1 in 4000	TBS	50 min RT
anti-Akt rabbit polyclonal antibody (Mouse Akt)	Cell Sigaling Technology, U.S.	Rabbit polyclonal	1 in 1500	TBS	Overnight 4 °C	Anti-rabbit IgG HRP-linked Antibody	Cell Signaling Technology, U.S.	Goat	1 in 4000	TBS	50 min RT
APC-107 (Mouse/Human BKα)	Cell Sigaling Technology, U.S.	Rabbit polyclonal	1 in 1500	TBS 0.1%BSA	Overnight 4 °C	Anti-rabbit IgG HRP-linked Antibody	Cell Signaling Technology, U.S.	Goat	1 in 4000	TBS	50 min RT
D2D4 (Mouse TNF-α)	Cell Sigaling Technology, U.S.	Rabbit monoclonal	1 in 1500	TBS	Overnight 4 °C	Anti-rabbit IgG HRP-linked Antibody	Cell Signaling Technology, U.S.	Goat	1 in 4000	TBS	50 min RT
D6A8(Mouse/Human β-actin)	Cell Sigaling Technology, U.S.	Rabbit monoclonal	1 in 2000	TBS	Overnight 4 °C	Anti-rabbit IgG HRP-linked Antibody	Cell Signaling Technology, U.S.	Goat	1 in 4000	TBS	50 min RT
DM3568 (Mouse IL-6Rα)	2B Scientific, UK	Rat monoclonal	1 in 500	TBS	Overnight 4 °C	Anti-rat IgG HRP-linked Antibody	Cell Signaling Technology, U.S.	Goat	1 in 4000	TBS	50 min RT

Table 2-5 Sources and experimental conditions for antibodies in Western blot

Description of antibodies (antibody name, source and experimental conditions) used in Western blot analysis. BSA: bovine serum albumin, TBS: tris-buffered saline, RT: room temperature, HRP: horse radish peroxidase.

Anti-rabbit IgG   Anti-mouse IgG

RAW264.7 Rat brain   RAW264.7 Rat brain
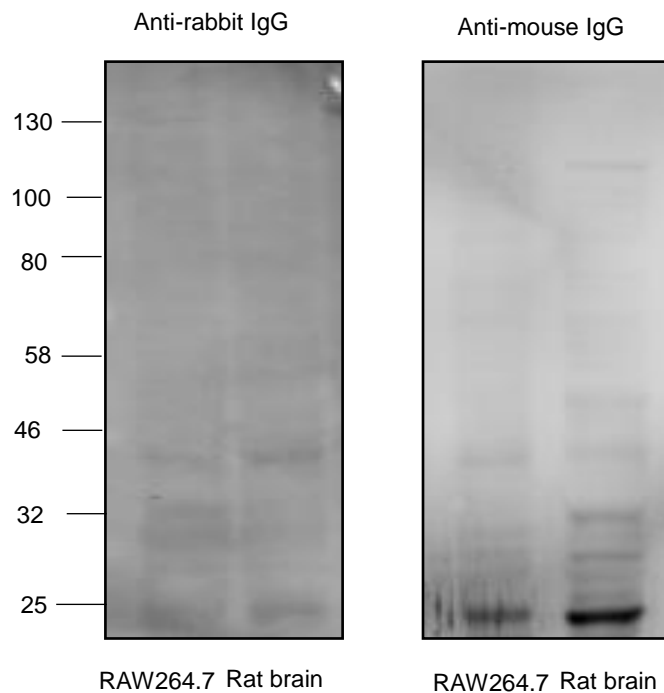
Figure 2-5 Blots stained with secondary antibodies without primary antibodies

Protein samples from whole cell lysate of RAW264.7 macrophages and rat brain lysates. Proteins were loaded 10 μg per each lane. Secondary antibodies, goat anti-rabbit IgG HRP-linked secondary antibody and goat anti-mouse IgG HRP-linked antibody were used at 1 in 4000 dilution. The experiments were repeated twice and blots show representative.

2.2.11 Electrophysiology

Whole cell voltage clamp recordings were performed at room temperature. Macrophages were plated on 13 mm glass coverslips chosen to fit the electrophysiology recording chamber. Pipettes were made using thin walled borosilicate glass (Harvard, Germany), heat-pulled and polished. When filled with pipette solution, the pipette had a resistance between 3.5 - 4 MΩ. Pipette solution was based on 120 mM K-acetate, 20 mM HEPES, 10 mM KCl, 5 mM EGTA, 1 mM MgCl$_2$ and 4 mM CaCl$_2$ with pH=7.2. Free Ca^{2+} in the solution was estimated as 1.6 μM using a software, MAXCHELATOR (Stanford University, U.S.). For initial recordings, pipette solution with free Ca^{2+} at 10 nM was also used, Table 2-2. The extracellular solution was a modified Kreb's; 125 mM NaCl, 26 mM NaHCO$_3$, 2.5 mM KCl, 1.26 mM NaH$_2$PO$_4$ H$_2$O, 25 mM D-glucose and 1 mM CaCl$_2$ with pH=7.4. The osmolality of the pipette solutions and extracellular solutions were maintained between 250-300 mOsmol. Currents were recorded using an Axopatch 200B amplifier (Axon Instruments, U.S.) at the sample rate of 5 kHz and filtered at 1kHz

with Digitata 1332A (Molecular Devices, U.S.). Once a high resistance seal (>2 GΩ) was formed, a ramp protocol (25 second with 10 second sweep ranging from -40 to 100 mV) was applied, Figure 2-6. 3 mM TEA and 30 nM IbTX were applied in extracellular solutions. pH of the extracellular solution was adjusted when TEA was used. For each treatment and control, ramp was repeated at least 5 times and the traces were averaged. There was 5-7 minutes interval between different drug applications. Both IbTX and TEA are reversible channel blockers and whole cell current are to recover during re-application of ramps in Kreb's. Macrophage possesses pseudopodia on their cell surfaces, and the blockade of glass pipette electrode could easily occur. To test whether reduction in current was due to the channel blocking, control ramps were repeated several times to observe recovery and after the blocker application. TEA- and IbTX-sensitive currents were obtained by subtracting average traces in presence of TEA or IbTX from control traces. Net membrane currents were plotted against membrane voltage. Recordings were carried out at room temperature. pCLAMP software (Molecular Devices, U.S.) was used to monitor current magnitude and duration, establish voltage ramp protocols and analyze the data.
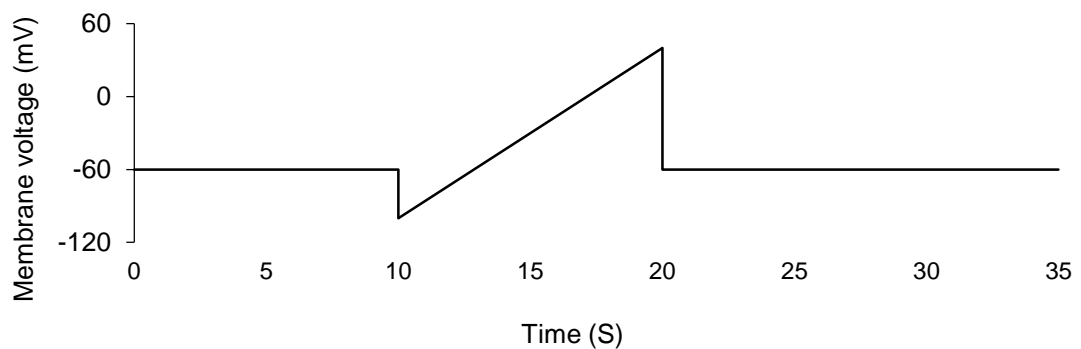
Figure 2-6 Voltage ramp protocol for whole cell recordings

A ramp protocol was established using pCLAMP software and applied in 35 second interval. Between 0 to 10 second voltage remained -60 mV. At 10 second, the membrane voltage was dropped to -100 mV and raised to 40 mV during 10 to 20 seconds. Between 20-35 second voltage was kept -60 mV and the protocol was repeated. The ramp protocol was applied at least 5 times per treatment and the obtained traces were averaged.

2.2.12 Cytokine and cytokine receptor assays

Macrophages were plated at 2.5×10^5 cells per well on 24 well plates and incubated overnight. The following day, the media was replaced and the cells received various drug treatments. After treatments, media was collected and kept in a -20°C freezer until analysis. Released cytokines and cytokine receptors, TNF-α, IL-6Rα and IL-6, from macrophages were assessed using ELISA kits (R & D Systems, U.S.), according to the manufacturer's protocol. All procedures were performed at room temperature. First the plate was coated with a relevant capture antibody in PBS overnight. Following day, the plates were washed with phosphate buffered saline with tween-20 (PBS-T) and blocked with 1% BSA in PBS for 1 hour. Cytokine/ cytokine receptor standards were prepared in a range between 0-1000 ng/ml in PBS containing 0.5% BSA. Samples were diluted in PBS containing 0.5% BSA, so as to achieve cytokine concentrations which fit with the standard curve of the kit. The standard and diluted samples were pipetted in duplicate. After 2 hours incubation, plates were washed with PBS-T and incubated with a secondary antibody, followed by wash and incubation with HRP. The color was developed using TMB substrate diluted in citrate buffer and optical density were measured in a microwell plate reader, Spectra MAXPlus (Molecular Devices, U.S.) at a wavelength 405 nm with 650 nm corrections. The results were averaged and a cytokine concentration in the samples was calculated using the standard curve. The detection limits of kits are 31.6 pg/ml for TNF-α and IL-6, or 15.6 pg/ml for IL-6Rα. Figure 2-7 shows typical standard curves for TNF-α, IL-6 and IL-6Rα.
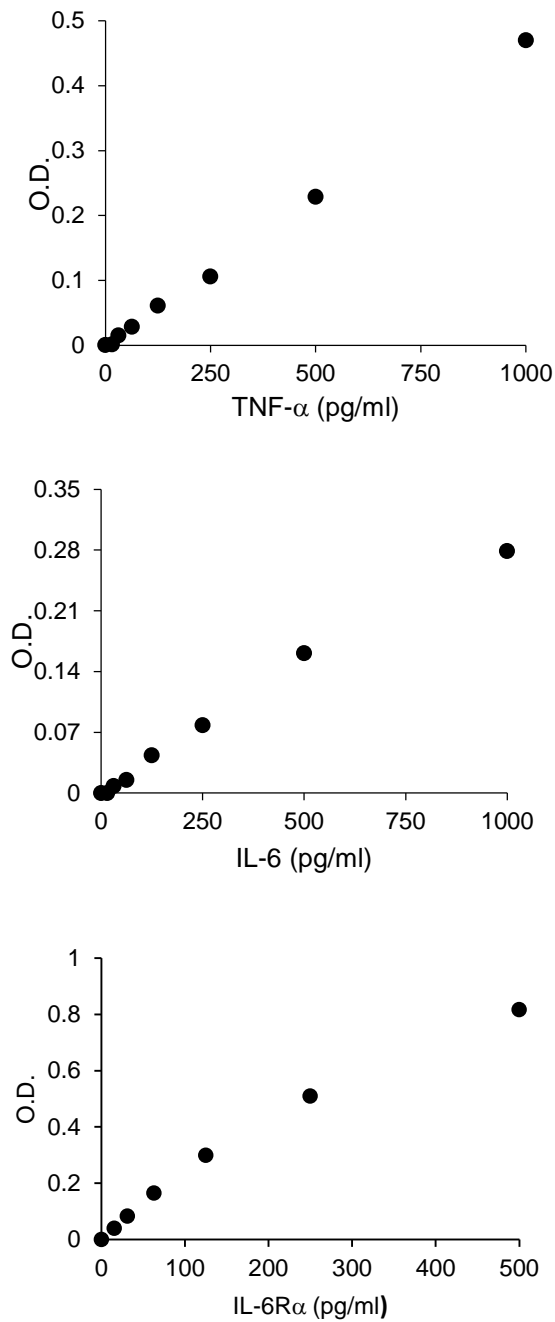
Figure 2-7 ELISA standard plots for TNF-α, IL-6 and IL-6Rα

TNF-α, IL-6 an IL-6Rα were prepared at the concentrations from 0-1000 pg/ml for TNF-α and IL-6 or 0-500 pg/m for IL-6Rα in PBS containing 0.5% BSA and used as a standard for each plate in ELISA. Standard plots were fitted to curves using non-liner regression analysis using Graph pad prism software (Graphpad, U.S.). O.D.: Optical density.

2.2.13 RNA extraction and cDNA synthesis

Total RNA was extracted from RAW264.7 macrophages using RNAsay mini-kit (Qiagen, UK) according to manufacturer's instruction. The procedure extracts RNA molecules longer than 200 nucleotides. This feature provides relatively selective isolation of mRNA and exclusion of shorter RNAs, rRNA and tRNAs (<200 nucleotides). Frozen cell pellets, containing $1x10^6$ cells per group, were lysed and homogenized in a supplied lysis buffer supplied with 0.1% β-metacaptoethanol (Sigma, UK) by votexing until participate clears. The lysates were centrifuged for 30 seconds at 13000 x g in RNase free collection tubes with gDNA eliminator column. Total RNA in flow through was combined with 70% ethanol and salt and captured in the RNA binding column. RNA binding column washed twice with supplied washing buffers and centrifugations at 13000 x g for 15 seconds twice. RNA was eluted in water and stored in a -20 ^oC freezer. The quality and purity of RNA were assessed by OD260/280 ratio, which is measured using a spectrophotometer (DU800; Beckman Coulter, U.S.). Complementary DNA (cDNA) was synthesized using the Superscript III Reverse transcriptase kit (Thermo Fisher Scientific, U.S.) with random primers (Thermo Fisher Scientific, U.S.) according to the manufacturer's instructions. 2 μg total RNA was mixed with 125 ng random primers, 10 ng dNTP Mix and RNase free DEPC treated water. The mixture was heated at 65°C for 5 minutes to denature RNA. The mixture containing single stranded RNA was mixed with 4 μl 5 x first stranded buffer, 200 units SuperScript™III RT, 1 nmol DTT and 1 μl RNaseOUT. After mixing, tubes were incubated at 25°C for 5 minutes for annealing. The mixture was heated at 50°C for 45 minutes to extend the strand. The reaction was inactivated by heating at 70°C for 15 minutes and cDNA for PCR template was obtained.

2.2.14 Real time-quantitative PCR

RT-QPCR was performed to assess mRNA level of TNF-α from cDNA. Taqman custom gene expression assay (Thermo Fisher Scientific, U.S.) and the ABI Prism 7900HT sequence detection system (Thermo Fisher Scientific, U.S.) were used. The probes for mouse TNF-α (Mm00443260_g1, Thermo Fisher Scientific, U.S.) and mouse β-actin (Mm00607939_s1, Thermo Fisher Scientific, U.S.) were used. The

assay was set up in accordance with Taqman protocols. cDNA samples were diluted in DEPC treated RNase DNase free water. Master mixes for TNF-α and β-actin were made and sample dilution was added to each mix. The sample was loaded on the plates in triplicate and blank control was DEPC RNase and DNase free water. The PCR was performed. The background signal was subtracted and values were averaged. TNF-α expression level was normalized to β-actin. Experiments were repeated with n=3 per treatment group and shows representative data and is expressed as mean+SEM.

2.2.15 Gene silencing

Most effective BKα silencing in RAW264.7 macrophages in this thesis was observed when Lipofectamine® RNAiMAX reagent was used (Thermo Fisher Scientific, U.S.). Two silencing siRNAs for mouse BKα, Mm_Kcnma1_1 FlexiTube siRNA, termed sequence 1 (Catalogue number: SI00194369, Qiagen UK) and Mm_Kcnma1_5 FlexiTube siRNA, termed sequence 5(Catalogue number: SI02670486 , Qiagen, UK) were used. Sequence 1 targets the sequence, CAC AAT GTC TAC AGT GGG TTA, and sequence 5 targets the sequence, CAG TTT CTG AAT ATC CTT AAA. These siRNAs were reconstituted in RNase free water to 10 μM and stored at -20 ^{o}C. A non-silencing siRNA, Negative Control siRNA (Catalogue number: 1022076, Qiagen, UK) targeting sequence AAT TCT CCG AAC GTG TCA CGT was used. Stocks for non-silencing siRNA was made in RNase free water at the concentration of 20 μM and stored at -20°C. RAW264.7 macrophages was plated in T25 cm^2 cell culture flasks at 1.25 x 10^6 cells per flasks and each flask had and 6 ml of complete culture media supplied with 10% FBS, 100 unit/ml penicillin and 100 μg/ml streptomycin. After overnight incubation, siRNAs and transfection reagents were diluted (siRNA 0.2 μM, Lipofectamine® RNAiMAX 1 in 25) in OptiMEM (Thermo Fisher Scientific, U.S.). After 5 minutes, siRNA and transfection reagents were mixed and the mixture was incubated for further 20 minutes for the transfection complex to form. 90 pmol of total siRNA and 27 μl of Lipofectamine® RNAiMAX were used per 25 cm^2 flasks which were used for each transfection the final siRNA concentration was 15 nM during the transfection. Macrophages were incubated with the transfection complex for 72 hours. The effect of silencing was determined by Western blot analysis of BKα.

In initial experiments, first GeneMute™ (SignaGen® Laboratories, U.S.) reagent was used in attempt to inhibit the expression of BKα in RAW264.7 macrophages. GeneMute™ regent was used following the manufacturer's instructions. Briefly, RAW264.7 macrophages were plated at 5 x 10^5 cells per well in 6 well plate and each well contained 1.5 ml complete media. siRNAs were diluted into 10 μM in 150 μl GeneMute™ reagent. The siRNA-transfection mixture was incubated for 15 minutes to form transfection complex. The complex was added to each well and the cells were incubated for 48 hours.

Second, Viromer® Blue (Lipocalyx, Germany) reagent was used in attempt to inhibit BKα expression in RAW264.7 macrophages. The reagent was used following the manufacture's instruction. Briefly RAW264.7 macrophages were plated at 5 X 10^5 cells per well in 6 well plate and each well contained 1.5 ml culture media. 15 pmol siRNA was diluted in Blue Buffer, supplied, and Viromer® transfection reagent was mixed. The mixture was incubated for 15 minutes at room temperature to allow transfection complex to form. 150 μl transfection complex was added to each well and after 48 hours of incubation. The cells were analyzed for the expression of BKα. See chapter 7 for the validation of silencing protocols.

2.2.16 ADAM17 activity assay

Proteolytic activity of ADAM17 was assessed by monitoring cleavage of TACE substrate II (fluorogenic) in living macrophages. The method was adapted from a paper by Alvarez-Iglesias *et al* (Alvarez-Iglesias *et al.*, 2005)*.* The enzyme substrate was added directly on to cells in culture and this configuration enabled the assessment of the plasma membrane expressed ADAM17 activity in living cells. RAW264.7 macrophages were plated at 4.8 x 10^4 cells per well on a 96 well fluorescence plate with complete DMEM and received relevant treatment. As the phenol red contained in normal DMEM interfered with fluorescence signal, the media was replaced with phenol red free DMEM supplemented with 4 mM L-glutamine (Thermo Fisher Scientific, U.S.) on the day of the activity assay. Three hours before the assay, the macrophages were activated with 150 ng/ml LPS. TACE substrate II fluorogenic (BML-P228, Enzo Life Sciences, UK) reconstituted in DMSO, directly dissolved in the assay media and applied to the cells at the final

concentration of 5 μM. Immediately, fluorescence signals were measured for 60 minutes using a fluorescence plate reader (Mithras LB 940, Thermo Fisher Scientific, U.S.) in 15 minutes interval. Samples containing no TACE substrate acted as negative control. A general inhibitor for membrane metalloproteases, 4.5 μM GM6001, and a selective inhibitor for ADAM17, 0.6 μM TAPI-0, were used to confirm that the fluorescence signal was due to the ADAM17 activity. Activity was calculated as change in fluorescence per minute in each well, this is expressed as fluorescence/minute for clarity. Results state per minute increase of fluorescence signal as mean+/-SEM and stated in text. Each experiment was repeated with n=3 or 4 per treatment group. Figure 2-8 shows the data from 150 ng/ml LPS stimulated RAW264.7 macrophages with or without 4.5 μM GM6001 or 0.3 μM TAPI-0.
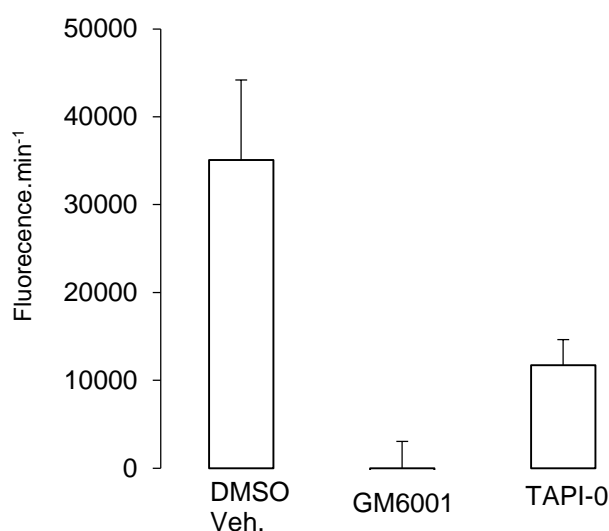
Figure 2-8 ADAM17 activity in macrophages and the effect of GM6001 and TAPI-0

RAW264.7 macrophages were stimulated with 150 ng/ml LPS for 3 hours and TACE II substrate was applied at 5 μM with/without inhibitors for ADAM17, 4.5 μM GM6001 or 0.3 μM TAPI-0. Control wells received DMSO and all wells had 0.15 % DMSO during assay. Fluorescence signals were monitored in 10 minutes interval for 60 minutes and the rate of change in fluorescence between 10 to 50 minutes was expressed as ADAM activity (fluorescence/minute). The graph shows results from n=3 repeated experiments.

2.2.17 Immune fluorescence imaging

RAW264.7 macrophages were plated at 1.3 x 10^4 cells per 13 mm circular glass coverslips. Macrophages were treated with 10 ng/ml LPS for up to 24 hours and fixed by incubation with 4% paraformaldehyde in PBS for 5 minutes and washed with PBS twice. The coverslips were blocked for one hour at room temperature on a shaker with 10% goat serum and 4% BSA in PBS. For staining of BKα, mouse monoclonal anti-moue BKα antibody, L6/60 (Millipore, UK), was used. RAW264.7 macrophage is a mouse cell line, and it was predicted that specific binding of Alex Fluor® 488 anti-mouse IgG secondary antibody (Thermo Fisher Scientific, U.S.) to the endogenous cellular like Ig molecules could result in high background. To avoid this problem, 1.25 μg/ml anti-mouse IgG was added to the block solution and incubated for 2 hours prior to the primary antibodies to mask endogenous Ig. The coverslip was washed twice with PBS. The coverslips were then incubated with L6/60 diluted to 1 in 750 in 5% goat serum and 2% BSA in PBS at 4°C overnight. The coverslips were washed twice for 5 minutes with PBS. Alex Fluor® 488 anti-mouse IgG secondary antibody was used to conjugate fluorescence dye to the primary antibody bind the cells. The secondary antibodies were diluted to 1 in 4000 in 5% goat serum and 2% BSA in PBS for 2 hours at room temperature. The coverslips were washed for 5 minutes twice. To visualize nuclei of macrophages, DAPI diluted 1 in 10000 in PBS, was applied for 5 minutes. The coverslips were washed for 5 minutes twice. The coverslips were mounted on glass slides with Vectashield (Vector Laboratories, U.S.). Fluorescence was visualized using a confocal microscopy (Zeiss LSM510 Meta, Carl Zeiss, Germany). Coverslips without primary antibody incubation were also prepared and the gain of microscope was adjusted so that no fluorescence signal was seen in these secondary antibody only control samples. This allowed to record the fluorescence signal due to the primary antibody binding and not resulting from non-specific binding of the secondary antibody to the cell to be recorded, 8. Images were taken from an area with 15-20 cells with the size indicated in the image. Experiments were repeated at least 3 times and resentative images are shown in figures.
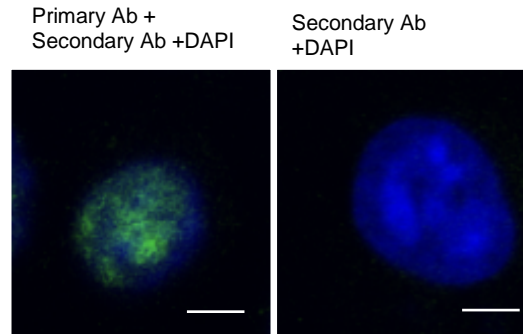
Figure 2-9 Immunofluorescence imaging of macrophages

RAW264.7 macrophages were paraformaldehyde fixed and stained with antibodies (Ab) and DAPI. Left panel shows a cell stained with anti-BKα (L6/60) following incubation with a secondary antibody and DAPI. The right panel shows a cell incubated with a secondary antibody and DAPI without primary antibody staining. Scale bar: 5 μm.

2.2.18 Statistical analysis

Statistical significance among treatment groups were tested using one-way ANOVA and the significance between control group and treatment group was tested by Dunnet's test following one-way ANOVA. Alternatively paired t-test was performed where there were only two groups. The name of test performed was indicated in each figure legend. Graphpad Prism (Graphpad Software, U.S.) was used to perform these tests. A p-value less than 0.05 was considered to be significant and expressed as *p<0.05, **p<0.01 and ***p<0.001 in figures.

Value stated in the text is from one example from repeated experiments. Figures in this thesis present both data from one experiment, which are quoted in text as well as combined data from all repeated experiments. Comments were made in the end of each result section to discuss these data from single experiment and aggregate data. The number of biological replicates, blots or cells for each experiment (n) is indicated in the figure legend.

Chapter 3 How macrophages change TNF-α, IL-6 and IL-6Rα release during TLR4 activation?

3.1   Introduction

Inflammatory stimuli are recognised by receptors expressed on immune cells and this recognition leads to the activation of inflammatory responses from the cell. Activated immune cells release a variety of inflammatory mediators which have important roles in controlling immune responses. Monocytes and macrophages are known to be the major source of these mediators during inflammation.

The aim of this short chapter is to characterise cytokine release from macrophages in response to TLR4 activation. Three proteins released from macrophages, TNF-α, IL-6 and IL-6Rα, were studied. LPS, a classical TLR4 activator, was used to activate macrophages at doses ranging from 3 to 1000 ng/ml. After 4 or 24 hours of LPS treatment, the concentration of these proteins in culture media was analysed.

3.2   Results

Stimulation of macrophages with LPS, 1 to 100 ng/ml, increased the release of TNF-α in dose-dependent manner. The maximum TNF-α release occurred with 100 ng/ml LPS and was 32.6+/-1.0 ng/ml at 4 hours and 41.7+/-3.0 ng/ml at 24 hours, Figure 3-1 a and b. LPS stimulation also induced the release of IL-6 in dose dependant manner at doses from 10 to 1000 ng/ml. The maximum IL-6 release occurred at LPS dose of 1000 ng/ml with 0.63+/-0.02 ng/ml at 4 hours and 2.3+/-0.08 ng/ml at 24 hours, Figure 3-2 a and b. IL-6Rα was constitutively released from macrophages and was 66.4+/-3.9 pg/ml at 4 hours and 328+/-14.8 pg/ml at 24 hours, Figure 3-3 a and b. LPS did not alter IL-6Rα release from macrophages during the first 4 hours of incubation and was 65.8+/-4.1 pg/ml with 100 ng/ml LPS, however after 24 hours, LPS dose-dependently inhibited IL-6Rα release with the minimum IL-6Rα release at 24 hours was occurring at 100 ng/ml LPS and was 104+/-10.3 pg/ml, Figure 3-3 a and b. Additional increases in the dose of LPS had no further effect, Figure 3-3 a and b. MTT assays indicated that LPS doses had no significant effect on cell viability at either 4 hours or 24 hours, Figure 3-4 a and b. The combined data, from repeated (≥ 3 times) experiments, for protein release and MTT was in line with the described results from individual experiments. These combined data were presented in Figure 3-1, 3-2, 3-3 and 3-4.
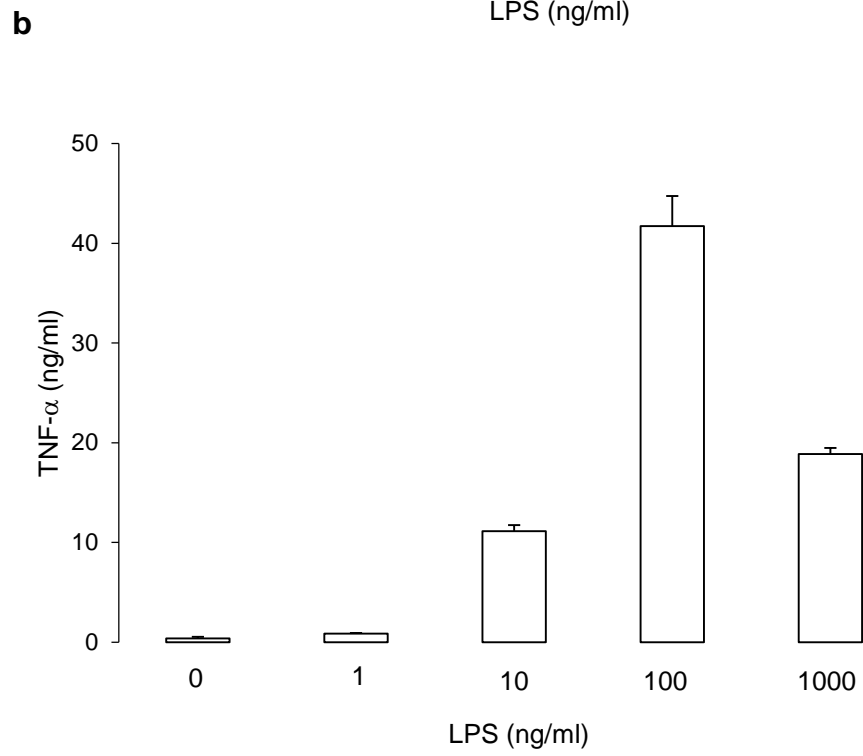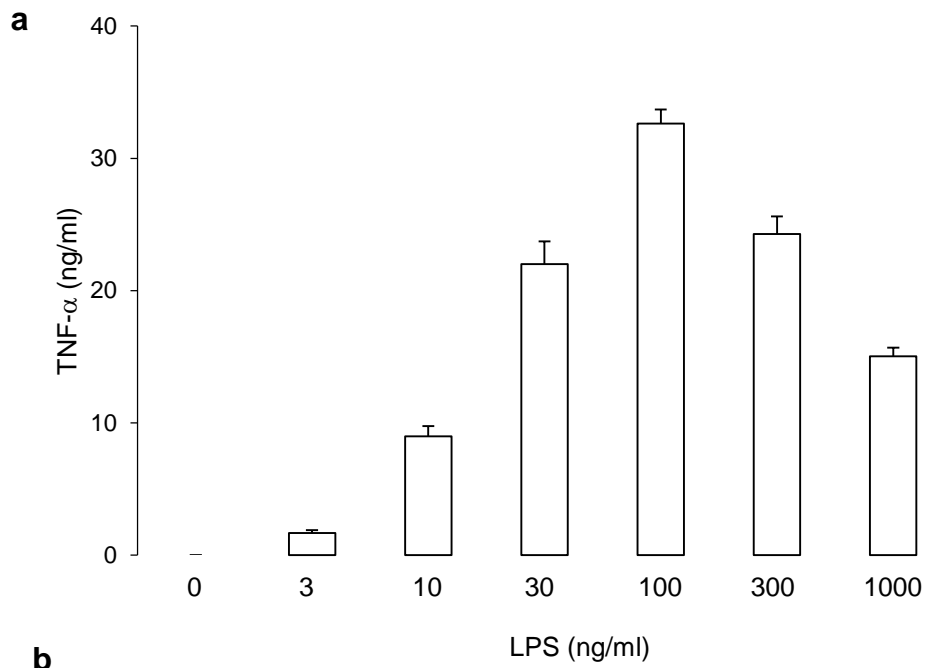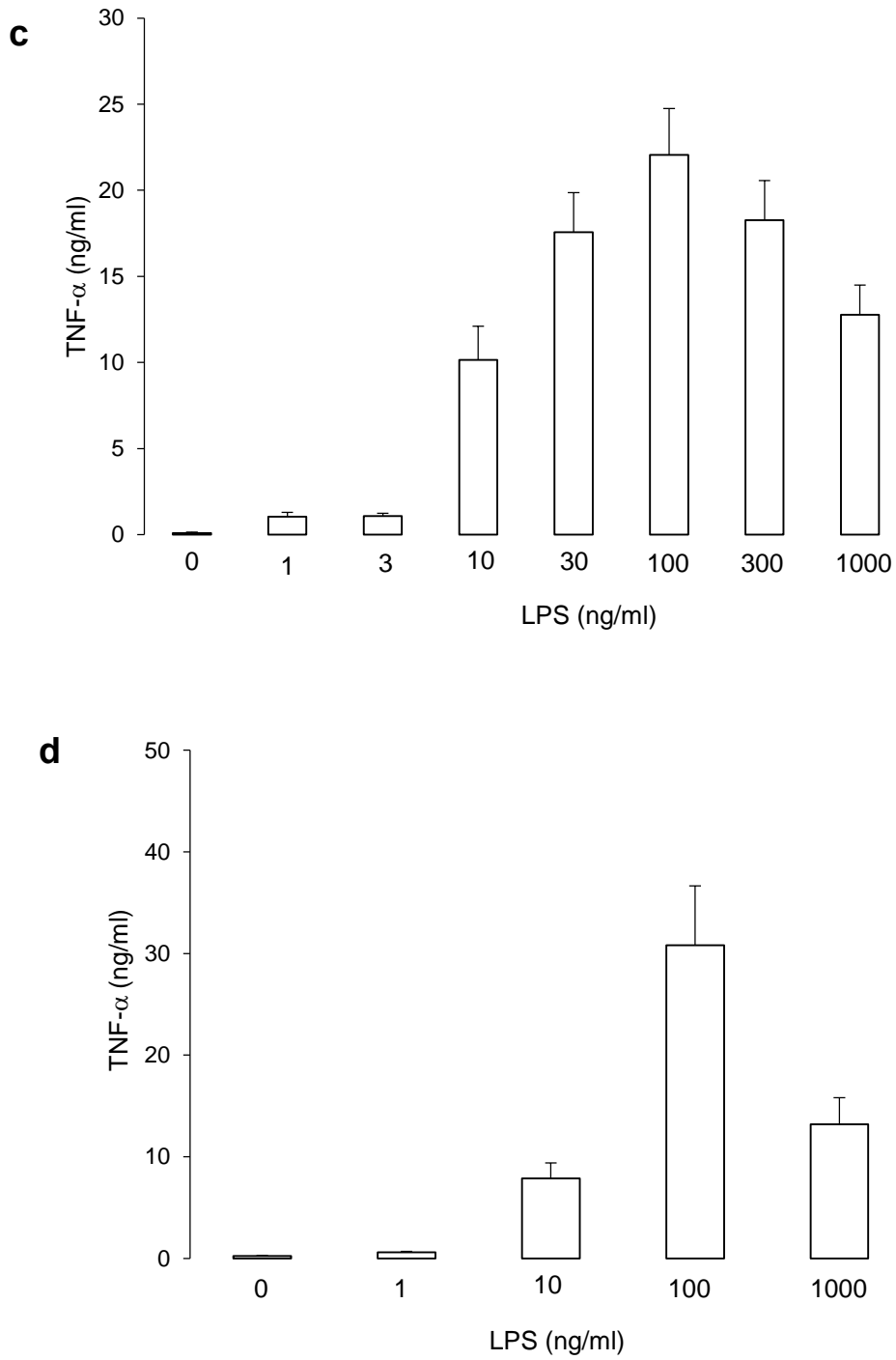
a

b

Figure 3-1 TNF-α release from LPS activated macrophages

RAW264.7 macrophages were treated with 0-1000 ng/ml LPS for a) & c) 4 hours or b) & d) 24 hours. TNF-α in conditioned was media measured by ELISA. Bars show mean+SEM (n≥3). a) & b) shows result from one experiment with n=4. c) & d) show combined data from 3 experiments.

a

b

c

d
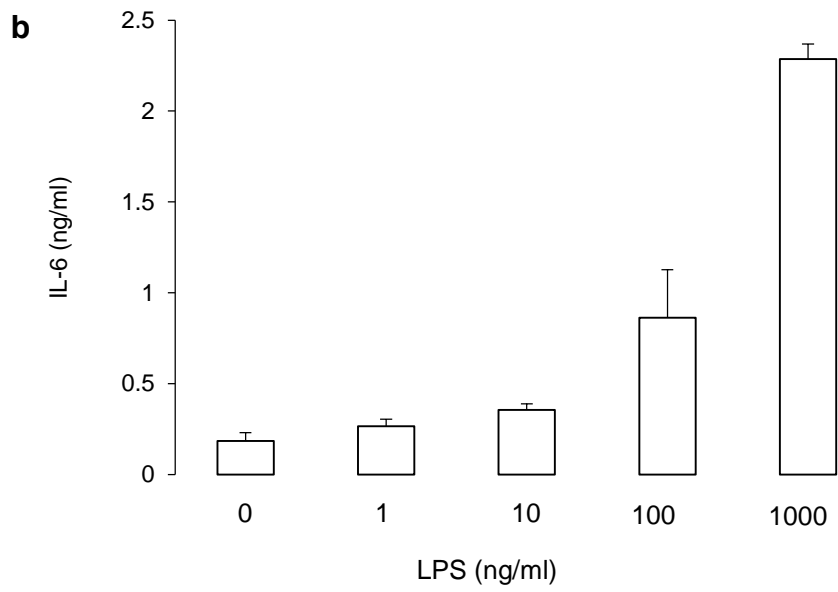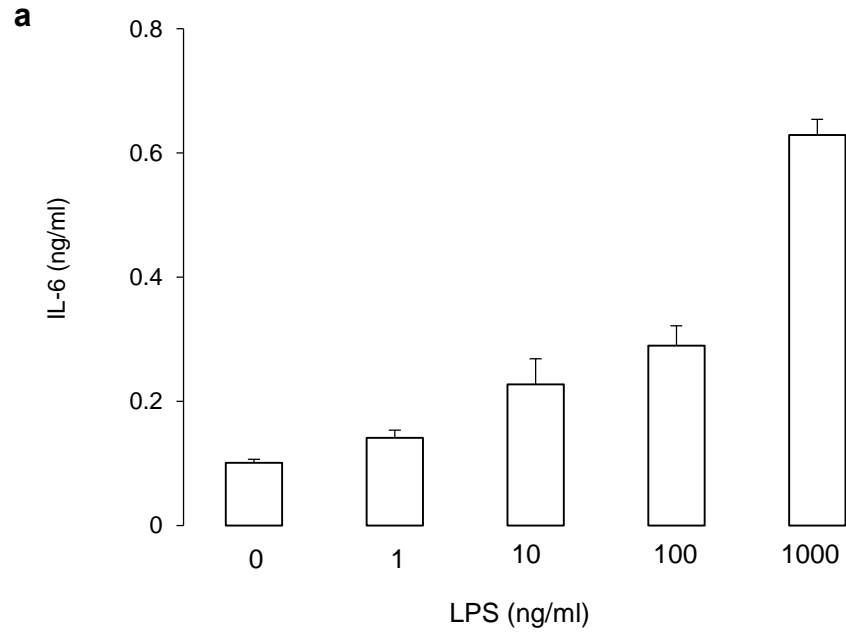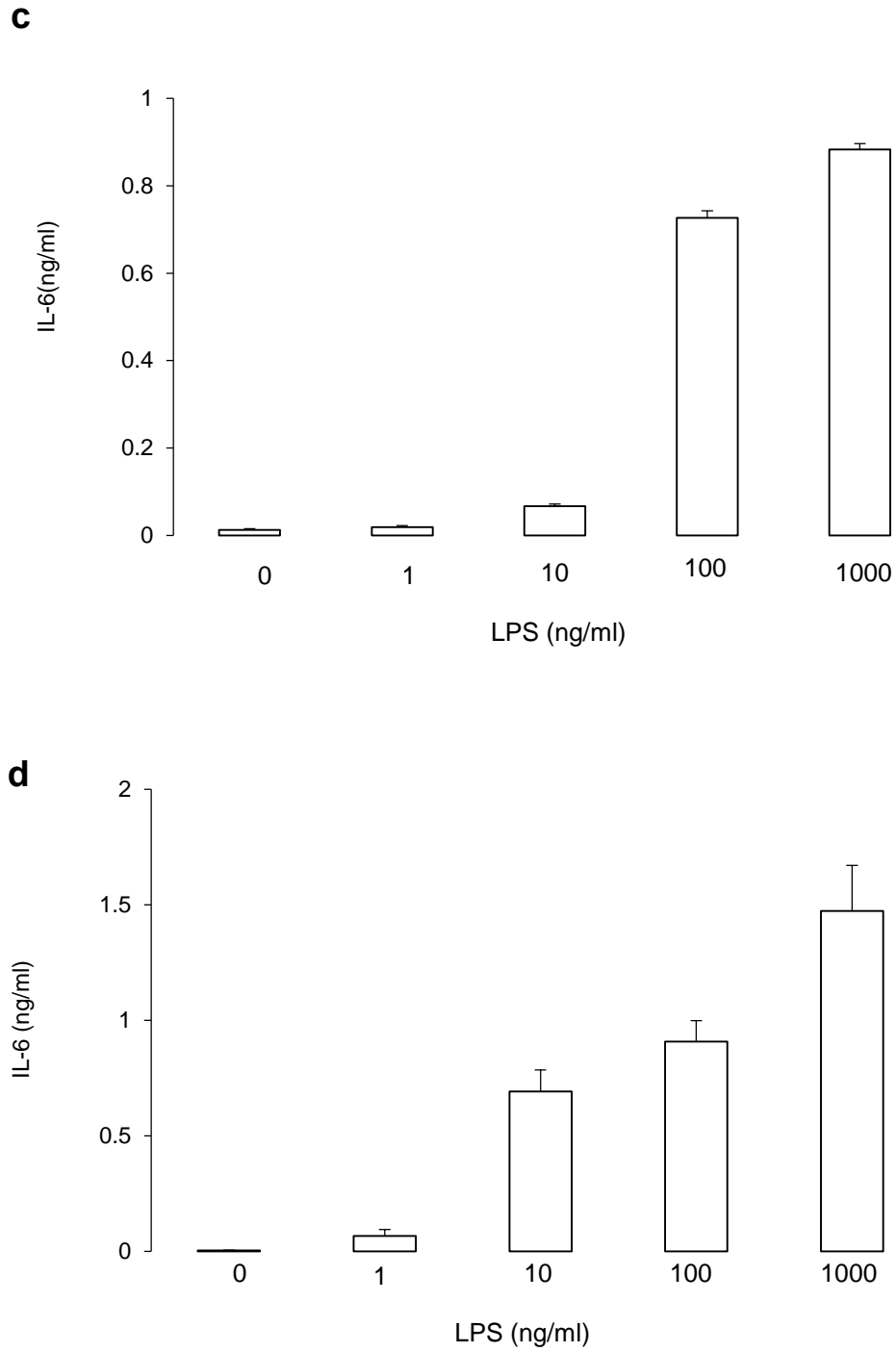
Figure 3-2 IL-6 release from LPS activated macrophages

RAW264.7 macrophages were treated with 0-1000 ng/ml LPS for a) & c) 4 hours or b) & d) 24 hours. IL-6 in conditioned was media measured by ELISA. Bars show mean+SEM (n≥3). a) & b) shows result from one experiment with n=3. c) & d) show combined data from 3 experiments.

a

b

c

d
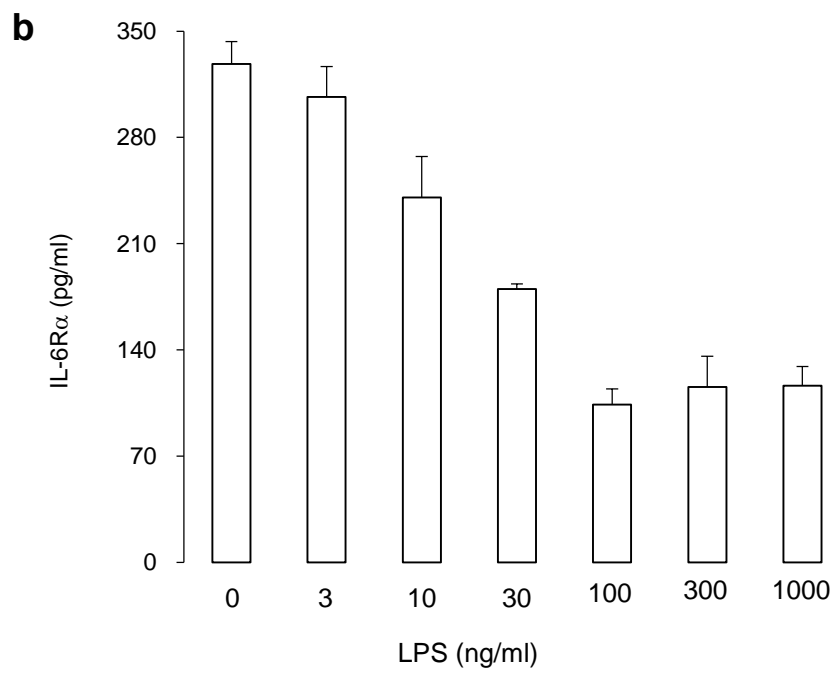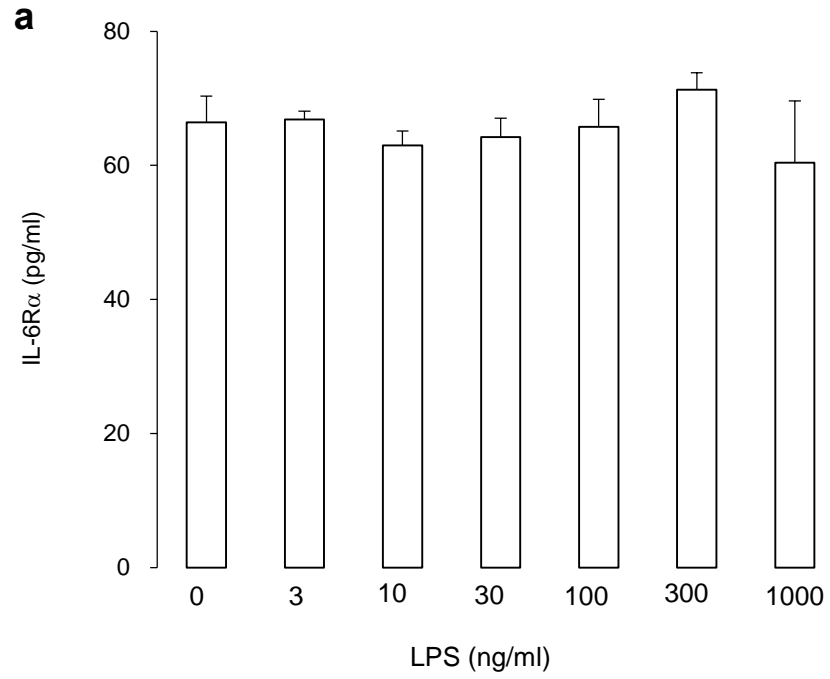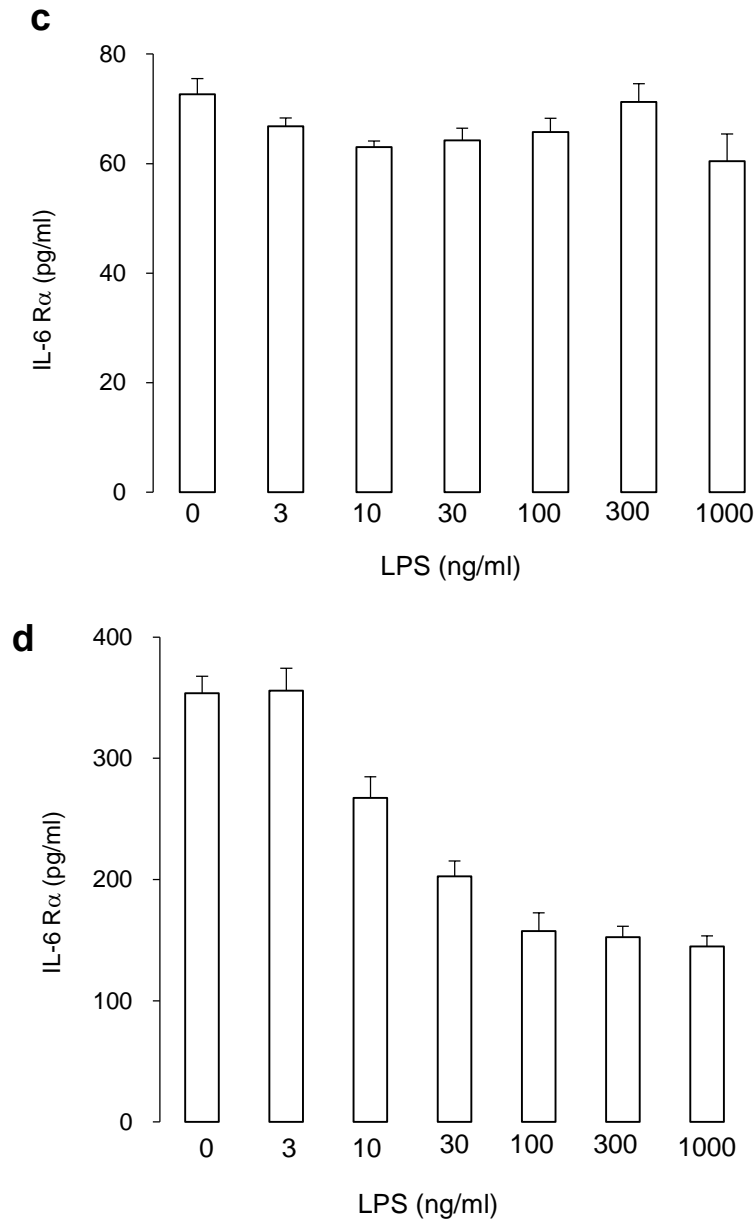
Figure 3-3 IL-6Rα release from LPS activated macrophages

RAW264.7 macrophages were treated with 0-1000 ng/ml LPS for a) & c) 4 hours or b) & d) 24 hours. IL-6Rα in conditioned was media measured by ELISA. Bars show mean+SEM (n≥3). a) & b) shows result from one experiment with n=3. c) & d) show combined data from 3 experiments.

a

b

c

d
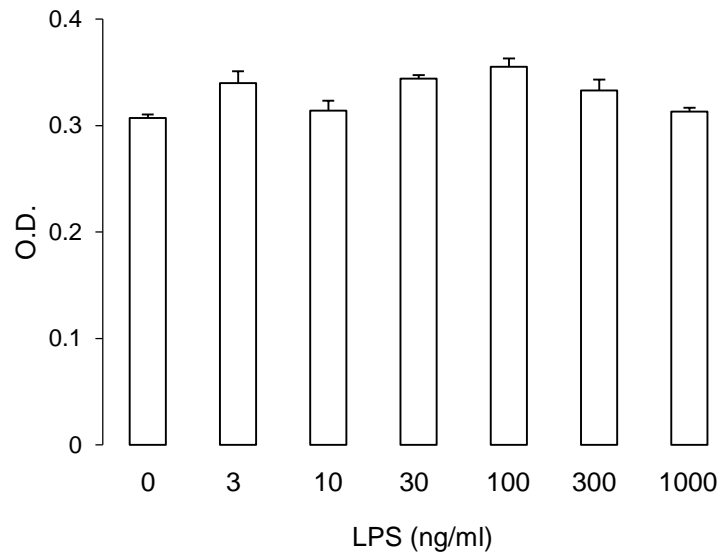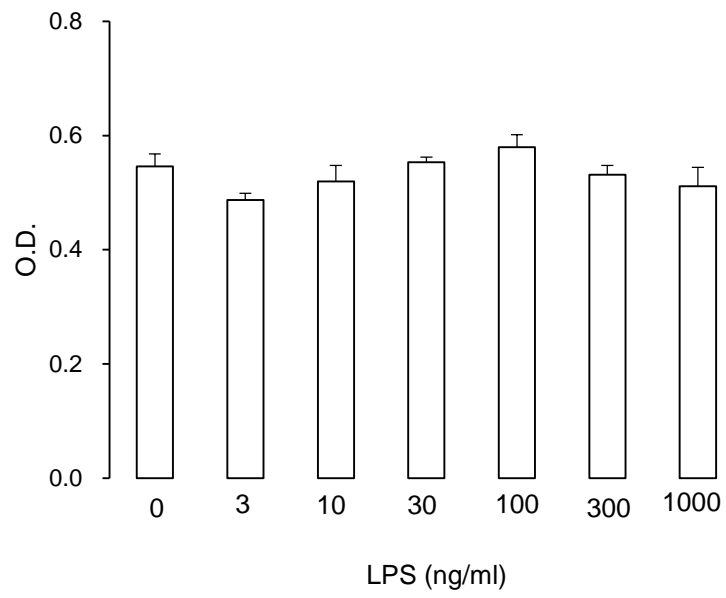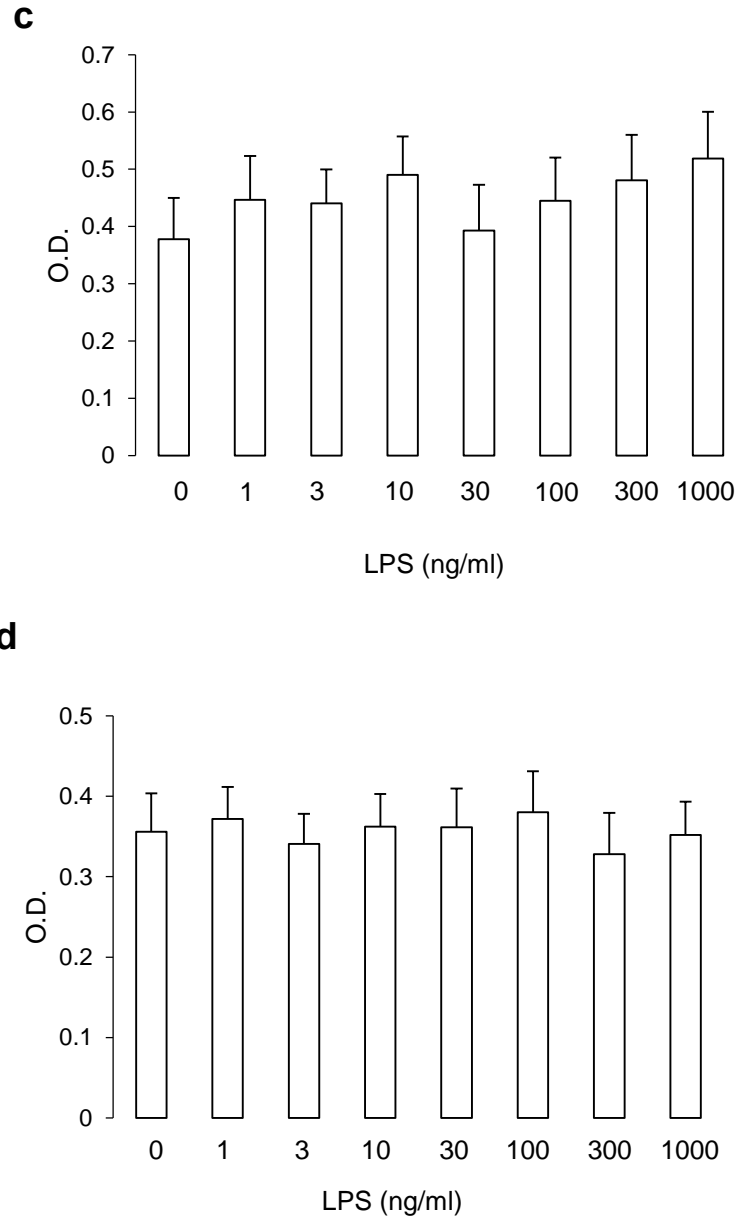
Figure 3-4 Effect of LPS treatment on macrophage cell viability

RAW264.7 macrophages were treated with 0-1000 ng/ml LPS for a) & c) 4 hours or b) & d) 24 hours. Cell viability was assessed by MTT. Bars show mean+SEM (n≥3). a) & b) show the result from one experiment with n=4 and c) & d) show combined data from 3 experiments.

### 3.3   Discussion

Ligation of LPS to TLR4 initiates inflammatory signalling cascades via intercellular adaptor proteins, MyD88 and/or TRIF, leading to the activation of transcription factors and the initiation of gene transcription. The transcription factors activated after LPS treatment include NF-κB, AP-1 and IRFs (Kawai and Akira, 2006; Watters *et al.*, 2007). The activation of these transcription factors leads to the induction of inflammatory molecules including TNF-α and IL-6. RAW264.7 macrophages are known to express TLR4 (He *et al.*, 2016). In agreement with previous observations, the results demonstrated that macrophages released increasing amounts of TNF-α and IL-6, upon the activation of TLR4.

TNF-α is a potent pro-inflammatory cytokine and the elevated levels of this cytokine are associated with much inflammatory pathology. TNF-α binds to TNFR1 and TNFR2 expressed on the plasma membrane of cells. Ligation of these TNF-α receptors ultimately causes the activation of NF-κB which results in the activation of further inflammation i.e. a positive feedback loop is established. TNF-α also acts directly on the hypothalamus, stimulates the release of corticotrophic releasing hormone and induces fever (Aggarwal *et al.*, 2012; Croft *et al.*, 2013).

TNF-α release was increased in a dose dependant manner up to 100 ng/ml LPS and began to decrease above 100 ng/ml LPS in RAW264.7 macrophages. However LPS did not affect the viability within the dose range, 1-1000 ng/ml, over 24 hours. Therefore the reduction in TNF-α release was unlikely to be due to the toxicity of LPS but possibly by other mechanisms. It is known that there are negative regulators of TNF-α production. For example, IL-10 released from macrophages is known to down-regulate the release of proinflammatory cytokines including TNF-α. Synaptotagmin XI (SytXI) is a specific inhibitor of TNF-α. SytXI has been shown to inhibit the fusion of TNF-α with the plasma membrane therefore decreasing the expression of the cytokine on the membrane. This, in turn, results in the decreased release of TNF-α from the cell (Duque *et al.*, 2013). It is possible that the decrease in TNF-α release at high concentration of LPS which has been observed in this section could be due to the activation of negative regulators rather than cell death.

IL-6 is known to exhibit both pro-inflammatory and anti-inflammatory effects. IL-6 signals through a receptor consisting of IL-6Rα in combination with gp130. IL-6Rα can be found as both soluble and membrane bound form with IL-6 being able to bind to either forms. The binding of IL-6 to either the soluble or membrane bound form of the receptor can leads to the activation of distinct signalling pathways which exert different biological responses. Signalling via soluble IL-6Rα, termed trans-signalling, elicits pro-inflammatory effects such as the increase in fever and induction of acute phase proteins. The trans-signalling is known to be important in the maintenance of T cells by inhibiting apoptosis of T helper 17 cells and promoting the development of regulatory T cells. Signalling via membrane bound IL-6Rα, is termed classical signalling, and known to be regenerative, mediating tissue remodelling (Hunter and Jones, 2015). IL-6 release from RAW264.7 macrophages continued to increase at the highest dose of LPS, which differed from TNF-α release. This phenomenon suggested that TNF-α and IL-6 have distinct mechanisms for controlling their release the downstream of TLR4 activation.

A previous report using RAW264.7 macrophages showed that IL-6 and TNF-α have differing production kinetics on their release, due to the segregation of TNF-α and IL-6 into different vesicles (Manderson *et al.*, 2007). The results in this chapter supported this idea of different kinetic in the release of TNF-α and IL-6. With 100 ng/ml LPS stimulation, the concentration of released TNF-α in media at 4 hours was 32.6 ng/ml, and 41.7 ng/ml at 24 hours. This result showed that the first 4 hours of activation accounts for 75% of total TNF-α release over 24 hours. IL-6 level was 0.63 ng/ml at 4 hours and 2.3 ng/ml at 24 hours suggesting that 27% of total IL-6 release in 24 hours was occurred during the first 4 hours i.e. suggesting a linear production of the cytokine over 24 hours. However, this analysis does not take into account the possible breakdown of these cytokines in the culture. Although the breakdown of cytokines has been poorly investigated, it is possible that TNF-α may have a faster decay rate than IL-6 in the system, although in this instance the decay of TNF-α would not be the same rate throughout the 24 hours.

It is known that IL-6Rα, a receptor for IL-6, is constantly released from macrophages and found at nM level in normal human serum (Jones et al., 2001). In line with this, culture media from resting RAW264.7 macrophages contained IL-6Rα. However,

LPS treatment appeared to inhibit the release of IL-6Rα at 24 hours in dose dependant manner and this inhibition in IL-6Rα release by LPS appeared at only later time point at 24 hours. It must be noted that there are few studies which characterized the release of IL-6Rα in macrophages. One possible explanation for the observed reduction in IL-6Rα release at later time point could be due to the binding of IL-6 to the IL-6Rα, which sharply increased after 24 hours of LPS stimulation. In this scenario the IL-6/IL-6Rα complex could not recognised by ELISA. This was tested in the laboratory and found that the addition of 3 ng/ml IL-6 only reduces the measurement in pg/ml range for IL-6Rα by 5%. Therefore the interference with IL-6 was not likely to be the cause of the reduction in IL-6Rα measurement, but suggests this reduction may be due to another biological effect. The control of IL-6 trans-signalling is of great interest in the treatment of autoimmune diseases and it is important to investigate further.

This chapter characterised the release of TNF-α, IL-6 and IL-6Rα from RAW264.7 macrophages during TLR4 activation. Next chapter investigated the BK channel expression in RAW264.7 macrophages.

Chapter 4 Do macrophages express BK channels and does TLR4 activation affect the channel expression?

4.1   Introduction

The aim of this chapter is to characterise the expression of BK channels in RAW264.7 macrophages. The expression, sub-cellular location of BK channels, the expression level and functionality were studied using immunofluorescence imaging, Western blot analysis and electrophysiological recordings. Macrophages are known to be plastic in nature with immune stimuli dramatically alter their phenotypes (Mosser and Edwards, 2008). It was hypothesised that immune activation may alter the expression of ion channels in macrophages. The BK channel expression was therefore characterised in LPS activated macrophages as well as in resting macrophages.

4.2   Results

4.2.1   BK channel expression in resting macrophages

Western blot analysis

Two antibodies against mouse BKα subunit, a rabbit polyclonal antibody, APC-107, and mouse monoclonal antibody, L6/60, were used in Western blot analysis of BKα in RAW264.7 macrophages. Both antibodies are designed to bind to the C-terminal region of BKα. Both primary antibodies detected the presence of protein bands at approximately 120 kDa in whole cell lysate from resting RAW264.7 macrophages, Figure 4-1 and Figure 4-2. Using the L6/60 antibody resulted in the appearance of doublet bands at 110 to 120 kDa, Figure 4-2. Protein bands at approximately 120kDa also appeared in rat brain lysates, Figure 4-2. For both APC-107 and L6/60 protein bands appeared at 100, 80, 60, 46, 32, and 25 kDa in whole cell lysates of RAW264.7 macrophages. However the lower band intensity appeared less than the band at 120 kDa when L6/60 was used. APC-107 gave less clear cut discrimination in signal intensities between the higher and lower molecular weight band, Figure 4-1 and Figure 4-2. In rat brain lysate, major bands appeared between 120-140 kDa. Lower protein bands at 110, 80, 45, 32 and 25 kDa were also appeared against both APC-107 and L6/60, Figure 4-1 and Figure 4-2.

When APC-107 was removed and the anti-rabbit IgG HRP-linked secondary antibody was applied on the membrane alone, most of the protein bands disappeared, although some faint bands could still be seen, Figure 4-1. When L6/60 was removed and anti-mouse IgG HRP-linked secondary antibody was applied alone, doublet bands between 110 to 120 kDa disappeared, Figure 4-2. Due to the specificity of L6/60 antibody for the 120 kDa band, which is predicted to be the complete BKα subunit, it was decided to use L6/60 to characterise BKα expression in following experiments.
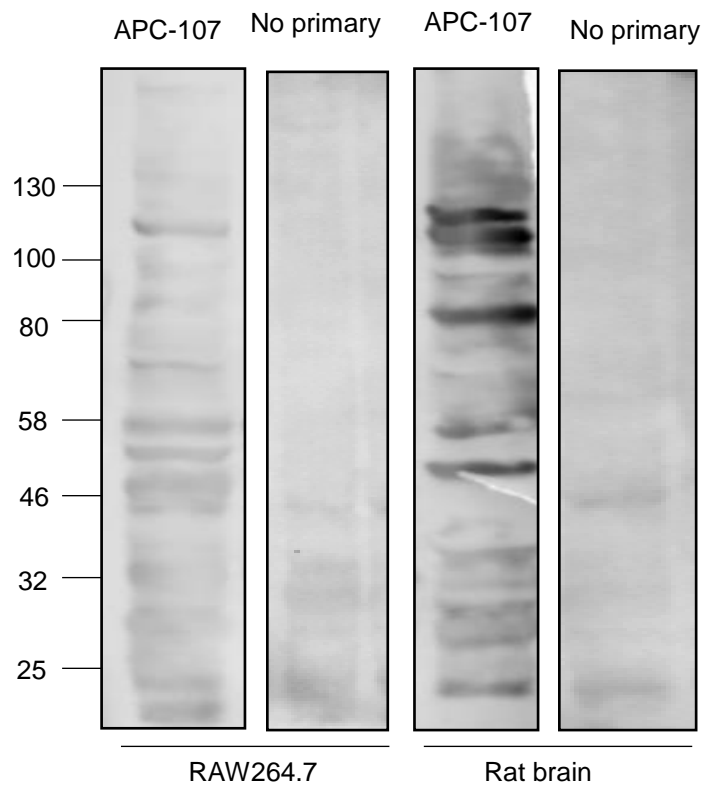
Figure 4-1 BKα expression in resting macrophages using a rabbit polyclonal anti-mouse BKα antibody, APC-107

BKα expression in the whole cell lysate of resting RAW264.7 macrophages (left) and rat brain (right) was analysed by Western blot using APC-107. No primary blot was made by omitting the primary antibody. Molecular marker in kDa is indicated in far left. 10 μg protein was loaded each lane. The experiment was repeated twice.
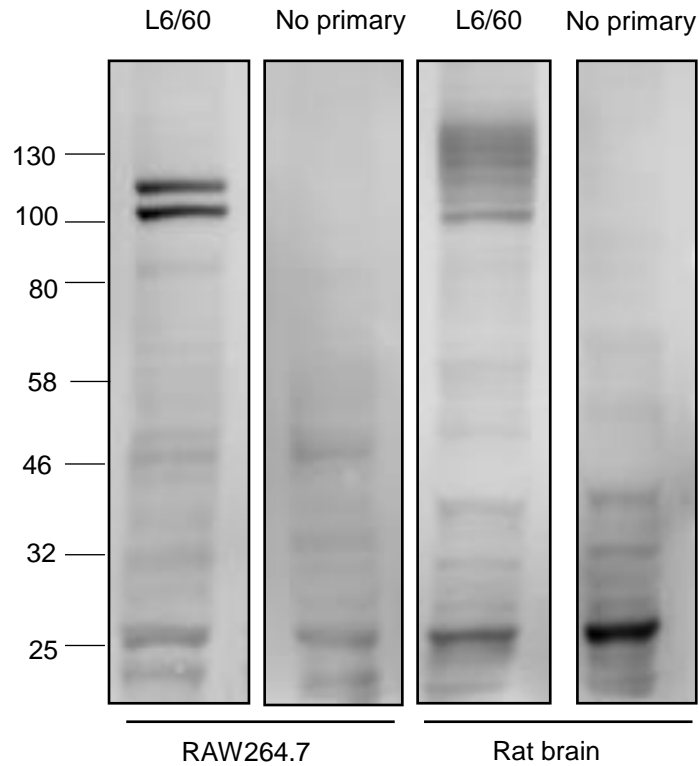
Figure 4-2 BKα expression in resting macrophages using a mouse monoclonal anti-mouse BKα antibody, L6/60

BKα expression in whole cell lysate of resting RAW264.7 macrophages (left) and rat brain (right) was analysed by Western blot using L6/60. No primary blot was made by omitting the primary antibody. Molecular marker in kDa is indicated in far left. 10 μg protein was loaded each lane. The experiment was repeated 5 times.

Immunolocalisation

The subcellular location of BK channels in resting RAW264.7 macrophages was analysed by immunofluorescence imaging techniques. BKα in the cells was analysed using L6/60. DAPI staining displayed nuclei in resting RAW264.7 cells, and positive staining for BKα were found in the nucleus, nuclear membrane and cytoplasm in resting macrophages, Figure 4-3. The plasma membrane appeared to be relatively free of BKα protein with only faint diffuse staining was seen, Figure 4-3. BKα was found to be associated with the nuclei BK in approximately 90% of resting macrophages, Figure 4-3.

a

Anti-BKα	DAPI	Merged	No primary

b
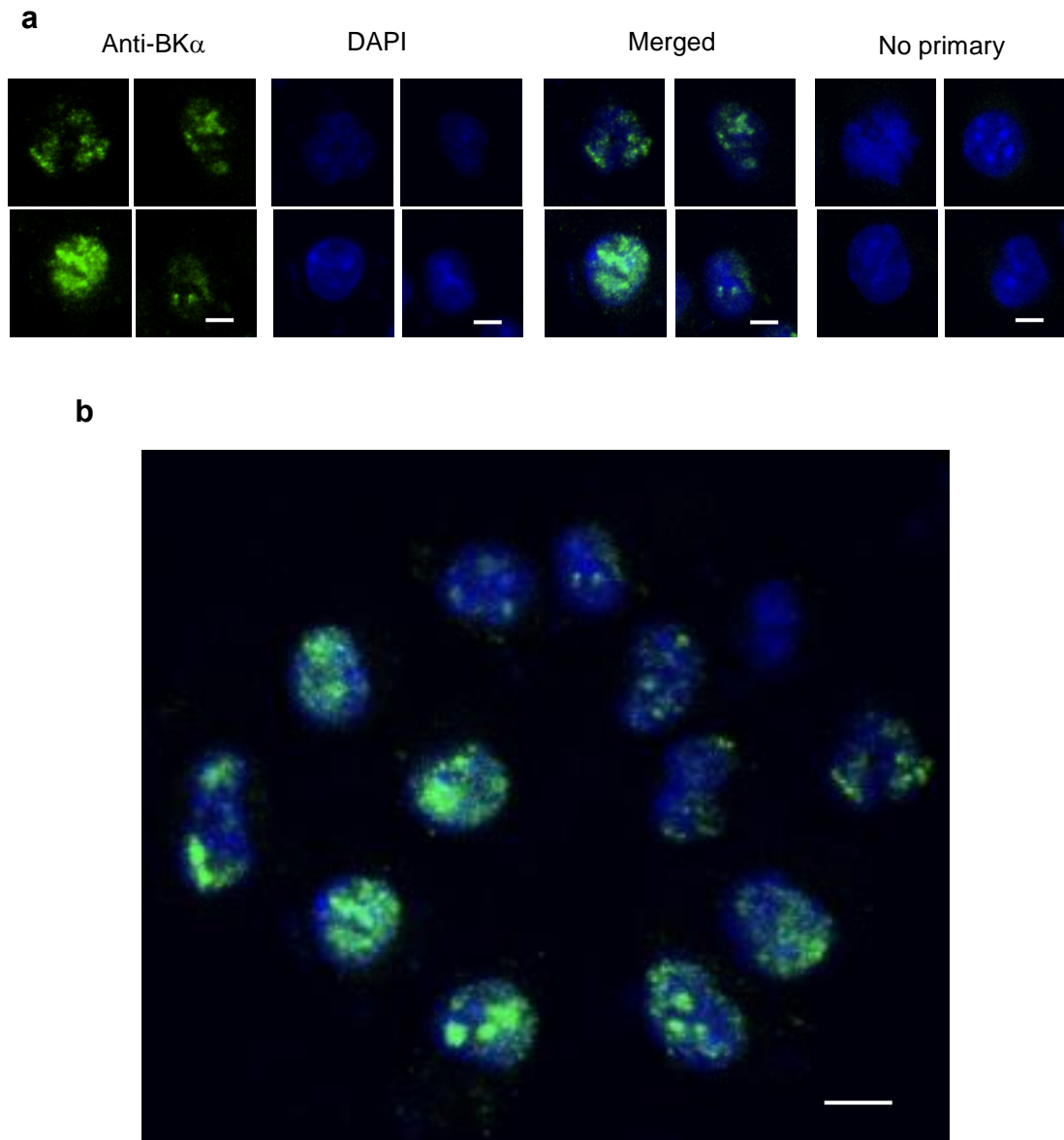
Figure 4-3 Localisation of BKα in resting macrophages

Resting RAW264.7 macrophages were paraformaldehyde fixed and stained for with DAPI (blue) and anti-BKα with L6/60 (green); merged DAPI+L6/60 and control in which there was no primary antibody but DAPI was present. a) single cell images (n=4, n: the number of cells) or b) area (n=11). Scale bar, 5μm. The experiment was repeated 4 times and images shown are representative. Pictures are taken from area containing approximately 15 cells.

Nuclei isolation

Nuclei from resting macrophages were isolated and analysed for BKα expression by Western blot. The blot indicated bands at 120 kDa and 80 kDa using L6/60 in samples of whole cell lysate and nuclei isolate. The protein band at 80 kDa in nuclei isolate appeared stronger than whole cell lysate, Figure 4-4.
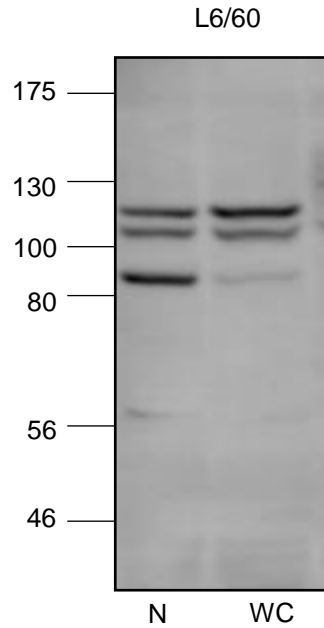
Figure 4-4 BKα expression in nuclei isolate of resting macrophages

BKα expression in nuclei (N) and whole cell (WC) lysates from resting RAW264.7 macrophages. 10 μg protein was loaded each lane. Left shows molecular weight marker in kDa. The experiment was repeated 3 times.

4.2.2 BK channels in TLR4 activated macrophages

In order to investigate if TLR4 activation changes the BK channel expression, macrophages were stimulated with LPS for up to 24 hours and the expression of BKα was analysed. In preliminary experiments, LPS was applied at the maximal dose, 150 ng/ml, however this resulted in a significant increase in membrane dynamics, see 4.2.3. Therefore 10 ng/ml LPS was selected to use to investigate the effect of TLR4 activation on the channel expression. This does of LPS, 10 ng/ml, had been shown to increase TNF-α and IL-6 release and decrease the release of IL-6Rα from RAW264.7 macrophages at 24 hours in chapter 3.

Immunolocalisation

In immunolocalisation studies, the major effect of stimulating RAW264.7 macrophage with LPS was the appearance of clusters of positive staining on some parts of the cell plasma membrane at 18 hours and 24 hours, the lack of DAPI staining at these clusters suggest it was not nuclei material. However the intensity of nuclei staining appeared to decrease after 24 hours of LPS treatment, while the proportion of cells showing nuclei staining remained approximately the same (83%; 10/12), Figure 4-5 and Figure 4-6.
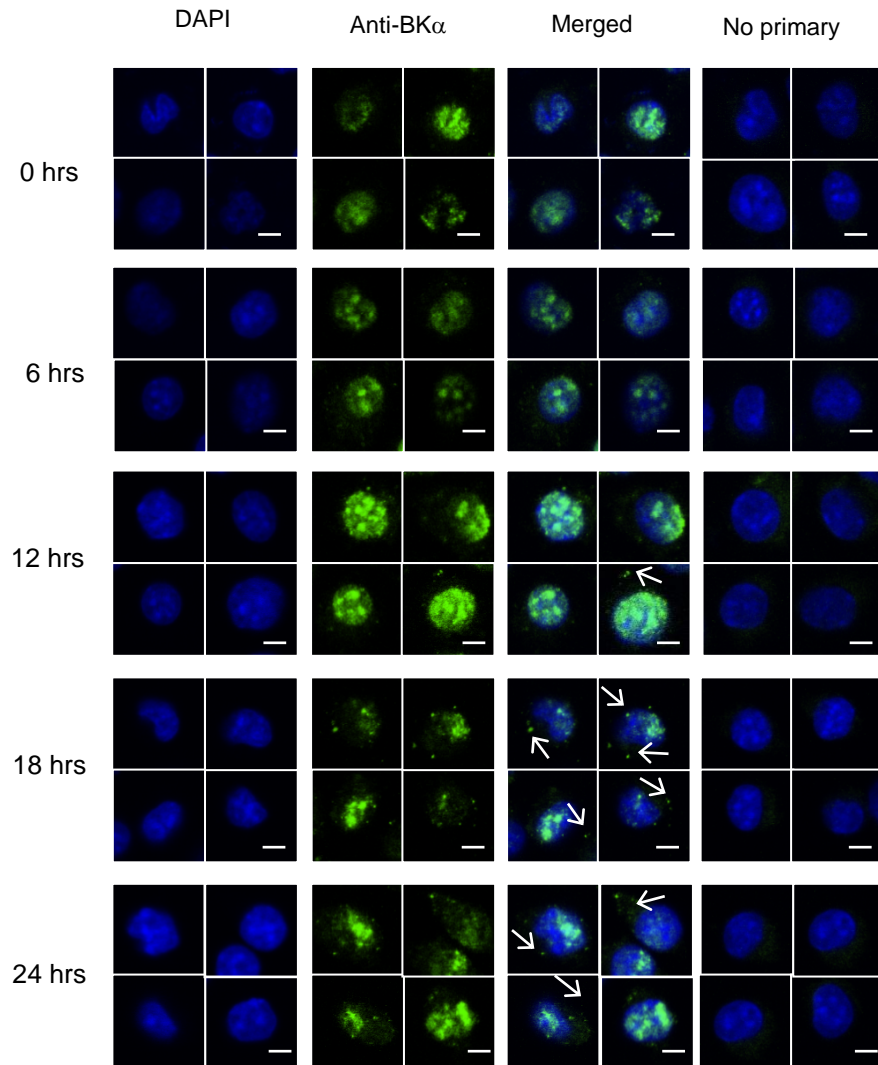
Figure 4-5 Localisation of BKα in LPS activated macrophages

RAW264.7 macrophages were activated with 10 ng/ml LPS and at indicated times cells were paraformaldehyde fixed and stained for nuclei with DAPI (blue) and anti-BKα with L6/60 (green); merged DAPI+L6/60 and control in which there was no primary antibody but DAPI was present. Scale bar, 5μm. Arrows indicate BKα staining on the plasma membrane. The experiment was repeated 3 times.
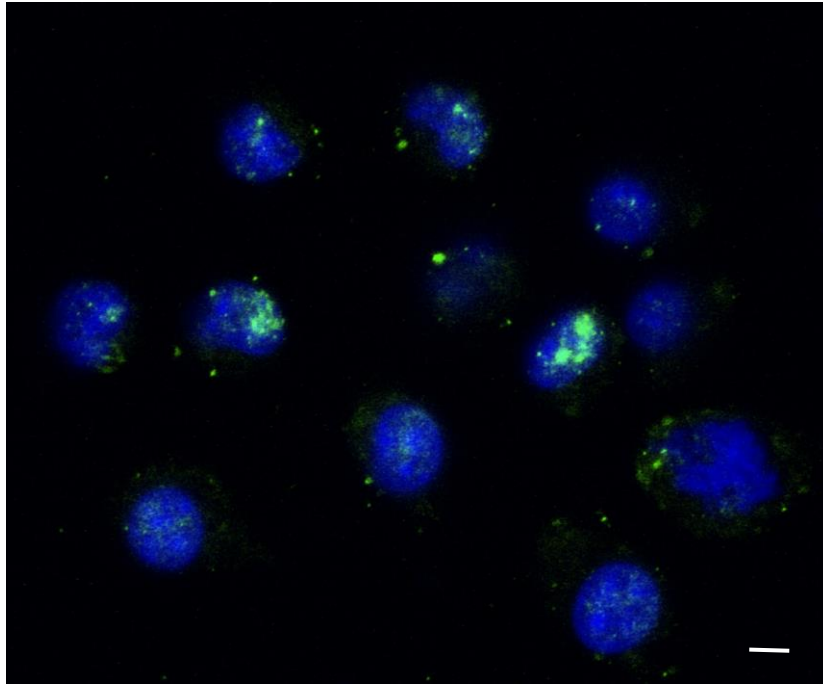
Figure 4-6 Localisation of BKα in LPS activated macrophages at population level

RAW264.7 macrophages were stimulated with 10 ng/ml LPS for 24 hours. Then the cells were paraformaldehyde fixed and stained for nuclei with DAPI (blue) and anti-BKα with L6/60 (green). Scale bar, 5μm. The experiment was repeated 4 times and image shown is representative. Pictures are taken from area containing approximately 12 cells.

Western blot analysis

To confirm the appearance of BK channel expression on the plasma membrane during TLR4 activation, whole cell protein and plasma membrane isolate from LPS activated RAW264.7 macrophages were analysed for BKα expression by Western blot. At whole cell level, BKα showed a small increase in expression after LPS treatment. Densitometry analysis showed that at whole cell level, the amount of BKα was increased by 25 % after 24 hours of LPS activation, N.S., Figure 4-7a and Figure 4-7c. In contrast, BKα was hardly detectable in isolated plasma membrane from resting RAW264.7 cells using the protocol described in 2.2.7. The expression of BKα on the plasma membrane increased during LPS treatment peaking around 18 hours, Figure 4-7b. The relative expression of plasma membrane associated BKα was 2.5 fold higher at 24 hour compared to that at 0 hour, p<0.05, Figure 4-7c.

a   WC

BKα
(120kDa)

β-actin
(42kDa)

Akt
(56kDa)

0   1   4   8   12   18   24

LPS (hrs)

b   PM

BKα
(120kDa)

β-actin
(42kDa)

Akt
(56kDa)

0   1   4   8   12   18   24   WC

LPS (hrs)

c
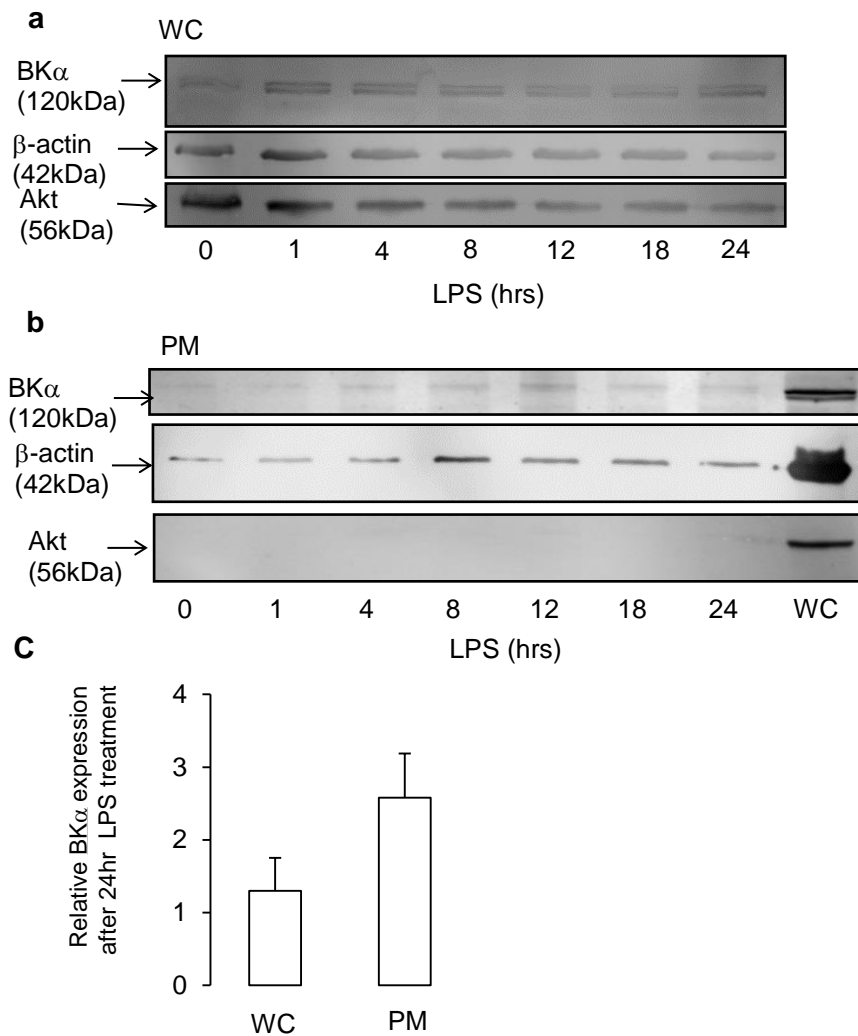
Figure 4-7 BKα expression in the plasma membrane isolate and whole cell lysate from RAW264.7 macrophages during LPS treatment

RAW264.7 macrophages were treated with 10 ng/ml LPS for up to 24 hours and a) whole cell (WC) and b) plasma membrane (PM) were collected. BKα expression, β-actin and Akt was analysed by Western blot. c) Densitometry analysis of relative BKα expression at 24 hours compared to at 0 hours. Bars represent mean+SEM, n=3, where n represents the number of blots used for analysis. The experiment was repeated 3 times.

4.2.3   Electrophysiological recording of resting and LPS treated macrophages

Whole cell voltage clamp experiments were performed to test for the functional BK channel expression on the plasma membrane of resting macrophages and macrophages activated with 10 ng/ml LPS for 24 hours. The following pharmacological reagents were used in electrophysiological recordings to study BK channel expression; 3 mM TEA, non-selective K^+ channel blocker, and 30 nM IbTX,

a BK channel selective inhibitor. Both reagents were applied in extracellular solutions for the justification of doses, see 4.3.

As mentioned in section 4.2.2, LPS was initially applied at the maximal dose at 150 ng/ml, however, at this maximal dose of LPS, macrophages were highly activated and became very difficult to make recordings from. This was due to an inability to make a stable seal with the electrode possibly because of the change in the membrane property. Therefore the submaximal dose of LPS was selected. Even after lowering LPS doses, it was to complete the cycle of drug treatments in macrophages and this limited the number of cells recorded in this thesis.

During the first series of experiments, the membrane properties of macrophages, probably the presence of pseudopodia prevented the formation of seal. To overcome this problem, a gentle air pressure applied into pipette using 1ml syringe when approaching cells. This is to repeal these pseudopodia and make relatively clean surface. This improved the formation of seal in the subsequent experiments.

Initially pipette solutions were prepared with 640 nM free Ca^{2+} in K^+-gluconate based solution, however, it was found that it was found difficult to determine free K^+ ions in the solution and this interfered with the data analysis. It was also suggested to increase the concentration of free Ca^{2+} for the activation of the channel. Therefore the pipette solution was changed to K^+-acetate based pipette solution, see Table 2-2, with 1.6 μM. free Ca^{2+}. Pipettes with various resistances from 2 to 4.5 MΩ were tested in RAW264.7 macrophages and it was decided to use pipette with the resistance between 3.5 and 4 MΩ.

3 mM TEA did not affect the whole cell current during voltage clamp (-100 mV to 40 mV, duration 10 s, Figure 2-5) in the majority of resting macrophages. In separate experiments, only 8.7% of resting macrophages had a K^+ current which was sensitive to 30 nM IbTX. After 24 hours of LPS treatment, the proportion of cells expressing TEA sensitive current increased. Importantly 30 nM IbTX blocked K^+ current in 41.5% macrophages. The 0 current potential of the I-V plot indicated both TEA and IbTX sensitive currents were carried via K^+ ions, Figure 4-8 and Figure 4-9.
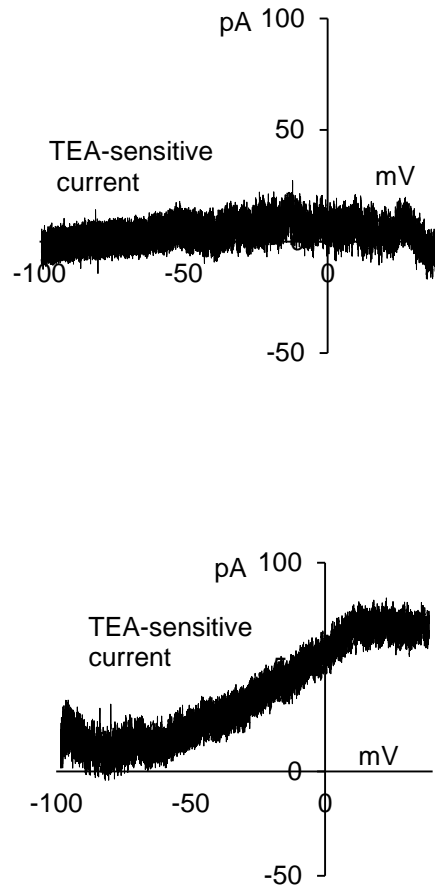
Figure 4-8 I-V plot of whole cell TEA-sensitive current in macrophages

Representative traces of TEA-sensitive current obtained by whole cell recordings from resting RAW264.7 macrophage or RAW264.7 macrophage stimulated for 24 hours with 10 ng/ml LPS. Voltage ramp (-100 mV to +40 mV, duration 10 s) was applied in presence or absence of 3 mM TEA in the extracellular solution. Representative graphs of TEA-sensitive current. The ramp protocol was run in individual cells at least 6 times per drug treatment and these traces were averaged. Sensitive currents were obtained by subtraction of traces with drug treatment from control traces and plotted against membrane voltage.
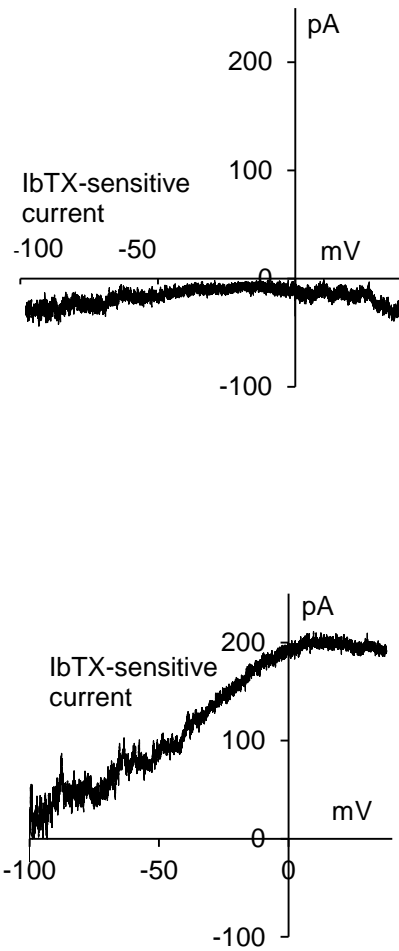
Figure 4-9 I-V plot for whole cell IbTX sensitive current in macrophages

Representative traces of IbTX-sensitive current obtained by whole cell recordings from resting RAW264.7 macrophages or RAW264.7 macrophages treated for 24 hours with 10 ng/ml LPS. Voltage ramp (-100 mV to +40 mV, duration 10 s) was applied in presence or absence of 30 nM IbTX in the extracellular solution. Representative graphs of IbTX-sensitive current. The ramp protocol was run in individual cells at least 6 times per drug treatment and these traces were averaged. Sensitive currents were obtained by subtraction of traces with drug treatment from control traces and plotted against membrane voltage.

LPS treatment	BK current present	Resting potential	Current amplitude of BK current at 0 mV
none	8.7%(2/23)	-60 to -50 mV (11 cells) -30 to -40 mV (7 cells) 0 to +10 mV (4 cells)	50 to 100 pA (1 cell) 150 to 200 pA (1 cell)
24 hrs	41.2% (7/17)	-60 to -50 mV (9 cells) -30 to -40 mV (4 cells) 0 to +10 mV (4 cells)	50 to 100 pA (2 cells) 100 to 150 pA (2 cells) 150 to 200 pA (3 cells)

Table 4-1 Summery of whole cell recordings in resting and LPS treated RAW264.7 macrophages

RAW264.7 macrophages received no treatment or received 10 ng/ml LPS for 24 hours prior to patch-clamp experiments. The percentage and the number of cells which expressed 30 nM IbTX-sensitive whole cell K^+ current /the total numbers of cells recorded are described.

4.3 Discussion

BK channels are expressed in various cellular locations including the plasma membrane, mitochondrial membrane and nuclear membrane. These channels are known to have location specific roles in cell biology (Xu *et al.*, 2002; Hoshi *et al.*, 2013; Li *et al.*, 2014; Balderas *et al.*, 2015). In addition, the gating properties of the BK channel are altered by tissue specific expression of accessory β- and/or γ-subunits or BKα gene splicing (Yan & Aldrich, 2010; Orio, et al., 2002). Endogenous molecules, such as proton, Heme, carbon monoxide and arachidonic acid also affect activation states of the channels (Hou, et al., 2009). Due to the variations in the localisation and differing opening properties of the BK channel, their expression pattern must be carefully examined before studying their biological roles.

The aim of this chapter was to characterise the expression of BK channel in resting and TLR4 activated RAW264.7 macrophages. This was investigated using three different techniques. Immunofluorescence imaging was used to visualise the subcellular location of BKα protein. Western blot analysis of the cellular fractions semi-quantified the BKα expression levels, indicated any possible splice variants and also confirmed the pattern of the cellular localisation observed in the immunofluorescence staining. Because of the various forms of post-translational regulation of the ion channels (Kyle and Braun, 2014), the mere existence of channel protein does not confirm that the channel is functional as an ion channel. Therefore, the whole cell voltage clamp experiment was performed to test the expression of the plasma membrane located channels.

In electrophysiological recordings, the assessment of the channel expression was mainly determined by its pharmacological properties. Two types of K^+ channel blockers were used, TEA and IbTX. TEA blocks most types of K^+ channels from both sides of lipid bilayer membranes in a voltage dependent manner and is known to exhibit higher affinity for BK channels compared to other types of K^+ channels (Yu et al., 2016). IbTX is a peptide toxin of 37 amino acid in length and is highly selective for BK channel. This toxin is membrane impermeable and blocks the channel pore from the outside. This drug is selective for BK channels located on the plasma membrane at concentrations at 100 nM and below (Galvez, et al., 1990).

The results from immunofluorescence imaging and Western blot analysis of cellular fractions consistently indicated the presence of BKα protein in resting RAW264.7 macrophages. Immunofluorescence images showed that BKα was predominantly associated with the nucleus and its surrounding region of cytoplasm. The BKα positive staining was hardly detectable on the plasma membrane in resting macrophages. This expression pattern was confirmed by Western blot analysis of the cellular fraction of the plasma membrane and nuclei. The expression of BK channels on nuclear membrane has been reported in neurons (Li *et al.*, 2014), however, this is the first time the expression of nuclear BK channels in macrophages has been reported to my knowledge. Consistent with the biochemical analysis, the electrophysiological recordings with TEA and IbTX also showed that few resting macrophages express functional BK channels on the plasma membrane.

However, there was a noticeable change in the expression of plasma membrane BK channel during LPS activation. BKα positive staining of distinct areas of the plasma membrane was observed in the immunofluorescence image between 18-24 hours of LPS stimulation. BKα staining pattern on the plasma membrane of macrophages resembled the channel clustering, which has been reported in central principal neurons of rats and mice (Kaufmann *et al.*, 2010). Western blot analysis also showed an increased expression of BKα protein in the plasma membrane isolate after LPS activation, with the relative expression at 24 hours was 2.5 fold higher than that of resting macrophages. An increase BKα expression was also observed at whole cell level; however, the magnitude of increase was 25%, which was 10 times smaller than that seen for the plasma membrane.

It was noted by a number of experienced electrophysiologists in the department that RAW264.7 macrophages were a particularly difficult cell to path-clamp. First, it was difficult to form GΩ seals. This may be due to the fact that the plasma membrane of macrophages is comparatively dynamic in nature. This property is important in the process of phagocytosis, however may have resulted in the difficulty in forming stable seal between the electrode and the membrane. Secondly the tip of electrode was often blocked by fine pseudopodia on macrophages. On the other hand, it was required to use a thin walled grass electrode in order to achieve effective dilation of cytoplasm, however this may have increased a chance of pseudopodia to slip into

the electrode. This condition was slightly improved by applying gentle air pressure to the pipette electrode when approaching a cell, to repeal the uneven structure of macrophage membrane such as pseudopodia. Even though, the percentage of cells, which completed the recording cycle, composed of approximately 20 ramps, was estimated to be approximately 3% of the total cells attempted. This highlights possible sampling problems when conducting electrophysiological studies of macrophages and their phenotypes. This problem became even more evident in LPS stimulated cells. The activation of cells is known to alter the cell surface molecule expression and membrane properties. It is possible that the plasma membrane of macrophages became more fluid and dynamic after TLR4 activation. It would be important to develop technique to achieve stable recordings in these cells. Possible experiments would be resting the cells in normal culture media for 1 hour after LPS activation to make them less active before carrying out recordings. It was also noticed that the cells which succeeded to record tended to share morphological characteristics. The macrophages existed in many shapes including spindly shape or round shape with various sizes. In this thesis, it was noticed that the recordings of macrophages with round shape were relatively successful compared to the cells with spindly shape. However as macrophages are heterogenic, the interpretation could be limited to these particular population. Again it would be important to develop techniques to consistently record these cells.

While technically challenging electrophysiological recordings did provide some evidence that the BK channel was upregulated on the plasma membrane in activated macrophages. The population of cells with TEA sensitive K^+ channel increased among macrophages treated with LPS for 24 hours. In line with this, the number of macrophages, which expressed IbTX sensitive K^+ current, increased 5 fold in LPS treated macrophages. Taken together, these results indicated that LPS activation led to an increase in the expression of functional BK channels on the cell surface in RAW264.7 macrophages. However it is important to note that not all macrophages upregulated BK channels on the plasma membrane during LPS activation. The upregulation of K^+ channels during immune cell activation has been observed in previous studies, suggesting a positive correlation between the immune cell activation and K^+ channel expression. The expression of K_{ir} currents was reported to increase after Phorbol 12-myristate 13-acetate (PMA) treatment in a mouse macrophage cell line J774.1 (Gallin and Sheehy, 1985) and mouse bone

marrow derived macrophages have been shown to induce the expression of K_{v1} type channel $\beta_{1.3}$–subunits after treatment with TNF-α (Vicente *et al.*, 2005).

Using two different BKα antibodies a protein band was detected in RAW264.7 macrophages at 120 kDa. This is close to the predicted molecule weight for mouse BKα protein of 130 kDa. However, it is important to note that studies often report the BKα being detected as a 120 kDa by Western blot analysis. When whole cell lysate is analysed, 120 kDa protein bands were observed as doublets in RAW264.7 macrophages. This doublet has been reported when using anti-BKα antibodies with rat brain tissue (Misonou *et al.*, 2006). However when plasma membrane isolates are analysed, the 120 kDa band is appeared in single band. It is possible that the doublet may result from various modifications of the channel, including mRNA splicing and glycosylation (Kyle and Braun, 2014). The absence of double band but repeated appearance of signal band in plasma membrane isolate could lead to assume that such modification occurs at different rate depending on channel cellular location. Further analysis with different cellular fractions may help to investigate the reason for doublet in whole cells and absence in plasma membrane isolate. Additional protein bands also appeared at smaller sizes, 110, 80, 60, 46, 32 and 25 kDa when using L6/60. Blots were the primary antibody was omitted indicated that these bands were likely due to non-specific binding of the secondary antibody. However, it cannot be totally exclude that a smaller sized BKα protein, possibly spliced variant, exists in the cell. To test this BKα mRNA expression could be analysed. When APC-107 was used bands at smaller sizes 60, 46, 32 and 25 kDa were also detected. Again removal of the primary antibody could not totally exclude the possibility that these where specific lower molecular weight BKα protein. Lower weights of BKα proteins have been reported in previous research. It is proposed that proteolysis of the C-terminal region of BKα occurs during the process of sample preparations and resulted in smaller fragments of 55 kDa and 25 kDa BKα (Knaus, et al., 1995) by a methodological effect. It is possible that this phenomenon occurred during the process of sample preparation in this thesis. However it is possible to say that both antibodies recognised a protein band at 120 kDa which appeared to be the regular form of the BKα protein.

It has been well appreciated that the co-expression of accessory subunits can alter the voltage dependence and Ca^{2+} sensitivity of BK channels (Hoshi, et al., 2013). In this study, the electrophysiological studies were limited to their pharmacological properties in RAW264.7 macrophages at whole cell level. I-V relation of the IbTX sensitive currents from macrophages described shallower I-V relationship, indicating the possibility that the BK channels on macrophages may have less voltage dependency compared to other cells. However this needs further investigation. It will be interesting to address the subunit expression in these cells by molecular and biochemical analysis and to characterise the electrophysiological properties of the channels in macrophages at the single channel level in the future.

In conclusion, BK channels are present in RAW264.7 macrophages. In the resting macrophages the channel are predominantly intracellular but sparse on the cell surface. TLR4 activation by LPS led to the upregulation of functional BK channels on the plasma membrane of these cells. In next chapter, the involvement of these plasma membrane located BK channels in the release of cytokine and cytokine receptors from TLR4 activated macrophages were studied.

Chapter 5 Does the plasma membrane BK channel have a role in TNF-α, IL-6 or IL-6Rα release from macrophages?

5.1 Introduction

Chapter 4 demonstrated that RAW264.7 macrophages express BK channels. In the resting condition or early time point of LPS activation, these channels are predominantly associated with intracellular sites with functional BK channels appearing sparse on the plasma membrane. However LPS treatment over 24 hours led to the appearance of the channels on the plasma membrane.

Functional BK channels have been described in different subcellular locations, including the mitochondrial membrane, nuclear membrane and plasma membrane and these studies have suggested the location specific roles for the channel (Xu *et al.*, 2002; Singh *et al.*, 2012; Hoshi *et al.*, 2013; Li *et al.*, 2014). The aim of this chapter was to investigate whether the plasma membrane expressed BK channels are involved in the release of TNF-α, IL-6 and IL-6Rα. These molecules were selected as they have been shown to be involved in the pathogenesis of a number of diseases, see chapter 1 and are current therapeutic targets for chronic inflammatory diseases.

First, the effect of BK channel blocking drugs, IbTX and paxilline on the release of these proteins from macrophages was investigated at a time when the expression of plasma membrane BK channels appeared low. This was done by applying these drugs on resting macrophages or during at the early time points, 0 to 4 hours of LPS stimulation. Second, the involvement of the plasma membrane BK channels in the release of these proteins was studied. This was done by treating macrophages with a low level of LPS for 24 hours prior to simulating with a higher dose of LPS. This protocol allows the investigation of the effect of BK channel blocking drugs on macrophage activation when the plasma membrane form of the BK channel is present.

5.2 Results

5.2.1 Effect of IbTX on TNF-α, IL-6 and IL-6Rα

IbTX is a water soluble peptide and is highly selective for BK channels. Previous studies have demonstrated that IbTX works at concentrations in nM range. Chapter 4 showed that 30 nM IbTX blocked BK-like currents and this concentration did not have any effect on cell viability. Therefore, this drug was applied at the concentrations from 3 to 30 nM. The macrophages were left unstimulated or stimulated with 10 or 150 ng/ml LPS for 4 hours with or without IbTX. This dose range was selected based on the results from chapter 3 & 4, which demonstrated that 10 ng/ml LPS caused the increase of BK channels on the plasma membrane. 150 ng/ml LPS caused maximal production of TNF-α. Proteins release from LPS stimulated macrophages was measured after 4 hours stimulation. The reasoning for this was that it had been shown that this time point was the optimum for TNF-α production in chapter 3. In addition, the expression of the plasma membrane BK channels was shown to be sparse at this time point after LPS stimulation, see chapter 4.

4 hours with IbTX, 3, 10 and 30 nM, did not induce the release of TNF-α or IL-6 nor alter the release of IL-6Rα from resting macrophages. The induction of TNF-α and IL-6 was below detection limit of ELISA kits, see section 2.2.11, and the level of IL-6Rα was 302+/-5.6 pg/ml in non-treated group and 304+/-12.7 pg/ml in the group treated with IbTX 30nM, Figure 5-1a. This indicated that the drug does not have a direct effect on the release of these proteins from macrophages. IbTX did not also change the release of TNF-α, IL-6 or IL-6Rα from macrophages activated with 10 ng/ml LPS. The level of TNF-α was 8.4+/-1.2 ng/ml from the group received 10 ng/ml LPS only and 8.1+/-1.6 ng/ml from the group received 10 ng/ml LPS and 30 nM IbTX, N.S., Figure 5-2a. The level of IL-6 was 0.44+/-0.45 ng/ml from the group received 10 ng/ml LPS only and 0.50+/-0.11 ng/ml from the group received 10 ng/ml LPS and 30 nM IbTX, N.S., Figure 5-2a. IL-6Rα was at 38.1+/-7.9 pg/ml from the group received 10 ng/ml LPS only and 44.0+/-11.4 ng/ml from the group received 10 ng/ml LPS and 30 nM IbTX, N.S., Figure 5-2a. Consistently, at 150 ng/ml LPS, IbTX did not alter the release of TNF-α, IL-6 or IL-6Rα. The level of TNF-α was 15.0+/-2.4 ng/ml from the group received 150 ng/ml LPS only and 15.6+/-1.2 ng/ml from the group received 150 ng/ml LPS and 30 nM IbTX, N.S., Figure 5-3a. IL-6 was at 0.62+/-0.017 ng/ml from the group received 150 ng/ml LPS only and 0.69+/-0.16

ng/ml from the group received 150 ng/ml LPS and 30 nM IbTX, N.S., Figure 5-3a. IL-6Rα was 32.9+/-5.7 pg/ml from the group received 150 ng/ml LPS only and 33.6+/-5.1 pg/ml from the group received 150 ng/ml LPS and 30 nM IbTX, N.S., Figure 5-3a. MTT assay indicated no effect on cell viability when it was applied alone or with either dose LPS, Figure 5-4a.

a
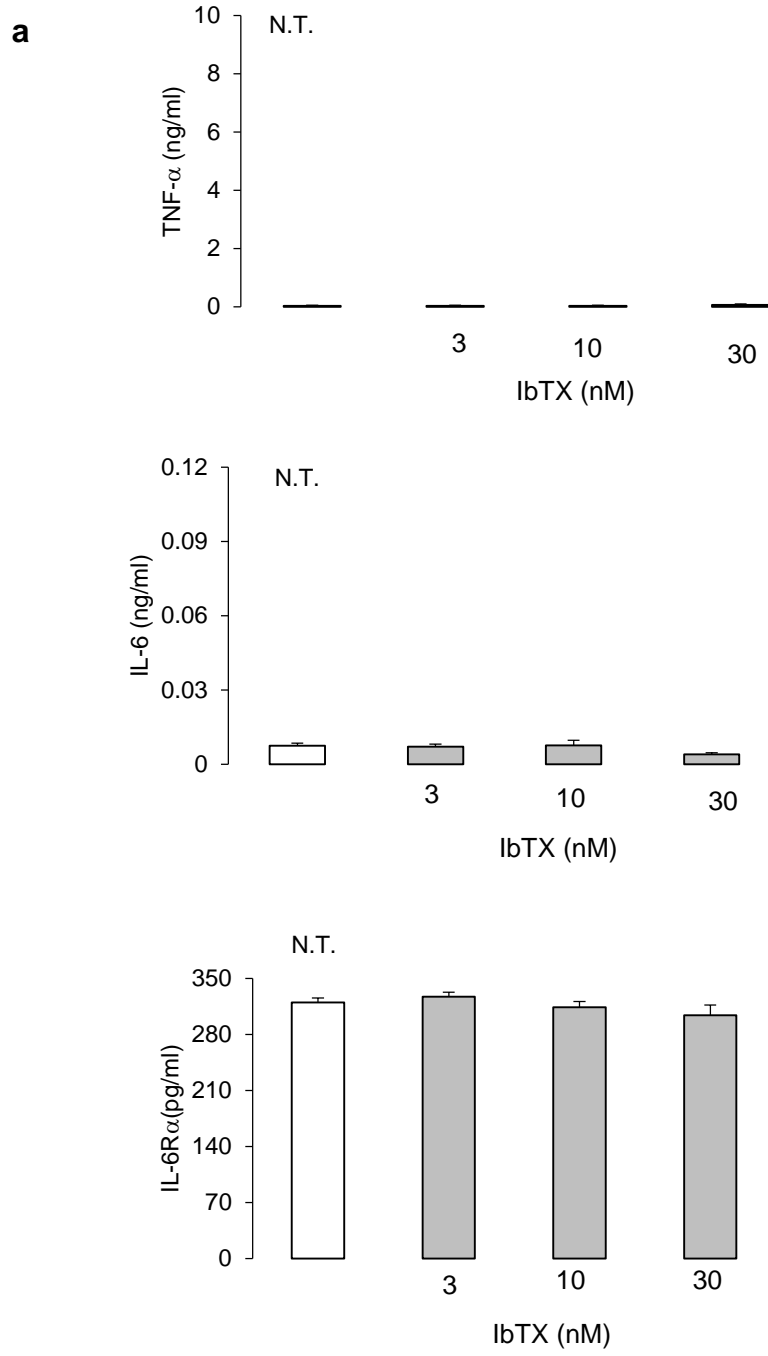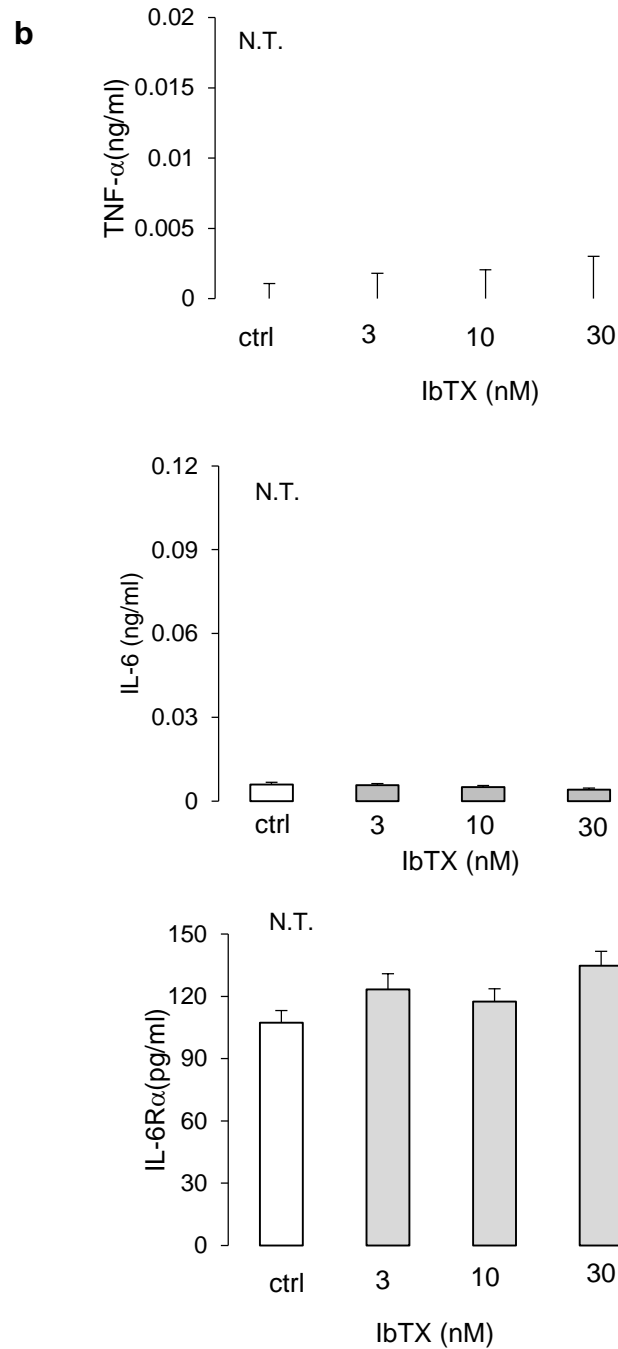
Figure 5-1 Effect of IbTX on TNF-α, IL-6 and IL-6Rα release from resting macrophages

RAW264.7 macrophages received 3-30 nM IbTX, shaded bars, or medium control, clear bar. After 4 hours culture media was collected. TNF-α, IL-6 and IL-6Rα in media was measured by ELISA. Bars represent mean+SEM (n≥3). a) shows results from one experiment with n=3. b) shows combined data from 3 experiments. N.T.: no treatment controls. Statistical significance of drug treatments against control (ctrl) was tested by one-way ANOVA followed by Dunnett's test.

a
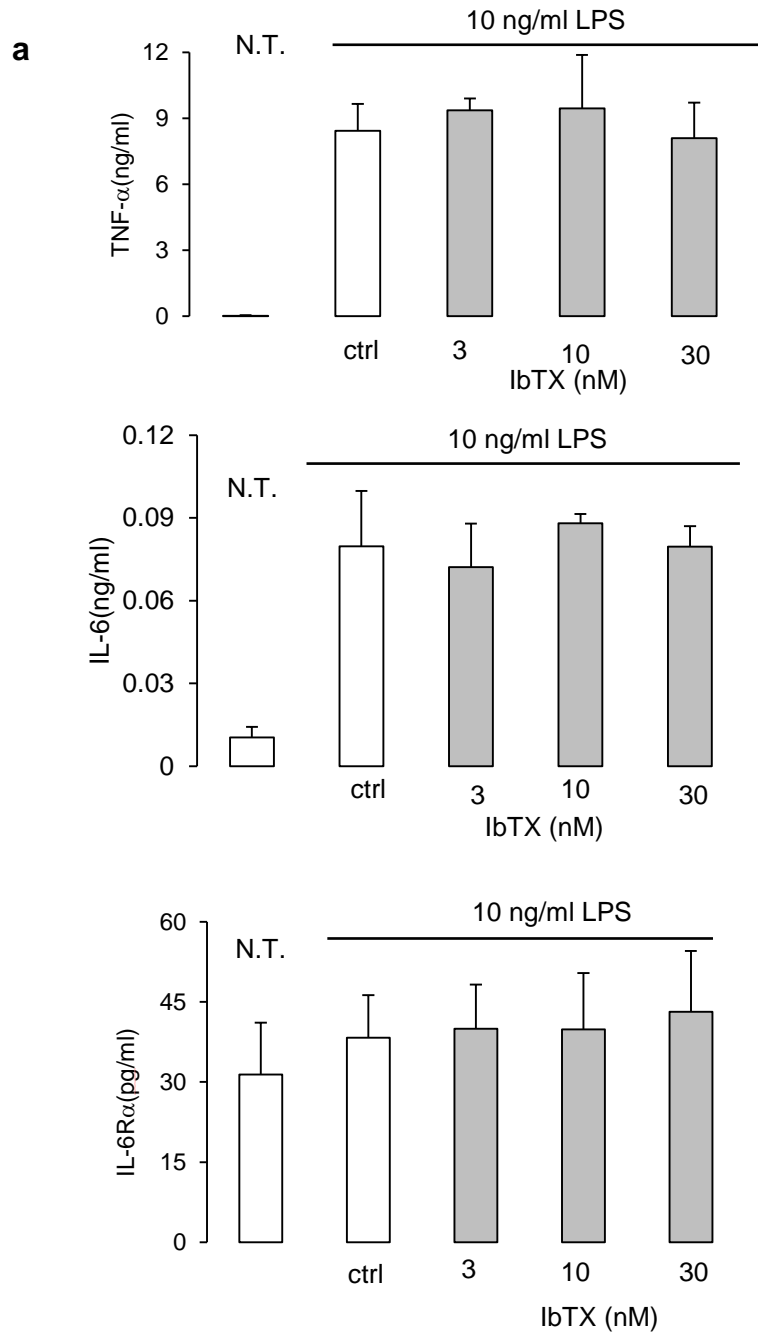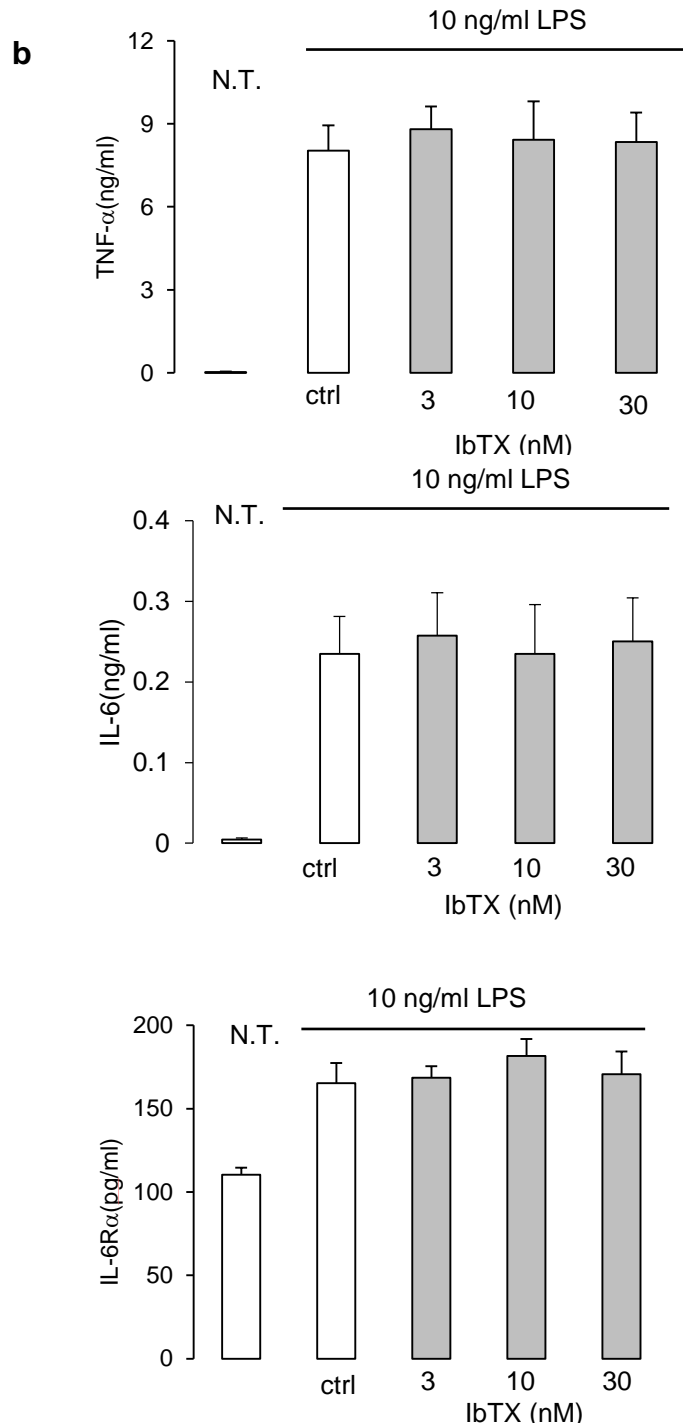
Figure 5-2 Effect of IbTX on TNF-α, IL-6 and IL-6Rα release from macrophages activated with a submaximal dose of LPS

RAW264.7 macrophages received 3-30 nM IbTX, shaded bars, or medium control, clear bars, during stimulation with 10 ng/ml LPS. After 4 hours, culture media was collected. TNF-α, IL-6 and IL-6Rα in media were measured by ELISA. Bars represent mean+SEM, (n$\geq$3). N.T.: no treatment controls. a) shows results from one experiment with n=4. b) shows combined data from 3 experiments. Statistical significance of drug treatments against control (ctrl) was tested by one-way ANOVA followed by Dunnett's test.

a

b
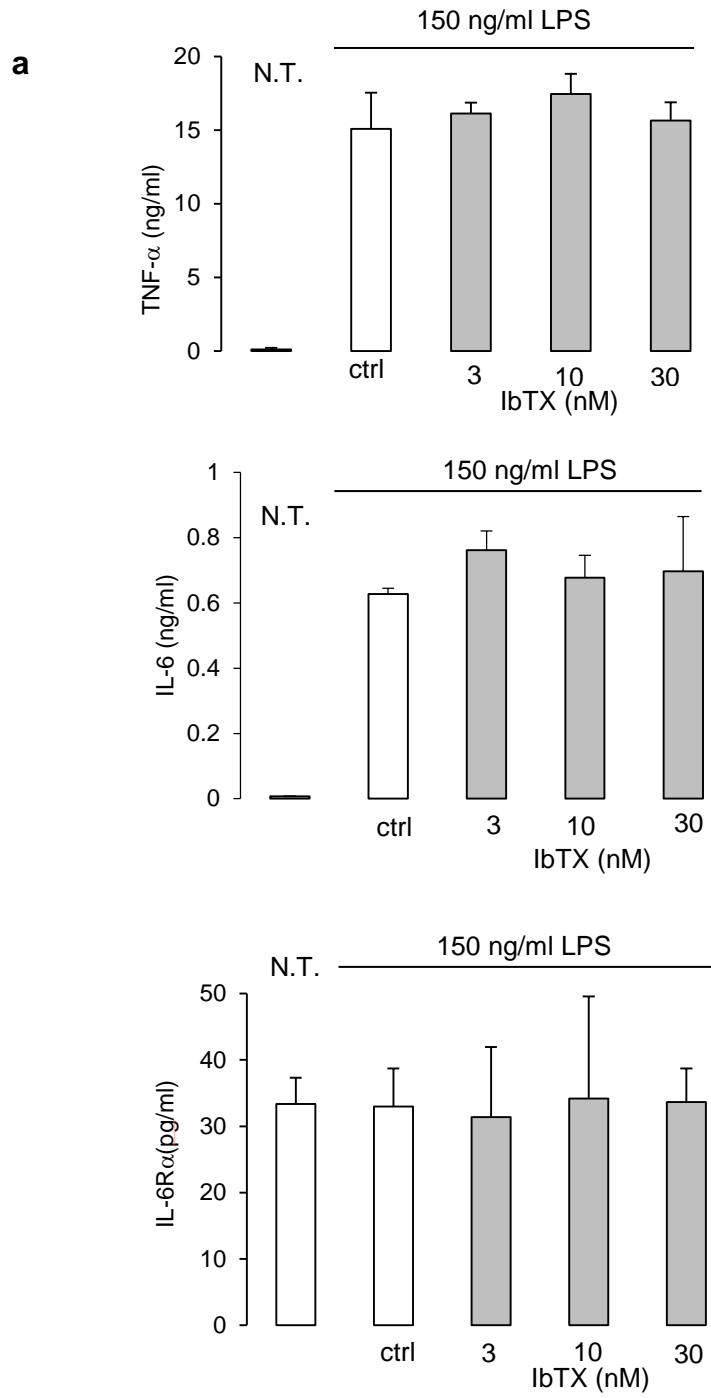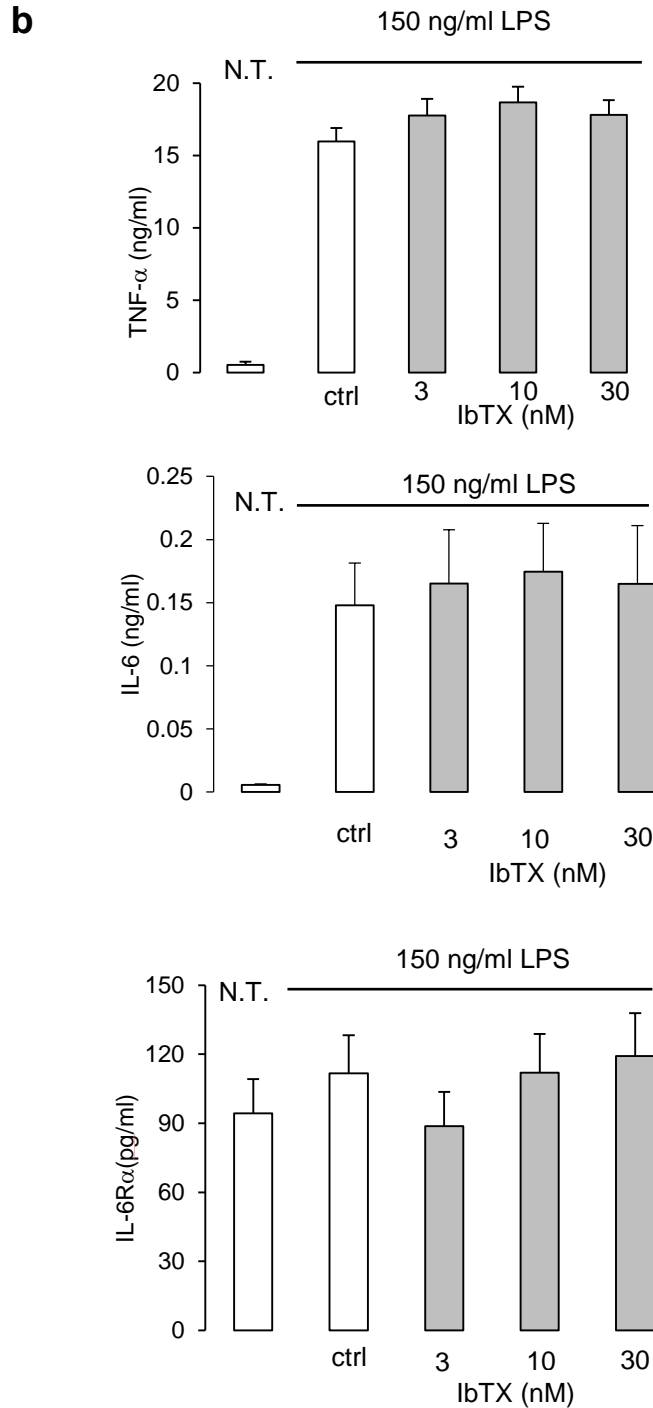
Figure 5-3 Effect of IbTX on TNF-α, IL-6 and IL-6Rα release from macrophages activated with a maximal dose of LPS

RAW264.7 macrophages received 3-30 nM IbTX, shaded bars, or medium control, clear bars, during stimulation with 150 ng/ml LPS. After 4 hours, culture media was collected. TNF-α, IL-6 and IL-6Rα in media were measured by ELISA. Bars represent mean+SEM, (n≥3). N.T.: no treatment controls. a) shows results from one experiment with n=4. b) shows combined data from 3 experiments. Statistical significance of drug treatments against control (ctrl) was tested by one-way ANOVA followed by Dunnett's test.

a
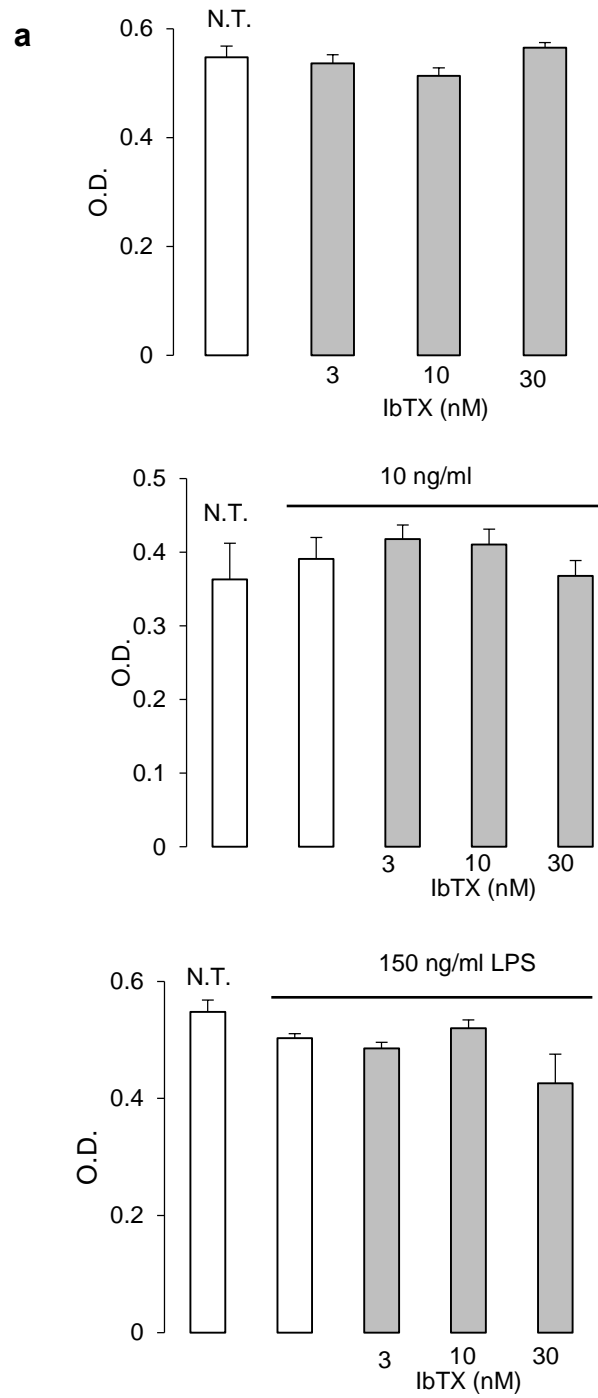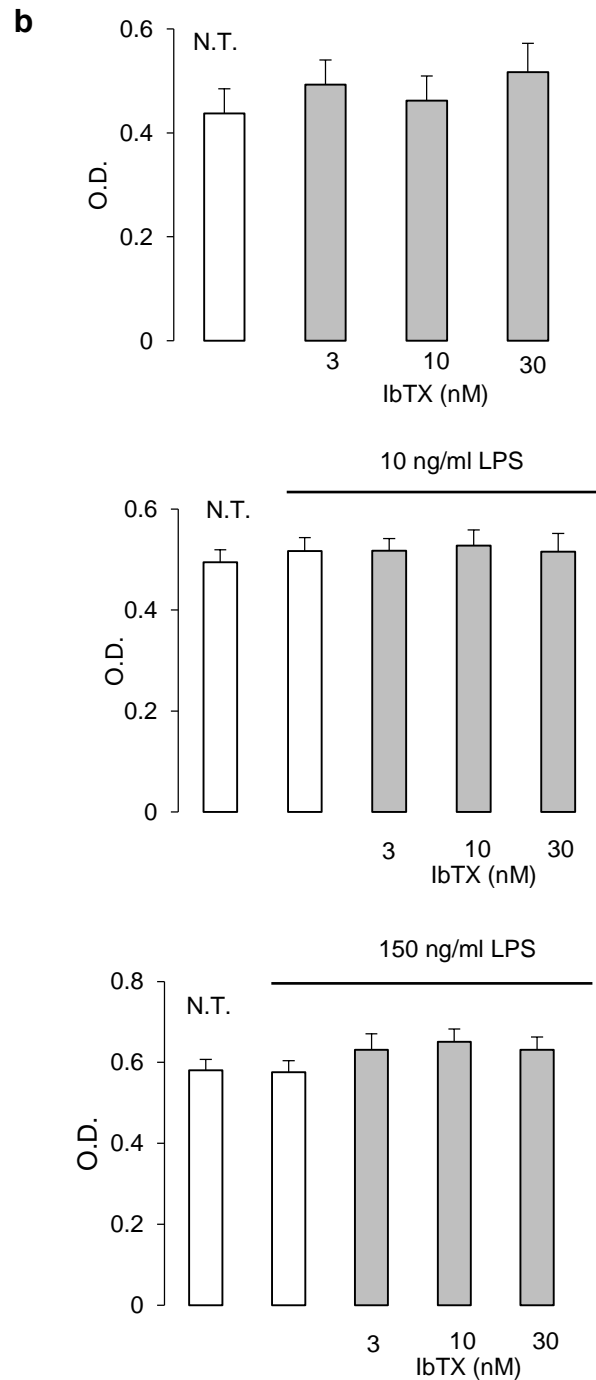
Figure 5-4 Cell viability of macrophages treated with IbTX and LPS

RAW264.7 macrophages received no treatment, 10 or 150 ng/ml LPS for 4 hours with, shaded bars or without, clear bars, 3-30 nM IbTX and cell vitality was assessed by MTT. Cell viability was measured by MTT. Bars represent mean+SEM, n≥3. N.T.: no treatment controls. a) shows data from one experiment with n=3 and b) shows combined data from 3 repeated experiments. Statistical significance of drug treatments against no treatment control was tested by one-way ANOVA followed by Dunnett's test.

5.2.2   Effect of paxilline on TNF-α release from early time point of TLR4 activation of macrophages

A second reported BK channel selective blocker, paxilline, was investigated. Due to the complexity of how paxilline blocks the channel, it was difficult to estimate the IC_{50} for this drug in this experiment. Therefore an initial cell culture experiment with paxilline was carried out to find the maximal tolerable dose of the drug in RAW264.7 macrophages. Paxilline, at 3 μM, significantly increased the release of TNF-α from resting macrophages, 601+/-225 pg/ml compared to vehicle control, which had no detectable production of TNF-α, p<0.05, Figure 5-5a. However, above 1 μM paxilline decreased MTT result, with measurements of 0.17+/-0.008 O.D. in vehicle control and 0.13+/-0.05 O.D. in 3 μM paxilline treatment group, p<0.05, Figure 5-5b. Therefore the maximum dose of paxilline used was set as 1 μM. The lower does was selected by estimating from the literature, which has been reported to selectively block closed BK channels and this is at 20 nM. Due to its poor solubility in aqueous solutions, paxilline was first dissolved in DMSO. The final concentration of DMSO used in culture wells was 0.015%. Initial experiments showed that this concentration of DMSO did not have an effect on TNF-α release.

Paxilline treatment for up to 24 hours at 0 to 1 μM did not induce TNF-α from resting macrophages, Figure 5-5a. In comparison, 20 nM paxilline enhanced TNF-α release from macrophages stimulated for 4 hours with 10 ng/ml LPS by 54% compared to vehicle control group, 4.8+/-0.34 ng/ml with 20 nM paxilline compared to 3.1+/-0.99 ng/ml DMSO vehicle control, p<0.05, Figure 5-6. 1 μM paxilline also significantly increased, p<0.05, TNF-α release by 61%, 5.0+/-1.2 ng/ml compared to the DMSO vehicle control, Figure 5-6a. Paxilline did not affect TNF-α release when 150 ng/ml LPS was used on the macrophages. MTT assay showed that 4 hours of incubation with paxilline did not affect the viability of the cells, Figure 5-6.
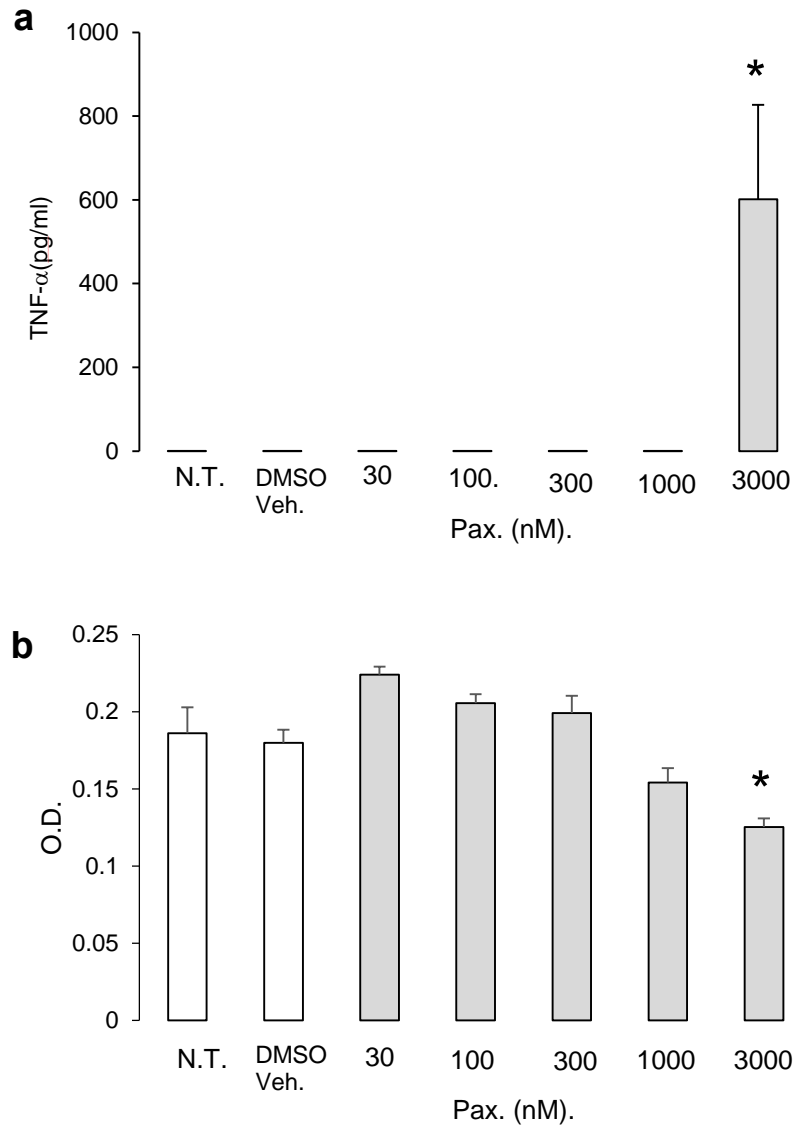
Figure 5-5 Preliminary data. Effect of paxilline on TNF-α release and cell viability in resting macrophages

RAW264.7 macrophages received no treatment (N.T.) or 3-3000 nM paxilline (Pax.), shaded bars, for 4 hours. Vehicle control (DMSO Veh.), clear bars, was made with DMSO. The final concentration of DMSO was 0.015% in controls, clear bars, and drug treatments, shaded bars. a) Concentration of TNF-α in conditioned media was measured by ELISA. b) Cell viability was assessed by MTT assay. Bars represent mean+SEM and shows result from one preliminary experiment with n=5. O.D.: optical density. Statistical significance of vehicle control (DMSO Veh) against drug treatments was tested by one–way ANOVA followed by Dunnett's t-test.* $p<0.05$.
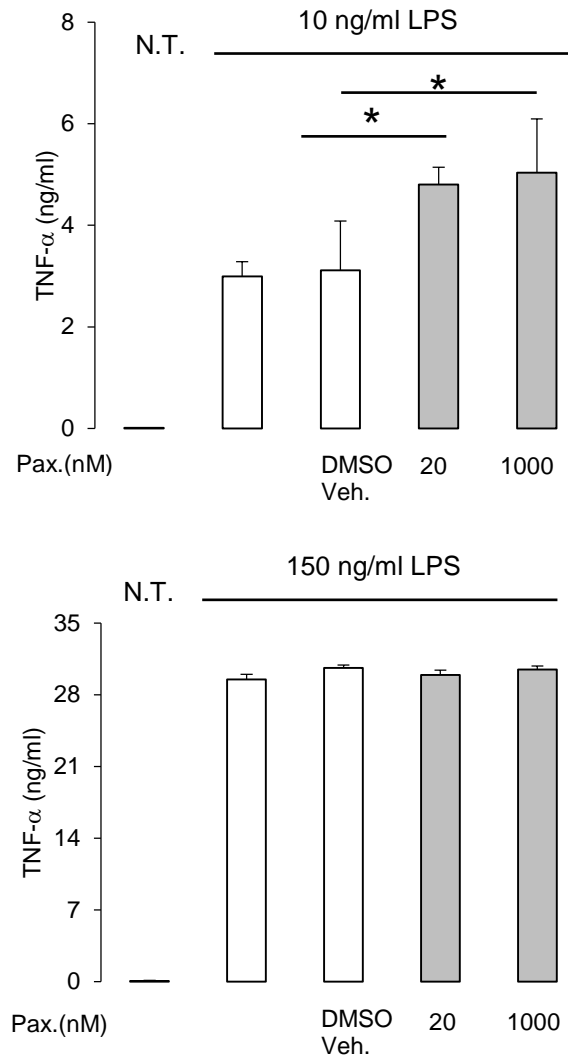
Figure 5-6 Preliminary data. Effect of paxilline on TNF-α release from LPS activated macrophages

 RAW264.7 macrophages received no treatment (N.T.), 10 or 150 ng/ml LPS with/without 20 or 1000 nM paxilline (Pax.) for 4 hours. Vehicle control (DMSO Veh.), clear bars, was DMSO. The final concentration of DMSO 0.015% in controls, clear bars, and drugs treatments, shaded bars. TNF-α in conditioned media was measured by ELISA. Bars represent mean+SEM with n=4. The experiment was repeated twice and graph shows result from one experiment with n=4. Statistical significance of vehicle control (DMSO Veh) against drug treatments was tested by one–way ANOVA followed by Dunnett's test.* $p < 0.05$.

5.2.3   LPS conditioning protocol and its effect on TNF-α, IL-6 and IL6Rα release from macrophages

The results from the previous section demonstrated that IbTX did not have any effect on the release of TNF-α, IL-6 and IL-6Rα during first 4 hours of LPS stimulation. However the results from chapter 4 demonstrated that this was not the optimum time for the expression of BK channels on the plasma membrane, but would suggest that the active BK channels only occurred on the plasma membrane of the RAW264.7 cells after 18-24 hours of stimulation with 10 ng/ml LPS. Therefore, to investigate the effect of IbTX on the release of these proteins at a time when BK channels were expressed on the plasma membrane, the following protocol was developed, Figure 5-7. First RAW264.7 macrophages were stimulated with 10 ng/ml LPS for 24 hours. After 24 hours, the culture media was changed and these 'conditioned macrophages' were treated with 150 ng/ml LPS for 4 hours in the presence or absence of 30 nM IbTX, Figure 5-7. The protocol is called 'LPS conditioning' protocol.
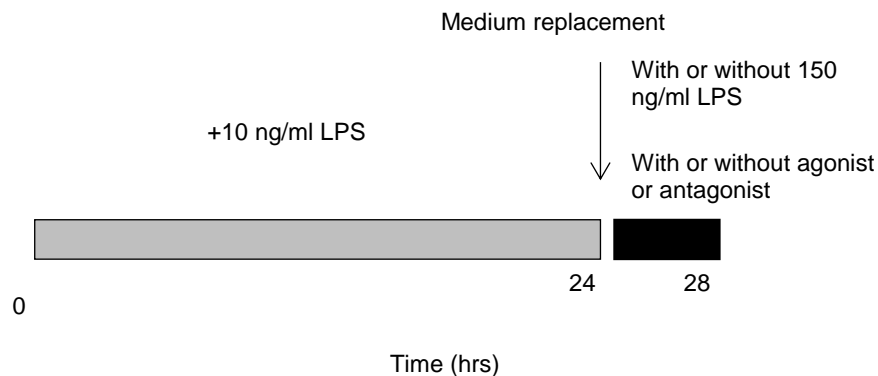
Figure 5-7 Protocol for investigating the effect of plasma membrane BK channel block by macrophages

RAW264.7 macrophages were treated with 10 ng/ml LPS for 24 hours. The media was replaced at 24 hours and subsequently, macrophages were activated with 150 ng/ml LPS with/without 30 nM IbTX. At 4 hours, cells and media were collected for analysis.

As described in chapter 1, TNF-α release can be regulated at the plasma membrane and it was decided to investigate the amount of cellular mTNF-α in the following experiments. mTNF-α was detected using a rabbit monoclonal anti-mouse TNF-α antibody, D2D4. D2D4 detected a protein band at 26 kDa in LPS stimulated cells and this protein band was absent in whole cell lysate from resting macrophages. Weaker bands also appeared between 30-40 kDa. The 26kDa band corresponded to the molecular weight of mTNF-α.
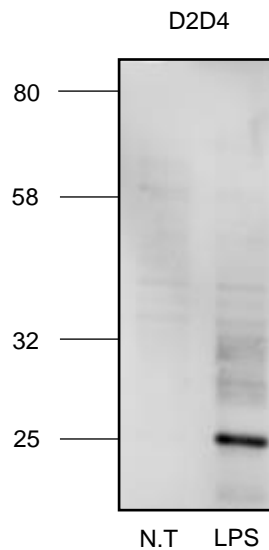
Figure 5-8 TNF-α expression in resting and LPS activated macrophages using a rabbit monoclonal anti-mouse TNF-α antibody, D2D4

RAW264.7 macrophages received no treatment or 150 ng/ml LPS for 4 hours. mTNF-α expression was assessed by Western blot. 10 µg protein was loaded per lane. Left indicates molecular weight marker in kDa. The experiment was repeated 5 times.

Before investigating the effect of the IbTX in this model, the effect of preconditioning the RAW264.7 macrophages with low dose LPS on the subsequent activation of the macrophages with 150ng/ml LPS was evaluated. LPS conditioning of macrophages resulted in approximately 38% reduction in TNF-α secretion in response to 150 ng/ml LPS for 4 hours compared to non-conditioned macrophages, 2.4+/-0.32 ng/ml and 3.9+/-0.64 ng/ml respectively, p<0.05, Figure 5-9a.

LPS conditioning also reduced the expression of the 26 kDa cellular mTNF-α LPS stimulation with 150 ng/ml LPS by 70%, Figure 5-9b. In contrast, release of IL-6

was potentiated in LPS conditioned group by 280%, non-conditioned group 0.34+/-0.08 ng/ml compared to condition group 1.3 +/-0.11 ng/ml, p<0.05, Figure 5-10a. IL-6Rα release was also increased by 25%, 14.0+/-0.54 pg/ml to 19.1 +/- 2.1 pg/ml, p<0.05, Figure 5-10a.

a

b
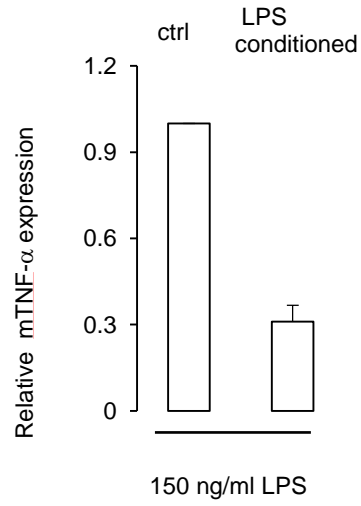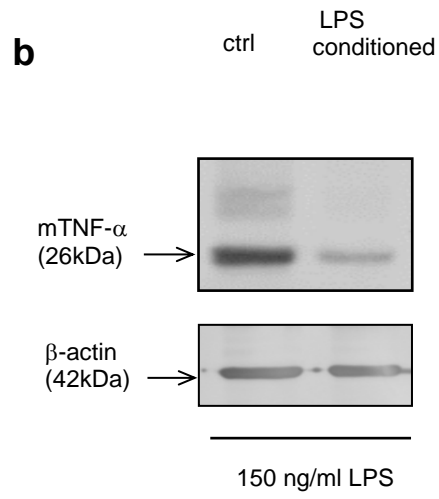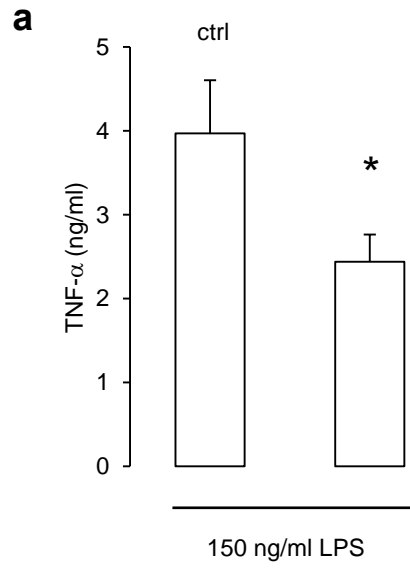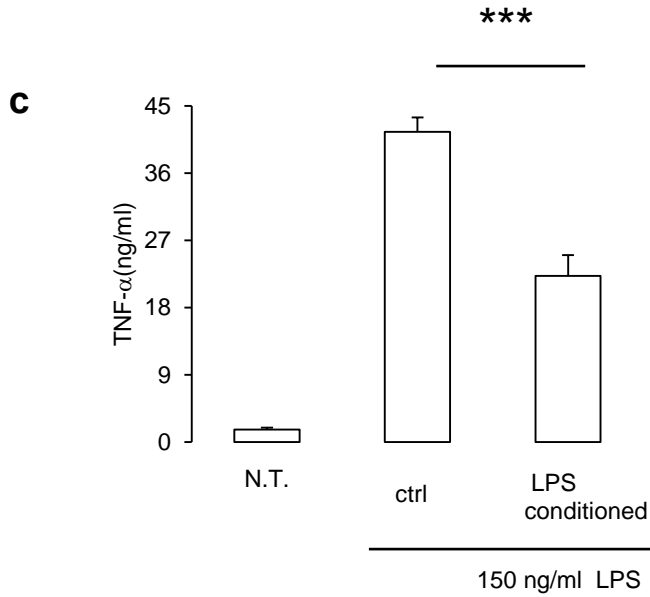
Figure 5-9 Effect of LPS conditioning on TNF-α release and mTNF-α expression in macrophages

RAW264.7 macrophages were incubated with 10 ng/ml LPS for 24 hours to produce LPS conditioned macrophages. Non conditioned macrophage (ctrl) did not receive this preconditioning. Subsequently the media was replaced and the conditioned and ctrl cells were activated with 150 ng/ml LPS for 4 hours. a) TNF-α release was measured by ELISA. Bars represent mean+SEM (n≥3). a) shows result from one experiment and c) shows combined data from 3 repeated experiments. b) Western blot analysis of mTNF-α and β-actin expression. Densitometry analysis shows relative mTNF-α expression in groups received LPS conditioning compared to the control groups without LPS conditioning (ctrl) and expressed. Bars represent mean+SEM with n=3, where n is number of blots used for the analysis. The experiment was repeated 3 times. Statistical significance was tested using paired t-test *p<0.05, **p<0.01, ***p<0.0001
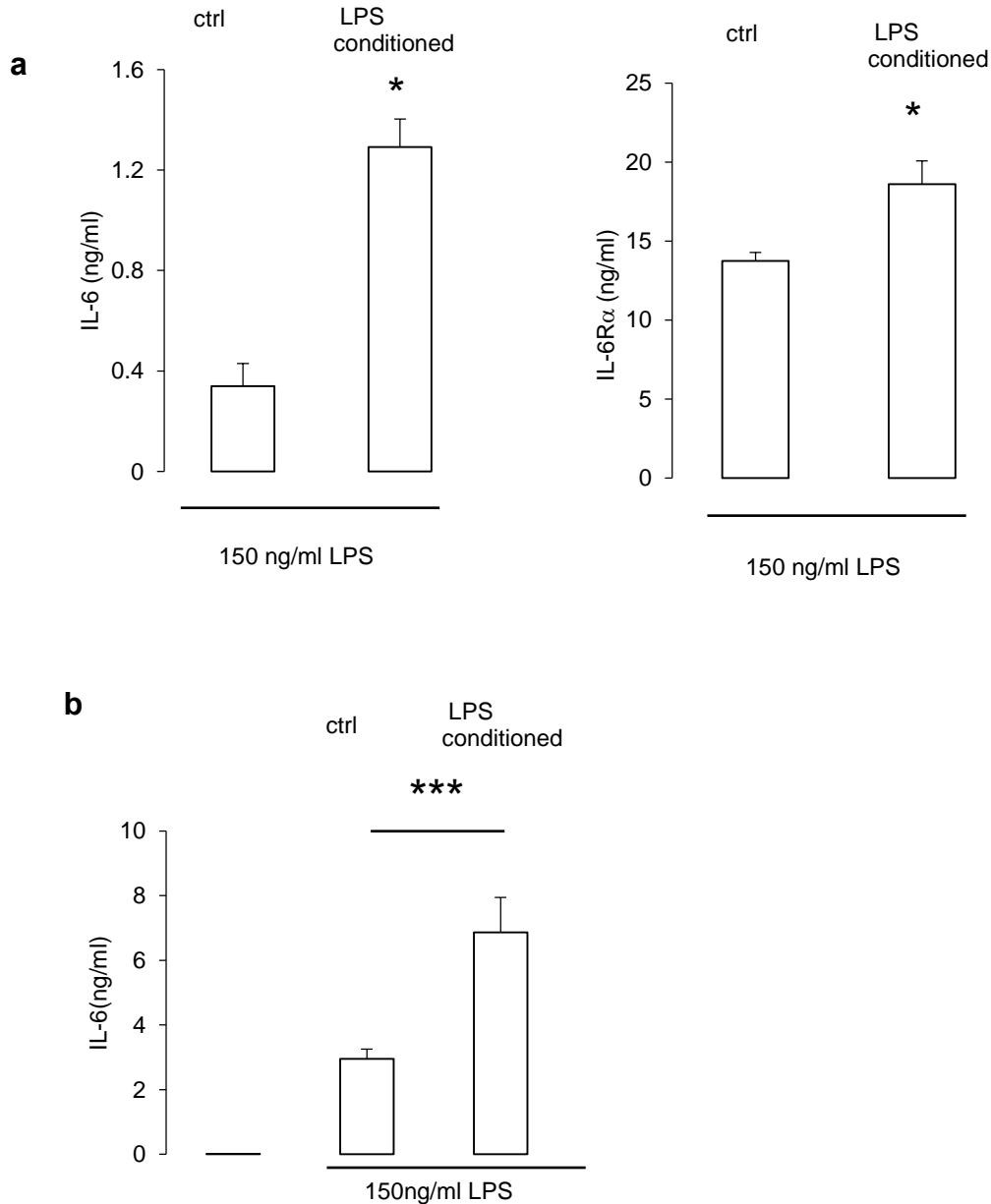
Figure 5-10 Effect of LPS conditioning on IL-6 and IL-6Rα release from macrophages

RAW264.7 macrophages were incubated with 10 ng/ml LPS for 24 hours to produce LPS conditioned macrophages. Non conditioned macrophage (ctrl) did not receive this preconditioning. Subsequently the media was replaced and the conditioned and ctrl cells were activated with 150 ng/ml LPS for 4 hours. IL-6 and IL-6Rα release was measured by ELISA. Bars represent mean+SEM (n≥3). a) shows results from one experiment with n=4. b) shows combined data from 3 repeated experiments. Statistical significance was tested using paired t-test *p<0.05. **p<0.01, ***p<0.0001.

5.2.4 Effect of IbTX on TNF-α, IL-6 and IL-6Rα release from LPS conditioned macrophages

In conditioned macrophages, the application of 30 nM IbTX significantly enhanced TNF-α release during 150 ng/ml LPS treatment compared to macrophages which did not receive the drug. Release was increased by approximately 65%, 2.4+/-0.32 ng/ml in LPS only group compared to 3.8+/-0.12 ng/ml in LPS with IbTX group, p<0.05, Figure 5-11a. IL-6Rα release from LPS stimulated conditioned macrophages was also shown to increase with IbTX treatment by approximately 80%, 30.1+/-3.1 pg/ml from the group received LPS only and 54.5+/-7.5 pg/ml from the group received LPS with IbTX, p<0.05, Figure 5-11a. In comparison, IL-6 release was not altered by IbTX treatment, showing 1.2+/-0.11 ng/ml in the group received LPS only and 1.3+/-0.24 ng/ml in the group received LPS with IbTX, Figure 5-11a. IbTX treatment did not affect the viability of the cells, Figure 5-11a.

a
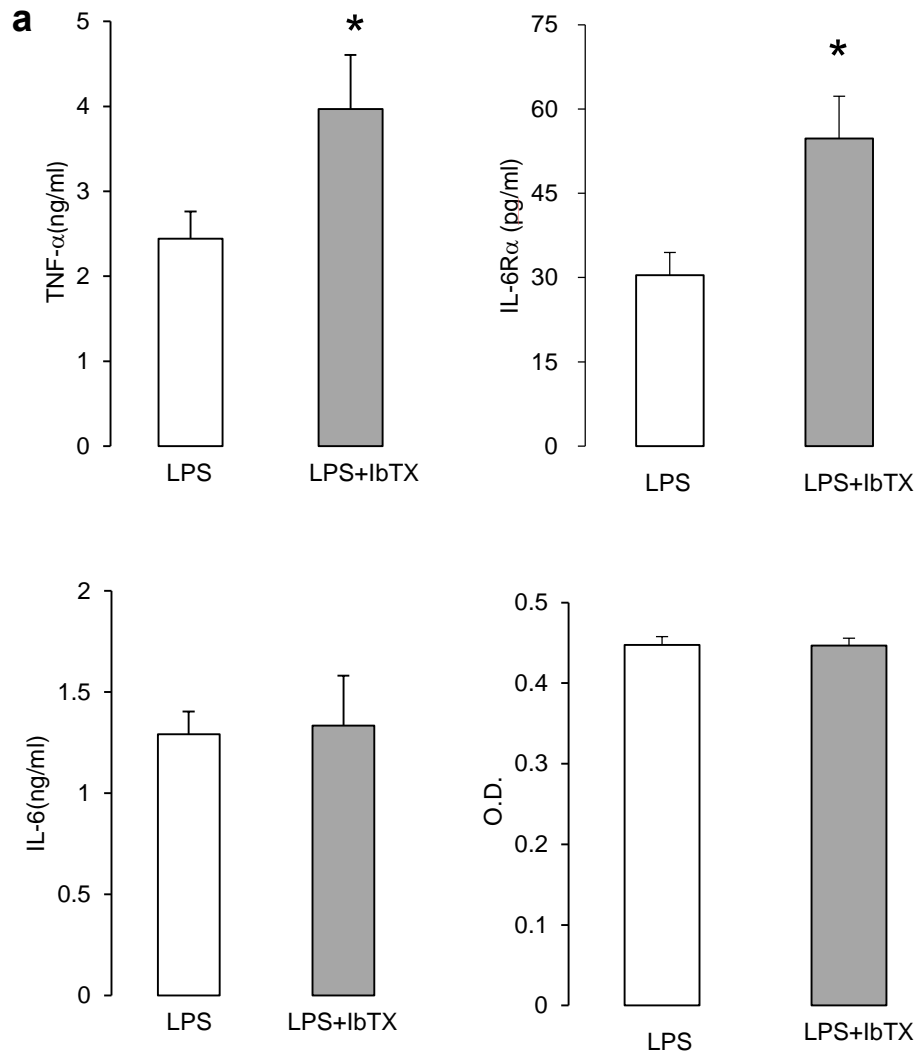
b
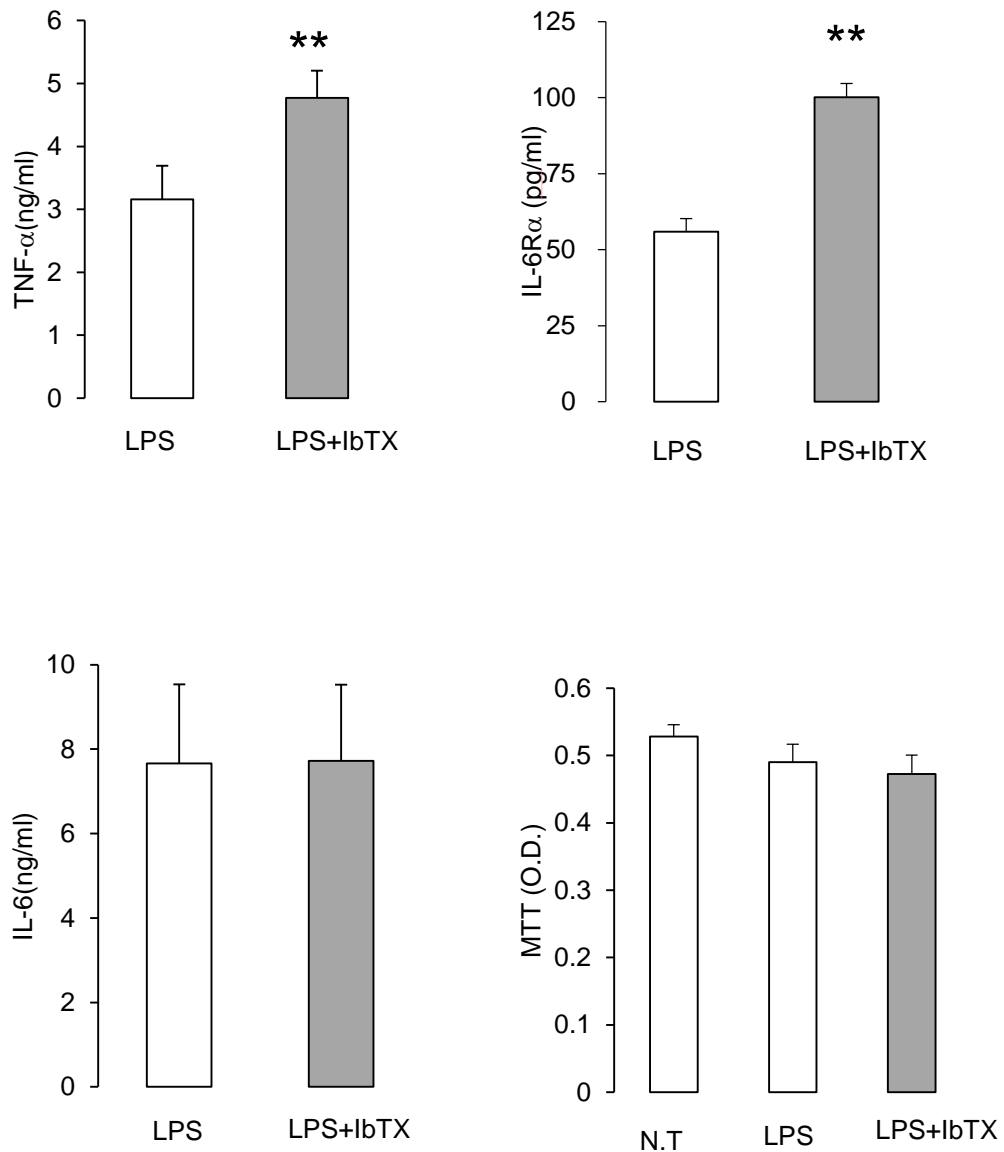
Figure 5-11 Effect of IbTX on the plasma membrane BK channels in TNF-α and IL-6Rα from LPS activated macrophages.

RAW264.7 macrophages were incubated with 10 ng/ml LPS for 24 hours to produce LPS conditioned macrophages. Subsequently the media was replaced and conditioned cells were activated with 150 ng/ml LPS with/without 30 nM IbTX. After 4 hours, culture media was collected and analysed by ELISA for TNF-α, IL-6Rα and IL-6. Cell viability was assessed by MTT. Bars show mean+SEM (n≥3). a) shows results from one experiment with n=3 and b) shows combined data from 3 repeated experiments. Statistical significance was tested by paired t-test. O.D.: optical density.*p<0.05, **p<0.01.

5.2.5   Regulation of TNF-α by IbTX

Previous section, 5.2.4, demonstrated that IbTX increases the release of TNF-α and IL-6Rα from the conditioned macrophages during LPS activation. TNF-α production is regulated at multiple levels including gene transcription, protein translation and membrane release. The increase in the release of TNF-α by IbTX could involve any or all these mechanisms. To identify at which step of TNF-α production IbTX modulated, TNF-α mRNA was analysed by RT-qPCR and the cellular contents of the cytokine protein was analysed by Western blot.

mRNA samples were collected from conditioned RAW264.7 macrophages after 4 hours LPS treatment with or without 30 nM IbTX and cDNA synthesised. The levels of TNF-α mRNA were subsequently analysed by RT-qPCR with levels normalised to β-actin, an internal control, Figure 5-12a. GAPDH had previously been shown not be a reliable internal control in this experiment. In spite of a significant increase in the levels of released TNF-α by IbTX, no significant difference in TNF-α mRNA expression was observed with IbTX, Figure 5-12a. In comparison, cellular levels of mTNF-α decreased with IbTX, Figure 5-12b and 5-12c. Taken together these results suggested that IbTX modulated the release of the cytokine and not gene transcription or translation.

To further investigate the role of BK channels in the system, a BK channel opener, 100 nM NS11021 was applied to LPS stimulated conditioned macrophages as a preliminary experiment. 100 nM NS11021 caused a significant decrease in TNF-α release, 9.8+/-0.22 ng/ml from LPS only group and 6.2+/-0.98 ng/ml from LPS with NS11021 group, $p < 0.05$, Figure 5-13. This result supports the role of BK channels in negatively regulating the release of the cytokine. However, it has to be noted that similar to paxilline, NS11021 is a small lipophilic molecule. Therefore the possibility that this drug caused the activation of other cytoplasmic BK channels as well as the activation of the plasma membrane BK channels cannot be excluded.

Initially it was attempted to study the expression of IL-6Rα in RAW264.7 macrophages and the effect of IbTX on the cellular expression of IL-6Rα. However only one available antibody, a rat monoclonal anti-mouse IL-6Rα antibody, DM3568,

was not able to detect any protein bands even after a series of optimization. Therefore, this study focused on the regulation of TNF-α.

The combined data, from repeated ($\geq$ 3 times) experiments, for protein release and MTT was in line with the described results from individual experiments. These combined data were presented in Figure 5-1, 5-2, 5-3, 5-4, 5-9 and 5-10. Statistical analysis of combined data and individual experimental data demonstrated a similar pattern of significance between treatment groups. It was noted combined data reached higher degree of significance.
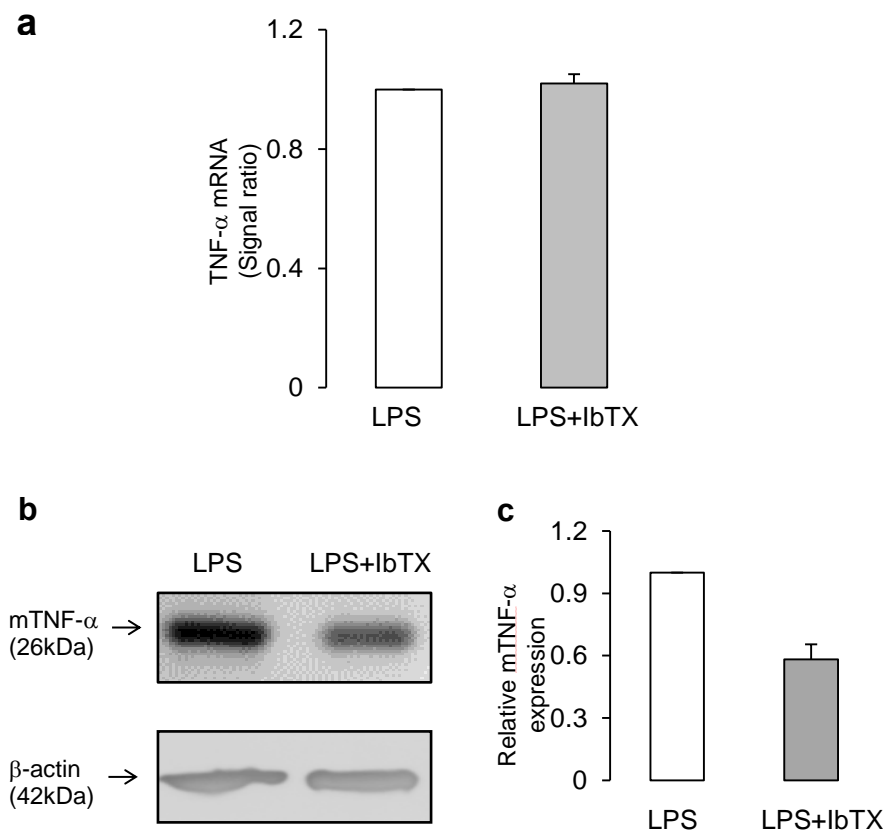
Figure 5-12 Effect of IbTX on TNF-α mRNA and mTNF-α expression

RAW264.7 macrophages were incubated with 10 ng/ml LPS for 24 hours to produce LPS conditioned macrophages. Subsequently the media was replaced and conditioned cells were activated with 150 ng/ml LPS with/without 30 nM IbTX. After 4 hours, cells were collected and analysed for a) TNF-α mRNA expression normalised to an internal control, β-actin. Bars represent mRNA signal ratio as mean+SEM, n=3 independent experiments. b) mTNF-α expression was analysed by Western blot. c) Densitometry analysis of TNF-α expression. Bars represent protein expression mean+SEM, n=3.
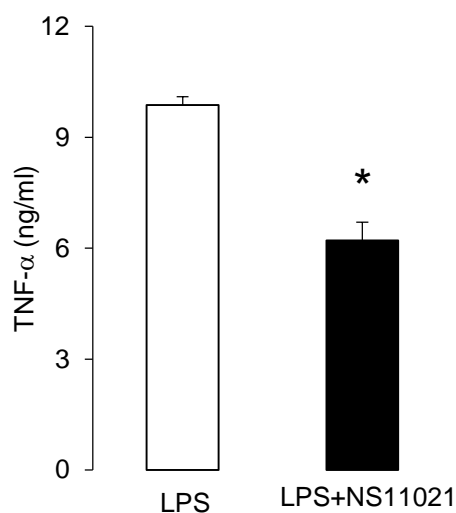
Figure 5-13 Preliminary data. Effect of NS11021 on TNF-α release from LPS conditioned macrophages.

RAW264.7 macrophages were incubated with 10 ng/ml LPS for 24 hours to produce LPS conditioned macrophages. Subsequently the media was replaced and conditioned cells were activated with 150 ng/ml LPS with/without 100 nM NS11021. After 4 hours, culture media was collected and analysed by ELISA for TNF-α. Graph show mean+ SEM from one experiment with n=4. Statistical significance was tested by paired t-test. O.D.:optical density.*p<0.05

5.3   Discussion

The first aim of this chapter was to investigate the effect of BK channel blockers, IbTX and paxilline, on the release of TNF-α, IL-6 and IL-6Rα. IbTX is a 37 amino acids peptide toxin isolated from scorpion venom. IbTX achieves a half maximum block of BK channels within the nM range and is highly selective for BK channels at 30 nM. This drug is impermeable to the lipid bilayer membranes and blocks the pore region of the channels from the outside (Galvez *et al.*, 1990; Yu *et al.*, 2016). Through PRRs, macrophages are known to respond to various microbial toxins. Therefore it was important to establish if IbTX lead to the direct activation of macrophages at the concentrations which the drug blocks BK channels. It was found that IbTX did not stimulate TNF-α, IL-6 release or alter IL-6Rα release from resting macrophages. The IbTX was not toxic to the cells over 4 hours. Taken together these results suggested that IbTX itself does not stimulate inflammatory cascades in macrophages.

The tremorgenic mycotoxin, paxilline is another selective blocker for BK channels. The size of paxilline is 435 Da and is highly lipophilic in nature (Knaus *et al.*, 1994b). Previous research has demonstrated that the paxilline blocks BK channels differently depending on the channels activation state. The affinity of this blocker to the channels has been reported to be inversely proportional to the open probability (P_o) of the channel. The IC$_{50}$ of this drug ranges from 10 nM, when the channels are closed, to 10 μM ,when the channels are opening at maximum rate (Zhou and Lingle, 2014). In this thesis, the paxilline doses above 1 μM appeared to affect the viability of the cells. Paxilline also significantly enhanced TNF-α secretion from macrophages, activated with submaximal dose of LPS. However this effect was lost when macrophages were stimulated with the optimal dose for TNF-α release. The result showed that paxilline modulated cytokine secretion from macrophages. If IbTX and paxilline are selective to BK channels how could they elicit differing effects? From chapter 4, it was demonstrated that RAW264.7 macrophages had low expression of BK channels on the plasma membrane in resting conditions and 4 hours after LPS activation. BK channels were abundant at intracellularly sites in resting RAW264.7 macrophages and at early time points of LPS activation. Owing to its lipophilic nature, it is possible that the paxilline entered cells and blocked intercellular BK channels whereas IbTX does not. Alternatively paxilline may

enhance TNF-α release by the off-target effect which is in addition to BK channel block. Additional targets for paxilline have been reported. At μM levels, paxilline inhibits Ca^{2+} ATPase and IP3 receptors (Longland *et al.*, 2000; Bilmen *et al.*, 2002). As this drug is widely used to study the BK channel, it would be worth investigating the mechanisms of how paxilline causes the activation of macrophages.

IbTX is considered to be a gold standard for the BK channel inhibition. Importantly, it only blocks BK channels located on the plasma membrane, thus provides a unique tool to selectively investigate plasma membrane located BK channels without affecting the intercellular pool of BK channels. For this reason, IbTX was used to block the plasma membrane located BK channel.

To investigate the effect of the plasma membrane BK channel block it was necessary for the cells to express functional BK channels on their plasma membrane. Results from chapter 4 have demonstrated that BK channels are upregulated on the plasma membrane 24 hours after stimulation with 10 ng/ml LPS, using this observation, a protocol was developed to investigate the role of the BK channel in activated macrophages. In this protocol, macrophages were stimulated for 24 hours with a sub-optimal dose of LPS to induce BK expression on the plasma membrane. These macrophages were termed 'LPS conditioned' macrophages. These cells were then activated with 150 ng/ml LPS for 4 hours and the drug could be applied during the activation to investigate BK channels role.

This protocol of low dose followed by high dose treatment with LPS is reminiscent of LPS/endotoxin tolerance, which is a well-appreciated immunological phenomenon (Morris *et al.*, 2015). In this response, a first challenge of cells, usually macrophages, with a low dose of LPS causes macrophages to become less responsive to subsequent challenge with a higher dose of LPS. In the tolerant state, immune cells have been reported to down-regulate the release of pro-inflammatory cytokines in response to the second challenge (Biswas and Lopez-Collazo, 2009). LPS tolerance is not only seen at cellular level, but also may be important in clinical settings where the immune system becomes unresponsive to a subsequent bacterial infections. To date multiple mechanisms have been implicated in the establishment/maintenance of endotoxin tolerance. Among these mechanisms, the downregulation of

proinflammatory cytokine transcription is considered to be most prominent. However, it is likely the multiple mechanisms are involved in tolerance. As expected, stimulation of macrophages with 10 ng/ml LPS generated the tolerance state and reduced the release of TNF-α form macrophages in response to secondary stimulation with 150 ng/ml. mTNF-α expression was also decreased in LPS conditioned RAW264.7 macrophages. However, in comparison to TNF-α, it was noted that IL-6 was significantly increased in LPS conditioned macrophages by 3 fold. There was also a significant increase in IL-6Rα release. This opposing effect on IL-6 release may rather represent the priming effect of immune cells. It has been known that low dose of LPS application could dramatically enhance the inflammatory response to subsequent LPS application (Morris *et al.*, 2015).

30 nM IbTX significantly increased TNF-α release by 55%. Indeed it appeared to reverse the effect of endotoxin tolerance in TNF-α release. However this was not associated with an increase in TNF-α mRNA, but at the post transcriptional site. To investigate the cellular contents of mTNF-α expression in these cells, Western blot was performed using a rabbit monoclonal anti-mouse TNF-α antibody D2D4. Firstly, in non-treated resting cells no protein band appeared, in LPS activated macrophages, the major band at 26 kDa and minor bands approximately at 30 kDa appeared indicating the production of TNF-α in response to TLR4 activation. The major band possibly corresponds to 26 kDa membrane anchored form TNF-α and minor bands to glycosylated form. In the LPS conditioned macrophages IbTX decreased the expression of mTNF-α by 44% which negatively correlated with the increase in the secretion of TNF-α from IbTX treated LPS conditioned cells. These results suggest that BK channels regulate TNF-α at the secretion from the cells and not earlier protein synthesis. In support of this, IbTX treatment did not affect the mRNA for TNF-α. In deed the most likely explanation is that the BK channel negatively regulates the release of TNF-α from the plasma membrane. In support of the negative effect of BK channel in the release of TNF-α, an application of 100 nM BK opener, NS11021, at the dose selective for BK channels resulted in a significant decrease in TNF-α release. However it is noted that NS11021 is lipophilic in nature and the interpretation of the results from this activator may not be limited in the activation of the plasma membrane BK channel.

TNF-α is initially expressed as its transmembrane form of 26 kDa mTNF-α. Membrane metalloproteases cleave mTNF-α to release the soluble 17 kDa TNF-α. ADAM17 is the primary enzyme to facilitate TNF-α ecotodomain shedding. This enzyme also cleaves IL-6Rα and is known to increase IL-6Rα in the circulation (Khokha *et al.*, 2013). It is noted that IL-6Rα is also reported as a substrate for a membrane metalloprotease, ADAM10 (Giebeler and Zigrino, 2016). IbTX further increased IL-6Rα release observed in LPS treated conditioned macrophages. Collectively, the data indicated possible interaction between the plasma membrane BK channel and the ADAMs.

IL-6, by contrast, is not expressed in a transmembrane form and is not subjected to cleavage by ADAM17 or other members of membrane metalloproteases family (Arango Duque and Descoteaux, 2014). IL-6 is produced in the endoplasmic reticulum and directed to Golgi. Accumulation has been reported to occur after 4 hours of LPS stimulation in RAW264.7 macrophages (Manderson *et al.*, 2007). IL-6 then exits from the Golgi, in vesicles and is secreted from the membrane via SNARE-mediated fusion with plasma membrane without processing as a transmembrane form. The block of the plasma membrane BK channels had no effect on IL-6 release during LPS stimulation of conditioned macrophages. Again this observation also supports the plasma membrane BK channels are working on the substrates of ADAM17. Therefore it was important to establish the role of ADAM17 in our system and interaction between its proteolytic activity and BK channels.

This chapter demonstrated that IbTX increased the release of TNF-α at the secretion in LPS conditioned macrophages. The release of IL-6Rα is also enhanced by IbTX however IL-6 was not affected. This opened up the hypothesis that BK channels located on the plasma membrane may be involved in the regulation of ADAM17 activity.

Chapter 6 Does ADAM17 have a role in TNF-α and/or IL-6Rα release in macrophages and does the plasma membrane BK channel regulate ADAM17 activity?

6.1   Introduction

Chapter 5 indicated a possible interaction between the plasma membrane BK channel and the release TNF-α and IL-6Rα. The release of TNF-α and IL-6Rα is mediated by ADAM17. It was hypothesised that the plasma membrane located BK channel may regulate ADAM17 activity. The aim of this chapter was to first investigate the expression and function of ADAM17 protein in RAW264.7 macrophages and secondly to study the effect of IbTX on the activity of ADAM17.

6.2   Results

6.2.1   ADAM17 expression in TLR4 activated macrophages

A rabbit polyclonal antibody for ADAM17, ab2051, which designed to bind the C-terminal region of the enzyme protein, was used to characterise the expression of ADAM17 in RAW264.7 macrophages. Figure 6-1 and Figure 6-2 show blots of ADAM17 in whole cell and plasma membrane isolate from RAW264.7 macrophages during treatment with 10 ng/ml LPS for up to 24 hours. ADAM17 has been reported to exist in a full length precursor 130 kDa and active 85 kDa forms. Ab2051 detected the presence of 85 and 130 kDa protein bands from whole cell lysates of RAW264.7 macrophages, Figure 6-1. In whole cell lysate, 10 ng/ml LPS treatment caused an increase in the expression level of 85 kDa protein bands, peaking around 24 hours of LPS stimulation, Figure 6-1. By contrast, protein bands at 130 kDa in whole cell lysate stayed relatively constant during the time course of LPS treatment except at 24 hours where the protein band appeared weaker, Figure 6-1. A cytosolic protein, Akt, which was used to validate isolation process, was present in whole cell lysate and absent in plasma membrane isolate indicating that the cell surface isolation appeared not to have the contamination of cytosolic contents, Figure 6-1 and Figure 6-2.

ADAM17
(130 kDa) →

ADAM17
(85 kDa) →

AkT
(56 kDa) →

β-actin
(42 kDa) →

| 0 | 1 | 4 | 8 | 12 | 18 | 24 |

LPS (hrs)
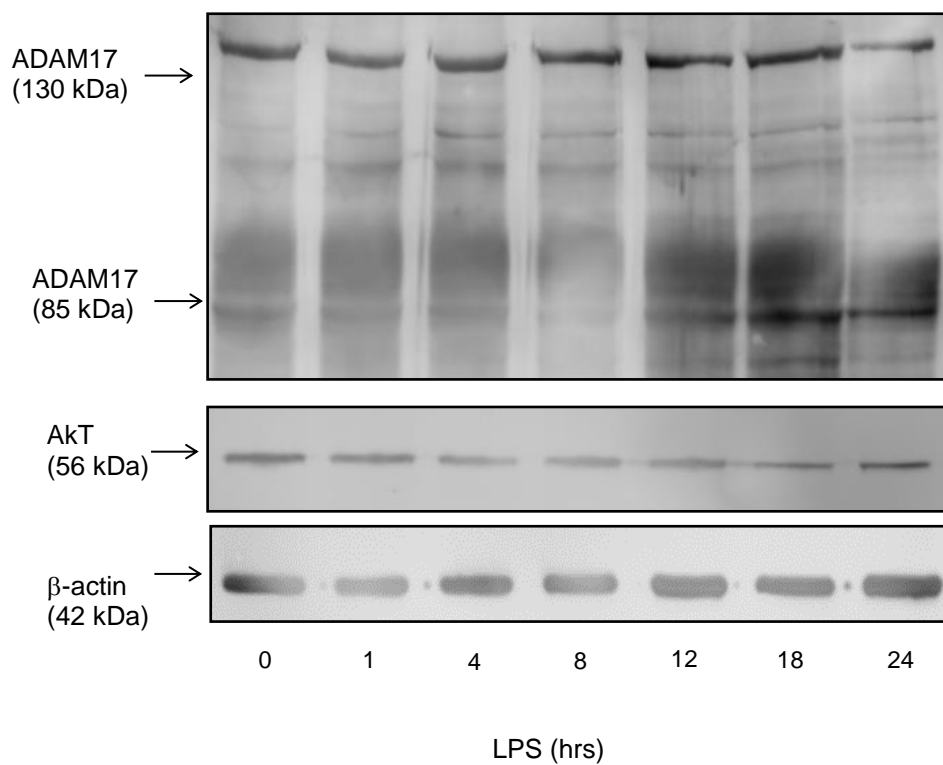
Figure 6-1 ADAM17 expression in whole cell lysate from LPS activated macrophages

RAW264.7 macrophages were treated with 10 ng/ml LPS for 0-24 hours. ADAM17, Akt and β-actin expression in whole cell lysate (WC) were analysed by Western blot. β-actin acted as a loading control. The experiment was repeated 3 times.

Western blot analysis of the plasma membrane isolates using an anti-ADAM17 antibody demonstrated the presence of protein bands at 85 and 130 kDa in plasma membrane isolate, Figure 6-2. It appeared that the level of 85 kDa form and the level of 130 kDa from ADAM17 stayed relatively constant during LPS treatment except that the expression level of 85 kDa form appeared highest at 12 hours of LPS treatment, Figure 6-2.
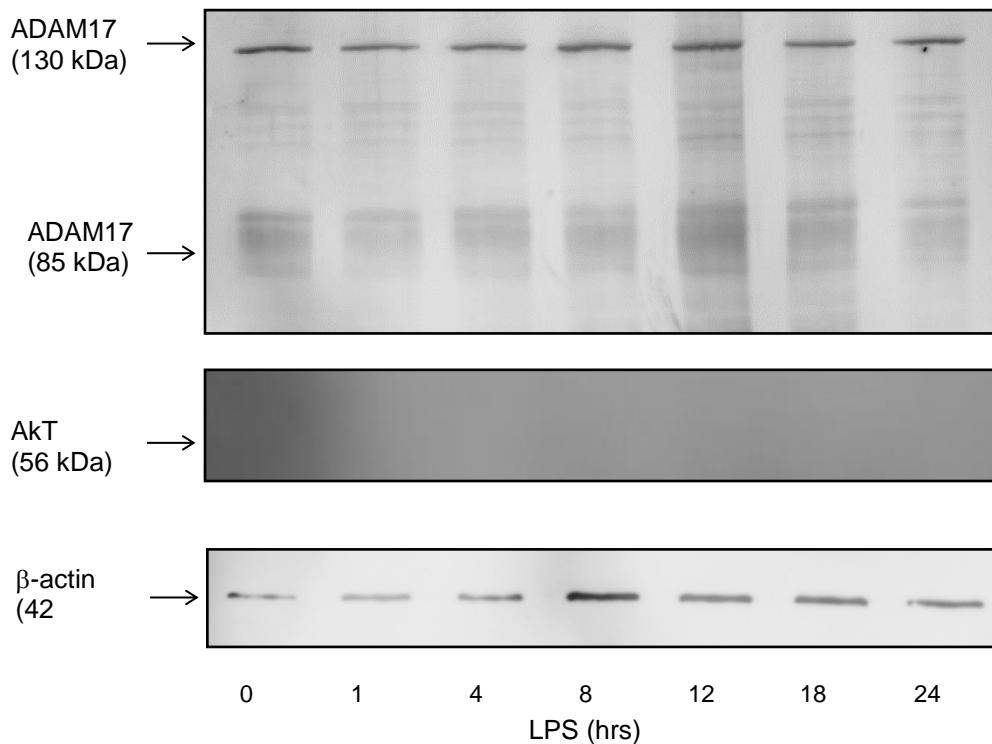
Figure 6-2 ADAM17 expression in plasma membrane isolate from LPS activated macrophages

RAW264.7 macrophages were treated with 10 ng/ml LPS for 0-24 hours. ADAM17, AkT and β-actin expression in plasma membrane isolate (PM) were analysed by Western blot. β-actin acted as a loading control. Absence of cytosolic protein AkT was used to check the contamination of cytosolic contents in isolation process. The experiment was repeated 4 times.

6.2.2   ADAM17 activity in TLR4 activated macrophages

The ultimate aim of this chapter was to investigate if the plasma membrane BK channel regulates the activity of ADAM17. To test this, it was required that ADAM17 activity was measured in the system which allowed the physical interaction between plasma membrane BK channel and ADAM17 to be maintained. Therefore, although the majority of ADAM17 assays have been done in cell-free systems, it was important that this assay was performed in live cells. Reported protocols were used and adapted to meet the requirement of the experiment (Alvarez-Iglesias *et al.*, 2005). After initial experiments, using fluorogenic TACE substrate II, a substrate for ADAM17 in this assay, it was found that the phenol red formulated in the media used and FBS lead to a high background by interfering with the fluorescence signal resulting from TACE substrate cleavage. Therefore enzyme activity assays were carried out with phenol red-free DMEM and FBS free DMEM.

The cells received LPS conditioning for 24 hours, as described in chapter 5, Figure 5-7. This protocol was demonstrated to upregulate the plasma membrane BK channels in macrophages in chapter 4. At 24 hours, the media was replaced with FBS and phenol red free DMEM during the macrophages activation with 150 ng/ml LPS for 3 hours, the substrate was added for the final hour. To preserve the spatial configuration of cellular components in the macrophages, the enzyme assay was carried out on plated live cells. As described in 2.15, the wells without TACE II substrate were prepared in order to eliminate the interference with the data from endogenous fluorescence of the cells. Per minute change in fluoresce signal in wells with TACE II substrate after the subtraction of the control measurement was estimated as ADAM17 membrane sheddase activity. ADAM17 activity data was reported as the rate of fluorescence signal increase per minute. In all experiments, ADAM17 inhibitors were used to confirm that increase in fluorescence was due to the enzyme activity of ADAM17.

The ADAM17 activity in the group which received LPS conditioning showed significantly higher activity compared to the group which did not receive LPS conditioning, 1718+/-261fluorescence/minute without LPS conditioning and 2459+/-119 fluorescence/minute in LPS conditioned cells, $p < 0.05$, Figure 6-3.

Application of 4.5 μM GM6001, a general inhibitor for membrane metalloproteases, diminished fluorescence signal by 86% in groups without LPS conditioning. The activity in DMSO control was 1718+/-261 fluorescence/minute and 235+/-344 fluorescence/minute in GM6001 treatment group, $p<0.05$, Figure 6-3. A reduction of 93% was also observed with GM6001 treatment in LPS conditioned macrophages, where DMSO control groups showed 2459+/-119 fluorescence/minute and GM6001 treatment group showed 183+/-96.4 fluorescence/minute, $p<0.001$, Figure 6-3. Treatment with 0.6 μM TAPI-0, a specific inhibitor for ADAM17, also significantly reduced the signal but at lesser degree compared to GM6001. The reduction in fluorescence signal was 70% in groups without conditioning, where DMSO control groups had 1718+/-26 fluorescence/minute and TAPI-0 treatment group had 528+/-13 fluorescence/minute, $p<0.05$, Figure 6-3. TAPI-0 also reduced ADAM17 activity by 59% in LPS conditioned groups, where DMSO control group had 2459+/-119 fluorescence/minute and TAPI-0 treatment group had 1019+/-232 fluorescence/minute, $p<0.05$, Figure 6-3.

The results demonstrated the presence of enzymatically active ADAM17 in TLR4 activated RAW264.7 macrophages. This section also showed that inhibitors for ADAM17, significantly down-regulated the substrate cleavage. Utilizing these inhibitors the next section was aimed to investigate its effect of ADAM17 inhibitors on the release of TNF-α, IL-6 and IL-6Rα.
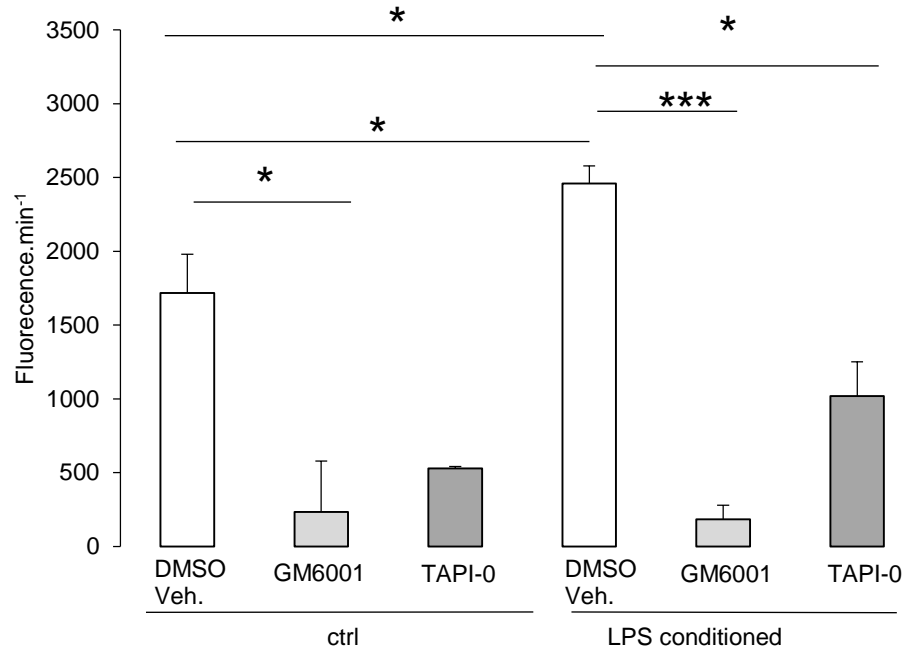
Figure 6-3 ADAM17 activity in LPS activated macrophages and the effect of LPS conditioning, GM6001 and TAPI-0

RAW264.7 macrophages were incubated with 10 ng/ml LPS for 24 hours to produce LPS conditioned macrophages. Non conditioned macrophages (ctrl) did not receive this preconditioning. Subsequently the media was replaced and the cells were stimulated with 150 ng/ml LPS for 3 hours and TACE II substrate was applied at 5 μM with/without inhibitors for ADAM17, 4.5 μM GM6001, light grey bars, or 0.3 μM TAPI-0, dark grey bars, for the final hour. Control wells received DMSO, clear bars, and the final concentration of DMSO in all wells was 0.15%. Fluorescence signals were monitored every 10 minutes for 60 minutes after the addition of the enzyme substrate and the rate of change in fluorescence between 10 to 50 minutes was expressed as ADAM activity (fluorescence/minute). Bars represent mean+SEM, n=4, repeated experiments. Statistical significance within groups received no LPS conditioning or within the groups received LPS conditioning was tested using one-way ANOVA followed by Dunnett's test. Statistical significance between non conditioned and LPS conditioned groups were tested using paired t-test. *p<0.05, ***p<0.001.

6.2.3   Effect of a general inhibitor for membrane metalloproteases, GM6001 and ADAM17 specific inhibitor, TAPI-0, on TNF-α and/or IL-6Rα release from TLR4 activated macrophages

GM6001 doses at 0.45-4.5 μM was applied during 150 ng/ml LPS activation of macrophages for 4 hours and its effect on TNF-α and IL-6Rα release was assessed. GM6001 dose dependently inhibited TNF-α release with the maximum decrease in TNF-α secretion by 86% at 4.5 μM GM6001. The level of TNF-α was 12.9+/-4.2 ng/ml in DMSO control and 1.8+/-0.48 ng/ml in the 4.5 μM GM6001 treatment group, p<0.001 Figure 6-4a. IL-6Rα release was also inhibited by GM6001 with the maximum reduction of 49% occurring at 1.5 μM GM6001. The level of IL-6Rα was 81.6+/-6.2 pg/ml in DMSO control group and 32.6+/-0.5 pg/ml in the group with 1.5 μM GM6001 treatment, p<0.05, Figure 6-4a.

TAPI-0 0.1- 0.6 μM was applied to RAW264.7 macrophages during 150 ng/ml LPS activation for 4 hours. TAPI-0 inhibited the release of TNF-α with the maximum reduction by 70% at 0.3 μM TAPI-0. The level of TNF-α was 13.0+/-2.2 ng/ml in DMSO control group and 3.9+/-0.24 ng/ml in the 0.3 μM TAPI-0 p<0.05, Figure 6-5a. TAPI-0 inhibited IL-6Rα release and with a maximum inhibition of 49% in the groups treated with 0.3 μM TAPI-0. The level of IL-6Rα was 79.2+/-8.7 pg/ml in DMSO control group and 41.3+/-12.8 pg/ml in 0.3 μM TAPI-0 group, Figure 6-5a.
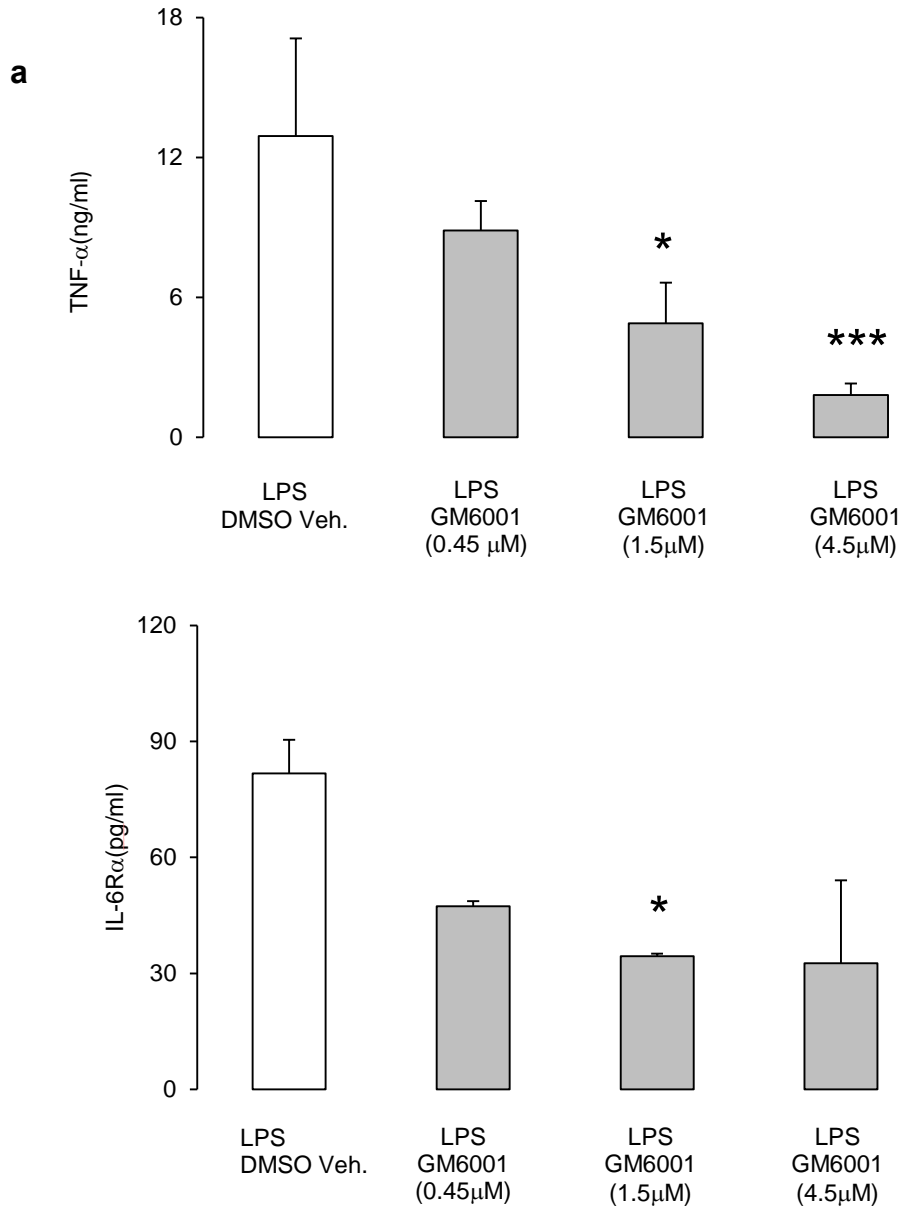
b
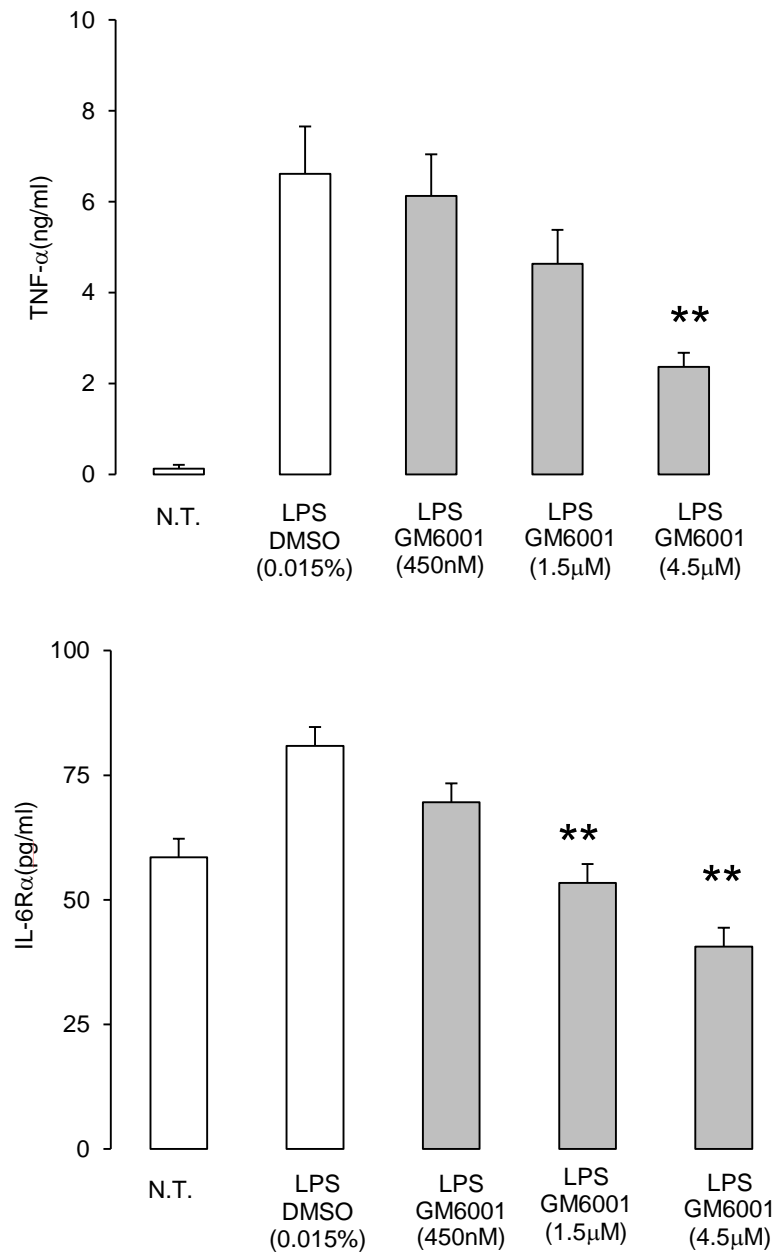
Figure 6-4 Effect of GM6001 on TNF-α and IL-6Rα release from LPS activated macrophages

RAW264.7 macrophages were treated with 150 ng/ml LPS with/without 0.45, 1.5 or 4.5 μM GM6001, grey bars, or vehicle control, clear bars. At 4 hours culture media was collected. The amount of TNF-α and IL-6Rα in conditioned media was measured by ELISA. Bars show mean+SEM (n≥3). a) shows results from one experiment with n=3 and b) shows combined data from 3 repeated experiments. Controls received DMSO vehicle (DMSO Veh.) and all wells had 0.015 % DMSO. Statistical significance of treatment groups compared to DMSO control group was tested using one-way ANOVA followed by Dunnett's test.*p<0.05, **p<0.001.

a

b
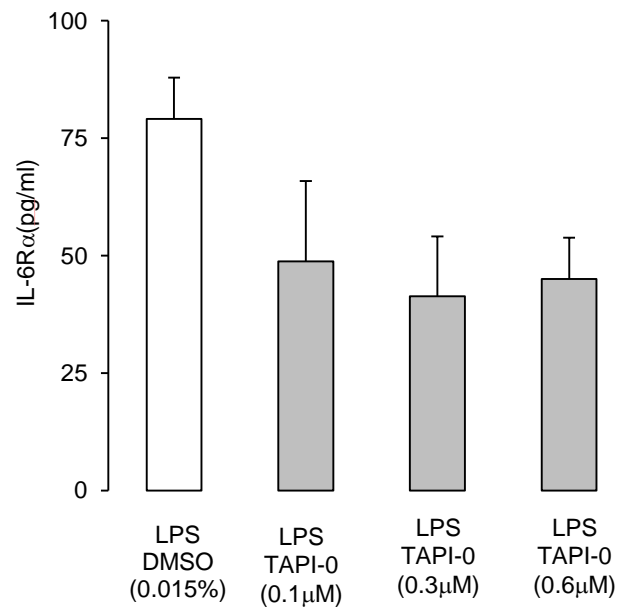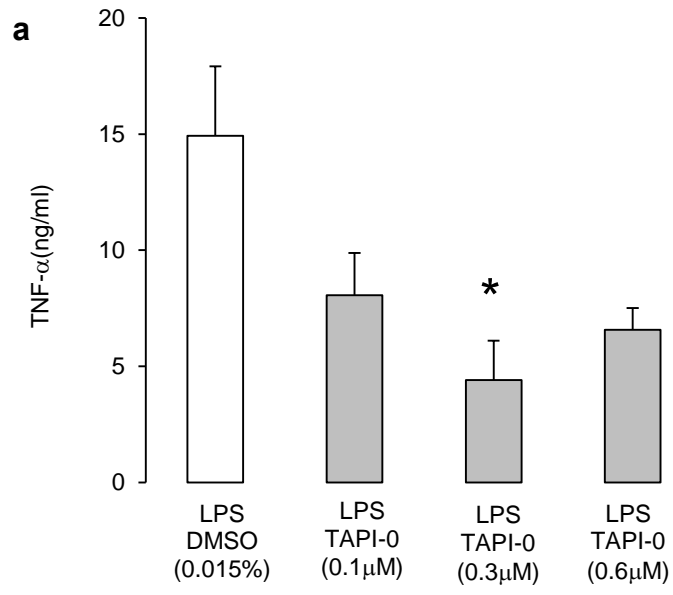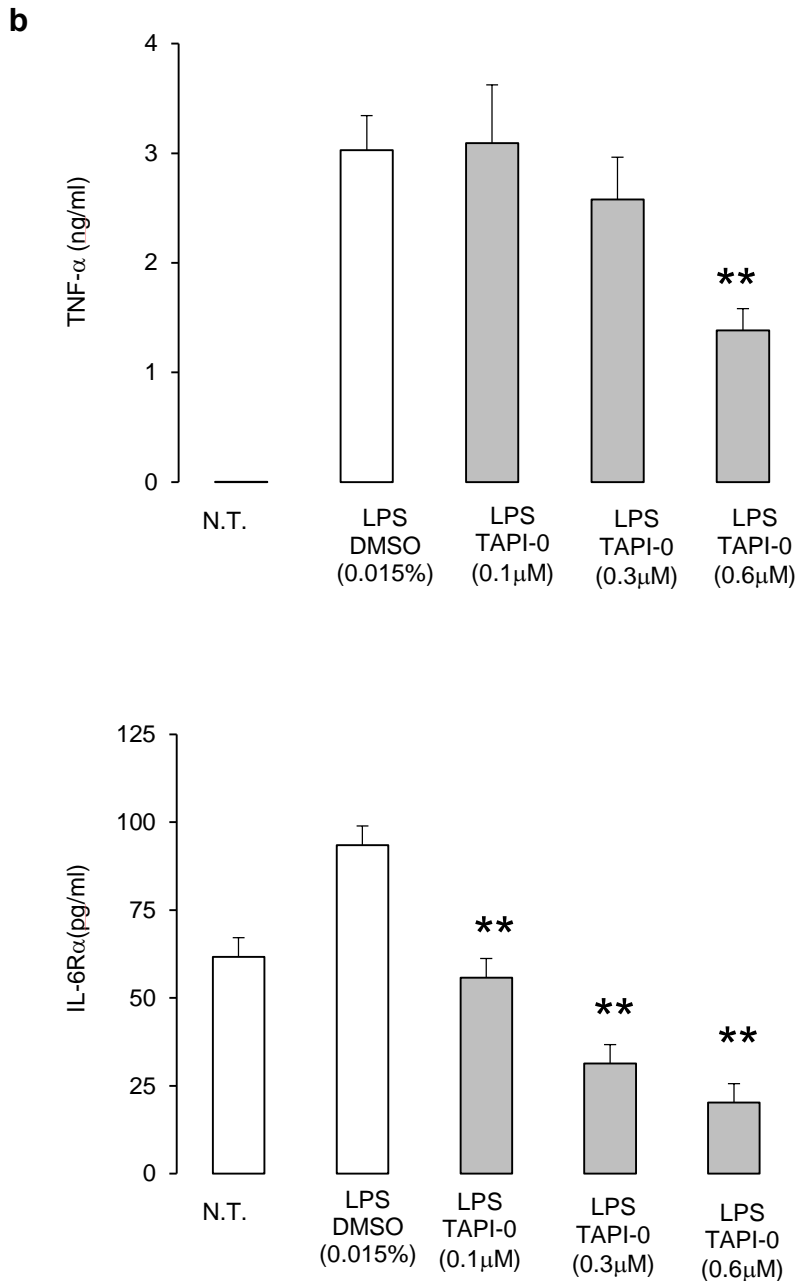
Figure 6-5 Effect of an ADAM17 inhibitor, TAPI-0, on TNF-α and IL-6Rα release from LPS activated macrophages

RAW264.7 macrophages were treated with 150 ng/ml LPS with/without 0.1, 0.3 or 0.6 μM TAPI-0, grey bars, or vehicle control, clear bars. At 4 hours culture media was collected. The amount of TNF-α and IL-6Rα in conditioned media was measured by ELISA. Bars represent mean+SEM (n≥3).a) shows result from one experiment with n=3 and b) shows combined data from 3 repeated experiments. Controls contained 0.015 % DMSO. Statistical significance of treatment groups compared to DMSO control group was tested using one-way ANOVA followed by Dunnett's test.*p<0.05, **p<0.01, ***p<0.0001.

6.2.4 Effect of GM6001 and TAPI-0 on IL-6 release from TLR4 activated macrophages

Application of GM6001 did not affect the release of IL-6. The level of IL-6 was recorded as 0.65+/-0.059 ng/ml from DMSO control group and 0.62+/-0.045 from 4.5 μM GM6001 treatment group, Figure 6-6a. TAPI-0 treatment did not affect the release of IL-6 and was 0.35+/-0.017 ng/ml in the DMSO control group and 0.32+/-0.0072 ng/ml in the group received 0.6 μM TAPI-0, Figure 6-6a. MTT assay showed that GM6001 and TAPI-0 treatments had no effect on the viability of cells, Figure 6-7a.

b
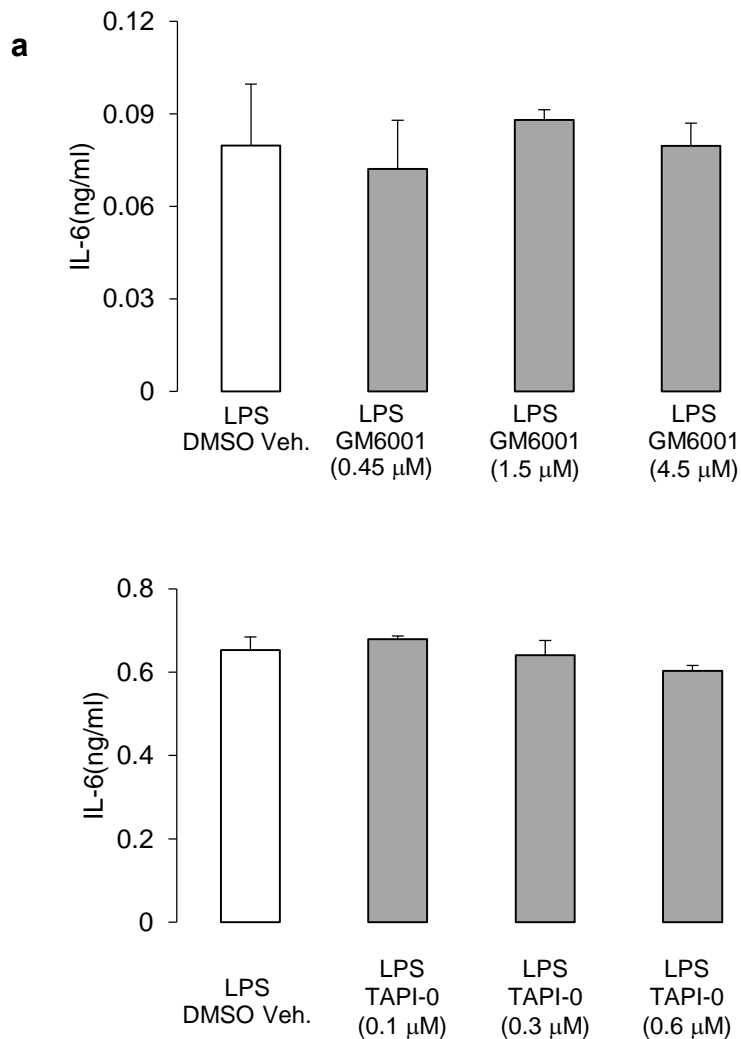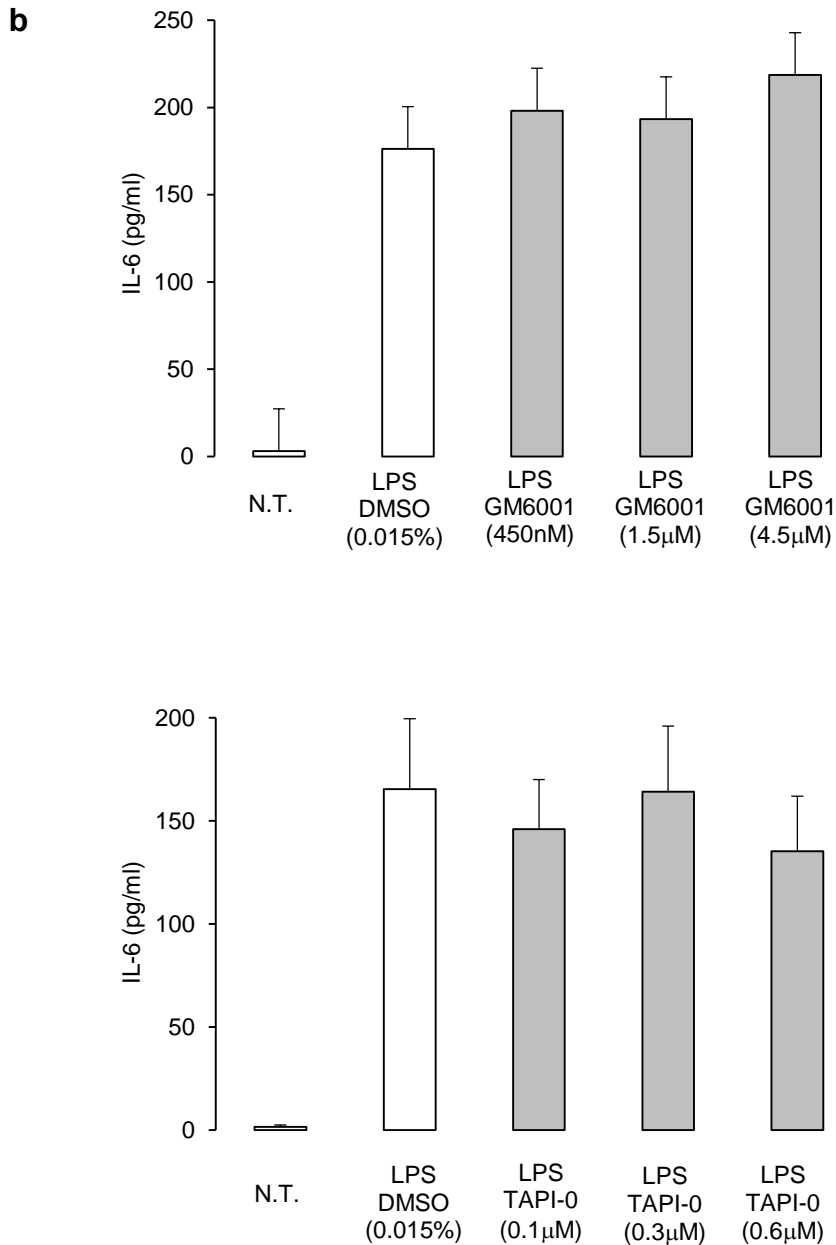
Figure 6-6 Effect of GM6001 and TAPI-0 on IL-6 release from LPS activated macrophages

RAW264.7 macrophages were treated with 150 ng/ml LPS with 0.45, 1.5 or 4.5 μM GM6001 or 0.1, 0.3 or 0.6 μM TAPI-0 grey bars, or vehicle control, clear bars. At 4 hours culture media was collected. The amount of IL-6 in conditioned media was measured by ELISA. Bars represent mean+SEM (n$\geq$3). a) shows result from one experiment and b) shows combined data from 3 repeated experiments. Controls groups received DMSO vehicle (DMSO Veh.) and all wells contained 0.015 % DMSO. Statistical significance of treatment groups compared to DMSO control group was tested using one-way ANOVA followed by Dunnett's test.

a

b
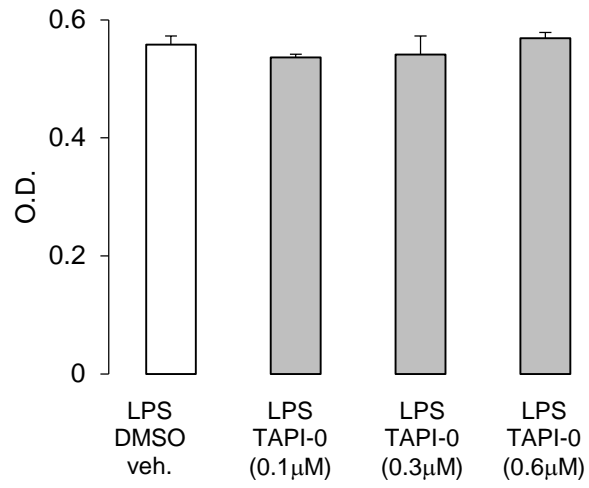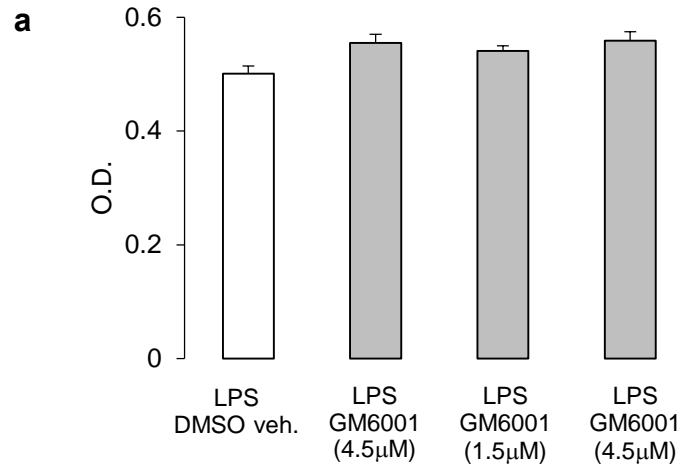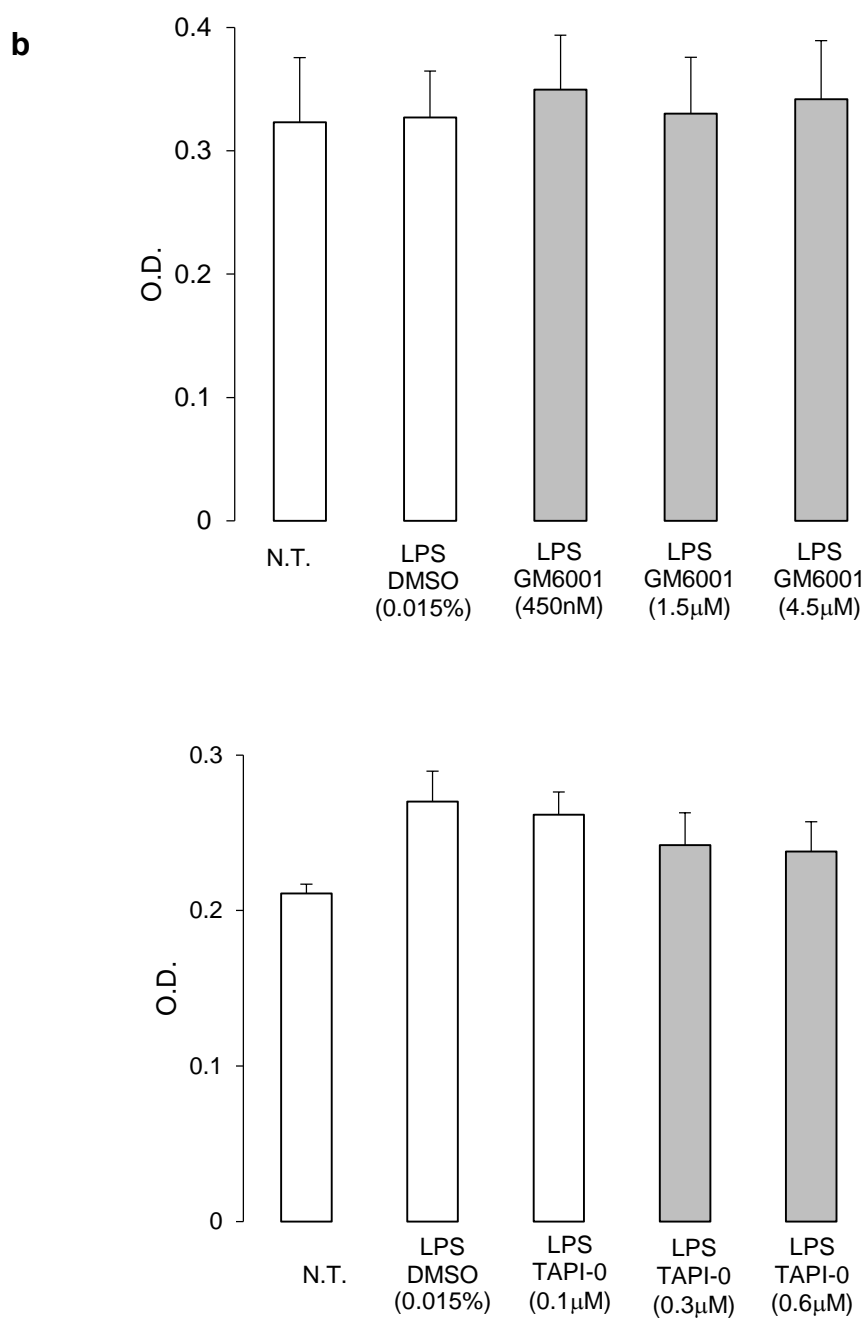
Figure 6-7 Effect of LPS, GM6001 or TAPI-0 treatments on cell viability

RAW264.7 macrophages were treated with 150 ng/ml LPS with 0.45, 1.5 or 4.5 μM GM6001 or 0.1, 0.3 or 0.6 μM TAPI-0, grey bars, or vehicle control, clear bars. At 4 hours cell viability was assessed by MTT assay and expressed as mean+SEM (n≥3). a) shows results from one experiment and b) shows combined data from 3 repeated experiments. O.D.: optical density. Controls groups received DMSO vehicle (DMSO Veh.) and all wells contained 0.015 % DMSO. Statistical significance of control group compared to treatment groups was tested using one-way ANOVA followed by Dunnet's test.

6.2.5   Effect of IbTX on ADAM17 activity in macrophages

IbTX had no effect on the activity of ADAM17 during 4 hours of LPS activation with activity being 1545+/-42 fluorescence/minute in LPS only group and 1457+/-108 fluorescence/minute in LPS with IbTX group, N.S., Figure 6-8. Next RAW264.7 macrophages received LPS conditioning to upregulate the plasma membrane BK channel. 30 nM IbTX was applied to these macrophages and its effect on ADAM17 activity was compared to conditioned macrophages which did not receive IbTX. In LPS conditioned cells, IbTX treatment dramatically increased ADAM17 activity by 150%. The activity was at 2560+/-228 fluorescence/minute in control LPS group and at 7095+/-1485 fluorescence/minute in IbTX treatment group, $p < 0.05$, Figure 6-9 . In all treatment groups, the increase in fluorescence was inhibited by 4.5 μM GM6001. The activity was 166+/-111 fluorescence/minute in the group received LPS and GM6001, $p < 0.01$ compared to LPS with DMSO control group, and at 394+/-99 fluorescence/minute in the group received LPS, IbTX and GM6001, $p < 0.001$ compared to control. This indicated that fluorescence signals were due to the activity of membrane bound metalloproteases. In LPS conditioned groups, application of 0.3 μM TAPI-0 also inhibited activity of ADAM17 but to a lesser degree than GM6001. The activity was 1515+/-216 fluorescence/minute in the group received LPS with TAPI-0, $p < 0.05$ compared to LPS with DMSO control group and was at 1008+/-453 fluorescence/minutes in the group received LPS, IbTX and TAPI-0, $p < 0.05$ compared to the group with LPS, IbTX and DMSO control, Figure 6-9.

The combined data, from repeated ($\geq$ 3 times) experiments, for protein release and MTT was in line with the described results from individual experiments. These combined data were presented in Figure 6-3, 6-4, 6-5, 6-6 and 6-7. Statistical analysis of combined data and individual experimental data demonstrated a similar pattern of significance between treatment groups. It was higher degree of significance was seen in combined data compared to individual experimental data.
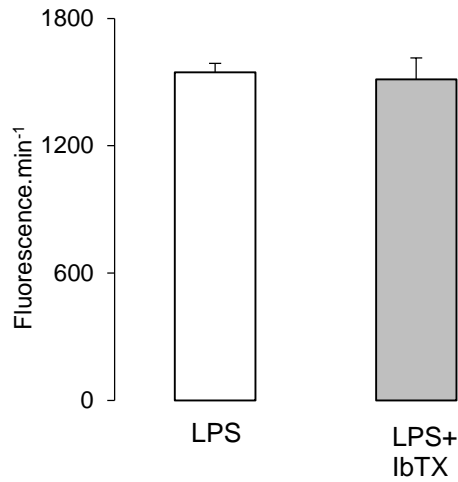
Figure 6-8 Effect of IbTX on ADAM17 activity of LPS activated of macrophages

RAW264.7 macrophages were stimulated with 150 ng/ml LPS with/without 30 nM IbTX for 3 hours and TACE II substrate was applied at 5 μM during the first 1 hour. Fluorescence signals were monitored in 10 minutes interval for 60 minutes and signals between 10 to 50 minutes used for analysis. The concentration of DMSO in all wells was at 0.15%. ADAM17 activity was measured as per minutes increase in fluorescence signal. Bars show mean+SEM with n=3 repeated experiments. Statistical significance was tested by paired t-test.
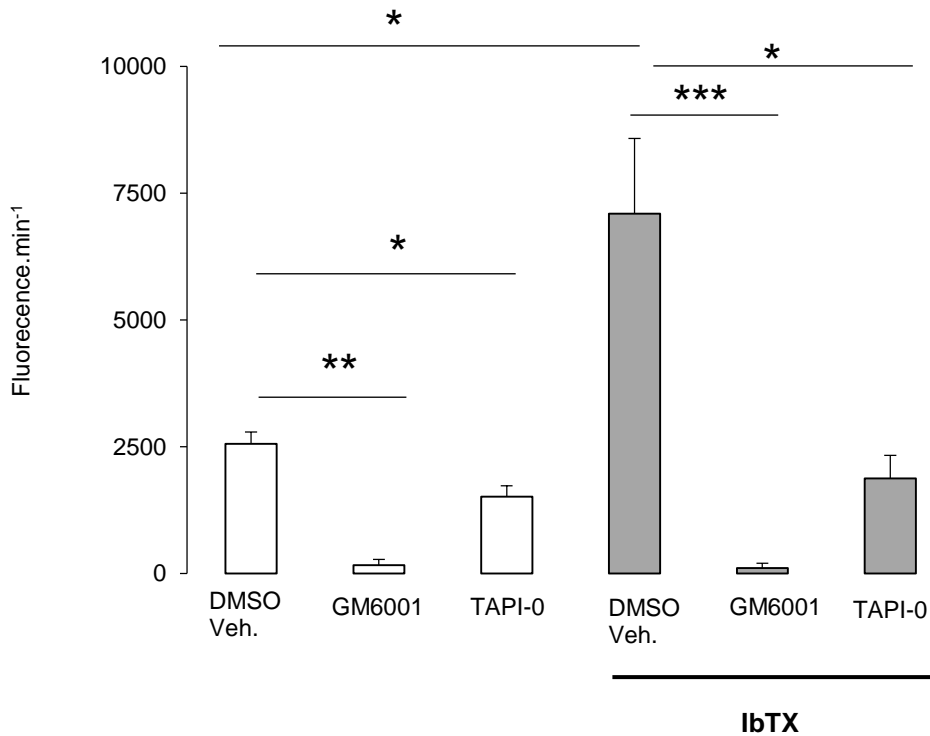
Figure 6-9 Effect of IbTX on ADAM17 activity in LPS conditioned macrophages

RAW264.7 macrophages were incubated with 10 ng/ml LPS for 24 hours to produce LPS conditioned macrophages. Subsequently these macrophages were stimulated with 150 ng/ml LPS for 3 hours and TACE II substrate was applied at 5 μM for the final hour. Cells recived IbTX, grey bars, or media alone, clear bars, with/without inhibitors for ADAM17, 4.5 μM GM6001 or 0.6 μM TAPI-0. The final DMSO concentration was 0.15 % and DMSO acted as the vehicle control (DMSO Veh.) Fluorescence signals were monitored in 10 minutes interval for 60 minutes and the rate of change in fluorescence between 10 to 50 minutes was used to assess ADAM activity (fluorescence/minute). Bars show mean+SEM with n=3 repeated experiments. Statistical significance between the treatment groups of interest versus the relevant control group is indicated by horizontal lines and tested using paired t-test. *p<0.05,**p<0.01,***p<0.0001.

6.2.6   Effect of IbTX on ADAM17 expression

The effect of IbTX on the expression of ADAM17 during LPS activation of conditioned macrophages was analysed by Western blot in a single preliminary study. It was difficult to obtain clean blot from this experiment. However at whole cell level there was 51% increase in the expression of 85 kDa protein band with IbTX treatment, while the level of 130 kDa protein was not affected, Figure 6-10.
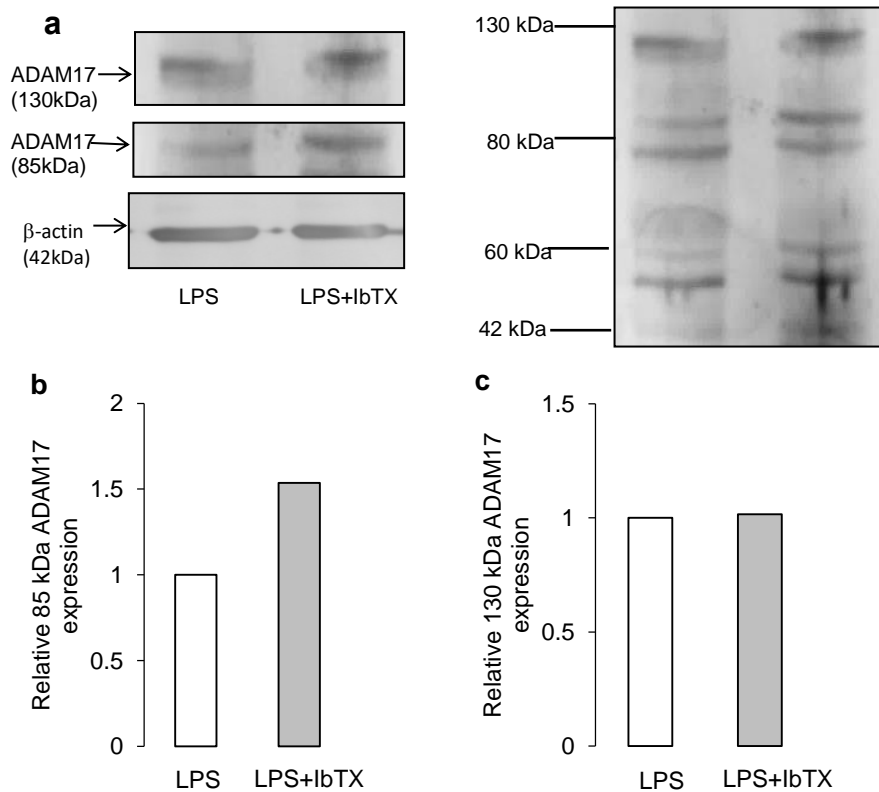
Figure 6-10 Preliminary data. Effect of IbTX on ADAM17 expression

RAW264.7 macrophages were incubated with 10 ng/ml LPS for 24 hours to produce LPS conditioned macrophages. Subsequently the media was replaced and the conditioned cells were activated with 150 ng/ml LPS for 4 hours with, grey bars, or without, clear bars, 30nM IbTX. a) ADAM17 expression was analysed by Western blot and β-actin acted as a loading control. Densitometry analysis shows relative expression of b) 85 kDa band or c) 130 kDa in IbTX treatment group compared to activated macrophage containing no IbTX only group. Blots were obtained from a single preliminary experiment.

6.3   Discussion

ADAM17 was first identified in 1997 as a membrane bound enzyme which release mTNF-α from the cell surface (Black *et al.*, 1997; Moss *et al.*, 1997). Since its discovery, a diverse range of molecules, including cytokines, growth factors, receptors and adhesion molecules have been found to be the targets for ADAM17. 76 proteins have been identified as substrates for the enzyme (Scheller *et al.*, 2011; Giebeler and Zigrino, 2016). Many of the substrates for ADAM17 are involved in the inflammatory responses as well as in other intercellular signalling mechanisms. Examples include the regulation of TNF-α signalling by the cleavage of TNF-α and its receptors, the initiation of epidermal growth factor receptor (EGFR)-mediated proliferation by ecotodomain shedding of heparin-binding EGF-like growth factor (HB-EGF) and the modulation of regulated intramembrane proteolysis by cleavage of Notch receptor. Taken together ADAM17 regulates a wide range of biological responses, including the immune response, cell survival and growth (Scheller *et al.*, 2011). However an essential question is how ADAM17 selectively regulates the release of these substrate molecules in a special manner to initiate specific cellular signalling pathways?

Due to its important role in biology, ADAM17 is one of the best characterised members of membrane metalloproteases family. While global ADAM17 knock-out animals are not viable, the significance of this enzyme is seen in the studies using a cell specific gene deletion, for example, mice deficient in myeloid ADAM17 are resistant to septic shock (Horiuchi *et al.*, 2007). The enzyme has been also shown to mediate key roles in the regeneration and resolution of inflammation. Using a novel transgenic technique termed exon-induced translational stop, it was demonstrated that epithelial cells with an approximately 95% reduction in ADAM17 expression had deficiencies in intestinal barrier function and poor recovery after intestine inflammation. This was due to insufficient TGFα and EGFR signalling (Chalaris *et al.*, 2010).

Perhaps reflecting its important role, the expression and activity of the protease is highly regulated, with the protein undergoing a series of maturation processes to become an active enzyme on the plasma membrane. It has been reported that ADAM17 is initially translated as a catalytically inactive form with pro-domain masking the catalytic site of this enzyme. At late Golgi compartment, the pro-domain

is cleaved by furin convertases, which is thought to be essential for ADAM17 protease activity. Due to this maturation process, the cellular ADAM17 is likely to appear at two distinct molecular weights, a 133 kDa full length precursor and 90 kDa matured enzyme without pro-domain peptide (Schlöndorff *et al.*, 2000). The enzyme is then transported to the plasma membrane by iRhom2. Research has reported that this translocation by iRhom2 is essential for the expression and function of ADAM17 at the plasma membrane (Adrain *et al.*, 2012; McIlwain *et al.*, 2012; Siggs *et al.*, 2012). Phosphorylation of cytoplasmic tail of ADAM17 by p38 at thereonine 735 has also been reported to increase the trafficking of ADAM17 to the cell surface (Soond *et al.*, 2005). At the cell surface, ADAM17 is thought to exist as a homo-dimer in association with tissue inhibitor of metalloproteinases-3 (TIMP-3) (Xu *et al.*, 2012b). Inflammatory signalling is believed to cause the dissociation of this dimer into an active monomer enzyme and the release of TIMP-3. Yet, the precise mechanism by which ADAM17 becomes activated is still controversial. A study has suggested that early in an inflammatory response, the release of TNF-α and L-selectin by ADAM17 does not require the removal of pro-domain of the enzyme nor TIMP-3 dissociation suggesting a more rapid and reversible activation of this enzyme. These authors speculated that early ADAM17 activation was determined by the local lipid bilayer microenvironment, composition and charge (Schwarz *et al.*, 2013). In another study it was demonstrated that the enzyme does not require the phosphorylation of C-terminal, but that the transmembrane region of the ADAM17 is essential in the control of substrate cleavage (Li *et al.*, 2007). However the majority of these studies are carried out in cell expression systems which may not contain all relevant regulatory mechanisms found for ADAM17 activation in other cells and interpretations of these results could be limited.

This chapter characterised the expression and function of ADAM17 and tested the hypothesis that BK channel on the plasma membrane regulated the activity of this enzyme. ADAM17 is expressed 85 kDa and 130 kDa protein in whole cell lysate and plasma membranes isolates from RAW264.7 macrophages. Protein bands at 130 kDa are believed to represent its precursor form with the 85 kDa form indicating the matured form of the enzyme. Previous research demonstrated that the sheddase activity of this enzyme is positively correlate with the mature form of the enzyme (Black *et al.*, 1997).

Interestingly, the expressions of ADAM17 followed a distinct pattern between whole cell and plasma membrane during LPS activation of RAW264.7 macrophages. At whole cell level, 130 kDa ADAM17 appeared to be present under resting condition and remained at similar level thought the time course of LPS activation. Taking this into account, it appeared that there was an increase in the mature form of ADAM17 at 85 kDa, 12 to 18 hours after LPS treatment. In this thesis the ADAM17 at 85 kDa did not appear as a distinct band, but appeared as smear. The existence of full-length ADAM17 on the plasma membrane of RAW264.7 macrophages contrasted with the conclusion from a study using human COS-7 cells, where full length form ADAM17 was hardly detected in the cell surface protein (Schlöndorff *et al.*, 2000). Possible explanations for this phenomenon may include differences in the cell surface protein isolation process, different mode of cell activation and/or species specific regulation of ADAM17 localisation. While the above measurement of ADAM17 protein in cell preparation is important, ADAM17 activity in living cells general gives a better insight into control mechanism for an enzyme.

The use of a fluorogenic substrate for ADAM17 indicated the presence of membrane sheddase activity of ADAM17 in RAW264.7 macrophages. The use of the general metalloproteases inhibitor, GM6001, also confirmed that the activity assay was measuring the membrane metalloproteases activity in RAW264.7 macrophages. The enzyme activity in these macrophages seemed to increase after LPS treatment. The data could indicate that LPS may have caused the upregulation of this enzymes activity in these cells. Importantly a selective inhibitor for ADAM17, TAPI-0 also inhibited the increased activity. This data support a role for ADAM17 in this assay and demonstrate the presence of ADAM17 on the plasma membrane on RAW264.7 macrophages. Comparing the degree of inhibition between GM6001 and TAPI-0, it appeared that the ADAM17 was the dominant metalloprotease responsible for the breakdown of TACE II substrate.

Cells release cytokines by a variety of mechanisms, such as membrane fusion of secretary granules and ecoto-domain shedding of transmembrane anchored cytokines by membrane bound proteases (Stow *et al.*, 2009). Macrophages release TNF-α via the latter mechanisms (Arango Duque and Descoteaux, 2014). In line with this, the inhibition of membrane metalloproteases by GM6001 significantly reduced the amount of TNF-α release from LPS activated RAW264.7 macrophages.

The release of TNF-α was also significantly reduced by the application of TAPI-0, a selective inhibitor of ADAM17. The maximum inhibition of TNF-α release achieved with this drug was approximately 70%, as compared with 90% with GM6001. The discrepancy in the inhibitory effects between GM6001 and TAPI-0 could suggest the involvement of other membrane metalloproteases such as ADAM10 in TNF-α release, with the greater effect of GM6001 being due to the inhibition of both ADAM10 and ADAM17. However the difference also may due to the potency and/or half-lives of the two drugs. In this thesis, TAPI-0 was found to have a maximal effect on TNF-α inhibition at 0.3 μM. It must be noted that at concentrations above 2 μM, TAPI-0 has been shown to inhibit other metalloproteinases. To further investigate the release of TNF-α in the system, it would be necessary to silence ADAM17 by gene silencing. However, it is difficult to achieve an effective silencing of protein expression in RAW264.7 cells as it will be discussed in chapter 7.

The inhibition of membrane metalloproteases by GM6001 and the inhibition of ADAM17 by TAPI-0 also effectively inhibited the release of IL-6Rα. It has been known that ADAM10 and ADAM17 are involved in the release of IL-6Rα. Another study has suggested that ADAM10 and ADAM17 may work on different regions for cleavage. ADAM17 requires its stalk region, a triple serine (3S) motif (Ser-359 to Ser-361) adjacent to the cleavage site for IL-6Rα in human, while ADAM10 does not (Riethmueller *et al.*, 2016). The result with TAPI-0 suggested the involvement of ADAM17 in releasing IL-6Rα. To clarify involvement and relative contribution of ADAM10 and ADAM17 in RAW264.7 macrophages, the application of selective inhibitors for ADAM10 and gene silencing of individual enzyme, especially ADAM17, would be suggested.

While GM6001 and TAPI-0 inhibited the release of IL-6Rα release, the inhibition of this receptor was to lesser degree compared to the inhibition observed in TNF-α release. In addition to membrane shedding by membrane metalloproteases, alternative splicing of IL-6Rα mRNA also leads to the soluble/circulating form of IL-6Rα, which is independent of membrane metalloproteases (Rose-John and Heinrich, 1994). It is believed that the contribution of mRNA splicing pathway to IL-6Rα production is relatively minor compared to the membrane metalloprotease mediated shedding. Collectively the results demonstrated that ADAM17 protein is expressed

in RAW264.7 macrophages and functions as a membrane sheddase for mTNF-α and IL-6Rα. Therefore although other metalloproteases than ADAM17 also cause the release of TNF-α and IL-6Rα, the data from this chapter would suggest that ADAM17 mediated sheddase activity is the major mechanism by which TNF-α is released from RAW264.7 macrophages.

Pharmacological inhibition of plasma membrane located BK channels in RAW264.7 macrophages by IbTX dramatically enhanced the activity of ADAM17. This result was in line with the observation from chapter 5, where IbTX significantly enhanced TNF-α and IL-6Rα release and reduced cellular mTNF-α. Importantly IbTX only increased ADAM17 in conditioned macrophages. The LPS pre-conditioning is required to increase the expression of the BK channel on the plasma membrane, and therefore the data is in line with a role for the channel in regulating ADAM17 activity. The results suggest that BK channels on the plasmas membrane of macrophages negatively regulate the activity of ADAM17. As a preliminary study, it was tested if IbTX changed in ADAM17 expression. IbTX appeared to increase the expression of 85 kDa ADAM17 in LPS stimulated RAW264.7 macrophages. However it should be noted that this data is from a single preliminary experiment and this interpretation is limited in the case that the level of 85 kDa ADAM17 expressions and its activity is directly proportional to each other. To confirm this phenomenon, further experiments is required. The experiments could be suggested would be first to investigate the correlation between 85 kDa form enzyme and the activity of ADAM17 in RAW264.7 cells and this experiment also need to be further repeat with plasma membrane isolate.

The data suggested a role for BK channels in regulating TNF-α and IL-6Rα from macrophages via activity of ADAM17. This links an ion channel activity to protein secretory mechanisms and suggests a novel regulatory process for ADAM17. However this analysis relays on the selectivity of IbTX for BK channels. Therefore in next chapter an alternative method to inhibit BK channels, gene silencing, was used.

Chapter 7 Does BK channel silencing upregulate ADAM17 activity in macrophages?

7.1 Introduction

Chapter 6 showed that a pharmacological inhibition of the plasma membrane BK channel increased the activity of ADAM17, suggesting a role for BK channels in regulating the activity of ADAM17. The aim of this chapter is to study the effect of genetic inhibition of BK channels on ADAM17 to validate the results using IbTX. The introduction of genetic materials into macrophages is known to be problematic as transfection reagents/vectors themselves can lead to the activation of macrophages. In addition stably transfected macrophages can lead to the generation of sub-clones from a heterogenic macrophage population which may show different activities compared to the original population. Therefore it was decided to use transient transfection with siRNA to knock-down BKα in RAW264.7 macrophages. The first part of this chapter attempted to optimize the transfection protocol to inhibit BKα expression in RAW264.7 macrophages. Secondly, the effect of BKα silencing on the release of TNF-α and IL-6Rα and the activity of ADAM17 was investigated.

7.2 Results

7.2.1 Optimization of siRNA protocol in macrophages

7.2.1.1 Transfection reagents for the inhibition of BKα protein expression

First objective of this chapter was to develop a protocol which silenced BK channels in RAW264.7 macrophages; two sequences for BKα silencing siRNA were acquired from Qiagen. These sequences were predesigned to be selective against BKα. These two sequences were named sequence 1 and sequence 5. siRNAs were used at the recommended concentration of 10 nM in the first set of experiments, which investigated different transfection reagents, namely GeneMute™, Viromer® and lipofectamine® RNAiMAX with transfection protocols followed as described in 2.2.15. Cells received either no treatment, transfection reagent alone, transfection reagent containing non-silencing siRNA and BKα silencing siRNAs, sequence 1 and 5. BKα expression was analysed by Western blot analysis using a mouse monoclonal anti-mouse BKα, L6/60.

GeneMute™ transfection reagent was applied to RAW264.7 macrophages at the concentration of 10 nM. This reagent utilises a liposome mediated delivery of siRNA.

In line with results from chapter 4, Western blot displayed the presence of protein bands at 120 kDa as a doublet. The application of GeneMute™ reagent by itself down regulated the expression of BKα and there was no apparent difference in the expression of BKα between the non-silencing siRNA and BKα silencing siRNA treatment groups. This suggested that GeneMute™ reagent had a non-specific inhibitory effect on the expression of the protein RAW264.7 cells, Figure 7-1a. The application of higher concentrations of siRNA with GeneMute™ caused the significant proportion of cell death. Secondly BKα silencing sequence was applied to macrophages using Viromer® Blue reagent at the concentration of 10 nM. This transfection reagent uses viral vector mediated delivery of siRNA. With Viromer® Blue, the addition of non-silencing or silencing siRNA did not alter the expression of BKα in RAW264.7 macrophages, Figure 7-1b. Similar results were obtained Lipofectamine® RNAiMAX, where BKα silencing siRNA had only a minor effect in the group treated with siRNA sequence 5, Figure 7-1c. Higher concentration of siRNA with Veromer® Blue resulted in a significant proportion of cell death during the incubation with siRNA. As a minor silencing effect was seen with Lipofectamine® RNAiMAX, further optimization was carried out with Lipofectamine® RNAiMAX.
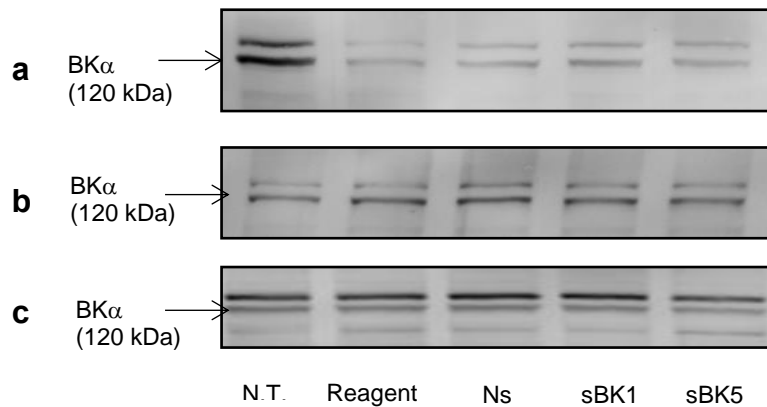
Figure 7-1 Effect of BKα silencing siRNA treatment on BKα expression using GeneMute™, Viromer ® Blue or lipofectamine® RNAiMAX reagents

RAW264.7 macrophages were not treated (N.T.) or treated with transection reagent only (Reagent), non-silencing siRNA (Ns), BKα silencing siRNA sequence 1 (sBK1), sequence 5 (sBK5). The transfection reagents used was a) GeneMute™, b) Viromer® Blue or c) lipofectamine® RNAiMAX. siRNA concentration was 10 nM. The expression of BKα was analysed by Western blot. The experiment was performed 1-2 times. Blots shown are representative of all experiments.

Due to the lack of the effect on BKα silencing by the siRNA at 10 nM, a second series of experiments were carried out using 15 nM siRNA. An additional group which contained both sequence 1 and sequence 5 (7.5 nM each) was included. Using Genemute® and Viromer® Blue as transfection reagents in this experiment resulted in cell death after 48 hours. In comparison, Lipofectamine® RNAiMAX in combination with non-silencing or silencing siRNA did not cause a noticeable change in cell morphology or adherence to the culture flasks for at least 72 hours. Using these conditions, a combination of silencing siRNA sequences 1 and 5 achieved the most effective silencing. However, the overall decrease in BKα expression was still limited to approximately 25% at whole cell lysates compared to the control which is non-silencing siRNA group, Figure 7-2. The concentration of siRNA used in subsequent experiments was 15 nM and incubation time was 72 hours.
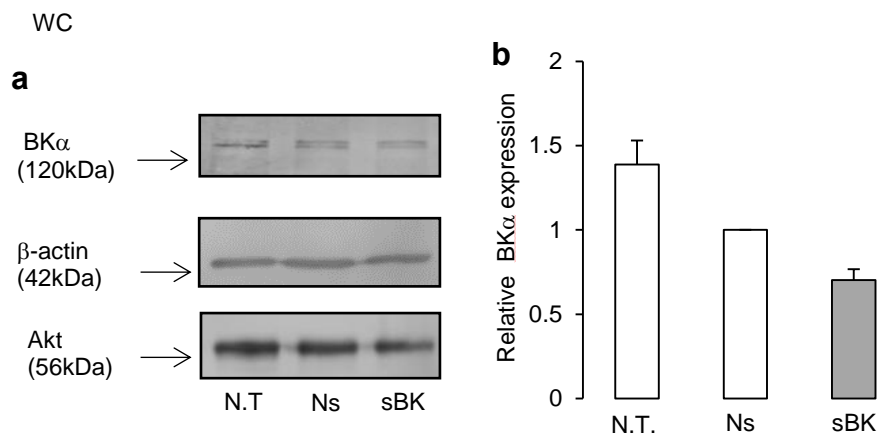
Figure 7-2 Effect of silencing siRNA on BKα expression at the whole cell in macrophages

RAW264.7 macrophages were not treated (N.T.) or treated with non-silencing siRNA (Ns) or BKα silencing siRNA (sBK), RNAiMAX was used as the transfection reagent. BKα , β-actin and Akt expression in whole cell lysate (WC) was assessed by Western blot. Densitometry analysis of relative BKα was normalised to β-actin. The amount of BKα expression in the no treatment group and BKα silencing siRNA treated group was compared to non-silencing siRNA control group. Bars represent mean+SEM with n=3 where n is number of blots used for analysis. The experiment was repeated 4 times.

.

7.2.2   Effect of BKα silencing siRNA on BKα expression on the plasma membrane
         isolate

As discussed in chapter 4, BK channels were found on the plasma membrane of RAW264.7 macrophages and at intracellular sites. As chapter 4, 5 and 6 suggested that it was the plasma membrane BK channel which was important in the regulation of ADAM17, the effect of siRNA treatment on the plasma membrane BK channel was assessed. BKα was almost undetected in plasma membrane lysate from non-treated cells, Figure 7-3a. These results were consistent with the observations made in chapter 4.   Notably, BKα was detected at 120 kDa in the plasma membrane isolate of the groups which received non-silencing siRNA, Figure 7-3a. Densitometry analysis indicated that there was approximately 5 fold increase in BKα expression on the plasma membrane in the non-silencing siRNA groups compared to the non-treated control groups, Figure 7-3b. BKα silencing siRNA reduced this expression on the plasma membrane with a 65% reduction when compared to non-silencing siRNA groups, Figure 7-3b. MTT assay was carried out to assess if the siRNA treatment affected the viability of the cells.
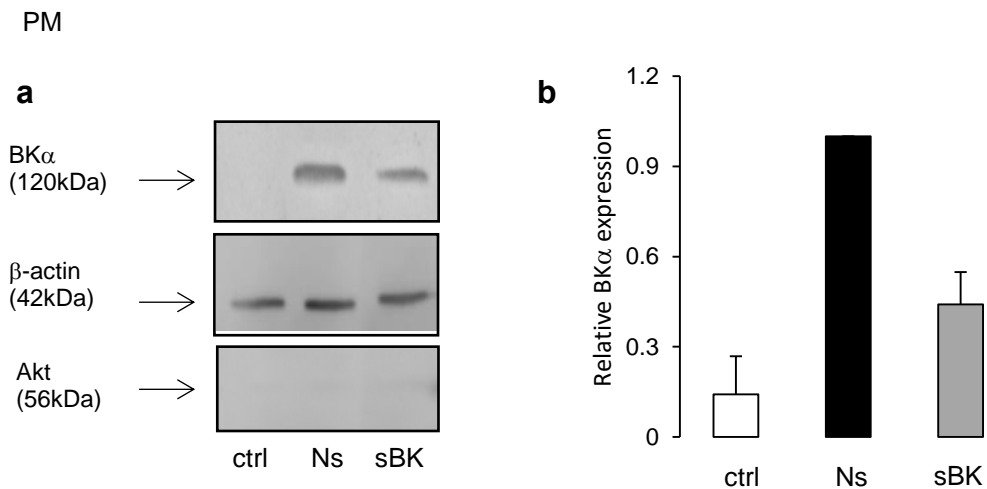
Figure 7-3 Effect of BKα silencing siRNA on BKα expression at the plasma membrane in macrophages

RAW264.7 macrophages were not treated (N.T.) or treated with non-silencing siRNA (Ns) or BKα silencing siRNA (sBK) using lipofectamine® RNAiMAX. BKα, β-actin and Akt expression in plasma membrane isolates (PM) was assessed by Western blot. Densitometry analysis of relative BKα was normalised to β-actin. The amount of BKα expression in the no treatment group and BKα silencing siRNA treated group was compared to non-silencing siRNA control group. Bars represent mean+SEM with n=3 where n is number of blots used for analysis. The experiment was repeated 3 times.

7.2.3 Effect of BKα silencing siRNA on TNF-α release and mTNF-α expression during TLR4 activation

The application of non-silencing siRNA caused the upregulation of BK channel on the plasma membranes, Figure 7-3. As this was the reason for using the conditioning protocol in chapter 5, which was applied to the cells in order to upregulate the BK channel on the plasma membrane, was no longer required in this chapter. siRNA treated cells were stimulated with 150 ng/ml LPS. BKα silencing significantly increased the release of TNF-α by 107%. The level of TNF-α was 8.1+/-0.15 ng/ml in non-silencing siRNA treatment group and 16.9+/-1.9 ng/ml in BKα silencing siRNA treatment group, $p < 0.05$, Figure 7-4a. BKα silencing siRNA also resulted in the reduction in mTNF-α expression and densitometry analysis indicated that BKα silencing caused a 66% reduction in mTNF-α relative to the expression seen in the non-silencing siRNA treated group, Figure 7-5. BKα silencing siRNA also significantly increased IL-6Rα release from RAW264.7 macrophages by 50% with 103+/-30 pg/ml and 159+/-7.3 pg/ml measured in the no-silencing and BKα silencing siRNA treatment group respectively, $p < 0.05$, Figure 7-6a.

The combined data, from repeated experiments over 3 times, for protein release and MTT was in line with the described results from individual experiments. These combined data were presented in Figure 7-4 c and d, and 7-6b. Statistical analysis of combined data and individual experimental data demonstrated a similar pattern of significance between treatment groups in TNF-α and IL-6Rα release. It was noted combined data from repeated experiments reached higher degree of significance in these molecules release. However the cell viability was shown to be affected by the siRNA application in combined data with approximately 40% degrease, Figure 7-4d. This may be due to reported off target effect of siRNA transfection to immune cells (De Arras *et al.*, 2014), which will be discussed in 7.3 discussion. However the decrease was equivalent in non-silencing siRNA, which is the control group and BKα silencing siRNA groups, which is the treatment group in the experiment. Therefore this did not affect the analysis nor interpretation of the effect of BK channel inhibition.
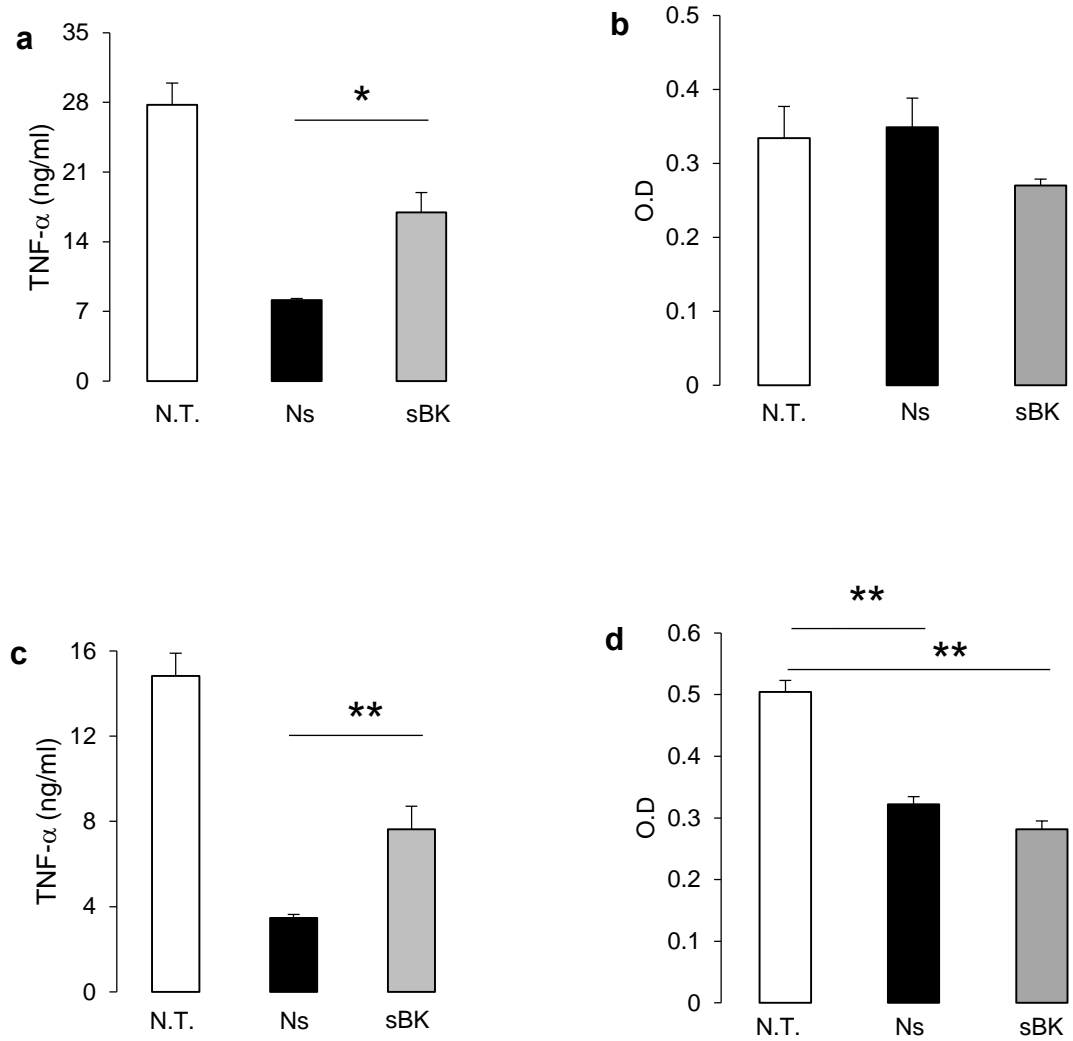
Figure 7-4 TNF-α release and cell viability in macrophages after treatment with BKα silencing siRNA

RAW264.7 macrophages were not treated (N.T), clear bar, or treated with non-silencing siRNA (Ns), black bars, or BKα silencing siRNA (sBK), grey bar followed by stimulation with 150 ng/ml LPS. After 4 hours cell culture media were collected. The level of TNF-α in conditioned media was measured by ELISA. Cell viability was assessed by MTT assay. Bars represent mean+SEM (n≥4). a) & b) shows result from one experiment with n=4 and c) & d) shows combined data from 3 repeated experiments.

a

mTNF-α
(26kDa)

β-actin
(42kDa)

Ns   sBK

b
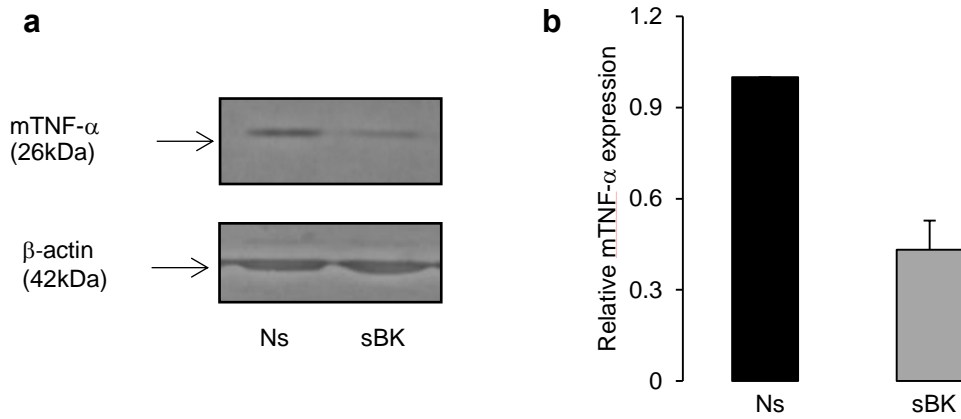
Figure 7-5 Effect of BKα silencing siRNA on mTNF-α expression in macrophages

RAW264.7 macrophages were treated with non-silencing siRNA (Ns), black bar, or BKα silencing siRNA (sBK), grey bar followed by stimulation with 150 ng/ml LPS. After 4 hours cell were collected for Western blot analysis a) mTNF-α and β-actin. b) Densitometry analysis shows relative mTNF-α expression in the BKα silencing siRNA treated group compared to non-silencing siRNA treated group. Bars represent mean+SEM (n=3), where n is the number of blots used for analysis. The experiment was repeated 4 times.
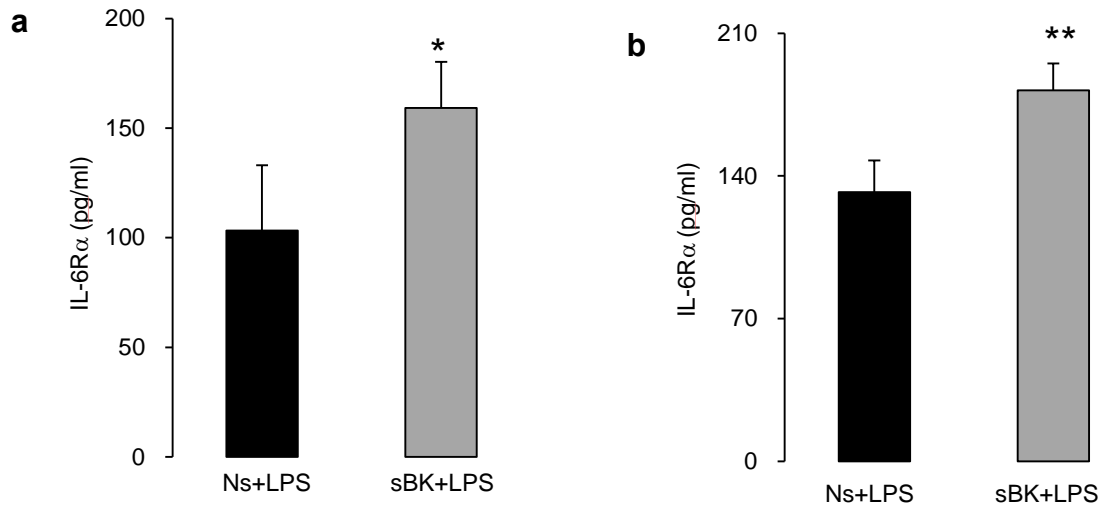
Figure 7-6   Effect of BKα silencing siRNA on IL-6Rα release from macrophages

RAW264.7 macrophages were treated with non-silencing siRNA (Ns), black bar, or BKα silencing siRNA (sBK), grey bars, followed by stimulation with 150 ng/ml LPS. After 4 hours medium was collected for IL-6Rα measurement by ELISA. Bars represent mean+SEM (n≥4). a) shows result from one experiment with n=4 and b) shows combined data from 3 repeated experiments. Statistical significance between the two treatment groups was tested using paired t-test. *p<0.05, **p<0.01.

7.2.4 Effect of BKα silencing siRNA on and ADAM17 activity

ADAM17 activity was assessed in BKα silenced and non-silenced RAW264.7 macrophages. As previously described, silenced or non-silenced macrophages were counted on the day of the assay in the suspended in phenol red free DMEM and directly plated onto the wells. The cells were stimulated with 150 ng/ml LPS and after 3 hours, TACE substrate II was directly added. Fluorescence signal was monitored for 1 hour duration. The groups treated with BKα silencing siRNA had doubled the activity of ADAM17 compared to non-silencing siRNA treatment. The activity was 10294+/-2704 fluorescence/minute in non-silencing siRNA and 20565+/-4723 fluorescence/minute in BKα silencing siRNA treated group, p<0.05, Figure 7-7. Treatment with GM6001 significantly reduced activity and with 2304+/-1430 fluorescence in non-silencing siRNA group and 4597+/-3981 fluorescence/minute in BKα silencing siRNA group being recorded, Figure 7-7. A preliminary experiment with Western blot analysis of 85 kDa ADAM17, which are considered to be biological active form of the enzyme, see 6-3 discussion, showed that there was 43% increase in the level of 85 kDa ADAM17 protein in the groups receiving BKα silencing siRNA compared to the non-silencing siRNA control groups, Figure 7-8 a and b.
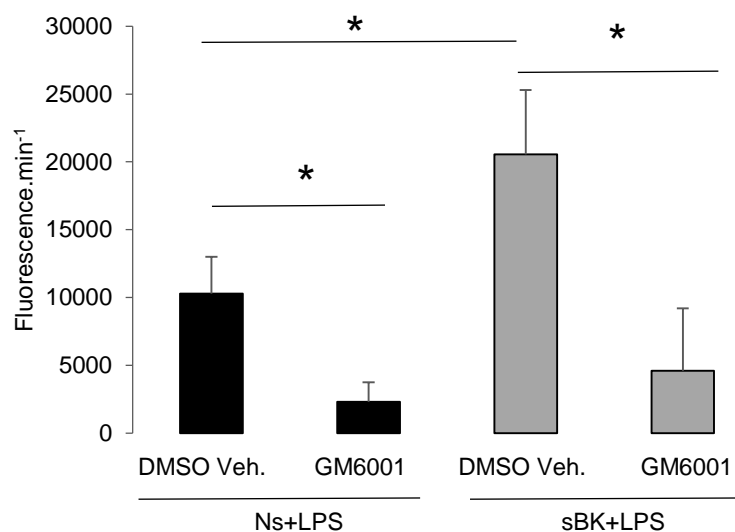
Figure 7-7 Effect of BKα silencing siRNA on ADAM17 activity in macrophages

RAW264.7 macrophages were treated with non-silencing siRNA (Ns), black bar, or BKα silencing siRNA (sBK), grey bars, and stimulated with 150 ng/ml LPS. After 3 hours, TACE substrate was applied. Control wells received DMSO (DMSO Veh.) with a final concentration of 0.15%. Per minute change in fluorescence signals (ADAM17 activity) were monitored in 10 minutes interval for 60 minutes and signals between 10 to 50 minutes used for analysis. Bars represent mean+SEM with n=4 repeated experiments. Horizontal lines represent statistical significance between groups and were tested by paired t-test. *p<0.05.

a

ADAM17
(85kDa) $\longrightarrow$

β-actin
(42kDa) $\longrightarrow$

Ns   sBK

b
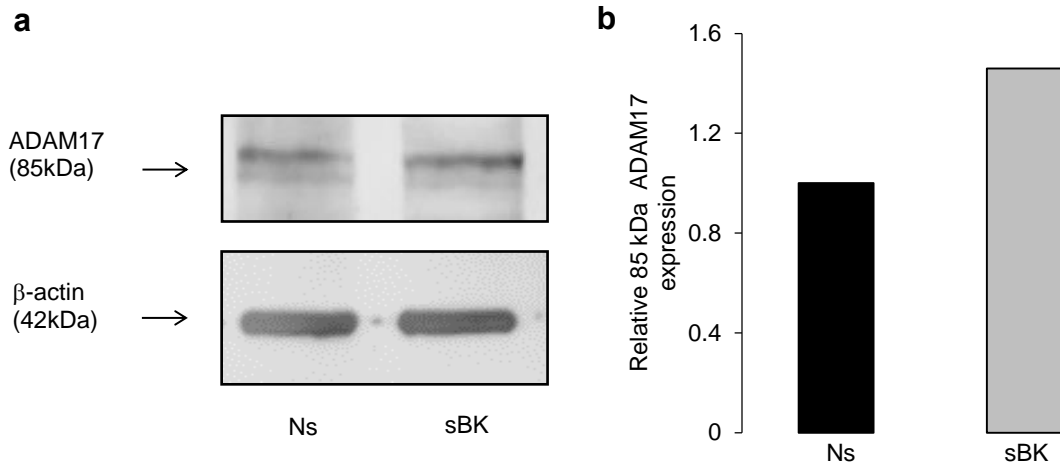
Figure 7-8 Preliminary data. Effect of BKα silencing on ADAM17 expression

RAW264.7 macrophages were treated with non-silencing siRNA (Ns), black bar, or BKα silencing siRNA (sBK), grey bars, followed by the stimulation with 150 ng/ml LPS. After 4 hours the cells were collected for Western blot analysis for a) ADAM17 and β-actin. b) Densitometry analysis shows relative mTNF-α expression in BKα silencing siRNA treated group compared to non-silencing siRNA treated group. Blots shown are from a single preliminary experiment.

7.3 Discussion

Gene silencing is mediated by the sequence specific degradation of RNA resulting from the insertion of a short double stranded RNA (small interference RNA: siRNA) (Hohjoh, 2004). While this technique provides a powerful tool to investigate the roles of the protein of interest, the effectiveness of silencing is known to vary significantly between the cell types. In addition, the application of siRNA may cause toxicity or cellular activation depending on the cellular system investigated. RAW264.7 macrophages and macrophages in general, are regarded as difficult cells to carry out genetic manipulation of protein expression *in vitro* (De Arras *et al.*, 2014). In this chapter, it was found the most efficient transfection protocol developed only resulted in 25% reduction in whole cell BKα expression in these macrophages. This is in line with a previous observation of RAW264.7 macrophages in which proteins have been attempted to be silenced (Thompson *et al.*, 1999).

Previous research has showed that siRNA can activate immune responses by TLR3, TLR7 and/or TLR8. These TLRs recognises double stranded RNA including siRNA and/or delivery vehicles used for siRNA transfection (Sioud, 2005). TLR3 is activated in a sequence independent manner and has been suggested to take a comparatively minor role in siRNA induced inflammation compared to that of TLR7 and TLR8. It has been suggested that the TLR7 and TLR8 preferentially recognise certain sequences of siRNA, which results in the release of TNF-α, IL-6 and or IFNγ (Karikó *et al.*, 2004; Sioud, 2005; Forsbach *et al.*, 2012). Unlike these observations, in the protocol used in the transfection did not stimulate TNF-α release from resting RAW264.7 macrophages. Although combined data showed a decrease in cell viability after non-silencing or silencing siRNA, the decrease in cell viability between non-silencing control group and silencing siRNA group were equivalent. Therefore this protocol was used to analyse the role of BK channels in these cells. Importantly it was noted that a purpose of this protocol was the upregulation of the plasma membrane BK channels in non-silencing siRNA controls. The silencing of BKα resulted in much lower level of expression of the plasma membrane BK channels, while not completely inhibiting it. It therefore appears that the reagent used in protocol, most likely upregulated the expression of BK channels on the plasma membrane. Fortuitously, this mimicked the effect of LPS conditioning which was used to upregulate the BK channel on the plasma membrane in chapter 4 and 5. Therefore the direct effect of BK silencing on TLR4 activation of macrophages was possible without conditioning the macrophages.

The reason why BKα silencing was 3 times more effective on the plasma membrane than at whole cells is not known. No literature could be found which investigated the difference in the effectiveness of siRNA silencing siRNA among cellular locations. However BK channels appeared on the plasma membranes of the macrophages after the transfection. It is possible to speculate that the BKα silencing siRNA preferentially inhibited the translation of the newly synthesised BKα which were directed to the cell surface. It would be important to test if the plasma membrane BK channel came from the pre-existing pool of BK channel protein, i.e. the intracellular pool, or was newly synthesized. To test this, it would be suggested to activate macrophages with 10 ng/ml LPS for 4 hours or the non-silencing siRNA to induce BK the appearance of the channel on the membrane in the presence or absence of transcription inhibitors and analyse the effect on the channel expression pattern. However, it must be noted that these experiments may be difficult to interpret. In addition, the silencing appeared to have less effect on intracellular sources of the BK channel. This result suggests that the effect which is seen in this chapter with BK channel silencing is likely to be due to the inhibition of the plasma membrane located BK channel and rather than the intracellular BK channel. The result also highlights a problem encountered when using other knockout technologies which prevent the expression of the channel globally i.e. all cellular location. This makes it important not only in the relation of a cellular function to the presence of protein, but also to its cellular location.

BK channel protein knock down increased the activity of the ADAM17 showing a 2.5 fold higher compared to non-silencing siRNA controls. These changes in TNF-α and IL-6Rα release profiles, mTNF-α expression and ADAM17 activity shown in BKα silenced cells were comparable to the effects seen with IbTX, a pharmacological inhibition of the plasma membrane BK channel, shown in chapter 5 and 6. Although the data was from a single preliminary experiment, the matured form ADAM17 at 85 kDa appeared upregulated by BKα silencing. It would be important to elucidate the connection between BK channel and ADAM17 activation processes.

In conclusion, non-silencing siRNA treatment led to the upregulation of BK channels on the plasma membrane in macrophages and BKα silencing siRNA significantly

down regulated this. Data from this chapter, using gene silencing, support the hypothesis that the plasma membrane located BK channel negatively regulates ADAM17 activity and enhances the release of TNF-α and IL-6Rα.

Chapter 8 General discussion

Inflammatory cytokines are important in facilitating acute inflammatory responses and essential in host defence. At the same time, prolonged and/or deregulated production of cytokines is associated with major diseases. Drugs which target cytokines and their receptors are used to treat many inflammatory diseases e.g. Remicade$^©$, an anti-TNF-α drug, and Actemra$^©$, an anti-IL-6Rα drug in rheumatoid arthritis. While many cytokines have been implicated in the inflammatory response TNF-α is considered the archetype pro-inflammatory cytokine. Macrophages are known to be the major source of TNF-α, along with a diverse array of other inflammatory mediators (Arango Duque and Descoteaux, 2014). It is therefore not surprising that a significant amount of research has investigated the cellular mechanisms which regulate the production of this cytokine from macrophages. However, the involvement of one class of plasma membrane protein, namely ion channels, in macrophage activation has received relatively little attention.

The general aim of this thesis was to use a variety of techniques to investigate the role of ion channels in the activation of macrophages *in vitro*. Specifically, the expression and role of BK channels in TNF-α production from macrophages during TLR4 activation was investigated.

BK channels are highly selective for K$^+$ ions and characterised by a large voltage conductance. The channel has important roles in regulating the membrane voltage and Ca^{2+} signalling. Their functions and biophysical properties have been extensively studied in excitable tissues such as in neurons and smooth muscle cells. Research has also revealed that BK channels are widely expressed in the body, in many different cell types and at different cellular locations. The BK channel is regulated by a diverse range of endogenous ligands. Importantly, many of the regulator ligands for BK channels opening have been hypothesised to have roles in inflammation e.g. CO. Previous work in the lab had suggested a role for CO producing enzyme, heme oxygenase, in regulating macrophage functions; however the precise mechanism by which this enzyme elicits its anti-inflammatory effect is yet to be elucidated. Finally, while not directly related to this thesis but of importance

in any possible follow-up research *in vivo*, BK channels had been conclusively shown to have no role in neutrophils in the innate immune response (Essin *et al.*, 2007).

It was therefore hypothesised that the BK channel may be involved in macrophage inflammatory responses. However not many studies had been carried out to characterise the expression of BK channels in these cells and the presence or absence of the channel in macrophages had not been determined and the technical approach to study ion channels in these cells had not been established. The challenge of this thesis was to first optimise the experiment to study ion channel in macrophages. Therefore a macrophage cell line, which tends to give more reproducibility to the experiments, was considered to be better for this study than primary cells. Furthermore literatures suggested that cultures of macrophages while expressing BK like channels did not show a homogenous expression across the populations (Gallin, 1991). This was probably because macrophages are highly heterogenic in nature (Gordon and Taylor, 2005). Human cell lines are not used predominately monocytic in nature and require to be differentiated before they become macrophages. The differentiation step adds another level of variability into a cellular system and produces macrophages which unlikely to be conducive for electrophysiological techniques. For these reasons, it was decided that a mouse macrophage cell line, RAW264.7 macrophage is suitable for this study. In addition, these cells are readily activated by the TLR4 ligand, LPS and TLR4 signalling has been well characterised in these cells. Therefore it was expected that these cells are clearer to investigate the effect of BK channel modulation on the TLR4.

The research progressed as follows;

1   The release of TNF-α, IL-6 and IL-6Rα, important proteins in inflammatory response, from RAW264.7 macrophages during activation of TLR4 was characterised. The effect of BK channel modulation drugs on the cytokine release was tested.

2   The expression of BKα protein in resting macrophages was investigated by biochemical analysis, and the channel functionality on the plasma membrane was tested by electrophysiological recordings.

3 BKα proteins were found in resting macrophages, therefore the effect of TLR4 activation on the BK channel expression pattern was investigated.

4 TLR4 activation led to upregulation of BK channels on the plasma membrane at later time point. The involvement of the plasma membrane expressed BK channels on the secretion of TNF-α, IL-6 and IL-6Rα was studied using a selective pharmacological inhibitor for BK channels, IbTX.

5 TNF-α release was found to be elevated by IbTX. Next the research proceed to identify at which steps of TNF-α production was affected by the channel inhibition; mRNA transcription, cellular protein synthesis or release was investigated.

6 BK channel inhibitor was found to alter the release and retention of mTNF-α. It was hypothesised that BK channels may interact with a TNF-α releasing enzyme, ADAM17. The functions of ADAM17, in macrophages were characterised. Subsequently the effect of IbTX on the activity of ADAM17 was studied.

7 As IbTX treatment enhanced ADAM17 activity, next BK channel was inhibited by gene silencing siRNA to verify the results from the pharmacological inhibition of BK channels.

These research objectives were investigated and the results were presented and analysed in chapter 3-7. In terms of the general aim of the thesis, if positive data on BK channel involvement in these cells had not be collected by objective 2, the role of other ions channels in these cells would have been investigated. This discussion chapter is aimed to integrate the results chapters, interpret the data in the light of the current literature and suggest further work arising from this thesis. This chapter also discusses the importance of this finding in inflammation and other physiological and/or pathological processes.

The main finding of this thesis is that the plasma membrane expressed BK channel regulates the activity of ADAM17 in TLR4 activated RAW264.7 macrophages, chapter 6 and 7. This was demonstrated using both a pharmacological approach and gene silencing approach. ADAM17 is a membrane sheddase which causes the release of TNF-α from the plasma membrane along with a number of other proteins, Table 8-1. Data in chapter 6 confirmed the role of this enzyme in the release TNF-α from RAW264.7 macrophages. ADAM17 also appeared to regulate the release of

IL-6Rα from macrophages. However the results indicated that the contribution of ADAM17 in overall IL-6Rα release is slightly less than that for TNF-α. An alternative mechanism by which IL-6Rα is released could include ADAM10, however the data with the pan metalloproteinase inhibiter, GM6001, would suggest this is not the case here. Instead, the result suggested the contribution of other mechanisms which are independent of membrane metalloproteinases. IL-6Rα is also released by the alternative splicing of the IL-6Rα gene (Horiuchi *et al.*, 1994) and this mechanism may account for the release of IL-6Rα from RAW264.7 macrophages. Nevertheless, the BK channel inhibition caused a significant enhancement in IL-6Rα release.

The analysis of the enzyme protein expression and the effect of membrane metalloprotease inhibitors supported the hypothesis that it was ADAM17, which is most likely to be regulated by BK channels, chapter 6 and 7. However the limitation of this analysis is that the specificity of the membrane metalloprotease inhibitors is not absolute due to the similarity of the cleavage sites recognised by these enzymes. Therefore there have been difficulties in synthesising selective inhibitors for each enzyme. In addition, the members of membrane metalloproteases family can have overlapping substrate specificities and different members can act on the same substrate (Khokha *et al.*, 2013). This means that the absence of one metalloproteinase can be compensates by the other members. A possibility that the BK channel regulated the activity of other member of ADAMs cannot be excluded. In particular ADAM10 can act as a sheddase for TNF-α and IL-6Rα Additional experiments with inhibitors of other metalloproteases and gene silencing may help to determine the relative contribution of various metalloproteinase to these proteins release.

Two previous papers (Papavlassopoulos *et al.*, 2006; Essin *et al.*, 2009) have investigated the role of BK channels in the production of TNF-α from macrophages. Essentially these papers reported that BK channels facilitated TNF-α production (Papavlassopoulos *et al.*, 2006) or had no role (Essin *et al.*, 2009). These results appear to oppose the finding from this thesis. This difference may due to various factors. This may include the use of different drugs in the paper, paxilline, instead of IbTX used in this thesis and the general knock-down of BK channels in these papers, while in this thesis, the experiments were designed to selectively inhibit plasma

membrane expressed BK channels without affecting intracellular BK channels. In the paper by Papavlassopoulos *et al*, paxilline, a different reagent from IbTX used in this thesis, was used as a BK channel blocker at 20 μM to confirm the involvement of the channel. However, in this thesis, paxilline at the concentrations of 3 μM and higher concentrations resulted in a toxic effect of paxilline. It is also noted that the IC$_{50}$ for BK channel block with paxilline can be relatively high. Paxilline was not extensively studied in these thesis because i) the above noted toxicity, ii) the possible effect on intracellular BK channels due to the lipid nature of the drug, iii) reported off-target effects of paxilline (Longland *et al.*, 2000; Bilmen *et al.*, 2002). In the second paper (Essin *et al.*, 2009), TNF-α function was investigated from macrophages isolated from BKα knockout mice. Interestingly these researchers found no effect of knocking out BKα channel on TNF-α release from macrophages stimulated for 24 hours with LPS. This thesis showed that only when BK channel appeared on the plasma membrane did IbTX have an effect and BK channel like current was sparse in resting macrophages. These authors also found a sparsity of IbTX sensitive currents in electrophysiological recordings from macrophages isolated from wildtype animals, which may have had similar phenotype to resting macrophages. Therefore this data on the BK channel expression in resting macrophages is also in line with this thesis.

An ELISA assay was used to measure release of TNF-α, IL-6 and IL-6Rα in the samples which were taken from repeated separate experiments. Although drug treatment caused relatively consistent effects in terms of ratio to the control groups, the level of protein release showed variations in some experiments. Similarly, after the activation with LPS, not all macrophages upregulated the plasma membrane BK channels and the membrane IbTX sensitive BK current was observed in only around 40% of the total cells recorded. The variability in response to LPS could be due to the phenotypic heterogeneity in macrophages. Macrophages are known to be highly plastic and heterogenetic in nature (Ravasi *et al.*, 2002; Gordon *et al.*, 2014). Their responses to immune stimuli could vary among some cell lines. Although the variability in basal levels, the results showed consistency in the effect of IbTX on cytokine release in terms of ratio to control groups, which would suggest that the interaction between BK channels and ADAM17 may occur consistently among macrophage populations.

Are there any *in vivo* studies which show a link between the BK channel and cytokine regulation? Three studies have investigated the involvement of BK channels in the models of sepsis (Cauwels and Brouckaert, 2008; O'Brien *et al.*, 2011; Xu *et al.*, 2012a). In the most recent study an exaggerated mortality was seen in mice by selective knock-out of β1 subunit, targeting vascular smooth muscle BK channels after the induction of sepsis (Xu *et al.*, 2012a). The study also showed that this was associated by an increased release of TNF-α and IL-6 in these knock-out animals, suggesting an inhibitory role for BK channel in TNF-α release. Although the data from this thesis does not agree completely, i.e. IL-6 release, this data on negative effect of BK channels in TNF-α release would be in line with the results within this thesis. Secondary another study suggested that the inhibition of BK channel and small conductance calcium dependent potassium channels have a protective effect in endotoxin shock (Cauwels and Brouckaert, 2008). In this study, animals treated with BK channel inhibitors showed a decreased survival to LPS but not TNF-α induced death. Again this could suggest that BK channels can regulate LPS activation mechanism. Finally, BKα deficient mice have been shown to have reduced survival in a model of polymicrobial sepsis via mechanisms independent of hypotension (O'Brien *et al.*, 2011). Again, it would be possible that this may related to the protective role of BK channels by reducing the release of TNF-α shown in this thesis.

How does the BK channel regulate ADAM17?

It is known that ADAM17 undergoes a series of maturation steps before being expressed as an active enzyme on the plasma membrane. Reported mechanisms which are believed to contribute to the control of ADAM17 activity include; cleavage of the enzyme pro-domain by furin proteases, translocation of ADAM17 to plasma membrane by iRhom2 and the conversion of ADAM17 dimers to active monomers by dissociation of the endogenous inhibitor TIMP-3 (Schlöndorff *et al.,* 2000; Adrain *et al.*, 2012; McIlwain *et al.*, 2012; Siggs *et al.*, 2012; Xu *et al.*, 2012b). The inhibition of BK channels appeared to show a mild effect on the protein expression of mature ADAM17, chapter 6 and Chapter 7 chapter 7. Therefore it appears that BK channels could regulate the enzyme activity at the level of expression or protein stability; however these results need further elucidation such as the expression at the plasma membrane level and the relationship between the molecular weight and the activity of ADAM17. In addition, alternative mechanisms for BK channel regulation of

ADAM17 cannot be discounted; for example, the opening of BK channel alters the membrane potential and ion compositions of the cells. These changes may directly or indirectly influence the activity of ADAM17. A recent paper suggested that the externalization of phosphatidylserine facilitates the interaction between the active site of the ADAM17 and cleavage site of its substrates via negatively charged residues on the phospholipid (Sommer *et al.*, 2016). In this light, it is possible to suggest that the membrane depolarization associated with BK channels could modulate the ADAM17 confirmation to inhibit its activity on the plasma membrane. However to confirm this, further experiments are needed. Firstly it would be suggested to investigate the effect on the membrane potential by the BK channel opening, and the link between membrane potentials and the activity of ADAM17 and its substrate release.

Cytokines, growth factors		Receptors			Adhesion molecules	Other molecules
TNF-α	SEMA4D	TNFR1	SORT1	GPIba	ICAM-1	APP
TGFα	LAG-3	TNFR2	CD91/APIER	GPV	VCAM-1	GP
AREG	DLL1	P75NTR	PTPRF,PTP-LAR	GPVI	NCAM	CA9
EREG	KL-1	IL-6Rα	EPCR	SDC1	ALCAM	PRNP, PrPc
EPGN, Epigen	KL-2	IL-1R2	ACE2	SDC4	L1-CAM	KL
NRG1, Heregulin	MICA	NTR1, TrkA	LOX-1	KDR,VEGR2	EpCAM	MUC-1
HB-EGF	MICB	GHR	NPR	CD89	DSG2	LYPD3, C4.4A
Pref1	Jagged	CSF1R, M-CSFR	HER4/ErbB4	Ptprz	CD62L	VASN
Fractalkine/ CX3CL1	LTA	SORL1	Notch 1	IGF2-R	CollagenXVII	CD163
TRANCE/RANKL	TMEFF2	SORCS1	TNFRSF8, CD30	M6P/IGF2R	PVRL4 Nectin-4	PMEL17
CSF-1	FLT-3L	SORCS3	TNFRSF5, CD40		CD44	

Table 8-1 ADAM17 substrates

Reported substrate molecules for ADAM17. Adapted from Scheller *et al.*, 2011 *Trends Immunol. 32*, 380–387.

What regulates the expression and activity of BK channels in macrophages?

Chapter 4 demonstrated that the activation of macrophages led to the upregulation BK channels on the plasma membrane. It is known that not only adaptive immune cells, but innate immune cells adjust their response to a subsequent stimuli (Netea *et al.*, 2016). Well-known examples include endotoxin tolerance and priming. Endotoxin tolerance is a phenomenon whereby the immune cells become unresponsive to the subsequent immune activation. This phenomenon is widely observed *in vitro*, *in vivo* and in clinical settings (Biswas and Lopez-Collazo, 2009). Priming is a elevating of inflammatory responses in a subsequent response after the first immune activation with a low dose of LPS. Chapter 5 showed the down regulation of released and cellular TNF-α protein, and an increase in IL-6 release in the groups received conditioning dose of LPS for 24 hours in prior to experiments. This result does not simply mimic the phenomenon of endotoxin tolerance or priming; however, it would be sufficient to say that the activation of these macrophages altered their phenotypes. Thus it can be suggested that the

upregulation of BK channels may be one of the adaptation mechanisms for macrophages to subsequent stimuli.

Mechanisms by how macrophages upregulate the BK channels are not clear. This could be the translocation of the channel protein from the cytosol, or newly synthesized. It has been reported that chemical modifications of the channel protein can upregulate the cell surface expression of BK channels (Jeffries *et al.*, 2010; Kyle and Braun, 2014). In the view of potential drug discovery, it would be useful to identify the mechanisms of BK channel expression change in macrophages.

Classically the opening of BK channels requires a rise in intracellular Ca^{2+} and hyperpolarization, which are often observed in the neurons and smooth muscle cells (Hoshi *et al.*, 2013). An important question is what increases the opening probability of BK channels in macrophages. In past decades, research has brought light into the new factors which markedly alter the activation states of the BK channel. Two possible factors must be considered when investigating the opening of BK channels, firstly the involvement/presence of endogenous signalling molecules and secondly the expression of unique BKα subtype or co-assembly with accessory subunits.

Firstly, several endogenous signalling molecules have been reported to activate BK channels (Hou *et al.*, 2009). Importantly many of these endogenous openers are known to be produced in macrophages during inflammatory responses. These molecules include CO, prostaglandin E_2 (PGE$_2$) and poly-unsaturated fatty acid (PUFA). It should be noted that these molecules are associated with down-regulation of inflammation in leukocytes. CO has been long recognised for its anti-inflammatory effect and the PUFA is known to promote the resolution of inflammation (Perretti *et al.*, 2015; Wallace *et al.*, 2015). Many of these openers are produced in macrophages and act intracellularly on the C-terminus (Hou *et al.*, 2009). In future work, it would be useful to analyse the production of these endogenous openers in TLR4 activated macrophages. In addition, recent paper has reported that the extracellular application of α-2-macroglobulin (α_2M) can activate BK channels. α_2M can be produced by the activated immune cells and therefore indicates possible connection between the BK channel activation and inflammatory response (Wakle-Prabagaran *et al.*, 2016).

However, the endogenous signalling molecules may not be the only factor when considering the opening of the channels. During the experiments, a few distinct resting membrane potential were observed in RAW264.7 cells, which were 60 mV, -35 mV and/or to -10 mV. This pattern did not change after 10 ng/ml LPS treatment for 24 hours. With the relatively low membrane potential ranges, it would be reasonable to assume that there would be other mechanisms which support these channels to open. The subtype of the BKα of macrophage BK channels and auxiliary subunit composition could alter the gating properties of this channel.

The subtype of BKα composition of the channel has not been determined in macrophages. A wide range of post transcriptional and/or post-translational modifications of the core channel protein modifies the gating properties of the channel (Kyle and Braun, 2014). These include alternative splicing of mRNA, chemical modifications such as phosphorylation and lipid insertion of the channel protein. Especially the alternative splicing of the channel mRNA results in a unique type of channel. For instance, BK channels found in glioma cells are known to have a distinct splice insert in BKα at C-terminus. This results in faster activation and higher Ca^{2+} sensitivity than those BK channels found in neurons and/or smooth muscle cells (Liu *et al.*, 2002). BK channels found in mitochondria are known to have a splice insert in C-terminus, which direct the channel to cardiac mitochondria. This mitochondrial BK channels are also known to exhibit a high conductance, voltage dependency and Ca^{2+} sensitivity (Balderas *et al.*, 2015). In RAW264.7 macrophages, BKα are found at a standard molecular weight of 120 kDa. In addition the auxiliary subunit composition can alter BK channel properties. γ1 subunit found in prostate cancer cells has been demonstrated to alter the gating of BK channels dramatically, enabling the channel to open at negative voltage with physiological Ca^{2+} concentrations (Yan and Aldrich, 2010). The co-expression of this subunit is suggested to enable the opening of this channel in non-excitable tissues. The other members of γ subunits: γ2-4 also alter the gating properties of the channel shifting the activation to a more negative voltage, but to a lesser degree than the γ subunit (Zhang and Yan, 2014). From the whole cell recordings, the steepness of I-V plot of the IbTX sensitive current from RAW264.7 cells indicated that the channels would be less dependent on membrane voltages to open. Therefore it would be useful to test the expression of any member of γ subunits in the RAW264.7 macrophages.

Furthermore the γ subunits of BK channels contain LRRs, which are an important motif for the pathogen recognition by TLRs (Yan and Aldrich, 2012). It would be suggested to study the sequence similarity of LRRs between BK channel γ subunits and TLRs, and intriguing could the BK channel be directly regulated by PAMPs or DAMPs.

What could be the consequence of BK channel regulation of ADAM17 for TNF-α and IL-6Rα function?

ADAM17 is one of the best characterised members of membrane metalloproteinases and known to facilitate the release of at least 76 transmembrane proteins from cell surface (Gooz, 2010; Scheller *et al.*, 2011; Giebeler and Zigrino, 2016). These substrates include inflammatory cytokines, growth factors, cell adhesion molecules and receptors, which are particularly important in the regulation of immune responses. Therefore the proposed interaction between BK channels and ADAM17 may assign the channel an important role in inflammatory response from macrophages.

It is known that not only circulating cytokines but membrane bound cytokines activate signalling cascades, leading to distinct physiological effects. Circulating TNF-α has been reported to preferentially act on the TNFR1, while mTNF-α binds to TNFR2 (Aggarwal *et al.*, 2012). These two signalling cascades have been reported to induce different cellular responses. The activation of TNFR1 by circulating TNF-α elicits a strong pro-inflammatory effect and the mTNF-α signalling through TNFR2 have been known to generate anti-inflammatory/regenerative responses, while still maintain an anti-microbial effect (McCoy and Tansey, 2008; Sedger and McDermott, 2014). In addition, it has been shown that mTNF-α also acts as receptor on the cell surface and the ligation of TNFRs on neighbouring cells can activate signalling in the cells. This form is termed reverse signalling and has been suggested to activate apoptosis in monocytes and macrophages (Juhász *et al.*, 2013). As a main membrane sheddase for TNF-α, ADAM17 regulates the ratio between circulating and membrane bound form of TNF-α and maintains the balance between the proinflammatory and tissue protective aspects of this cytokine. The inhibition of BK channels resulted in the enhanced activity of ADAM17. The increased activity of ADAM17 resulted in a decrease in mTNF-α expression and the increased release of

TNF-α in LPS activated RAW264.7 macrophages, chapter 6 and chapter 7. It is possible that active plasma membrane BK channel could shift TNF-α away from a predominant pro-inflammatory effect towards a tissue protective by increasing proportion of mTNF-α compared to its circulating form. The brain may represent a particular interesting area in which to look at this relationship (Probert, 2015).

IL-6Rα is expressed as both transmembrane form and circulating form. ADAM17 together with ADAM10 are known to facilitate the ecotodomain shedding of IL-6Rα. Both membrane bound IL-6Rα and circulating form IL-6Rα are able to initiate IL-6 signalling in combination with gp130. However, the signalling via membrane-bound IL-6Rα and signalling via circulating IL-6Rα have different cellular responses (Schöbitz *et al.*, 1995). IL-6 signalling via transmembrane IL-6Rα, termed classical signalling, leads to anti-inflammatory and regenerative process but signalling via circulating IL-6Rα is termed trans-signalling and known to promote inflammation. Especially, the circulating level of IL-6Rα has the impact on IL-6 trans-signalling process, which has been shown to have proinflammatory effect. Over activation of this IL-6 trans-signalling is associated with many inflammatory diseases, including rheumatoid arthritis and the control of circulating level of IL-6Rα is important in the treatment of these diseases (Hunter and Jones, 2015). Cleavage of ecotodomain of IL-6Rα by ADAM17 together with ADAM10, could modulate the balance between the two different signalling pathways, which may represent a new therapeutic target (Hunter and Jones, 2015).

The ADAM17 is widely expressed and the substrates for ADAM17 are implicated in numerous fields of biology. Investigation of the proposed BK-ADAM17 interaction in other tissues which express ADAM17 and BK channels would be useful. In particular, endothelial cells are abundant in BK and ADAM17. ADAM17 mediated shedding of growth factors, cytokines and cell adhesion molecules are known to be important in controlling vascular biology (Dreymueller *et al.*, 2012). In particular, ADAM17 mediated EGF-like growth factors are involved in endothelial migration (Maretzky *et al.*, 2011) and have implications in vascular tissue maintenance. Moreover ADAM17 facilitates the shedding of VCAM-1 and regulates the leukocytes migration into the tissues, which are essential during acute inflammatory responses (Garton *et al.*, 2006). It would be useful to study if the modulation of endothelial BK

channels have an impact on the phenomenon. Another cells would be important is glioma cells. These cells express unique variant BK channels as well as ADAM17. In U87 glioma cells, the enzyme has been suggested to promote migration, self-renewal and development of malignant phenotype (Zheng *et al.*, 2012; Chen *et al.*, 2013a, 2013b). It would be important to study the effect of BK channel modulation in on glioma cell phenotypes.

The BK channel-ADAM17 axis in biology?

This study was carried out in RAW264.7 macrophages. It would be important to evaluate the plasma membrane BK channel regulation of ADAM17 in animal models. However upon application to any other models, cautions have to be made to selectively modulate BK channels which are expressed on the plasma membrane. The channel has been reported at variable cellular localisation and location specific functions. In this thesis, nuclear BK channels are found in RAW264.7 macrophages and further variations in the channel location can be assumed in any types of macrophages. The conclusion from this thesis does not agree with the data from a paper using BK knock out mice which showed the down regulation of TNF-α in BK channel deficient animals (Essin *et al.*, 2009). In this thesis, the plasma membrane BK channels are selectively inhibited by IbTX and siRNA treatment. The difference in the results in Essin *et al*'s paper and this thesis may be due to the difference between pan BK channel inhibition by knock down and the selective inhibition of the plasma membrane BK channels. When investigating this phenomenon in BK transgenic models, first it would be important to generate a model, which selectively silences the plasma membrane BK channel to achieve the selective inhibition.

The thesis confirmed the expression of BK channels in nucleus of macrophages. The role for the nuclear BK channels in macrophage inflammatory response would be investigated in future. A report has shown that BK channel exit in nuclear membrane of rodent neurons and regulates CREB mediated transcription (Li *et al.*, 2014). CREB is known to regulate innate inflammatory responses (Wen *et al.*, 2010). It would be interesting to address whether the nuclear BK channels in macrophages may interact with the CREB mediated transcription.

Future works arising from this thesis

As discussed above, this thesis opened up many possible directions of future research.

Does this finding have physiological relevance? The application of this study into animal models would give insight into the significance of the phenomenon of plasma membrane BK channel regulation of ADAM17 observed in RAW264.7 macrophages. It is important that the plasma membrane BK channel is selectively inhibited upon application on animal models.

How BK channels regulate ADAM17? In this thesis, the mechanisms of how plasma membrane BK channels regulate ADAM17 activity was not addressed. It is important to investigate this question in the future. Preliminary data suggested that the BK channel inhibition appeared to affect the expression level of 85 kDa ADAM17 protein, which is considered to be biological active form. The relationship between the expression level of biological active ADAM17 on plasma membrane and BK channels could be elucidate further.

Do immune stimuli regulate BK channel expression in macrophages? This thesis has shown that LPS caused upregulation of BK channels on the plasma membrane of the macrophages. Also previous research suggested the general trend of upregulation of K^+ channels upon the activation or differentiation of immune cells (Feske *et al.*, 2015). It would be interesting to investigate if LPS or other immune stimuli such as IFNγ or TNF-α have this effect on human macrophages.

What is the subtype and subunit compositions of BK channels in macrophages? The subtype of BKα or β/γ subunit expression was not determined from this thesis. It is important to study the expression of subunits and BKα subtype to elucidate how these channel could function in inflammatory responses. Also this characterization of macrophage BK channels may suggest the possible way of selectively inhibiting the channels in macrophages.

Would ADAM17 and BK channels interact in other types of cells? ADAM17 and BK channels are widely expressed in the body. These two molecules are observed in other types of cells including endothelial cells and glioma cells, which express tissue specific type of BK channels (Baron *et al.*, 1997; Liu *et al.*, 2002). It is useful to repeat this study of the BK channel regulation of ADAM17 activity to further elucidate this phenomenon.

Conclusion

In conclusion, inflammatory response is a protective process, which facilitates the host defence and the maintenance of homeostasis; however, at the same time deregulated inflammation could lead to many diseases. Signalling cascades mediated by inflammatory cytokines are essential in the regulation of inflammatory responses. This thesis investigated the role of BK channels in TNF-α production from macrophages. The BK channels are upregulated on the plasma membrane of macrophages during the TLR4 activation or siRNA transfection, suggesting the possible involvement of these channels in adaptation of innate inflammatory responses. Using the pharmacological modulators and gene silencing, this thesis demonstrated that the plasma membrane BK channel regulates the activity of ADAM17 and the release of ADAM17 substrates from RAW264.7 macrophages during TLR4 activation. ADAM17 is an important regulator of numerous cell signalling during inflammatory responses, tissue regeneration, growth, respiratory and cardiovascular systems, and tumour growth. This mechanism of ADAM17 regulation by BK channels would possibly suggest a novel signalling axis, which directly link an ion channel and the activity of membrane metalloproteinase and would stimulate future research in these fields. Indeed further work is required, especially in vivo model, it is hoped that this finding may open up new therapeutic interventions.
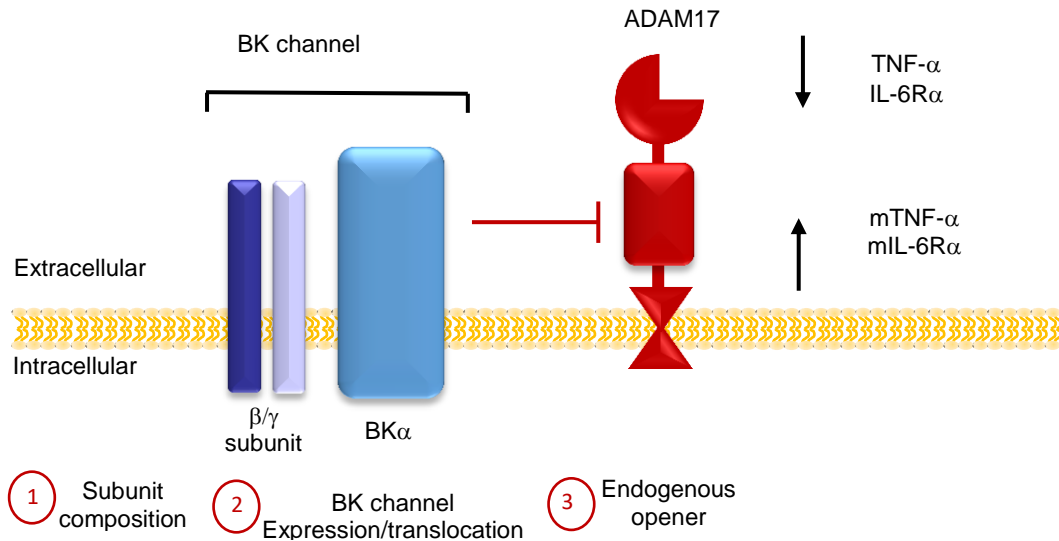
Figure 8-1 BK channels opening down regulate ADAM17 activity

The possible mechanisms for BK channels opening may be the (1) co-expression with accessory β/γ subunits which modify BK channel gating properties. (2) LPS activation and/or siRNA treatment lead to the upregulation of BKα on the plasma membrane of macrophages. The upregulated BK channels opening appeared to down regulates ADAM17 activity and decreased the release of TNF-α and IL6Rα. (3) Binding of endogenous signalling molecule.

Chapter 9 Reference

Adrain, C., Zettl, M., Christova, Y., Taylor, N., and Freeman, M. (2012). Tumor necrosis factor signaling requires iRhom2 to promote trafficking and activation of TACE. Science *335*, 225–228.

Aggarwal, B. B., Gupta, S. C., and Kim, J. H. (2012). Historical perspectives on tumor necrosis factor and its superfamily: 25 years later, a golden journey. Blood *119*, 651–665.

Akira, S., Uematsu, S., and Takeuchi, O. (2006). Pathogen recognition and innate immunity. Cell *124*, 783–801.

Aloj, G., Giardino, G., Valentino, L., Maio, F., Gallo, V., Esposito, T., Naddei, R., Cirillo, E., and Pignata, C. (2012). Severe combined immunodeficiences: new and old scenarios. Int. Rev. Immunol. *31*, 43–65.

Alvarez-Iglesias, M., Wayne, G., O'Dea, K. P., Amour, A., and Takata, M. (2005). Continuous real-time measurement of tumor necrosis factor-α converting enzyme activity on live cells. Lab. Invest. *85*, 1440–1448.

Angus, D. C., and van der Poll, T. (2013). Severe sepsis and septic shock. N. Engl. J. Med. *369*, 840–851.

Antalis, T. M., and Godbolt, D. (1991). Isolation of intact nuclei from hematopoietic cell types. Nucleic Acids Res. *19*, 4301.

Arango Duque, G., and Descoteaux, A. (2014). Macrophage cytokines: involvement in immunity and infectious diseases. Front. Immunol. *5*, 491.

Balderas, E., Zhang, J., Stefani, E., and Toro, L. (2015). Mitochondrial BK_{Ca} channel. Front. Physiol. *6*. 104

Baron, A., Frieden, M., and Bény, J.-L. (1997). Epoxyeicosatrienoic acids activate a high-conductance, Ca^{2+}-dependent K^+ channel on pig coronary artery endothelial cells. J. Physiol. *504*, 537–543.

Behrens, R., Nolting, A., Reimann, F., Schwarz, M., Waldschütz, R., and Pongs, O. (2000). hKCNMB3 and hKCNMB4, cloning and characterization of two members of the large-conductance calcium-activated potassium channel β subunit family. FEBS Lett. *474*, 99–106.

Bentzen, B. H., Nardi, A., Calloe, K., Madsen, L. S., Olesen, S.-P., and Grunnet, M. (2007). The small molecule NS11021 is a potent and specific activator of Ca^{2+}-activated big-conductance K^+ channels. Mol. Pharmacol. *72*, 1033–1044.

Bentzen, B. H., Olesen, S.-P., Rønn, L. C. B., and Grunnet, M. (2014). BK channel activators and their therapeutic perspectives. Front. Physiol. *5*. 389.

Berthier, A. *et al.* (2004). Involvement of a calcium-dependent dephosphorylation of BAD associated with the localization of TRPC-1 within lipid rafts in 7-ketocholesterol-induced THP-1 cell apoptosis. Cell Death Differ. *11*, 897–905.

Bilmen, J. G., Wootton, L. L., and Michelangeli, F. (2002). The mechanism of inhibition of the sarco/endoplasmic reticulum Ca^{2+} ATPase by paxilline. Arch. Biochem. Biophys. *406*, 55–64.

Biswas, S. K., and Lopez-Collazo, E. (2009). Endotoxin tolerance: new mechanisms, molecules and clinical significance. Trends Immunol. *30*, 475–487.

Black, R. A. *et al.* (1997). A metalloproteinase disintegrin that releases tumour-necrosis factor-α from cells. Nature *385*, 729–733.

Boghner, B. S., and Lichtenstein, L. M. (1991). Anaphylaxis. N. Engl. J. Med. *324*, 1785–1790.

Bonizzi, G., and Karin, M. (2004). The two NF-κB activation pathways and their role in innate and adaptive immunity. Trends Immunol. *25*, 280–288.

Brenner, R., Jegla, T. J., Wickenden, A., Liu, Y., and Aldrich, R. W. (2000). Cloning and functional characterization of novel large conductance calcium-activated potassium channel β subunits, hKCNMB3 and hKCNMB4. J. Biol. Chem. *275*, 6453–6461.

Bringmann, A., Skatchkov, S. N., Biedermann, B., Faude, F., and Reichenbach, A. (1998). Alterations of potassium channel activity in retinal Müller glial cells induced by arachidonic acid. Neuroscience *86*, 1291–1306.

Cahalan, M. D., and Chandy, K. G. (2009). The functional network of ion channels in T lymphocytes. Immunol. Rev. *231*, 59–87.

Campbell, I. L., Erta, M., Lim, S. L., Frausto, R., May, U., Rose-John, S., Scheller, J., and Hidalgo, J. (2014). Trans-signaling is a dominant mechanism for the pathogenic actions of interleukin-6 in the brain. J. Neurosci. *34*, 2503–2513.

Candia, S., Garcia, M. L., and Latorre, R. (1992). Mode of action of iberiotoxin, a potent blocker of the large conductance Ca^{2+}-activated K^+ channel. Biophys. J. *63*, 583–590.

Carpenter, S., Ricci, E. P., Mercier, B. C., Moore, M. J., and Fitzgerald, K. A. (2014). Post-transcriptional regulation of gene expression in innate immunity. Nat. Rev. Immunol. *14*, 361–376.

Carvacho, I., Gonzalez, W., Torres, Y. P., Brauchi, S., Alvarez, O., Gonzalez-Nilo, F. D., and Latorre, R. (2008). Intrinsic electrostatic potential in the BK channel pore: role in determining single channel conductance and block. J. Gen. Physiol. *131*, 147–161.

Cauwels, A., and Brouckaert, P. (2008). Critical role for small and large conductance calcium-dependent potassium channels in endotoxemia and TNF toxicity. Shock Augusta Ga *29*, 577–582.

Cavaliere, F., Dinkel, K., and Reymann, K. (2005). Microglia response and P2 receptor participation in oxygen/glucose deprivation-induced cortical damage. Neuroscience *136*, 615–623.

Cecchi, X., Wolff, D., Alvarez, O., and Latorre, R. (1987). Mechanisms of Cs+ blockade in a Ca^{2+}-activated K^+ channel from smooth muscle. Biophys. J. *52*, 707–716.

Chalaris, A. *et al.* (2010). Critical role of the disintegrin metalloprotease ADAM17 for intestinal inflammation and regeneration in mice. J. Exp. Med. *207*, 1617–1624.

Charles A Janeway, J., Travers, P., Walport, M., and Shlomchik, M. J. (2001). Principles of innate and adaptive immunity. Immunobiology: the immune system in health and disease. 5th edition. 711 Third Avenue, 8th Floor New York, NY 10017. Garland Science Ltd. 1-35.

Chen, X., Chen, L., Chen, J., Hu, W., Gao, H., Xie, B., Wang, X., Yin, Z., Li, S., and Wang, X. (2013a). ADAM17 promotes U87 glioblastoma stem cell migration and invasion. Brain Res. *1538*, 151–158.

Chen, X., Chen, L., Zhang, R., Yi, Y., Ma, Y., Yan, K., Jiang, X., and Wang, X. (2013b). ADAM17 regulates self-renewal and differentiation of U87 glioblastoma stem cells. Neurosci. Lett. *537*, 44–49.

Chen, Z. J. (2005). Ubiquitin signalling in the NF-κB pathway. Nat. Cell Biol. *7*, 758–765.

Clark, A. R., Dean, J. L. E., and Saklatvala, J. (2003). Post-transcriptional regulation of gene expression by mitogen-activated protein kinase p38. FEBS Lett. *546*, 37–44.

Coiret, G., Borowiec, A.-S., Mariot, P., Ouadid-Ahidouch, H., and Matifat, F. (2007). The antiestrogen tamoxifen activates BK channels and stimulates proliferation of MCF-7 breast cancer cells. Mol. Pharmacol. *71*, 843–851.

Contreras, G. F. *et al.* (2013). A BK (Slo1) channel journey from molecule to physiology. Channels *7*, 442–458.

Contreras, G. F., Neely, A., Alvarez, O., Gonzalez, C., and Latorre, R. (2012). Modulation of BK channel voltage gating by different auxiliary β subunits. Proc. Natl. Acad. Sci. U. S. A. *109*, 18991–18996.

Crawford, E. K., Ensor, J. E., Kalvakolanu, I., and Hasday, J. D. (1997). The role of 3' poly(A) tail metabolism in tumor necrosis factor-alpha regulation. J. Biol. Chem. *272*, 21120–21127.

Croft, M., Benedict, C. A., and Ware, C. F. (2013). Clinical targeting of the TNF and TNFR superfamilies. Nat. Rev. Drug Discov. *12*, 147–168.

Cui, J., Yang, H., and Lee, U. S. (2009). Molecular mechanisms of BK channel activation. Cell. Mol. Life Sci. CMLS *66*, 852–875.

Davies, L. C., Jenkins, S. J., Allen, J. E., and Taylor, P. R. (2013). Tissue-resident macrophages. Nat. Immunol. *14*, 986–995.

De Arras, L., Guthrie, B. S., and Alper, S. (2014). Using RNA-interference to investigate the innate immune response in mouse macrophages. J. Vis. Exp. *93*, 51306.

DeCoursey, T. E., and Cherny, V. V. (1996). Voltage-activated proton currents in human THP-1 monocytes. J. Membr. Biol. *152*, 131–140.

DeCoursey, T. E., Kim, S. Y., Silver, M. R., and Quandt, F. N. (1996). Ion channel expression in PMA-differentiated human THP-1 macrophages. J. Membr. Biol. *152*, 141–157.

Deng, L., Wang, C., Spencer, E., Yang, L., Braun, A., You, J., Slaughter, C., Pickart, C., and Chen, Z. J. (2000). Activation of the IκB kinase complex by TRAF6 requires a dimeric ubiquitin-conjugating enzyme complex and a unique polyubiquitin chain. Cell *103*, 351–361.

Di, A., Gao, X.-P., Qian, F., Kawamura, T., Han, J., Hecquet, C., Ye, R. D., Vogel, S. M., and Malik, A. B. (2011). The redox-sensitive cation channel TRPM2 modulates phagocyte ROS production and inflammation. Nat. Immunol. *13*, 29–34.

Donnelly, N., Gorman, A. M., Gupta, S., and Samali, A. (2013). The eIF2α kinases: their structures and functions. Cell. Mol. Life Sci. CMLS *70*, 3493–3511.

Douglas, R. M., Lai, J. C. K., Bian, S., Cummins, L., Moczydlowski, E., and Haddad, G. G. (2006). The calcium-sensitive large-conductance potassium channel (BK/MAXI K) is present in the inner mitochondrial membrane of rat brain. Neuroscience *139*, 1249–1261.

Dreymueller, D., Pruessmeyer, J., Groth, E., and Ludwig, A. (2012). The role of ADAM-mediated shedding in vascular biology. Eur. J. Cell Biol. *91*, 472–485.

Duque, G. A., Fukuda, M., and Descoteaux, A. (2013). Synaptotagmin XI regulates phagocytosis and cytokine secretion in macrophages. J. Immunol. *190*, 1737–1745.

Essin, K. *et al.* (2007). Large-conductance calcium-activated potassium channel activity is absent in human and mouse neutrophils and is not required for innate immunity. Am. J. Physiol. - Cell Physiol. *293*, C45–C54.

Essin, K. *et al.* (2009). BK channels in innate immune functions of neutrophils and macrophages. Blood *113*, 1326–1331.

Feske, S. (2009). ORAI1 and STIM1 deficiency in human and mice: roles of store-operated Ca^{2+} entry in the immune system and beyond. Immunol. Rev. *231*, 189–209.

Feske, S., Wulff, H., and Skolnik, E. Y. (2015). Ion channels in innate and adaptive immunity. Annu. Rev. Immunol. *33*, 291–353.

Finney-Hayward, T. K. *et al.* (2010). Expression of transient receptor potential c6 channels in human lung macrophages. Am. J. Respir. Cell Mol. Biol. *43*, 296–304.

Fitzgerald, K. A. *et al.* (2001). Mal (MyD88-adapter-like) is required for toll-like receptor-4 signal transduction. Nature *413*, 78–83.

Flannagan, R. S., Jaumouillé, V., and Grinstein, S. (2012). The cell biology of phagocytosis. Annu. Rev. Pathol. Mech. Dis. *7*, 61–98.

Forsbach, A., Müller, C., Montino, C., Kritzler, A., Curdt, R., Benahmed, A., Jurk, M., and Vollmer, J. (2012). Impact of delivery systems on siRNA immune activation and RNA interference. Immunol. Lett. *141*, 169–180.

Gessmer, G., Cui, Y-M., Otani, Y., Soom, M., Hoshi, T., and Heinemann, H. S. (2012). Molecular mechanism of pharmacological activation of BK channels, molecular mechanism of pharmacological activation of BK channels. Proc. Natl. Acad. Sci. U. S. *109*, 3552–3557.

Gallin, E. K. (1984). Calcium- and voltage-activated potassium channels in human macrophages. Biophys. J. *46*, 821–825.

Gallin, E. K. (1991). Ion channels in leukocytes. Physiol. Rev. *71*, 775–811.

Gallin, E. K., and Sheehy, P. A. (1985). Differential expression of inward and outward potassium currents in the macrophage-like cell line J774.1. J. Physiol. *369*, 475–499.

Galvez, A., Gimenez-Gallego, G., Reuben, J. P., Roy-Contancin, L., Feigenbaum, P., Kaczorowski, G. J., and Garcia, M. L. (1990). Purification and characterization of a unique, potent, peptidyl probe for the high conductance calcium-activated potassium channel from venom of the scorpion Buthus tamulus. J. Biol. Chem. *265*, 11083–11090.

Gao, Y., Hanley, P. J., Rinné, S., Zuzarte, M., and Daut, J. (2010). Calcium-activated K$^+$ channel (K$_{Ca3.1}$) activity during Ca^{2+} store depletion and store-operated Ca^{2+} entry in human macrophages. Cell Calcium *48*, 19–27.

Garton, K. J., Gough, P. J., and Raines, E. W. (2006). Emerging roles for ectodomain shedding in the regulation of inflammatory responses. J. Leukoc. Biol. *79*, 1105–1116.

Ghatta, S., Nimmagadda, D., Xu, X., and O'Rourke, S. T. (2006). Large-conductance, calcium-activated potassium channels: structural and functional implications. Pharmacol. Ther. *110*, 103–116.

Giebeler, N., and Zigrino, P. (2016). A disintegrin and metalloprotease (ADAM): historical overview of their functions. Toxins *8*, 122.

Gooz, M. (2010). ADAM-17: the enzyme that does it all. Crit. Rev. Biochem. Mol. Biol. *45*, 146–169.

Gordon, S., and Martinez, F. O. (2010). Alternative activation of macrophages: mechanism and functions. Immunity *32*, 593–604.

Gordon, S., Plüddemann, A., and Martinez Estrada, F. (2014). Macrophage heterogeneity in tissues: phenotypic diversity and functions. Immunol. Rev. *262*, 36–55.

Gordon, S., and Taylor, P. R. (2005). Monocyte and macrophage heterogeneity. Nat. Rev. Immunol. *5*, 953–964.

Guerra, A. N. *et al.* (2003). Purinergic receptor regulation of LPS-induced signaling and pathophysiology. J. Endotoxin Res. *9*, 256–263.

Häcker, H., Tseng, P.-H., and Karin, M. (2011). Expanding TRAF function: TRAF3 as a tri-faced immune regulator. Nat. Rev. Immunol. *11*, 457–468.

Hagar, J. A., Powell, D. A., Aachoui, Y., Ernst, R. K., and Miao, E. A. (2013). Cytoplasmic LPS activates caspase-11: implications in TLR4-independent endotoxic shock. Science *341*, 1250–1253.

He, L., Duan, H., Li, X., Wang, S., Zhang, Y., Lei, L., Xu, J., Liu, S., and Li, X. (2016). Sinomenine down-regulates TLR4/TRAF6 expression and attenuates lipopolysaccharide-induced osteoclastogenesis and osteolysis. Eur. J. Pharmacol. *779*, 66–79.

Hercule, H. C., Salanova, B., Essin, K., Honeck, H., Falck, J. R., Sausbier, M., Ruth, P., Schunck, W.-H., Luft, F. C., and Gollasch, M. (2007). The vasodilator 17,18-epoxyeicosatetraenoic acid targets the pore-forming BK α channel subunit in rodents. Exp. Physiol. *92*, 1067–1076.

Hohjoh, H. (2004). Enhancement of RNAi activity by improved siRNA duplexes. FEBS Lett. *557*, 193–198.

Horiuchi, K., Kimura, T., Miyamoto, T., Takaishi, H., Okada, Y., Toyama, Y., and Blobel, C. P. (2007). Cutting edge: TNF-α-converting enzyme (TACE/ADAM17) inactivation in mouse myeloid cells prevents lethality from endotoxin shock. J. Immunol. *179*, 2686–2689.

Horiuchi, S., Koyanagiu, Y., Zhouu, Y., Miyamotou, H., Tanakau, Y., Waki, M., Matsumoto, A., Yamamotou, M., and Yamamotof, N. (1994). Soluble interleukin-6 receptors released from T cell or granulocyte/macrophage cell lines and human peripheral blood mononuclear cells are generated through an alternative splicing mechanism. Eur. J. Immunol. *24*, 1945–1948.

Horng, T., Barton, G. M., Flavell, R. A., and Medzhitov, R. (2002). The adaptor molecule TIRAP provides signalling specificity for toll-like receptors. Nature *420*, 329–333.

Horrigan, F. T., Heinemann, S. H., and Hoshi, T. (2005). Heme regulates allosteric activation of the Slo1 BK channel. J. Gen. Physiol. *126*, 7–21.

Hoshi, T., Pantazis, A., and Olcese, R. (2013). Transduction of voltage and Ca^{2+} signals by Slo1 BK channels. Physiology *28*, 172–189.

Hotamisligil, G. S., Shargill, N. S., and Spiegelman, B. M. (1993). Adipose expression of tumor necrosis factor-alpha: direct role in obesity-linked insulin resistance. Science *259*, 87–91.

Hou, S., Heinemann, S. H., and Hoshi, T. (2009). Modulation of BK_{Ca} channel gating by endogenous signaling molecules. Physiology *24*, 26–35.

Hunter, C. A., and Jones, S. A. (2015). IL-6 as a keystone cytokine in health and disease. Nat. Immunol. *16*, 448–457.

Jeffries, O., Geiger, N., Rowe, I. C. M., Tian, L., McClafferty, H., Chen, L., Bi, D., Knaus, H. G., Ruth, P., and Shipston, M. J. (2010). Palmitoylation of the S0-S1 linker regulates cell surface expression of voltage- and calcium-activated potassium (BK) channels. J. Biol. Chem. *285*, 33307–33314.

Jenkins, K. A., and Mansell, A. (2010). TIR-containing adaptors in toll-like receptor signalling. Cytokine *49*, 237–244.

Jiang, D. *et al.* (2005). Regulation of lung injury and repair by toll-like receptors and hyaluronan. Nat. Med. *11*, 1173–1179.

Jones, S. A., Horiuchi, S., Topley, N., Yamamoto, N., and Fuller, G. M. (2001). The soluble interleukin 6 receptor: mechanisms of production and implications in disease. FASEB J. *15*, 43–58.

Juhász, K., Buzás, K., and Duda, E. (2013). Importance of reverse signaling of the TNF superfamily in immune regulation. Expert Rev. Clin. Immunol. *9*, 335–348.

Kaczorowski, G. J., and Garcia, M. L. (1999). Pharmacology of voltage-gated and calcium-activated potassium channels. Curr. Opin. Chem. Biol. *3*, 448–458.

Kagan, J. C., Su, T., Horng, T., Chow, A., Akira, S., and Medzhitov, R. (2008). TRAM couples endocytosis of toll-like receptor 4 to the induction of interferon-β. Nat. Immunol. *9*, 361–368.

Kang, J. Y., and Lee, J.-O. (2011). Structural biology of the toll-like receptor family. Annu. Rev. Biochem. *80*, 917–941.

Karikó, K., Bhuyan, P., Capodici, J., and Weissman, D. (2004). Small interfering RNAs mediate sequence-independent gene suppression and induce immune activation by signaling through toll-like receptor 3. J. Immunol. *172*, 6545–6549.

Kaufmann, W. A., Kasugai, Y., Ferraguti, F., and Storm, J. F. (2010). Two distinct pools of large-conductance calcium-activated potassium channels in the somatic plasma membrane of central principal neurons. Neuroscience *169*, 974–986.

Kawai, T., Adachi, O., Ogawa, T., Takeda, K., and Akira, S. (1999). Unresponsiveness of MyD88-deficient mice to endotoxin. Immunity *11*, 115–122.

Kawai, T., and Akira, S. (2006). TLR signaling. Cell death differ. *13*, 816–825.

Khokha, R., Murthy, A., and Weiss, A. (2013). Metalloproteinases and their natural inhibitors in inflammation and immunity. Nat. Rev. Immunol. *13*, 649–665.

Klimpel, G. R. (1980). Soluble factor(s) from LPS-activated macrophages induce cytotoxic T cell differentiation from alloantigen-primed spleen cells. J. Immunol. *125*, 1243–1249.

Knaus, H. G., Folander, K., Garcia-Calvo, M., Garcia, M. L., Kaczorowski, G. J., Smith, M., and Swanson, R. (1994a). Primary sequence and immunological characterization of beta-subunit of high conductance Ca^{2+}-activated K^+ channel from smooth muscle. J. Biol. Chem. *269*, 17274–17278.

Knaus, H.-G., McManus, O. B., Lee, S. H., Schmalhofer, W. A., Garcia-Calvo, M., Helms, L. M. H., Sanchez, M., Giangiacomo, K., and Reuben, J. P. (1994b). Tremorgenic indole alkaloids potently inhibit smooth muscle high-conductance calcium-activated potassium channels. Biochemistry *33*, 5819–5828.

Kobe, B., and Deisenhofer, J. (1995). Proteins with leucine-rich repeats. Curr. Opin. Struct. Biol. *5*, 409–416.

Kopf, M., Baumann, H., Freer, G., Freudenberg, M., Lamers, M., Kishimoto, T., Zinkernagel, R., Bluethmann, H., and Köhler, G. (1994). Impaired immune and acute-phase responses in interleukin-6-deficient mice. Nature *368*, 339–342.

Kyle, B. D., and Braun, A. P. (2014). The regulation of BK channel activity by pre- and post-translational modifications. Membr. Physiol. Membr. Biophys. *5*, 316.

Launay, P., Cheng, H., Srivatsan, S., Penner, R., Fleig, A., and Kinet, J.-P. (2004). TRPM4 regulates calcium oscillations after T cell activation. Science *306*, 1374–1377.

Lenzo, J. C., Turner, A. L., Cook, A. D., Vlahos, R., Anderson, G. P., Reynolds, E. C., and Hamilton, J. A. (2012). Control of macrophage lineage populations by CSF-1 receptor and GM-CSF in homeostasis and inflammation. Immunol. Cell Biol. *90*, 429–440.

Li, B. *et al.* (2014). Nuclear BK channels regulate gene expression via the control of nuclear calcium signaling. Nat. Neurosci. *17*, 1055–1063.

Li, G., and Cheung, D. W. (1999). Effects of paxilline on K^+ channels in rat mesenteric arterial cells. Eur. J. Pharmacol. *372*, 103–107.

Li, X., Pérez, L., Pan, Z., and Fan, H. (2007). The transmembrane domain of TACE regulates protein ectodomain shedding. Cell Res. *17*, 985–998.

Liu, D. Y., Scholze, A., Kreutz, R., Wehland-von-Trebra, M., Zidek, W., Zhu, Z. M., and Tepel, M. (2007). Monocytes from spontaneously hypertensive rats show increased store-operated and second messenger-operated calcium influx mediated by transient receptor potential canonical type 3 channels. Am. J. Hypertens. *20*, 1111–1118.

Liu, R. *et al.* (2013). Human β-defensin 2 is a novel opener of Ca^{2+}-activated potassium channels and induces vasodilation and hypotension in monkeys novelty and significance. Hypertension *62*, 415–425.

Liu, X., Chang, Y., Reinhart, P. H., and Sontheimer, H. (2002). Cloning and characterization of glioma BK, a novel BK channel isoform highly expressed in human glioma cells. J. Neurosci. *22*, 1840–1849.

Longland, C. L., Dyer, J. L., and Michelangeli, F. (2000). The mycotoxin paxilline inhibits the cerebellar inositol 1,4,5-trisphosphate receptor. Eur. J. Pharmacol. *408*, 219–225.

Lord Florey (1970). Inflammation in general pathology, 49 Newman Street London: Lloyd-Luke (Medical Books) Ltd, 22–123.

Mackenzie, A. B., Chirakkal, H., and North, R. A. (2003). Kv1.3 potassium channels in human alveolar macrophages. Am. J. Physiol. - Lung Cell. Mol. Physiol. *285*, L862–L868.

Manderson, A. P., Kay, J. G., Hammond, L. A., Brown, D. L., and Stow, J. L. (2007). Subcompartments of the macrophage recycling endosome direct the differential secretion of IL-6 and TNFα. J. Cell Biol. *178*, 57–69.

Maretzky, T., Evers, A., Zhou, W., Swendeman, S. L., Wong, P.-M., Rafii, S., Reiss, K., and Blobel, C. P. (2011). Migration of growth factor-stimulated epithelial and endothelial cells depends on EGFR transactivation by ADAM17. Nat. Commun. *2*, 229.

McCoy, M. K., and Tansey, M. G. (2008). TNF signaling inhibition in the CNS: implications for normal brain function and neurodegenerative disease. J. Neuroinflammation *5*, 45.

McGettrick, A. F., Brint, E. K., Palsson-McDermott, E. M., Rowe, D. C., Golenbock, D. T., Gay, N. J., Fitzgerald, K. A., and O'Neill, L. A. J. (2006). TRIF-related adapter molecule is phosphorylated by PKCε during toll-like receptor 4 signaling. Proc. Natl. Acad. Sci. U. S. A. *103*, 9196–9201.

McIlwain, D. R. *et al.* (2012). iRhom2 regulation of TACE controls TNF-mediated protection against listeria and responses to LPS. Science *335*, 229–232.

Medzhitov, R. (2008). Origin and physiological roles of inflammation. Nature *454*, 428–435.

Meera, P., Wallner, M., and Toro, L. (2000). A neuronal β subunit (KCNMB4) makes the large conductance, voltage- and Ca^{2+}-activated K^+ channel resistant to charybdotoxin and iberiotoxin. Proc. Natl. Acad. Sci. *97*, 5562–5567.

Metschnikoff, P. E. (1884). Ueber die beziehung der phagocyten zu milzbrandbacillen. Arch. Für Pathol. Anat. Physiol. Für Klin. Med. *97*, 502–526.

Mills, C. D., Kincaid, K., Alt, J. M., Heilman, M. J., and Hill, A. M. (2000). M-1/M-2 macrophages and the Th1/Th2 paradigm. J. Immunol. *164*, 6166–6173.

Misonou, H., Menegola, M., Buchwalder, L., Park, E. W., Meredith, A., Rhodes, K. J., Aldrich, R. W., and Trimmer, J. S. (2006). Immunolocalization of the Ca^{2+}-activated K^+ channel Slo1 in axons and nerve terminals of mammalian brain and cultured neurons. J. Comp. Neurol. *496*, 289–302.

Miyake, K. (2006). Invited review: Roles for accessory molecules in microbial recognition by toll-like receptors. J. Endotoxin Res. *12*, 195–204.

Morris, M. C., Gilliam, E. A., and Li, L. (2015). Innate immune programing by endotoxin and its pathological consequences. Mol. Innate Immun. *5*, 680.

Moss, M. L. *et al.* (1997). Cloning of a disintegrin metalloproteinase that processes precursor tumour-necrosis factor-α. Nature *385*, 733–736.

Mosser, D. M., and Edwards, J. P. (2008). Exploring the full spectrum of macrophage activation. Nat. Rev. Immunol. *8*, 958–969.

Mukhopadhyay, S., Plüddemann, A., and Gordon, S. (2009). Macrophage pattern recognition receptors in immunity, homeostasis and self tolerance. Adv. Exp. Med. Biol. *653*, 1–14.

Murray, P. J., and Wynn, T. A. (2011). Protective and pathogenic functions of macrophage subsets. Nat. Rev. Immunol. *11*, 723–737.

Nagasawa, M., Nakagawa, Y., Tanaka, S., and Kojima, I. (2007). Chemotactic peptide fMetLeuPhe induces translocation of the TRPV2 channel in macrophages. J. Cell. Physiol. *210*, 692–702.

Napetschnig, J., and Wu, H. (2013). Molecular basis of NF-κB signaling. Annu. Rev. Biophys. *42*, 443–468.

Nardi, A., Calderone, V., Chericoni, S., and Morelli, I. (2003). Natural modulators of large-conductance calcium-activated potassium channels. Planta Med. *69*, 885–892.

Nathan, C. (2002). Points of control in inflammation. Nature *420*, 846–852.

Netea, M. G., Joosten, L. A. B., Latz, E., Mills, K. H. G., Natoli, G., Stunnenberg, H. G., O'Neill, L. A. J., and Xavier, R. J. (2016). Trained immunity: a program of innate immune memory in health and disease. Science *352*, aaf1098.

O'Brien, A. J., Terala, D., Orie, N. N., Davies, N. A., Zolfaghari, P., Singer, M., and Clapp, L. H. (2011). BK large conductance Ca^{2+}-activated K^+ channel deficient mice are not resistant to hypotension and display reduced survival benefit following polymicrobial sepsis. Shock *35*, 485–491.

Olesen, S. P., Munch, E., Moldt, P., and Drejer, J. (1994). Selective activation of Ca^{2+}-dependent K^+ channels by novel benzimidazolone. Eur. J. Pharmacol. *251*, 53–59.

O'Neill, L. A. J., and Bowie, A. G. (2007). The family of five: TIR-domain-containing adaptors in toll-like receptor signalling. Nat. Rev. Immunol. *7*, 353–364.

Orio, P., Rojas, P., Ferreira, G., and Latorre, R. (2002). New disguises for an old channel: maxiK channel β-subunits. Physiology *17*, 156–161.

Papavlassopoulos, M., Stamme, C., Thon, L., Adam, D., Hillemann, D., Seydel, U., and Schromm, A. B. (2006). MaxiK blockade selectively inhibits the lipopolysaccharide-induced IκB-α/NF-κB signaling pathway in macrophages. J. Immunol. *177*, 4086–4093.

Perdiguero, E. G., and Geissmann, F. (2016). The development and maintenance of resident macrophages. Nat. Immunol. *17*, 2–8.

Perretti, M., Leroy, X., Bland, E. J., and Montero-Melendez, T. (2015). Resolution pharmacology: opportunities for therapeutic innovation in inflammation. Trends Pharmacol. Sci. *36*, 737–755.

Poltorak, A. *et al.* (1998). Defective LPS signaling In C3H/Hej and C57BL/10SCCR mice: mutations In TLR4 gene. Science *282*, 2085–2088.

Probert, L. (2015). TNF and its receptors in the CNS: The essential, the desirable and the deleterious effects. Neuroscience *302*, 2–22.

Rabani, M. *et al.* (2011). Metabolic labeling of RNA uncovers principles of RNA production and degradation dynamics in mammalian cells. Nat. Biotechnol. *29*, 436–442.

Raetz, C. R. H., and Whitfield, C. (2002). Lipopolysaccharide endotoxins. Annu. Rev. Biochem. *71*, 635–700.

Ravasi, T., Wells, C., Forest, A., Underhill, D. M., Wainwright, B. J., Aderem, A., Grimmond, S., and Hume, D. A. (2002). Generation of diversity in the innate immune system: macrophage heterogeneity arises from gene-autonomous transcriptional probability of individual inducible genes. J. Immunol. Baltim. Md 1950 *168*, 44–50.

Riethmueller, S., Ehlers, J. C., Lokau, J., Düsterhöft, S., Knittler, K., Dombrowsky, G., Grötzinger, J., Rabe, B., Rose-John, S., and Garbers, C. (2016). Cleavage site localization differentially controls interleukin-6 receptor proteolysis by ADAM10 and ADAM17. Sci. Rep. *6*, 25550.

Roos, D. *et al.* (1996). Mutations in the X-linked and autosomal recessive forms of chronic granulomatous disease. Blood *87*, 1663–1681.

Rose-John, S. (2013). ADAM17, shedding, TACE as therapeutic targets. Pharmacol. Res. *71*, 19–22.

Rose-John, S., and Heinrich, P. C. (1994). Soluble receptors for cytokines and growth factors: generation and biological function. Biochem. J. *300*, 281–290.

Rowe, D. C., McGettrick, A. F., Latz, E., Monks, B. G., Gay, N. J., Yamamoto, M., Akira, S., O'Neill, L. A., Fitzgerald, K. A., and Golenbock, D. T. (2006). The myristoylation of TRIF-related adaptor molecule is essential for toll-like receptor 4 signal transduction. Proc. Natl. Acad. Sci. *103*, 6299–6304.

Roy, S., Morayo Akande, A., Large, R. J., Webb, T. I., Camarasu, C., Sergeant, G. P., McHale, N. G., Thornbury, K. D., and Hollywood, M. A. (2012). Structure-activity relationships of a novel group of large-conductance Ca^{2+}-activated K^+ (BK) channel modulators: the GoSlo-SR family. ChemMedChem *7*, 1763–1769.

Rutledge, H. R., Jiang, W., Yang, J., Warg, L. A., Schwartz, D. A., Pisetsky, D. S., and Yang, I. V. (2012). Gene expression profiles of RAW264.7 macrophages stimulated with preparations of LPS differing in isolation and purity. Innate Immun. *18*, 80–88.

Santoni, G., Farfariello, V., Liberati, S., Morelli, M. B., Nabissi, M., Santoni, M., and Amantini, C. (2013). The role of transient receptor potential vanilloid type-2 ion channels in innate and adaptive immune responses. Front. Immunol. *4*.34

Sato, S., Sugiyama, M., Yamamoto, M., Watanabe, Y., Kawai, T., Takeda, K., and Akira, S. (2003). Toll/IL-1 receptor domain-containing adaptor inducing IFN-beta (TRIF) associates with TNF receptor-associated factor 6 and TANK-binding kinase 1, and activates two distinct transcription factors, NF-kappa B and IFN-regulatory factor-3, in the toll-like receptor signaling. J. Immunol. Baltim. Md 1950 *171*, 4304–4310.

Scheller, J., Chalaris, A., Garbers, C., and Rose-John, S. (2011). ADAM17: a molecular switch to control inflammation and tissue regeneration. Trends Immunol. *32*, 380–387.

Schilling, T., and Eder, C. (2009). Non-selective cation channel activity is required for lysophosphatidylcholine-induced monocyte migration. J. Cell. Physiol. *221*, 325–334.

Schlöndorff, J., Becherer, J. D., and Blobel, C. P. (2000). Intracellular maturation and localization of the tumour necrosis factor alpha convertase (TACE). Biochem. J. *347*, 131–138.

Schöbitz, B., Pezeshki, G., Pohl, T., Hemmann, U., Heinrich, P. C., Holsboer, F., and Reul, J. M. (1995). Soluble interleukin-6 (IL-6) receptor augments central effects of IL-6 in vivo. FASEB J. *9*, 659–664.

Schwarz, J. *et al.* (2013). Short-term TNFα shedding is independent of cytoplasmic phosphorylation or furin cleavage of ADAM17. Biochim. Biophys. Acta BBA - Mol. Cell Res. *1833*, 3355–3367.

Sedger, L. M., and McDermott, M. F. (2014). TNF and TNF-receptors: From mediators of cell death and inflammation to therapeutic giants – past, present and future. Cytokine Growth Factor Rev. *25*, 453–472.

Shaw, G., and Kamen, R. (1986). A conserved AU sequence from the 3′ untranslated region of GM-CSF mRNA mediates selective mRNA degradation. Cell *46*, 659–667.

Shurety, W., Merino-Trigo, A., Brown, D., Hume, D. A., and Stow, J. L. (2000). Localization and post-golgi trafficking of tumor necrosis factor-alpha in macrophages. J. Interferon Cytokine Res. *20*, 427–438.

Siggs, O. M., Xiao, N., Wang, Y., Shi, H., Tomisato, W., Li, X., Xia, Y., and Beutler, B. (2012). iRhom2 is required for the secretion of mouse TNFα. Blood *119*, 5769–5771.

Singh, H., Stefani, E., and Toro, L. (2012). Intracellular BK_{Ca} (iBK_{Ca}) channels. J. Physiol. *590*, 5937–5947.

Sioud, M. (2005). Induction of inflammatory cytokines and interferon responses by double-stranded and single-stranded siRNAs is sequence-dependent and requires endosomal localization. J. Mol. Biol. *348*, 1079–1090.

Sommer, A. *et al.* (2016). Phosphatidylserine exposure is required for ADAM17 sheddase function. Nat. Commun. *7*, 11523.

Song, D. H., and Lee, J.-O. (2012). Sensing of microbial molecular patterns by toll-like receptors. Immunol. Rev. *250*, 216–229.

Soond, S. M., Everson, B., Riches, D. W. H., and Murphy, G. (2005). ERK-mediated phosphorylation of Thr735 in TNFα-converting enzyme and its potential role in TACE protein trafficking. J. Cell Sci. *118*, 2371–2380.

Srivastava, S., Zhdanova, O., Di, L., Li, Z., Albaqumi, M., Wulff, H., and Skolnik, E. Y. (2008). Protein histidine phosphatase 1 negatively regulates CD4 T cells by inhibiting the K^+ channel $K_{Ca3.1}$. Proc. Natl. Acad. Sci. *105*, 14442–14446.

Stebbing, M. J., Cottee, J. M., and Rana, I. (2015). The role of ion channels in microglial activation and proliferation – a complex interplay between ligand-gated ion channels, K^+ channels, and intracellular Ca^{2+} in innate and adaptive responses, Front. Immuno.*4*, 34

Stoecklin, G., Lu, M., Rattenbacher, B., and Moroni, C. (2003). A constitutive decay element promotes tumor necrosis factor alpha mRNA degradation via an AU-rich element-independent pathway. Mol. Cell. Biol. *23*, 3506–3515.

Stoecklin, G., Stubbs, T., Kedersha, N., Wax, S., Rigby, W. F. C., Blackwell, T. K., and Anderson, P. (2004). MK2-induced tristetraprolin:14-3-3 complexes prevent stress granule association and ARE-mRNA decay. EMBO J. *23*, 1313–1324.

Stow, J. L., Ching Low, P., Offenhäuser, C., and Sangermani, D. (2009). Cytokine secretion in macrophages and other cells: pathways and mediators. Immunobiology *214*, 601–612.

Takeuchi, O., and Akira, S. (2010). Pattern recognition receptors and inflammation. Cell *140*, 805–820.

Takeuchi, O., Hoshino, K., and Akira, S. (2000). Cutting edge: TLR2-deficient and MyD88-deficient mice are highly susceptible to staphylococcus aureus infection. J. Immunol. *165*, 5392–5396.

Tanaka, T., Narazaki, M., Ogata, A., and Kishimoto, T. (2014). A new era for the treatment of inflammatory autoimmune diseases by interleukin-6 blockade strategy. Semin. Immunol. *26*, 88–96.

Tang, X. D., Garcia, M. L., Heinemann, S. H., and Hoshi, T. (2004). Reactive oxygen species impair Slo1 BK channel function by altering cysteine-mediated calcium sensing. Nat. Struct. Mol. Biol. *11*, 171–178.

Thompson, C. D., Frazier-Jessen, M. R., Rawat, R., Nordan, R. P., and Brown, R. T. (1999). Evaluation of methods for transient transfection of a murine macrophage cell line, RAW 264.7. BioTechniques *27*, 824–826.

Tiedje, C., Ronkina, N., Tehrani, M., Dhamija, S., Laass, K., Holtmann, H., Kotlyarov, A., and Gaestel, M. (2012). The p38/MK2-driven exchange between tristetraprolin and HuR regulates AU-rich element-dependent translation. PLoS Genet. *8*, e1002977.

Tzachanis, D., Berezovskaya, A., Nadler, L. M., and Boussiotis, V. A. (2002). Blockade of B7/CD28 in mixed lymphocyte reaction cultures results in the generation of alternatively activated macrophages, which suppress T-cell responses. Blood *99*, 1465–1473.

Vallabhapurapu, S., and Karin, M. (2009). Regulation and function of NF-κB transcription factors in the immune system. Annu. Rev. Immunol. *27*, 693–733.

Valverde, M. A., Rojas, P., Amigo, J., Cosmelli, D., Orio, P., Bahamonde, M. I., Mann, G. E., Vergara, C., and Latorre, R. (1999). Acute activation of maxi-K channels (hslo) by estradiol binding to the β subunit. Science *285*, 1929–1931.

Vergara, C., Alvarez, O., and Latorre, R. (1999). Localization of the K^+ lock-in and the Ba^{2+} binding sites in a voltage-gated calcium-modulated channel. J. Gen. Physiol. *114*, 365–376.

Vicente, R., Escalada, A., Soler, C., Grande, M., Celada, A., Tamkun, M. M., Solsona, C., and Felipe, A. (2005). Pattern of Kv beta subunit expression in

macrophages depends upon proliferation and the mode of activation. J. Immunol. Baltim. Md 1950 *174*, 4736–4744.

Villarroel, A., Alvarez, O., Oberhauser, A., and Latorre, R. (1988). Probing a Ca^{2+}-activated K^+ channel with quaternary ammonium ions. Pflüg. Arch. *413*, 118–126.

Wakle-Prabagaran, M., Lorca, R. A., Ma, X., Stamnes, S. J., Amazu, C., Hsiao, J. J., Karch, C. M., Hyrc, K. L., Wright, M. E., and England, S. K. (2016). BKCa channel regulates calcium oscillations induced by alpha-2-macroglobulin in human myometrial smooth muscle cells. Proc. Natl. Acad. Sci. *113*, E2335–E2344.

Wallace, J. L., Ianaro, A., Flannigan, K. L., and Cirino, G. (2015). Gaseous mediators in resolution of inflammation. Semin. Immunol. *27*, 227–233.

Wallner, M., Meera, P., and Toro, L. (1999). Molecular basis of fast inactivation in voltage and Ca^{2+}-activated K^+ channels: A transmembrane β-subunit homolog. Proc. Natl. Acad. Sci. *96*, 4137–4142.

Walsh, M. C., Lee, J., and Choi, Y. (2015). Tumor necrosis factor receptor-associated factor 6 (TRAF6) regulation of development, function, and homeostasis of the immune system. Immunol. Rev. *266*, 72–92.

Wang, C., Deng, L., Hong, M., Akkaraju, G. R., Inoue, J., and Chen, Z. J. (2001). TAK1 is a ubiquitin-dependent kinase of MKK and IKK. Nature *412*, 346–351.

Watters, T. M., Kenny, E. F., and O'Neill, L. A. J. (2007). Structure, function and regulation of the toll/IL-1 receptor adaptor proteins. Immunol. Cell Biol. *85*, 411–419.

Weischenfeldt, J., Damgaard, I., Bryder, D., Theilgaard-Mönch, K., Thoren, L. A., Nielsen, F. C., Jacobsen, S. E. W., Nerlov, C., and Porse, B. T. (2008). NMD is essential for hematopoietic stem and progenitor cells and for eliminating by-products of programmed DNA rearrangements. Genes Dev. *22*, 1381–1396.

Wen, A. Y., Sakamoto, K. M., and Miller, L. S. (2010). The role of the transcription factor CREB in immune function. J. Immunol. *185*, 6413–6419.

Whitt, J. P., Montgomery, J. R., and Meredith, A. L. (2016). BK channel inactivation gates daytime excitability in the circadian clock. Nat. Commun. *7*, 10837.

Woloski, B. M., and Fuller, G. M. (1985). Identification and partial characterization of hepatocyte-stimulating factor from leukemia cell lines: comparison with interleukin 1. Proc. Natl. Acad. Sci. *82*, 1443–1447.

Wu, Y., Yang, Y., Ye, S., and Jiang, Y. (2010). Structure of the gating ring from the human large-conductance Ca^{2+}-gated K^+ channel. Nature *466*, 393–397.

Wynn, T. A., Chawla, A., and Pollard, J. W. (2013). Macrophage biology in development, homeostasis and disease. Nature *496*, 445–455.

Xu, H., Wang, Y., Garver, H., Galligan, J. J., and Fink, G. D. (2012a). Vascular BK channel deficiency exacerbates organ damage and mortality in endotoxemic mice. J. Cardiovasc. Pharmacol. *59*, 207–214.

Xu, N., Chen, C. Y., and Shyu, A. B. (1997). Modulation of the fate of cytoplasmic mRNA by AU-rich elements: key sequence features controlling mRNA deadenylation and decay. Mol. Cell. Biol. *17*, 4611–4621.

Xu, P., Liu, J., Sakaki-Yumoto, M., and Derynck, R. (2012b). TACE activation by MAPK-mediated regulation of cell surface dimerization and TIMP3 association. Sci. Signal. *5*, ra34-ra34.

Xu, W., Liu, Y., Wang, S., McDonald, T., Eyk, J. E. V., Sidor, A., and O'Rourke, B. (2002). Cytoprotective role of Ca^{2+}- activated K^+ channels in the cardiac inner mitochondrial membrane. Science *298*, 1029–1033.

Yamamoto, M. *et al.* (2002). Essential role for TIRAP in activation of the signalling cascade shared by TLR2 and TLR4. Nature *420*, 324–329.

Yamamoto, M. *et al.* (2003a). Role of adaptor TRIF in the MyD88-independent toll-like receptor signaling pathway. Science *301*, 640–643.

Yamamoto, M., Sato, S., Hemmi, H., Uematsu, S., Hoshino, K., Kaisho, T., Takeuchi, O., Takeda, K., and Akira, S. (2003b). TRAM is specifically involved in the toll-like receptor 4-mediated MyD88-independent signaling pathway. Nat. Immunol. *4*, 1144–1150.

Yamamoto, S. *et al.* (2008). TRPM2-mediated Ca^{2+} influx induces chemokine production in monocytes that aggravates inflammatory neutrophil infiltration. Nat. Med. *14*, 738–747.

Yan, J., and Aldrich, R. W. (2010). LRRC26 auxiliary protein allows BK channel activation at resting voltage without calcium. Nature *466*, 513–516.

Yan, J., and Aldrich, R. W. (2012). BK potassium channel modulation by leucine-rich repeat-containing proteins. Proc. Natl. Acad. Sci. U. S. A. *109*, 7917–7922.

Yasukawa, K., Hirano, T., Watanabe, Y., Muratani, K., Matsuda, T., Nakai, S., and Kishimoto, T. (1987). Structure and expression of human B cell stimulatory factor-2 (BSF-2/IL-6) gene. EMBO J. *6*, 2939–2945.

Yoshizaki, K., Nakagawa, T., Fukunaga, K., Tseng, L. T., Yamamura, Y., and Kishimoto, T. (1984). Isolation and characterization of B cell differentiation factor (BCDF) secreted from a human B lymphoblastoid cell line. J. Immunol. *132*, 2948–2954.

Yu, M., Liu, S., Sun, P., Pan, H., Tian, C., and Zhang, L. (2016). Peptide toxins and small-molecule blockers of BK channels. Acta Pharmacol. Sin. *37*, 56–66.

Yuan, P., Leonetti, M. D., Pico, A. R., Hsiung, Y., and MacKinnon, R. (2010). Structure of the human BK channel Ca^{2+}-activation apparatus at 3.0 å resolution. Science *329*, 182–186.

Zhang, J., and Yan, J. (2014). Regulation of BK channels by auxiliary γ subunits. Membr. Physiol. Membr. Biophys. *5*, 401.

Zheng, X., Jiang, F., Katakowski, M., Lu, Y., and Chopp, M. (2012). ADAM17 promotes glioma cell malignant phenotype. Mol. Carcinog. *51*, 150–164.

Zhou, Y., and Lingle, C. J. (2014). Paxilline inhibits BK channels by an almost exclusively closed-channel block mechanism. J. Gen. Physiol. *144*, 415–440.

Appendix

Prizes

Finalist, The New Investigator Award, A novel role for BK channel in regulating metalloprotease activity, *12th World Congress on Inflammation*, August 2015 Boston.

Published abstracts

Yoshida, M., Gibb. A. J., Willis. D. (2012) Iberiotoxin block of endotoxin tolerance in a mouse macrophage cell line. P008. *British Pharmacological Society Winter Meeting,* December 2012 London.

Yoshida, M., Willis, D. (2015) A novel role for BK channel in regulating metalloprotease activity. B266. *12th World Congress on Inflammation*, August 2015 Boston.

Scholarship

University College London Old Students' Association Trust Scholarships, 2014